University of Alberta

Starch morphological and molecular structural relations to amylolysis

by

Sabaratnam Naguleswaran

A thesis submitted to the Faculty of Graduate Studies and Research
in partial fulfillment of the requirements for the degree of

Doctor of Philosophy

in

Food Science and Technology

Department of Agricultural, Food and Nutritional Science

Spring 2013
Edmonton, Alberta

DEDICATION

This dissertation is lovingly dedicated to my wife Sumithira and son Tharun.

ABSTRACT

The objective of this research was to investigate the impact of variation in starch morphology and molecular structure among starches isolated from triticale, wheat, corn and barley (normal, waxy, and high-amylose genotypes) on amylolysis. Native starch granules in their unfractionated and fractionated (large and small granules) forms were characterized in terms of their composition, morphology, physicochemical properties and molecular structure [amylopectin (AP) and amylose (AM)]. The degree of hydrolysis (DH) was determined (55^{o}C for 1h and then at 30^{o}C for 72h) using a mixture of α-amylase and glucoamylase. SEM and CLSM studies revealed that surface pores and internal channels were mainly present in large granules of triticale, wheat and corn starches. In corn starches, the surface pores and channels were filled with protein and phospholipids. AM content and crystallinity of starches varied among genotypes, and between large and small granules within a source. Regardless of genotypes, the DH at the initial stage (1h) of hydrolysis of unfractionated triticale was higher than wheat, corn and barley starches. In fractionated starches, small granules were hydrolyzed (at 1h) to a greater extent than large granules due to their larger surface area per unit mass. The data on AP molecular characteristics showed that the average chain length (average-*CL*) was negatively correlated to weight-average molecular weight (M_w), molecular-size or radius of gyration (R_z), molecular density (ρ) and degree of branching (*DB*). The enzyme hydrolysis data indicated that, at all stages of hydrolysis, AP was hydrolyzed to a greater extent

than AM. Whereas, variation in DH among isolated AP or isolated AM from different starch sources was generally insignificant at all stages of hydrolysis. Furthermore, it was observed that the DH (at 1h) of native unfractionated starches was negatively correlated to average-*CL*, but positively correlated to M_w, R_z, ρ and *DB*. Overall, this study indicated that starch amylolysis is influenced by the interplay among: 1) composition (AM content), 2) morphological characteristics (granule size, channels/pores, and associated proteins and phospholipids) and 3) difference in granular architecture (resulting from variation in the AP average-*CL*).

ACKNOWLEDGEMENT

I would like to express my sincere thanks to the following individuals and organizations for their contribution and support during my Ph.D. program.

My first and foremost gratitude goes to Dr. Thava Vasanthan, for his guidance, advice, patience and encouragement throughout my research studies. I am fortunate to work with him for my Doctor of Philosophy.

I appreciate very much the financial support to my research studies from the Natural Science and Engineering Research Council (NSERC) of Canada through the Discovery Grant to Dr. T. Vasanthan, the Agriculture Bio-innovation Program (ABIP) of Agriculture and Agri-Food Canada through the funding from Canadian Triticale Biorefinery Initiative (CTBI), and the Biorefining Conversions Network (BCN) at the University of Alberta. I gratefully acknowledge the Graduate Student Scholarship from the Alberta Innovates-Technology Futures in Edmonton, Canada and also the travel grants from the Faculty of Graduate Studies and Research, the Department of Agricultural, Food and Nutritional Science and the Graduate Students' Association, University of Alberta.

I would like to extend my appreciation to Dr. Michael Eskin (External examiner), Dr. Phillip Choi (Examination committee member), Dr. David Bressler (Supervisory committee member and collaborator) and Dr. Michael Gaenzle (Supervisory committee member) for serving in my final defense examination committee.

Thanks also extended to Drs. Ratnajothi Hoover and Jihong Li for their valuable suggestions and comments on manuscripts preparation for publications. Dr. J. Lan, Gao, Wong, Haiyan, Mariana, Amin, Tem, Tian, Ankur, Safia, Ehsan and Koel, your friendly assistance and co-operation during my Ph.D. studies will always be remembered. In addition, my appreciation goes to all staff and graduate students in the Department of Agricultural, Food and Nutritional Science for their routine assistance and making a pleasant environment where I worked.

Last but not least, my lovable gratefulness to my wife Sumithira and son Tharun for their valuable support, encouragement and love throughout my life. Finally, thanks to my parents and rest of my family for encouraging me to achieve my academic goals.

TABLE OF CONTENTS

LIST OF TABLES

LIST OF FIGURES

LIST OF SYMBOLS AND ABBREVIATIONS

1G	First Generation
2G	Second Generation
3G	Third Generation
AACC	American Association of Cereal Chemists
AC	Agriculture and Agri-Food Canada
ACS	American Chemical Society
AFM	Atomic Force Microscopy
AM	Amylose
AP	Amylopectin
APTS	8-aminopyrene-1,3,6-trisulfonic acid
B	Number of branch points
CBO	Cross Beam Optics
CBQCA	3-(4-carboxybenzoyl)-quinoline-2-carboxaldehyde
CDC	Crop Development Center
CL	Chain Length
CLSM	Confocal Laser Scanning Microscopy
CPS	Canada Prairie Spring

DB	Degree of Branching
DDGS	Dried Distiller's Grains plus Solubles
DH	Degree of Hydrolysis
DM	Dry-Milling
DMSO	Dimethylsulfoxide
DP	Degree of Polymerization
DP_n	Number-average Degree of Polymerization
DP_w	Weight-average Degree of Polymerization
DSC	Differential Scanning Calorimetry
FAO	Food and Agriculture Organization
FFF	Field-Flow Fractionation
FID	Flame-Ionization-Detector
GAU	Glucoamylase Unit
GC	Gas Chromatography
GH	Glycoside Hydrolase
GHG	Greenhouse Gas
GLM	General Linear Model
gM	Branching ratio or Shrinking factor

GSHE	Granular Starch Hydrolyzing Enzyme
HA	High-Amylose
HPLC	High-Performance Liquid Chromatography
HPSEC	High-Performance Size Exclusion Chromatography
HSD	Honestly Significant Difference
LPL	Lysophospholipid
LSD	Least Significant Differences
MALLS	Multi-Angle Laser Light Scattering
M_n	Number-average Molecular Weight
M_w	Weight-average Molecular Weight
NM	Normal
PDI	Polydispersity Index
RC	Relative Crystallinity
RHF	Raw-starch Hydrolysis and Fermentation
RID	Refractive Index Detector
RS	Resistant Starch
R_w	Weight-average Radius of Gyration
R_z	Z-average Radius of Gyration

SAS	Statistical Analysis System
SAXS	Small Angle X-Ray Scattering
SDS	Sodium Dodecyl Sulfate
SEM	Scanning Electron Microscopy
SHF	Separate Hydrolysis and Fermentation
SSF	Simultaneous Saccharification and Fermentation
SV_g	Specific Volume for Gyration
T_c	Conclusion or End gelatinization temperature
TEM	Transmission Electron Microscopy
TN	Total Nitrogen
T_o	Onset gelatinization temperature
T_p	Peak or Mid-point gelatinization temperature
WAXD	Wide Angle X-Ray Diffraction
WX	Waxy
WM	Wet-Milling
db	dry basis
ρ	Molecular Density
ΔH	Enthalpy of gelatinization

CHAPTER 1
INTRODUCTION AND OBJECTIVES

1.1. INTRODUCTION

The uses of starch sharply increased in both food and industrial applications. Cereal grains are a major source of starch that is currently utilized in various foods, industrial and cosmetic applications. A clear understanding of starch structure-function relationship is an essential factor in deciding the application of a particular starch. The highly organized semicrystalline structure of starch granule makes it a unique polysaccharide with numerous functionalities. For instance, starch is the major energy source for both plant and animals. Highly processed foods utilize various functionalities of starch-derived products such as sugars, dextrins, or modified starches, which confer many specific physicochemical properties. Furthermore, a rapidly growing trend in processed food is a shift toward more natural and healthy products. One of the current trends is the consumption of starchy products that are resistant to digestion, so called resistant starches (RS). Some of these can be a source of dietary fiber (i.e. completely resistant to enzyme hydrolysis) and others are known as slowly digestible starches (Englyst, et al., 1992), demonstrated to assist in controlling sugar metabolism in diabetics. Thus, understanding the relationship between starch structure and its enzymatic hydrolysis is important in developing novel food products from various starch sources.

On the other hand, a fast growing global demand for energy, progressive depletion of fossil fuel and a concern on global warming due to increased greenhouse gases have resulted in efforts to find alternative energy sources, which are renewable and environmentally friendly. Biofuels have been shown to have the potential to accomplish the aforementioned requirements. Of all biofuels, bioethanol is the most utilized liquid biofuel either as a fuel or as a gasoline extender or additive. Bioethanol produced from energy crops or agricultural crops (ex: sugarcane or cereal grains) is referred to as a first-generation biofuel (Gomez, et al., 2008). Conventional large-scale ethanol production is a batch process and it requires starch from agricultural crops to be enzymatically hydrolyzed (liquefaction at 90-110^{o}C followed by saccharification at 60-70^{o}C) completely to sugars (glucose, maltose and maltotriose), which are subsequently fermented to ethanol by yeast (Chen, et al., 2008; Sharma, et al., 2007). The current trend in bioethanol production towards continuous process involves the saccharification of dextrin (liquefied starch) into sugars in parallel to yeast fermentation in a single reactor, so called simultaneous saccharification and fermentation, SSF (Balat, 2009; das Neves, et al., 2007). Regardless of technologies, the initial step in current bioethanol production that converts native starch into sugars (amylolysis) is expensive since excessive heat energy is used in gelatinizing starch. An improved granular starch hydrolyzing enzyme cocktail (a mixture of α-amylase and glucoamylase) was developed to hydrolyze native starch granules into fermentable sugars at sub-gelatinization temperature

(raw starch hydrolysis). It is used in SSF at low temperature, thus reduces the cost of production and can effectively work on uncooked (raw) starches. In addition, raw starch hydrolysis has been shown to produce a better recovery of value-added co-products such as dried distiller's grain plus solubles (DDGS) due to the high stability of components such as proteins at low temperature (Gibreel, et al., 2009).

Despite the extensive collection of starch hydrolysis (by amylases) studies reported in the literature, a substantial research gap yet exists in this area of science. There is no information available on how amylose (AM) and amylopectin (AP) would be hydrolyzed by amylases when isolated from the starch granule. A comparison of the reactivity of amylases towards the intact native granule and its isolated components (AM and AP) would help us to understand the role played by AM and AP in starch amylolysis. Understanding the structural basis among the multitude of intrinsic starch factors (composition, morphology and molecular structure) which influence the starch amylolysis is critically important for providing a structural target for breeding or genetic research programs. Regardless of whether starches are selected to be resistant to digestion, as in the case with health food products, or are selected to be readily hydrolyzed at lower, more efficient temperatures, as required for ethanol production, the same industrial problem and research question arise and need answering: how do the compositional, morphological, architectural, and molecular properties of starch influence amylolysis? Thus, this study is geared towards understanding how

variations in the structural properties of starch from various botanical origins (corn, barley, wheat, and triticale) would influence the starch susceptibility towards amylolysis by amylases. The outcome of this study may provide some novel information for precise control of starch liquefaction and saccharification of bioconversions during hydrolysis and fermentation process in bioethanol production, and may help food industries in formulating variety of low-glycemic food products from the selected cereal grains.

REFERENCES

Balat M. (2009). Bioethanol as a vehicular fuel: A critical review. *Energy Sources Part A – Recovery, Utilization, and Environmental Effects, 31*, 1242-1255.

Chen J., Wu K., & Fukuda H. (2008). Bioethanol production from uncooked raw starch by immobilized surface-engineered yeast cells. *Applied Biochemistry and Biotechnology, 145*, 59-67.

das Neves M. A., Kimura T., Shimizu C., & Nakajima M. (2007). State of the art and future trends of bioethanol production. *Dynamic Biochemistry, Process Biotechnology and Molecular Biology, 1*, 1-14.

Englyst H. N., Kingman S. M., & Cummings J. H. (1992). Classification and measurement of nutritionally important starch fractions. *European Journal of Clinical Nutrition, 46*, 33-50.

Gibreel A., Sandercock J. R., Lan J., Goonewardene L. A., Zijlstra R. T., Curtis J. M., & Bressler D. C. (2009). Fermentation of barley by using *Saccharomyces cerevisiae*: Examination of barley as a feedstock for bioethanol production and value-added products. *Applied and Environmental Microbiology, 75*, 1363-1372.

Gomez L. D., Steele-King C. G., & McQueen-Mason S. J. (2008). Sustainable liquid biofuels from biomass: the writing's on the walls. *New Phytologist, 178*, 473-485.

Sharma V., Rausch K. D., Tumbleson M. E., & Singh V. (2007). Comparison between granular starch hydrolyzing enzyme and conventional enzymes for ethanol production from maize starch with different amylose: amylopectin ratios. *Starch-Starke, 59*, 549-556.

1.2. OBJECTIVES AND HYPOTHESES

The overall objective of this thesis was to understand the relationship between the starch factors (morphology, composition, architecture and molecular properties), and amylolysis of native starches from some cereals such as triticale, corn, wheat, and barley.

The entire study was designed based on the following major objectives.

Objective 1:

To characterize the distribution of surface pores, internal channels, and starch-associated protein and phospholipids within starch granules in relation to amylolysis by using two common microscopy techniques such as scanning electron microscopy (SEM) and confocal laser scanning microscopy (CLSM).

Hypothesis: The surface pores and internal channels of native starch granules facilitate the diffusion of amylase enzymes for better hydrolysis.

Objective 2:

To understand the relationship among starch morphology, architectural and physicochemical characteristics, and the degree of amylolysis of large and small starch granules from normal genotypes of triticale, wheat and corn using granular starch hydrolyzing enzymes at sub-gelatinization temperatures.

Hypothesis: Difference in granule size of native starches with similar amylose content significantly influences the degree of amylolysis.

Objective 3:

To understand the relationship among starch morphology, architectural and physicochemical characteristics, and the degree of hydrolysis of unfractionated and fractionated (large and small) starch granules from waxy (<10% amylose), normal (20–30% amylose) and high-amylose (>40% amylose) hull-less barley in comparison with corn starches of varying amylose content (0–70%) using granular starch hydrolyzing enzymes at sub-gelatinization temperatures.

Hypothesis: The native starches differ in granule size and amylose content significantly influence the degree of amylolysis.

Objective 4:

To understand the relationship among granule architecture and molecular characteristics of amylose and amylopectin, and the degree of hydrolysis of triticale, wheat, corn and barley starches using granular starch hydrolyzing enzymes at sub-gelatinization temperatures.

Hypothesis: The granule architecture and molecular structure of amylose and amylopectin significantly influence the degree of amylolysis.

CHAPTER 2

LITERATURE REVIEW

2.1. STARCH

Starch is the second foremost natural polysaccharide solely present in higher plants next to cellulose. This biopolymer is important source of energy for many plants and animals, including humans. Indeed, the uses of starch are not limited for food consumption; it can be a raw material for various industrial applications. For instance, starch is popularly known for manufacturing of paper and boards, textiles, cosmetics, pharmaceuticals, agrochemicals, detergents, bioplastics, and for bioethanol production (Liu, 2005; Murthy, et al., 2011). In plants, starch is deposited as granules in the amyloplast of storage organs. For example, in cereal grains (ex: barley), granules are embedded in the protein matrix of endosperm wherein each cell compartment is clearly distinguished by cell walls (Figure 2.1). The most important starch sources are the cereal grains, legume seeds (pulses), tubers and some roots. In cereals, the starch content varies from 57 to 89% (Liu, 2005). In North America, corn and wheat are more widely cultivated than barley and triticale, and are used for various food and industrial applications. The Canadian and total world production of corn, wheat, barley, and triticale in 2010 is presented in Figure 2.2 (FAO Statistics Division, 2012). In Canada, wheat was number one in production (23.2 MT) in 2010 followed by corn (11.7 MT), barley (7.6 MT) and triticale (0.07 MT).

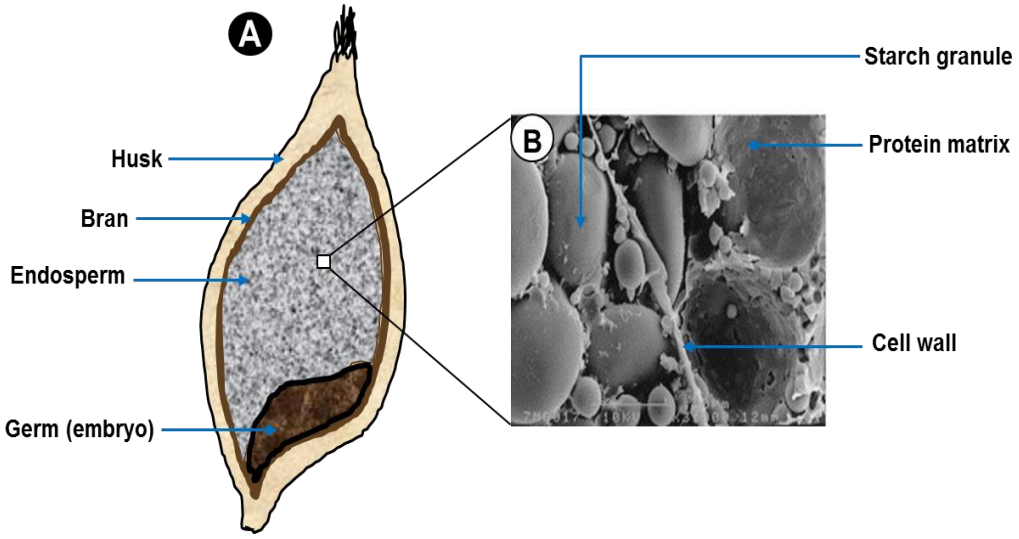

Figure 2.1: (**A**)-Representation of a barley grain, and (**B**)-Scanning electron microscopy image of barley endosperm [(**B**)-Adapted from the publication of Izydorczyk and Dexter (2008) with permission of Elsevier Ltd.]

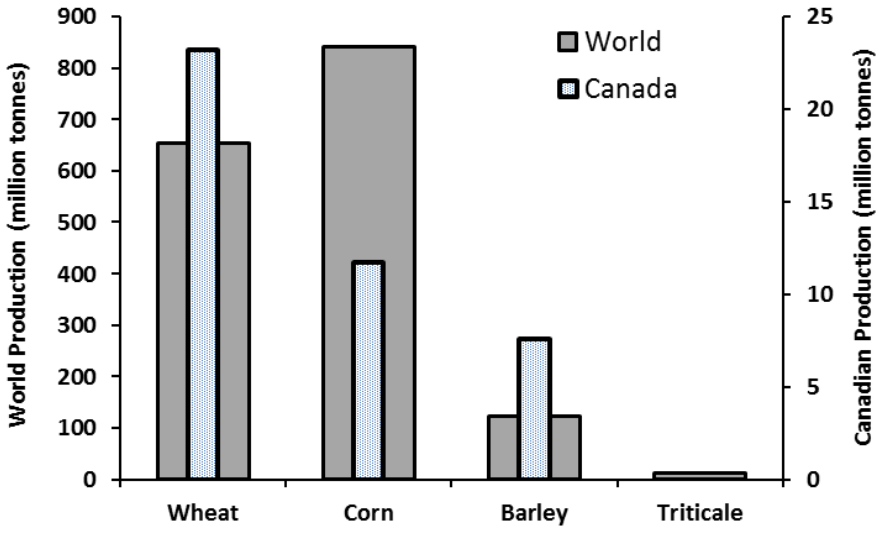

Figure 2.2: Canadian and total world production of wheat, corn, barley and triticale in 2010.

2.1.1. Granule morphology

The size and shape of the starch granules vary with plant species and maturity of the storage organs (Ao & Jane, 2007; Huber & Praznik, 2004). In most cereal starches, size of the granules ranges from 2 to 36 µm with a bimodal size distribution, where the ratio of small to large granules varies with plant source (Jane, 2009). For example, wheat, triticale, barley, and rye have a bimodal size distribution while corn starches have unimodal distribution (Jane, 2009; Tester, et al., 2006). Most of the large A-granules in cereal starches are lenticular (ex: wheat) or polygonal (ex: corn) while small B-granules are round or spherical in shape. In high-amylose corn starch, although majority of granules are polygonal in shape, some of them are elongated or filamentous granules (Liu, 2005).

Various microscopy methods such as scanning electron microscopy (SEM), transmission electron microscopy (TEM), atomic force microscopy (AFM) and recently confocal laser scanning microscopy (CLSM) have been used to study the granule morphology of starches. When observed under SEM, the surface of corn, wheat, barley, rye, sorghum and millet starch granules appeared to be distributed with pores (Jane, 2009; Liu, 2005, Sujka & Jamroz, 2007). Based on the diameter, the starch pores can be classified into: 1) macropores [>50 nm], 2) mesopores [2 – 50 nm] and 3) micropores [<2 nm] (Sujka & Jamroz, 2007). The diameter and distribution of pores on starch granules vary with starch sources, size of the starch granules, maturity of a storage organ, and the location of

starch granule in a storage organ. Most of the large granules in cereal starches have relatively more pores compared to small granules. Starch granules located closer to germ have numerous pores than the granules in other parts of the cereal grain. In addition, starch granules in cereal grain (ex: corn) harvested at the later stage of maturity have more pores than granules harvested at the early stage of maturity. The pores on starch granules are the external openings of channels that run internally to connect the cavity in hilum region of the granule (Dhital, et al., 2010; Jane, 2009; Sujka & Jamroz, 2007). The size and shape of the cavity differ with starch sources. For instance, the cavities of rice and wheat starch granules are spherical in shape but in corn starches, the cavities are irregular in shape or star shaped (Jane, 2009).

A schematic showing the morphological features of a starch granule is presented in Figure 2.3 in comparison with the SEM images of a native granule. The pores, channels and cavities are naturally existing granule features in starches and are possibly important for enzyme or chemical diffusions (Dhital, et al., 2010; Liu, 2005; Sujka & Jamroz, 2010). However, the granule surface pores and channels may or may not be associated with minor components of starch such as protein and phospholipids (Han & BeMiller, 2008; Han & Hamaker, 2002a; Han, et al., 2005; Lee & BeMiller, 2008). The effect of such components on chemical and enzyme reaction sites of starch granules have also been investigated (Chung & Lai, 2006; Gray & BeMiller, 2004; Israkarn, et al., 2007; Mira, et al., 2007), and the findings are discussed in Chapter 3.1.

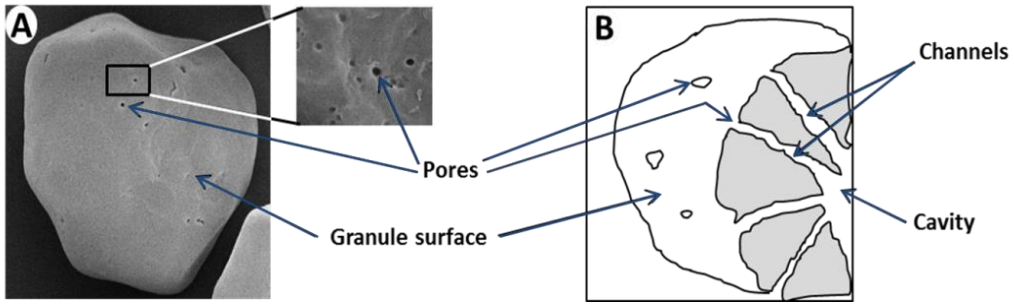

Figure 2.3: (A)-Scanning electron microscopy image of native corn starch granule, and **(B)**-Representation of a starch granule showing pores, channels and cavity.

2.1.2. Granule architecture

Structurally, the starch granules are semicrystalline in nature (Vermeylen, et al., 2005). The architecture of a starch granule is built up by two polymers: (1) amylose (AM), essentially linear with a few long-chain branches consists of 500-20000 glucose units joined by α-(1,4)-glycosidic linkage (Figure 2.4A), and (2) amylopectin (AP), a heavily branched molecule in which about 200000 glucose units are linearly joined by α-(1,4)-glycosidic linkage with branch points (≈5%) linked by α-(1,6)-glycosidic bonds (Figure 2.4B) (Gilbert, et al., 2010; Gomand, et al., 2012; Murthy, et al., 2011). The AM and AP are highly organized through intra- and inter-molecular hydrogen-bonding to form the architecture of a starch granule. However, the architecture differs in starch granules since the proportion of AM and AP varies with different starch sources and among genotypes within a source (Li, et al., 2003; Liu, 2005). In cereal starches, the AM content varies between ≈0% (ex: waxy corn) and 70% (ex: high-amylose corn), and also

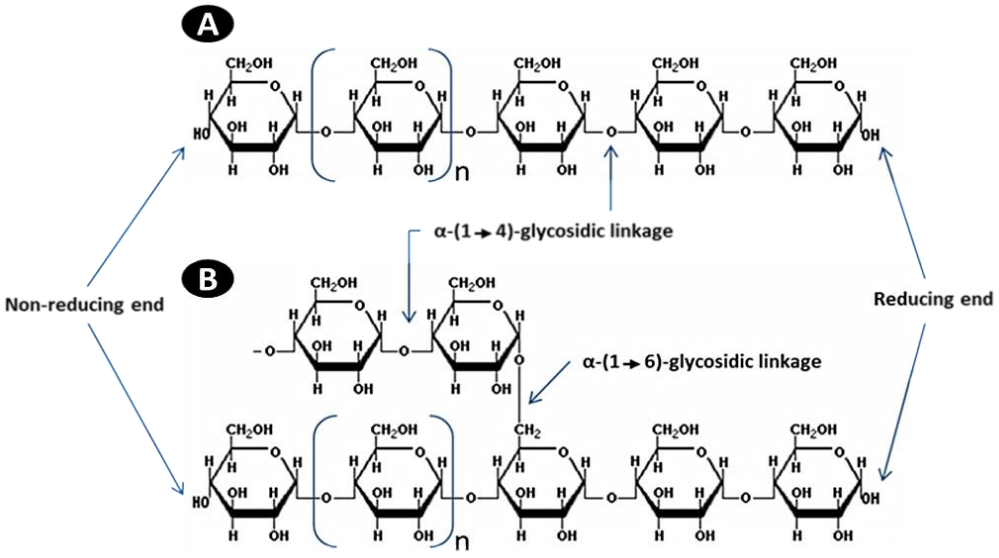

Figure 2.4: Molecular structure of amylose (**A**) and amylopectin (**B**). Adapted and modified from Tester, et al. (2004) with permission of Elsevier Ltd.

between sizes of granules within a source. For example, large A-granules of wheat, triticale, and barley starches contain more AM than their small B-granules (Ao & Jane, 2007). The AM in starches may exist in free form, in networking with AP branch points, and in the form of AM-lipid complexes. The lipids in AM-lipid complex of cereal starches are mostly phospholipids (Ao & Jane, 2007). The formation of a helical complex between AM and iodine results in the deep blue color of starch dispersions and forms the basis for quantitative determination of AM content.

Figure 2.5 illustrates the two different models, using blocklet (Gallant, et al., 1997) and using growth rings (Jenkins, et al., 1994), which have been proposed to explain the architecture of a starch granule. The blocklet model

(Figure 2.5A) structurally distinguishes the interior of a native starch granule into an amorphous central region (hilum), which is composed mainly of AM and a periphery region, which is occupied by alternatively arranged crystalline hard shells and semicrystalline soft shells. The crystalline shell and semicrystalline shell are composed of several blocklets in different sizes. The size of the blocklet ranges from 20 to 500 nm depending on the botanical origin of the starch and its location within a granule (Gallant, et al., 1997). In addition, the size of a blocklet in semicrystalline shell is smaller than that in crystalline shell. A blocklet is further composed of alternatively arranged crystalline lamellae (≈7 nm), which has a highly ordered double-helical crystallites of AP, and amorphous lamellae (≈2 nm), where the branch-points of AP are located (Ao & Jane, 2007; Li, et al., 2003; Liu, 2005; Vermeylen, et al., 2005). Thus, the shape, size, and structure of starch granules are primarily determined by the structure and arrangement of AP molecules.

The architecture of a starch granule in the second model (Figure 2.5B) is also described based on the configuration of two distinct regions. In this model, several semicrystalline and amorphous layers are alternately arranged to form growth rings, ranging in width between 120 and 400 nm depending on the sources of starch. The semicrystalline growth rings are further composed of alternatively organized crystalline lamellae (5–6 nm) and amorphous lamellae (2–5 nm) of the AP molecules. Accordingly, the A-chains of AP form double helices, which are regularly packed as clusters to form the crystalline lamellae,

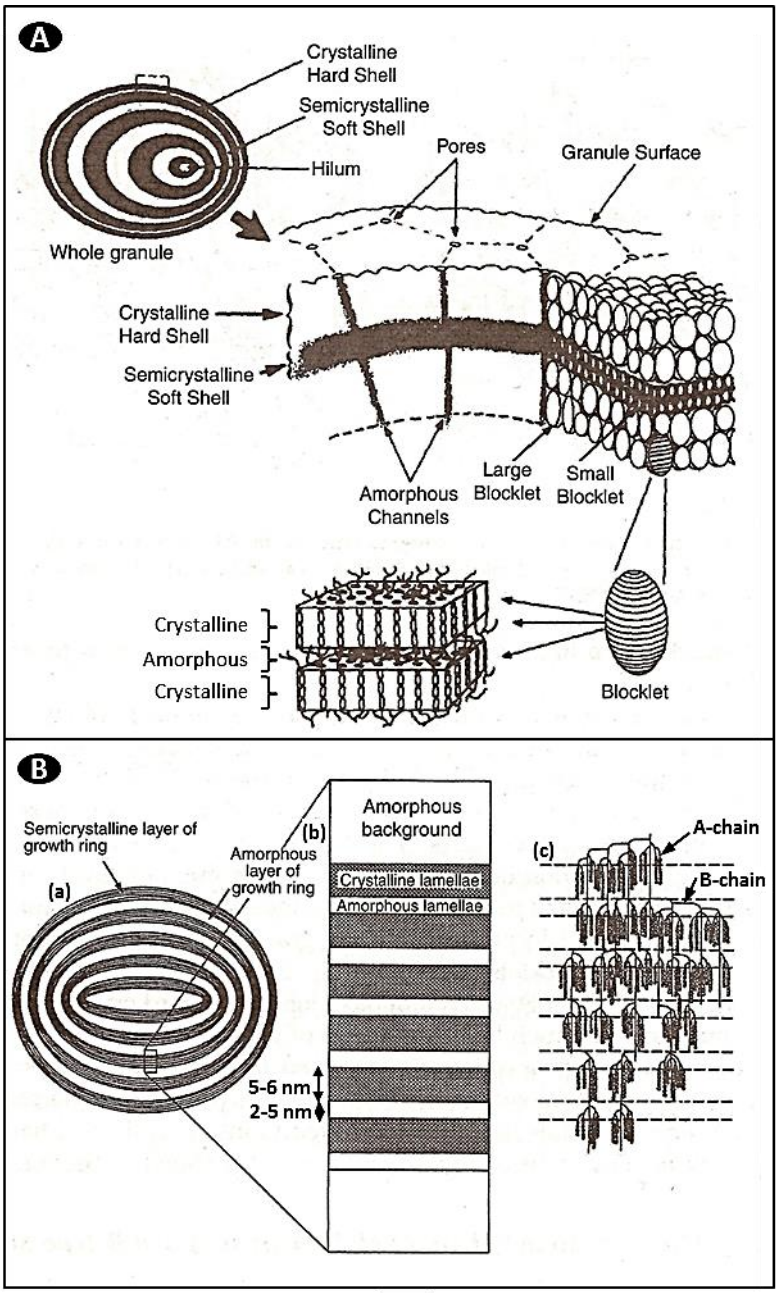

Figure 2.5: Different representations of the structure of a starch granule: (**A**) Blocklet model, and (**B**) Growth rings model, (**a**) – A single granule, consisting of alternatively arranged amorphous and semicrystalline layers of growth rings, (**b**) – an expanded view of the semicrystalline layer of growth ring, and (**c**) – the cluster structure of amylopectin within the semicrystalline layer of growth ring. **(A)** – adapted from Gallant, et al. (1997), and **(B)** – adapted from Jenkins, et al. (1994) with permissions of Elsevier Ltd.

whereas the B-chains of AP provide connections between the clusters. The amorphous lamellae have the branching points for both A- and B-chains of AP (Jenkins, et al., 1994).

The AM molecules in both models are believed to present in the central amorphous region (hilum) of a granule and in networking with branch points of AP in the amorphous lamellae of growth ring or of a blocklet (Gallant, et al., 1997; Huber & Praznik, 2004). The amorphous regions of a starch granule are susceptible to chemical and enzyme reactions, and are also responsible for the swelling property of native starches (Ao & Jane, 2007; Jenkins, et al., 1994; Liu, 2005).

A number of cluster models have been proposed to illustrate the structure of AP. Among them, four models such as French; Robin; Manners & Matheson; and Hizukuri are presented in Figures 2.6A, B, C, and D, respectively. Generally, in a cluster model, short and long chains of glucose monomer are glycosidically linked through α-(1,4)-glycosidic (linear) and α-(1,6)-glycosidic (branch point) linkages to form an AP molecule (Goesaert, et al., 2010; Rolland-Sabate, et al., 2007). The model that has been proposed by Manners and Matheson (1981) is based on the models proposed by French (1972) and Robin et al. (1974). In addition, a model (Figure 2.6D) that proposed by Hizukuri (1986) is reasonably used to describe the AP structure (Jane, 2009). By considering this model, the un-branched A-chains are linked to B- or C-chains by their reducing

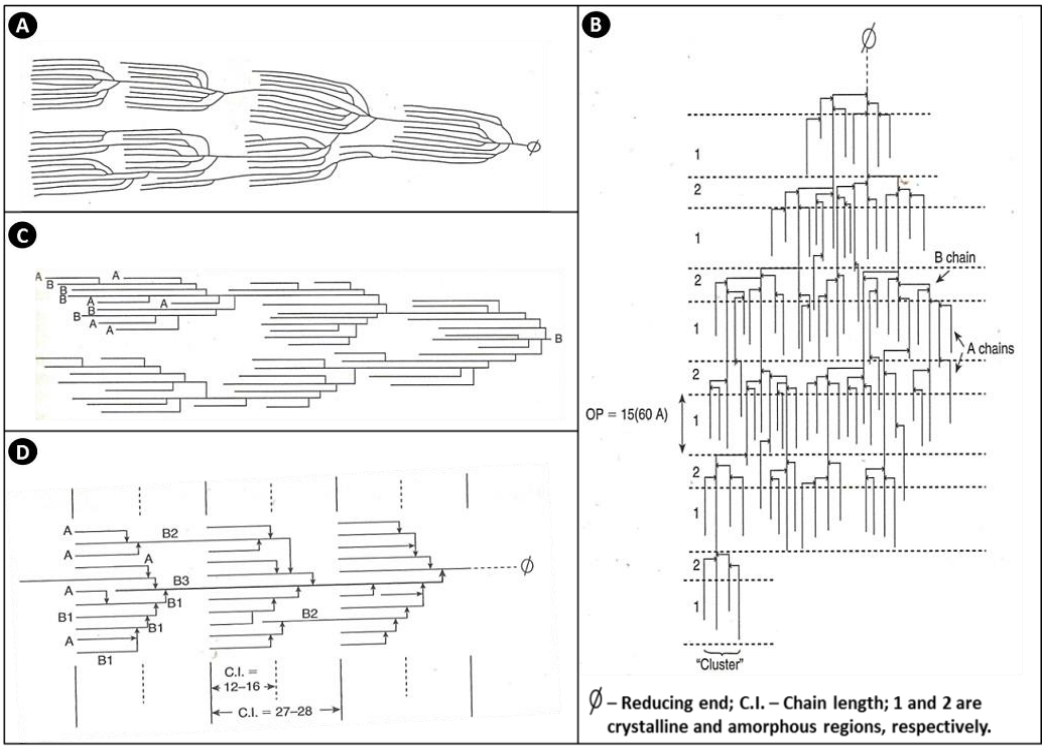

Figure 2.6: Cluster models of amylopectin: (**A**) French model (Adapted from French, 1972), (**B**) Robin et al. model (Adapted from Robin, et al., 1974 with permission of Copyright Clearance Center), (**C**) Manners and Matheson model (Adapted from Manners and Matheson, 1981 with permission of Elsevier Ltd.), and (**D**) Hizukuri model (Adapted from Hizukuri, 1986 with permission of Elsevier Ltd.)

ends through α-D-(1,6)-linkages. The B-chains (B1, B2, B3, or B4) are branched at O-6 of a glucose unit to connect A-chains or another B-chain and linked to a C-chain. Each AP molecule has a single reducing end at its only C-chain (Figure 2.6D). The unit chains of AP are relatively short as compared to AM molecules (Tester, et al., 2004). The short un-branched A-chains (DP 6–12) and branched B1-chains (DP 13–24) in a single cluster form double helices, which laterally associate themselves to form crystallites between intra- and inter-AP molecules within the native starch granules (Tester, et al., 2004). Furthermore, the long

branched chains such as B2 (DP 25–36), B3 (DP 37–75) and B4 (DP 104–140) extend into 2, 3 and 4 or more clusters, respectively, to make up the backbone of the AP structure (Goesaert, et al., 2010; Jane, 2009). The average length of unit-chains in an AP highly depends on source of the starch, maturity of storage organ, and location of molecules within a starch granule. In cereal starches, the average chain-length varies between 18 and 31 glucose units long (Jane, 2009).

Using X-ray diffraction analysis, Wu and Sarko (1978) identified two types, A- and B-types, of crystallites in starches (Figure 2.7). Although the individual double helices in the two types are very similar, the structures of A- and B-types differ in their organization. In the A-type, left-handed, parallel-stranded double helices are compactly organized in a monocline space where less number (≈12) of inter-helical water molecules are associated. In contrast, double helices are less compactly organized in the hexagonal space wherein more (≈36) water molecules are trapped in the B-type crystals (Huber & Praznik, 2004; Liu, 2005; Wu & Sarko, 1978). A more stable structure of A-type crystallites is characteristics of cereal starches whereas less stable crystallites are found in high-amylose corn, tuber and root starches (Liu, 2005). The amount of crystallinity within starch granules varies between 0 and 100%. The 0% reference represents 'fully amorphous' material (ex: freeze-dried gelatinized starch) with the 100% reference usually being generated by extensive acid hydrolysis of starch in which all the amorphous (but not crystalline) material has been eroded

(Tester, et al., 2004). Generally, in cereal starches, the percentage of relative crystallinity ranges from 22 to 40%.

In the quantitative determination of AP, iodine does not form a stable blue complex with AP due to the short length of the unit chains (need at least DP 40 to form blue complex with iodine), but instead forms a purple color. Thus, AP content of a starch sample is usually measured based on its AM content, where the AP content equals to 100 minus AM content (%) assuming that the starch granules are solely composed of AP and AM.

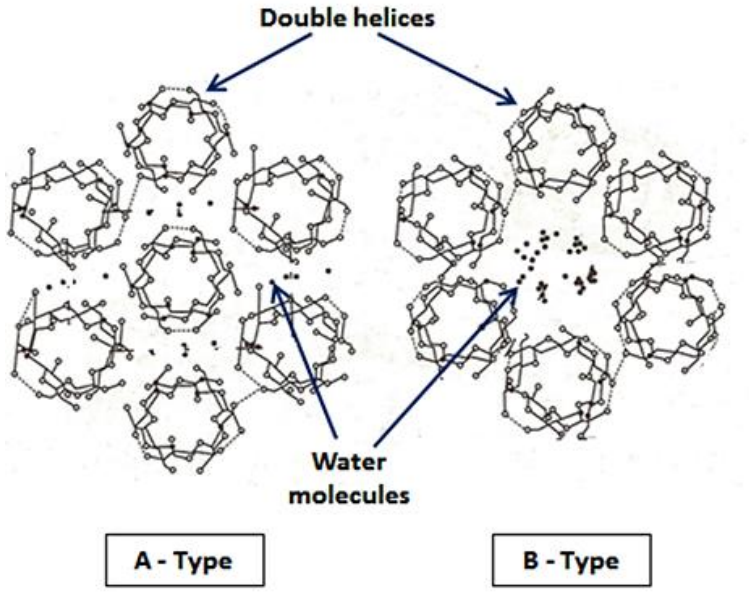

Figure 2.7: Comparison of unit cells and helix packing in A- and B-type crystallites: dashed lines indicate hydrogen bonds. Adapted and modified from the publication of Wu and Sarko, (1978) with permission of Elsevier Ltd.

2.2. STARCH AMYLOLYSIS

The major type of enzymes involved in the breakdown of starch molecules are amylases (also known as amylolytic enzymes) and these glycoside hydrolases (GHs) are commonly found in plants, animals and microbes (bacteria and fungi). The amylases from bacteria and fungi have been widely used for industrial applications such as textile, brewing, and bioethanol production, where starch is used as a raw material (Gangadharan, et al., 2009). In cereal grains, the triticale has high levels of auto-amylolytic enzymes (Pejin, et al., 2009) whereas barley, wheat, rye and rice have very low levels of α-amylases that are commonly inactive. However, the amylase activity of the above grains is rapidly increased during the germination process (Hizukuri, et al., 2006). The amylases can be further classified into α-amylases (GH family 13), β-amylases (GH family 14), glucoamylases (GH family 15) and debranching enzymes, depending on the configuration of the substrate involved or products formed (Goesaert, et al., 2009; Hizukuri, et al., 2006). In addition, the amylases have two major classes, endo- and exo-acting enzymes, according to their mode of action on substrates. Figure 2.8 clearly illustrates the types and classes of different amylases involved in the degradation of starch molecules (ex: amylopectin).

Conventional type α-amylases (EC 3.2.1.1) are endo-acting enzymes that hydrolyses α-D-(1,4)-glycosidic linkages randomly, but internally yielding soluble products such as oligosaccharides, and branched and low molecular weight

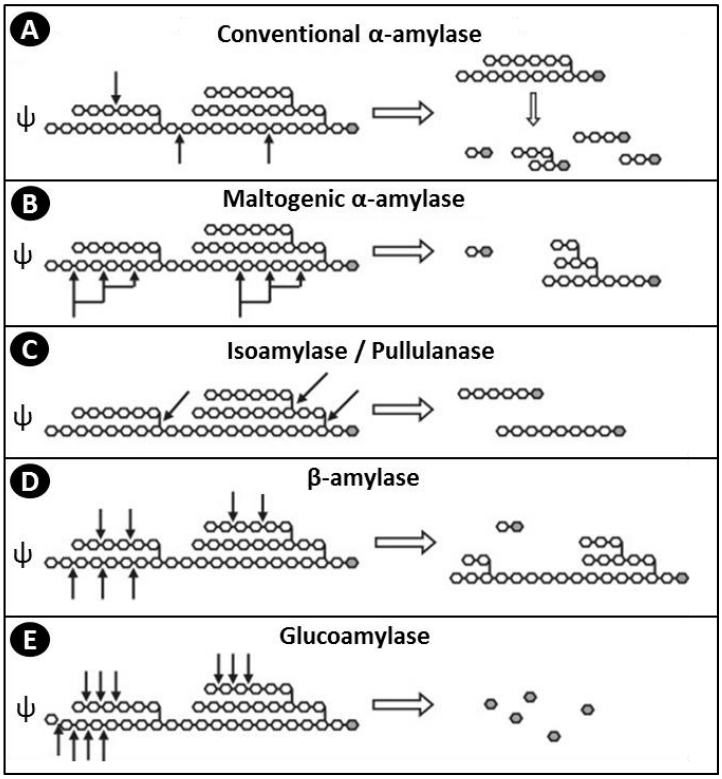

Figure 2.8: Representation of the action of different amylolytic enzymes on starch polymers (amylopectin). Ψ-indicates the side, where the non-reducing ends are present in an amylopectin molecule and the gray ring structure represents a glucose residue, which has the reducing end. Adapted and modified from Goesaert, et al. (2009) with permission of Elsevier Ltd.

α-limit dextrins (Figure 2.8A). However, the maltogenic α-amylases (EC 3.2.1.133) have an exo-action, which hydrolyze the α-D-(1,4)-glycosidic linkages from the non-reducing end resulting in the production of mainly α-maltose molecules (Figure 2.8B). Isoamylase (EC 3.2.1.68) and pullulanase (EC 3.2.1.41) are debranching enzymes which hydrolyses only the α-D-(1,6)-glycosidic bonds to form the linear short chains of glucan polymers (Figure 2.8C). As shown in Figure 2.8D, the β-amylases (EC 3.2.1.2) are exo-acting enzymes which hydrolyses the α-(1,4)-linkages beginning from the non-reducing ends of starch

molecules to form β-maltose and β-limit dextrins. However, β-amylase action stops at branch point since it cannot hydrolyze or bypass the α-(1,6)-linkage. Glucoamylase or amyloglucosidase (EC 3.2.1.3) typically has exo-acting hydrolysis pattern on starch polymers from their non-reducing end towards reducing end and it depolymerize both α-(1,4)- and α-(1,6)-linkages to completely convert the starch molecules into glucose monomers (Figure 2.8E). It has been reported that the glucoamylase can hydrolyze α-(1,4)-glycosidic linkage ≈20 times faster than the α-(1,6)-branch points (Goesaert, et al., 2010; Hizukuri, et al., 2006; Murthy, et al., 2011).

2.2.1. Factors affecting the native starch amylolysis

Several unit operations are carried out in converting the complex native starch granules into simple forms (ex: mono- and di-saccharides) for various food and industrial applications. For instance, the processing operations such as gelatinization (cooking) or modification convert the starch granules from their semicrystalline state to amorphous form resulting in highly susceptible to hydrolysis by amylases (Tester, et al., 2006). However, the native starch granules resist hydrolysis or exhibit a slow hydrolysis to amylolytic enzymes due to their highly ordered and complex semicrystalline structure, and inability to soluble in water. Studies on hydrolysis of native starches have shown that the amylases can hydrolyze starch granules, but the degree of hydrolysis mainly depends on the type of starch and type amylase used for hydrolysis (Robyt, 2009).

Native starch hydrolysis by amylases occurs in several steps, which include diffusion to the solid surface, adsorption, and finally catalysis; the rate of hydrolysis is initially fast, but continues at a slower and more persistent rate (Oates, 1997). In general, the amylases hydrolyze starch granules in two ways: 1) exocorrosion (erosion of the entire granule surface or sections of it resulting in fissures and pits), and 2) endocorrosion (hydrolysis of the channels from selected points on the surface towards the center of granule resulting in granule fragmentation) (Oates, 1997; Sujka & Jamroz, 2007; Sujka & Jamroz, 2009). For example, the lenticular starch granules from wheat, barley, rye, and triticale exhibit an endocorrosion pattern, whereas normal corn starch shows an exocorrosion pattern of hydrolysis. The hydrolysis of native starch granules can also be described as a series of reactions (Tester, et al., 2006). Firstly, the amylases randomly diffuse on the granule surface to certain points. Secondly, the hydrolysis initiates from these points and continues radially (centripetal pattern) causing the formation of pores. Thirdly, the pores continue as channels towards the granule core. Finally, the enzymes that are trapped within the granule cause hydrolysis further towards granule surface (centrifugal pattern). In general, the cereal starches such as corn, rice, and wheat have shown to be hydrolyzed by means of both centrifugal and centripetal patterns (Tester, et al., 2006).

Several factors have been reported that influence the native starch hydrolysis. The size and shape of the starch granules are among them, and they

widely vary with plant origin and genotypes. When compared to large granules, the small granules of starches hydrolyzed faster due to their higher surface area to volume ratio for better reaction by amylases (Dhital, et al., 2010; Stevnebø, et al., 2006; Tester, et al., 2006). The shape of the granules likely affects the surface area to volume ratio, thereby potentially influencing the hydrolysis (Tester, et al., 2006). The AM to AP ratio is another intrinsic factor that affects the hydrolysis of starches. The AM content inversely affects the degree of hydrolysis of native starches (Sharma, et al., 2007; Tester, et al., 2006). Starch associated minor components such as protein, lipids, and phosphorus also influence the enzyme adsorption and hydrolysis of starch. The proteins and phospholipids that found on surface or in channels of the granules can reduce the accessibility of enzymes by blocking the adsorption sites, thereby inversely influencing the hydrolysis (Oates, 1997; Svihus, et al., 2005). The starch associated protein content proportionally increase with the surface area of the starch granules; the proteins on the granule surface are in a size ranging from 5 to 60 kDa while internally associated proteins mainly range from 60 to 150 kDa (Baldwin, 2001). Starch lipids can also exist in the form of amylose-lipid complexes. Several amylose-lipid complexes pack to form the amylose-lipid crystals (V-type crystallites). The AM molecules in V-type crystallites are much less readily accessible to amylases because of two reasons: 1) the contact between enzyme active site and AM is reduced, and 2) the water molecules, important for the hydrolysis reaction, are hindered by the hydrophobicity of lipids. However, the amylose in a complex is

not completely resistant to enzymes (Oates, 1997; Svihus, et al., 2005; Tester, et al., 2006; Vasanthan & Bhatty, 1996). The phosphorus in starches is present in three forms: 1) phosphate monoesters, 2) phospholipids, and 3) inorganic phosphates. Among them, the phospholipids in the form of lysophospholipid (LPL) highly present in *Triticeae* (ex: wheat and triticale) starches (Svihus, et al., 2005; Tester, et al., 2006). Phosphorus is believed to hinder the hydrolysis by either making new bonds with starch molecules, which are resistant to conventional amylases, or blocking the active sites of starch for amylase reactions when it is associated with phospholipids. A number of non-starch components such as fiber (soluble and insoluble), storage protein, phenolics and phytic acid can also influence the hydrolysis of starch by amylases.

As discussed in previous section, granule architecture predominantly influences the native starch hydrolysis. The structural features on the granule surface such as pores, channels, and equatorial groove are assumed to have direct effect on hydrolysis by providing the number of active adsorption sites for enzymes (Oates, 1997; Tester, et al., 2006). Furthermore, the amount of double helices, and type and distribution of crystallites present in native granules significantly influence the rate and extent of hydrolysis. Interestingly, the normal genotypes of cereals which have highly ordered A-type crystallites are hydrolyzed more rapidly by α-amylases than the high-amylose genotypes of cereals or tuber starches which have less compactly packed B-type crystallites (Planchot, et al., 1997; Tester, et al., 2006). Although the amorphous regions are

composed of AM molecules or branch points of AP, they are not readily hydrolyzed by amylases; in contrast, they may influence the hydrolysis of starches at their later stage (Tester, et al., 2006). In addition, the molecular structural features of AM and AP influence the starch hydrolysis. The molecular characteristics of AP such as molar mass (molecular weight), molecular dimension or size (radius of gyration), molecular density, branching degree, and distribution of short-chains have been shown to influence the hydrolysis of starches by amylases (Goesaert, et al., 2010; Miao, et al., 2011; Murthy, et al., 2011). A higher number of short-chains with a greater degree of branching resulting in more compact structure (high molecular density), high molar mass and small molecular size of AP molecule. The AP molecule with the above characteristics potentially shows less hydrolysis by amylases. Besides, the source of amylases, concentrations of enzyme and substrate (solid content), and conditions for enzyme reaction during hydrolysis such as temperature, pH and duration or time are some other factors that could influence the hydrolysis of native starches.

2.2.2. Gelatinization and retrogradation of native starches

Native starch granules are relatively resistant to penetration by both water and hydrolytic enzymes at room temperature, due to the formation of hydrogen bonds within the same molecule and between neighboring molecules (Power, 2003). However, these granules undergo an order-disorder phase transition phenomenon when heated over a critical temperature range in the presence of

excess water, called gelatinization. A drawing to show the steps in gelatinization process of starches is presented in Figure 2.9 (I-IIB). In the presence of water and elevated temperature, the above phase transition is associated with the diffusion of water into the granule, rupture of hydrogen bonds within the granule, hydration, and radial swelling in the amorphous regions of the granules. During gelatinization, some other physical changes also occur in starch granules such as loss of crystallinity, loss of optical birefringence, uncoiling and dissociation of double helices (in the crystalline regions), decreased relaxation time of water molecules, and amylose leaching resulting in a highly viscous solution with gelatinous consistency (Hoover & Sosulski, 1991; Oates, 1997; Ratnayake, et al., 2002). Gelatinization increases the reactivity of starch for chemicals and amylolytic enzymes, since the highly ordered compact granule structure of native starch no longer exists. As a result, the starches or starch sources are cooked in manufacturing of starch syrups (ex: high glucose and high fructose syrups) and in bioethanol production, where complete conversion of starch into sugars by amylolytic enzymes is important.

Differential scanning calorimetry (DSC) has been widely used to study the gelatinization parameters of starches and it measures the gelatinization transition temperatures: onset (T_o), mid-point or peak (T_p), conclusion or end (T_c) and gives a path to study the effect of water content on gelatinization temperature (Hoover & Sosulski, 1991; Ratnayake, et al., 2002). In fact, the gelatinization transition temperatures are the temperatures at which the melting

of starch crystals or crystallites occurs, thereby reflecting the perfection of starch crystallites (Liu, 2005). T_o is the temperature at which weaker starch crystals melt whereas T_c is temperature at which stronger crystals melt. The enthalpy of gelatinization (ΔH) measures the amount of energy required to melt the starch crystals within starch granules. The gelatinization and swelling properties of starches depend on molecular structure of AP (unit chain length, branching degree, molecular weight, and polydispersity), starch composition (amylose/amylopectin ratio, AM-lipid complex and phosphorus content), and granule architecture (crystalline/amorphous ratio) (Hoover & Ratnayake, 2002; Ratnayake, et al., 2002).

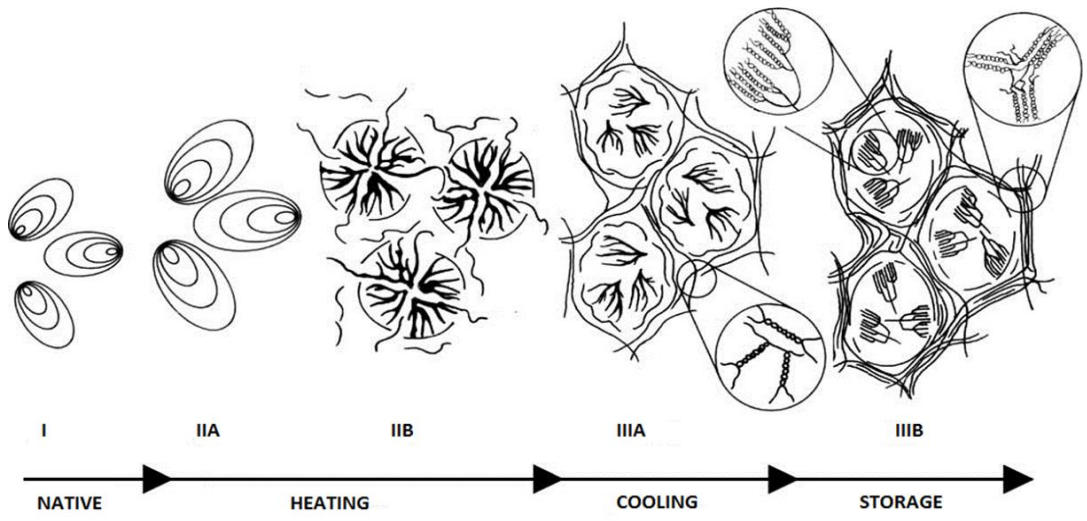

Figure 2.9: Representation of changes that occur in starch–water mixture during heating, cooling, and storage: (**I**) Native starch granules; (**IIA**) swelling of granules and (**IIB**) amylose leaching and partial granule disruption, resulting in the formation of a starch paste; (**IIIA**) formation of an amylose network (amylose retrogradation) during cooling of the starch paste and (**IIIB**) formation of ordered or crystalline amylopectin molecules (amylopectin retrogradation) during storage. **I – IIB** represent the gelatinization process, and **IIIA – B** represent the retrogradation process. (Adapted and modified from Goesaert, et al., 2005, with permission of Elsevier Ltd.)

Starch granules when heated in excess water above their gelatinization temperature undergo irreversible swelling, resulting in amylose leaching into the solution. In the presence of sufficient starch concentration, this suspension will form an elastic gel upon cooling. The molecular interactions between AM–AM, AM–AP or AP–AP (mainly hydrogen bonding between the –OH groups of the starch chains) that occur during cooling are referred to as retrogradation. Figure 2.9 (IIIA and IIIB) illustrates the steps associated with the retrogradation process of gelatinized starch. The interactions in retrogradation process are found to be time and temperature dependent (Ratnayake, et al., 2002). Starch retrogradation is influenced by the botanical source, the fine structure of amylopectin (ex: chain length and distribution), amylose:amylopectin content ratio, and molecular size and size distribution of starch (Liu, 2005). During retrogradation, AM forms double-helical associations of 40–70 glucose units long, whereas AP crystallization occurs by association of the outermost short branches (DP 14–17) (Hoover & Sosulski, 1991). Although the retrograded starch contains both crystalline and amorphous regions (Ratnayake, et al., 2002), it is highly resistant to amylase hydrolysis. It has been reported that the amylases hydrolyze the glycosidic bonds located in the amorphous regions of the retrograded starches, leaving the crystalline double helical regions intact (Robyt, 2009). However, because the starch retrogradation is a kinetically controlled process, the alteration of time, temperature and water content during processing can produce a variety of products (Liu, 2005).

2.2.3. Importance of starch hydrolysis in food and industrial applications

2.2.3.1. Food applications

In the preparation of several food products, the cereal groats (grains without hull) are either milled into flours to make breads, pizzas and other baked products or flaked, rolled, and puffed to make variety of ready-to-eat snacks and breakfast cereals. The food processing unit-operations such as baking, cooking, extrusion, drum drying, and heating convert the native intact starch granules into highly digestible form through the gelatinization process. However, the type of cereal (ex: wheat vs. corn), form of raw materials (groats or flour), structure of starch granules within a source and their resistance to processing steps primarily influence the end-use applications of native starches in cereals.

With respect to starch digestion, some starches are not completely digested and absorbed in the small intestine by pancreatic amylases; instead, they are fermented in the colon or hindgut by anaerobic bacteria to producing certain short-chain fatty acids (SCFA) such as acetic, propionic and butyric acids. These SCFA maintain the health of colon by stimulating colonic blood flow and fluid, and electrolyte uptake (Mason, 2009). The starches that resist digestion are called resistant starches (RS) and their physiological functions are similar to dietary fiber. Fermentation of RS mainly produces butyrate than the other types of SCFA. Resistant starches (RS) have been classified into five major types: 1) RS1, physically entrapped starch granules within the protein matrix and cell walls of endosperm or cotyledon cells in which the amylases find difficulty to bypass

such barriers (ex: whole grain cereal flour), however, fine grinding of flour may remove the effect of RS1, 2) RS2, a higher crystallinity of un-swollen starch granules protects them from amylases (ex: green banana and high-amylose corn), therefore cooking of starches may remove the effect of RS2, 3) RS3, gelatinized and retrograded starches in which intentionally formed AM-AM crystals are completely amylase-resistant like dietary fiber, 4) RS4, starches chemically modified (ex: cross-linking or substitution) to improve the functional properties, where the newly formed chemical bonds are resistant to amylase, thus partially digestible, and 5) RS5, starch or amylose-lipid complex formed during heating or cooking of starchy foods in the presence of fats or lipids, and this complex resists enzymatic digestion (Liu, 2005; Mason, 2009).

Resistant starches can be used as a functional food ingredient for making variety of food products, since they have been shown to be associated with certain physiological impacts on human health similar to conventional dietary fibers. The important physiological effects of RS are: 1) decreasing dietary calorie values for body fat deposition result in preventing obesity, 2) lowering glycemic index which is important for diabetic patients, 3) reducing blood cholesterol levels to prevent and control cardiovascular diseases, and 4) decreasing the risk of colon cancer through enhancing short-chain (butyrate) fatty acid production (Liu, 2005). Thereby, a better understanding of relationship between starch structure (in particular morphology and molecular structure) and amylolysis is essential in formulating a variety of food products.

2.2.3.2. Industrial applications

The complete amylolysis of starch to sugars is essential for an industrial application, for example, bioethanol production where the sugars are fermented into ethanol by yeasts. Ethanol is a renewable source of energy when it is produced from a biological material (ex: grains), and it offers social and economic benefits when compared to petroleum-based fuels. Cereal grains are one of the raw materials used for ethanol production, where corn and wheat are used more commonly than barley, rye, and triticale (das Neves, et al., 2007; Sanchez & Cardona, 2008). Technically, bioethanol production from grain or flour mainly includes starch amylolysis and fermentation. Starch amylolysis comprises two enzymatic processes: 1) the dextrinization or liquefaction, which is a conversion of concentrated starch suspension into a low-viscosity solution by α-amylases, and 2) saccharification where liquefied starch or soluble dextrin is converted mainly into D-glucose monomers by glucoamylases (Gangadharan, et al., 2009; Power, 2003). The following sections discuss in detail about the production of bioethanol from cereal grains.

2.3. BIOETHANOL PRODUCTION

2.3.1. Ethanol around the world

The current automobile industries are considering certain factors such as environmental concerns (zero or very low emissions), increasing cost of fossil fuel, and health, safety and choice of consumers in designing the vehicles for

transportation (Rosillo-Calle & Walter, 2006). Designing a vehicle that can run with biofuels (bioethanol, biodiesel, pyrolysis oils, gasification fuels and various other alcohol-based fuels) has the potential to solve the aforementioned considerations of automobile industries. For example, flexible-fuel vehicles manufactured to use both biofuel and petroleum-based fuels. Of all biofuels, bioethanol is the most utilized liquid biofuel either as a fuel or as a gasoline extender or additive. When compared to gasoline, fuel ethanol offers many advantages: 1) higher octane number (109) than gasoline (98), 2) less evaporative emissions due to its lower vapor pressure (16 KPa) than gasoline (71 KPa), 3) less chances for vehicle to catch fire due to its low flammability in air (1.3–7.6%, v/v) than gasoline (3.5–19%, v/v) (Balat, 2009; das Neves, et al., 2007). In addition, according to Natural Resources of Canada (2011), about 35% reduction in greenhouse gas (GHG) emissions is possible when we use corn-based ethanol (85% ethanol) instead of gasoline under typical Canadian conditions. However, it cannot be concluded that ethanol is a complete fuel like gasoline. Its drawbacks over gasoline include lower energy density, lower flame luminosity, corrosiveness, miscibility in water, toxicity to ecosystems as well as its lower vapor pressure making the cold-start problem particularly during wintertime in Canada (Balat, 2009; das Neves, et al., 2007). In Canada, there are two grades of fuel ethanol available such as E10 (5–10% ethanol by volume with gasoline) and E85 (85% ethanol by volume with gasoline), however, utilization of E85 to publics' vehicle is limited (Natural Resources Canada, 2011). According to

Baier et al. (2009), about 67.5 billion liters of ethanol were produced worldwide in 2008, particularly in USA (36 billion liters) and Brazil (22 billion liters), and the production is yet steadily increasing (Figure 2.10). It is estimated that about 120 billion liters of ethanol will be produced in 2017 (Figure 2.10).

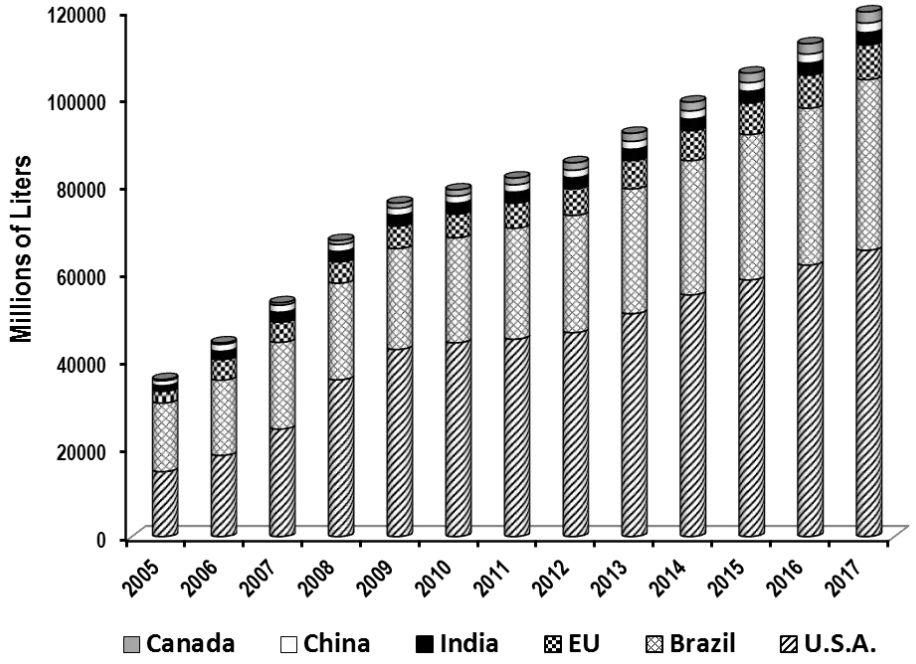

Figure 2.10: World ethanol producing countries and their production in millions of liters (Source: Baier, et al., 2009)

There are primarily two groups of energy sources such as sugar based crops (ex: sugarcane) and starch rich cereal grains (ex: corn) used globally in the production of ethanol. As shown in Figure 2.11 (Berg, 2012), USA (mainly from corn grains) and Brazil (solely from sugarcane) were world leading ethanol producers in 1993. In 20 years, several other countries have been gradually joined in the list, yet

USA and Brazil are still leading in the production. As a result, bioethanol from different sources is anticipated to be one of the dominating renewable biofuels (or may substitute up to 10–20% of gasoline) in the transport sector in few years (das Neves, et al., 2007; Rosillo-Calle & Walter, 2006).

In Canada, wheat grains are the main raw material used for fuel ethanol production, particularly in Western Canada. A higher price of wheat and less availability of corn necessitated Western Canada to find alternative feedstock for ethanol production that are less expensive, but comparable to wheat and corn (Wang, et al., 1997). Regardless of certain technical challenges, barley, oat, triticale and rye grains have been shown to be a potential feedstock for fuel ethanol production comparable to wheat and corn (Gibreel, et al., 2009; Pejin, et al., 2009; Wang, et al., 1997). However, there are some basic aspects that have to be considered in selecting a grain for industrial energy use such as: 1) grain yield and price competitiveness with other grains, 2) plump kernels with a low percentage thins, 3) high starch content and high conversion rates to ethanol, 4) a market for co-products, 5) regularized grain supply chain, and 6) sufficient tax or other incentives for ethanol to be competitive with gasoline in the fuel market (Alberta Agriculture and Rural Development, 2006). Triticale grains have many agronomical (ex: higher grain yield), biological (ex: resistance to pest and diseases), and economical (ex: rich in autoamylolytic enzymes and low price of grains) advantages for utilizing as a feedstock for ethanol production in Canada (Pejin, et al., 2009; Wang, et al., 1997).

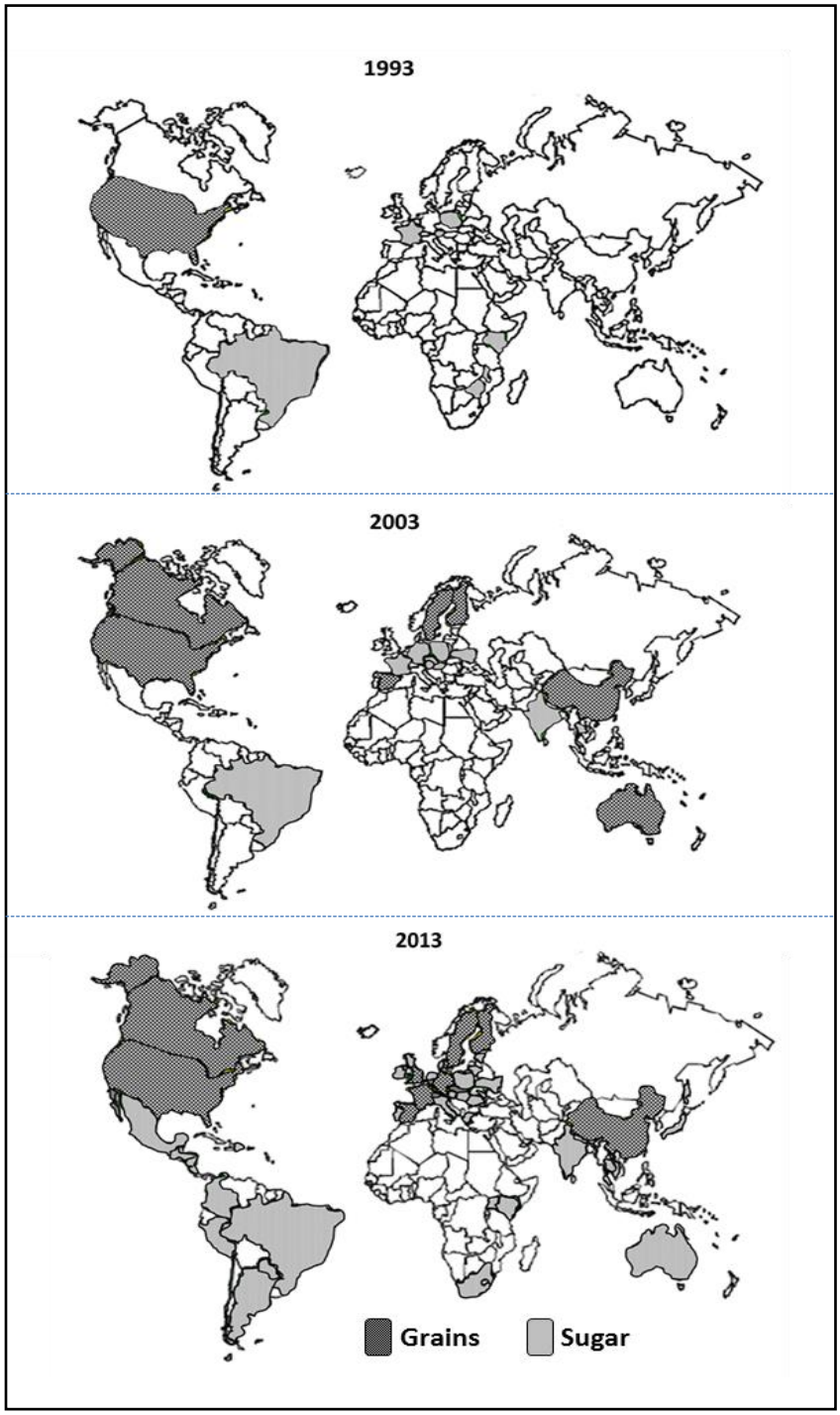

Figure 2.11: Distribution of energy-crops based bioethanol-producing countries from 1993 to 2013. (Source: Berg, 2012)

2.3.2. Current technologies in bioethanol production

Bioethanol from agricultural crops has been produced since the 1800s, with the ethanol from this production technique is referred to as first generation (1G) bioethanol. In contrast, utilization of energy crops for fuel production could create food scarcity in the near future, so that the world must find alternatives for bioethanol production. As a result, second (2G) and third (3G) generations of biofuel productions have emerged. In the 2G technique, bioethanol is produced from a feedstock (biomass) not directly used for food purposes. There are six groups of lignocellulosic biomasses that can be used for bioethanol production such as: 1) crop residues (cane bagasse, corn stover, wheat straw, rice straw, rice hulls, etc.), 2) hardwood (aspen, poplar, etc.), 3) softwood (pine, spruce, etc.), 4) cellulose wastes (newsprint, waste office papers, recycled papers, etc.), 5) herbaceous biomass (alfalfa hay, switch grass, thimothy grass, etc.) and 6) municipal solid wastes (Sanchez & Cardona, 2008). Cellulose is the polysaccharide of glucose monomers, which is structurally protected by hemicellulose and lignin in the lignocellulosic biomass. Thereby, the conversion of such non-starch polysaccharide into sugars for yeast fermentation is not as easy as starch to sugar conversion. There are several pre-treatments such as chemical (ex: acid), physical (ex: steam explosion) and biological (ex: enzymes of microbes) that need to be performed to break the biomass complex in order to access the cellulose for 2G bioethanol production; thus, it has more challenges than the 1G technique.

To be more sustainable than the 1G bioethanol concerning the competition between food and fuel, and to be less challenging than 2G bioethanol regarding the conversion of cellulose in the complex biomass to sugars, third generation (3G) bioethanol production emerged using algae and seaweeds as feedstock (Choi, et al., 2010; Goh & Lee, 2010). Algae and seaweed are naturally grown in marine sources and in nutrient poor land without having much attention in their cultivation. They are good source of fermentable sugars in the form of starch and non-starch polysaccharides such as cellulose and carrageenan, and the conversion process of such polysaccharides into ethanol is also easier than the process in 2G bioethanol (Choi, et al., 2010; Goh & Lee, 2010). However, more investigations on 3G bioethanol require optimizing the conversion of galactose to glucose for yeast fermentation, since carrageenan is composed of galactose and most of the yeast strains cannot directly ferment the galactose.

2.3.3. Starch based bioethanol production processes

North American distilleries are predominantly using starch-based feedstock (corn and wheat grains) for bioethanol production. There are two types of milling processes such as dry-milling (DM) and wet-milling (WM) currently practiced in North America for ethanol production from grains (das Neves, et al., 2007; Naik, et al., 2010; Rosillo-Calle & Walter, 2006; Sanchez & Cardona, 2008). Figure 2.12 shows the key differences between DM and WM processes. The DM process uses dry-ground grain flour whereas WM process needs whole grains. With respect to products, DM will have two co-products, ethanol and dried distillers'

grains with solubles (DDGS). As DDGS are composed of residual starch (mostly escaped from the enzyme actions, thus resistant starch), soluble and insoluble protein, soluble and insoluble fiber, lipids, organic acids, yeast biomass, soluble sugars, fermentation by-products and other minor components, they are commonly used as animal feed (Reed, 2012). On the other hand, in WM process, the insoluble protein, oil in germ, fiber, and some solids that separated initially as co-products and only the starch slurry pumped out to the ethanol production line. Regardless of processes, the starch in flour or slurry is enzymatically converted into sugars, which are then fermented to ethanol by yeast.

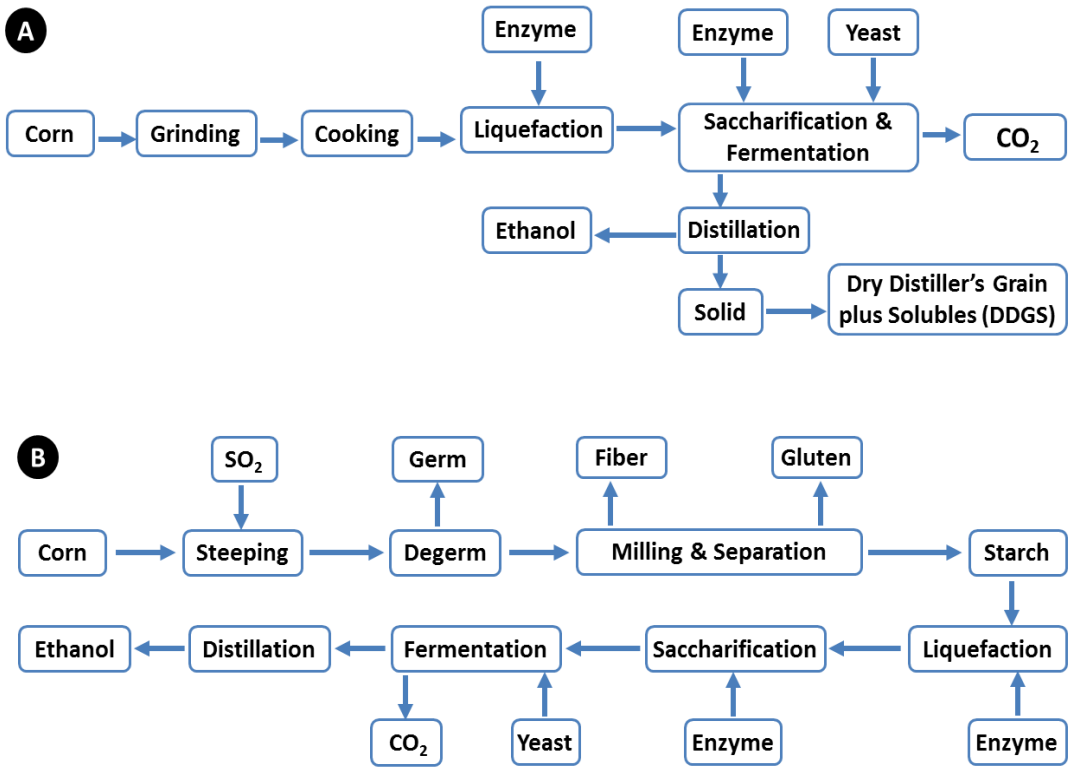

Figure 2.12: Representations of dry-milling (**A**) and wet-milling (**B**) processes involved in bioethanol production. Adapted and modified from Naik, et al. (2010) with permission of Elsevier Ltd.

Yeast (*Saccharomyces cerevisiae*), commonly used in industrial bioethanol production, cannot directly ferment the starch to ethanol since it lacks the amylolytic enzymes to liberate glucose from starch (Power, 2003). Thus, a complete bioconversion of starch to sugars by amylases is important prior to yeast fermentation, and it is generally achieved in two steps such as liquefaction and saccharification. During liquefaction, the insoluble starch is converted to soluble dextrin by α-amylase, and this step can be accompanied with a cooking process (ex: jet cooking) to gelatinize the starch as seen in DM process (Figure 2.12A). As discussed in section 2.1.2, the gelatinization of starch is important to rupture the complex structure of starch granules, thereby making the starch polymers (amylose and amylopectin) readily accessible to the amylolytic enzymes. However, cooking of a starchy feedstock at high temperature prior to liquefaction is an energy intensive process, causing considerable cost to industries (Chen, et al., 2008).

Saccharification is important in ethanol production, because during this step glucoamylase converts the liquefied starch or dextrin into sugars to feed yeast. Depending on the milling process, the abovementioned starch hydrolysis (amylolytic) steps and fermentation are carried out in three distinct configurations, separate hydrolysis and fermentation (SHF) or simultaneous saccharification and fermentation (SSF) or raw-starch hydrolysis and fermentation (RHF).

2.3.3.1. Separate Hydrolysis and Fermentation (SHF)

As illustrated in Figure 2.12B for WM process, the starch hydrolysis and fermentation steps are performed separately in distinct reactors (Balat, 2009; das Neves, et al., 2007). In the first reactor, liquefaction followed by the saccharification processes are performed to hydrolyze the starch completely into sugars. The sugars then transferred to another reactor in which yeast is added for fermentation. A benefit of this configuration is that the starch hydrolysis and sugar fermentation steps are not interacted, making it a more flexible process. In addition, this configuration produces a better ethanol yield than the other types (das Neves, et al., 2007). However, during starch hydrolysis, amylase activity could be inhibited by the accumulation of sugars, thereby reducing the yield of ethanol (Balat, 2009; das Neves, et al., 2007). Furthermore, this conventional type of configuration consumes more time and energy to complete production due to the sequential processes of liquefaction, saccharification, and fermentation (Vinh, 2003).

2.3.3.2. Simultaneous Saccharification and Fermentation (SSF)

The key steps in the SSF configuration are essentially similar to the SHF, except that the saccharification and fermentation steps are combined and performed in one reactor. As shown in Figure 2.12A for DM process, immediately after the liquefaction step, the content is transferred into another reactor where glucoamylase (saccharification enzyme) and yeast are added concurrently. Thus,

the sugars produced by saccharification are simultaneously fermented by yeast. A major benefit of this configuration over SHF is that the presence of yeast along with glucoamylase enzyme in a single reactor reduces the sugar accumulation (Balat, 2009; das Neves, et al., 2007), making a higher conversion rate of starch to ethanol is possible. Furthermore, the presence of ethanol during SSF process makes the reactor safe against the contamination by number of unwanted microbes. Compared to SHF, the SSF technique saves time up to 25% (Vinh, 2003). However, the flexibility of process is reduced particularly in controlling the fermentation, since SSF is performed in a single vessel.

2.3.3.3. Raw-starch Hydrolysis and Fermentation (RHF)

With the development of improved granular starch hydrolyzing enzymes (GSHE), the bioethanol industries are interested in raw-starch hydrolysis and fermentation technique. Compared to traditional process of cooking the starch (at 90-95^{o}C) with (liquefaction) or without thermostable amylase enzymes, the new approach of non-cooking with a comparable ethanol production efficiency is getting more popular (Gibreel, et al., 2009; Gibreel, et al., 2011). Since it is an alternative to high temperature cooking process, this technique also called as the cold-cook process (Reed, 2012). The key difference between this technique and SHF or SSF is the number of unit operations involved. Starch hydrolysis and fermentation can be performed in a single reactor under low temperature (i.e. sub-gelatinization temperature of <58^{o}C) condition. However, a short incubation

time is essential to obtain a certain amount of sugars to boost the activity of yeast before introducing them into the reactor. The GSHE is a mixture of α-amylase and glucoamylase with some other enzymes in a cocktail produced from genetically engineered microorganisms. For example, Stargen 001™ and Stargen 002™ are two common GSHE that have been developed by Genencor International (USA). This company has claimed that many potential advantages are associated with the GSHE for bioethanol production such as improved productivity, lower energy consumption, higher ethanol yield, and savings on capital expenses by reducing the number of unit operations (Genencor International, 2009). Additionally, the DDGS produced from this technique have shown to be rich in good quality protein, sterols, tocopherols, tocotrienols, and fatty acids likely due to low temperature process (Gibreel, et al., 2009; Gibreel, et al., 2011).

However, how effective are these GSHE in converting the native starches into sugars with respect to diverse granular structure of starches, is a big challenge in RHF technique. A clear understanding of the starch structure-function relationship is essential in order to answer the above question. Thus, this thesis was designed to understand the influence of morphology, granule architecture and molecular structure (i.e. structure of amylose and amylopectin) of native starch granules towards amylolysis by using a commercial GSHE at sub-gelatinization temperatures.

REFERENCES

Alberta Agriculture and Rural Development (2006). Triticale grain for other uses. http://www1.agric.gov.ab.ca.login.ezproxy.library.ualberta.ca/$department/deptdocs.nsf/all/fcd10568. Accessed on July 19, 2012.

Ao Z. & Jane J. (2007). Characterization and modeling of the A- and B-granule starches of wheat, triticale, and barley. *Carbohydrate Polymers, 67*, 46-55.

Baier S., Clements M., Griffiths C., & Ihrig J. (2009). Biofuels impact on crop and food prices: using an interactive spreadsheet. *International Finance Discussion Papers, 967*, 1-32.

Balat M. (2009). Bioethanol as a Vehicular Fuel: A Critical Review. *Energy Sources Part A-Recovery Utilization and Environmental Effects, 31*, 1242-1255.

Baldwin P. M. (2001). Starch granule-associated proteins and polypeptides: A review. *Starch-Starke, 53*, 475-503.

Berg C. (2012). World fuel ethanol: Analysis and outlook. http://www.meti.go.jp/report/downloadfiles/g30819b40j.pdf. Accessed on Mar 11, 2012.

Chen J., Wu K., & Fukuda H. (2008). Bioethanol production from uncooked raw starch by immobilized surface-engineered yeast cells. *Applied Biochemistry and Biotechnology, 145*, 59-67.

Choi S. P., Nguyen M. T., & Sim S. J. (2010). Enzymatic pretreatment of Chlamydomonas reinhardtii biomass for ethanol production. *Bioresource Technology, 101*, 5330-5336.

Chung Y. & Lai H. (2006). Molecular and granular characteristics of corn starch modified by HCl-methanol at different temperatures. *Carbohydrate Polymers, 63*, 527-534.

das Neves M. A., Kimura T., Shimizu C., & Nakajima M. (2007). State of the art and future trends of bioethanol production. *Dynamic Biochemistry, Process Biotechnology and Molecular Biology, 1*, 1-14.

Dhital S., Shrestha A. K., & Gidley M. J. (2010). Relationship between granule size and in vitro digestibility of maize and potato starches. *Carbohydrate Polymers, 82*, 480-488.

FAO Statistics Division (2012). http://faostat.fao.org. Accessed on Oct 9, 2012.

French A. D. (1972). Fine structure of starch and its relationship to the organization of the granules. *Journal of Japanese Society Starch Science, 19*, 8-25.

Gallant D. J., Bouchet B., & Baldwin P. M. (1997). Microscopy of starch: Evidence of a new level of granule organization. *Carbohydrate Polymers, 32*, 177-191.

Gangadharan D., Nampoothiri K. M., Sivaramakrishnan S., & Pandey A. (2009). Biochemical Characterization of Raw-starch-digesting Alpha Amylase Purified from Bacillus amyloliquefaciens. *Applied Biochemistry and Biotechnology, 158*, 653-662.

Genencor International (2009). Transforming the ethanol industry. http://www.genencor.com/cms/resources/file/ebf95c076d3afc7/STARGEN%20Backgrounder.pdf. Accessed on Sep 15, 2009.

Gibreel A., Sandercock J. R., Lan J., Goonewardene L. A., Scott A. C., Zijlstra R. T., Curtis J. M., & Bressler D. C. (2011). Evaluation of value-added components of dried distiller's grain with solubles from triticale and wheat. *Bioresource Technology, 102*, 6920-6927.

Gibreel A., Sandercock J. R., Lan J., Goonewardene L. A., Zijlstra R. T., Curtis J. M., & Bressler D. C. (2009). Fermentation of barley by using *Saccharomyces cerevisiae*: Examination of barley as a feedstock for bioethanol production and value-added products. *Applied and Environmental Microbiology, 75*, 1363-1372.

Gilbert R. G., Gidley M. J., Hill S., Kilz P., Rolland-Sabate A., Stevenson D. G., & Cave R. A. (2010). Characterizing the Size and Molecular Weight Distribution of Stach: Why it Is Important and Why it Is Hard. *Cereal Foods World, 55*, 139-143.

Goesaert H., Bijttebier A., & Delcour J. A. (2010). Hydrolysis of amylopectin by amylolytic enzymes: level of inner chain attack as an important analytical differentiation criterion. *Carbohydrate Research, 345*, 397-401.

Goesaert H., Brijs K., Veraverbeke W. S., Courtin C. M., Gebruers K., & Delcour J. A. (2005). Wheat flour constituents: how they impact bread quality, and how to impact their functionality. *Trends in Food Science & Technology, 16*, 12-16.

Goesaert H., Slade L., Levine H., & Delcour J. A. (2009). Amylases and bread firming – an integrated view. *Journal of Cereal Science, 50*, 345-352.

Goh C. S. & Lee K. T. (2010). A visionary and conceptual macroalgae-based third-generation bioethanol (TGB) biorefinery in Sabah, Malaysia as an underlay for renewable and sustainable development. *Renewable & Sustainable Energy Reviews, 14*, 842-848.

Gomand S. V., Lamberts L., Gommes C. J., Visser R. G. F., Delcour J. A., & Goderis B. (2012). Molecular and Morphological Aspects of Annealing-Induced Stabilization of Starch Crystallites. *Biomacromolecules, 13*, 1361-1370.

Gray J. A. & BeMiller J. N. (2004). Development and utilization of reflectance confocal laser scanning microscopy to locate reaction sites in modified starch granules. *Cereal Chemistry, 81*, 278-286.

Han J. & BeMiller J. N. (2008). Effects of protein on crosslinking of normal maize, waxy maize, and potato starches. *Carbohydrate Polymers, 73*, 532-540.

Han X., Benmoussa M., Gray J., BeMiller J., & Hamaker B. (2005). Detection of proteins in starch granule channels. *Cereal Chemistry, 82*, 351-355.

Han X. & Hamaker B. (2002a). Location of starch granule-associated proteins revealed by confocal laser scanning microscopy. *Journal of Cereal Science, 35*, 109-116.

Hizukuri S. (1986). Polymodal Distribution of the Chain Lengths of Amylopectins, and its Significance. *Carbohydrate Research, 147*, 342-347.

Hizukuri, S., Abe, J., & Hanashiro, I. (2006). Starch: Analytical aspects. In A. Eliasson (Ed.). *Carbohydrates in Food* (pp. 305-390). Boca Raton, FL, USA.: CRS Press, Taylor & Francis Group, LLC.

Hoover R. & Ratnayake W. S. (2002). Starch characteristics of black bean, chick pea, lentil, navy bean and pinto bean cultivars grown in Canada. *Food Chemistry, 78*, 489-498.

Hoover R. & Sosulski F. W. (1991). Composition, Structure, Functionality, and Chemical Modification of Legume Starches - a Review. *Canadian Journal of Physiology and Pharmacology, 69*, 79-92.

Huber, A. & Praznik, W. (2004). Analysis of Molecular characteristics of starch polysaccharides. In P. Thomasik (Ed.). *Chemical and Functional Properties of Food Saccharides* (pp. 333-353). Boca Raton, Florida, USA.: CRC Press LLC.

Israkarn K., Hongsprabhas P., & Hongsprabhas P. (2007). Influences of granule-associated proteins on physicochemical properties of mungbean and cassava starches. *Carbohydrate Polymers, 68*, 314-322.

Izydorczyk M. S. & Dexter J. E. (2008). Barley β-glucans and arabinoxylans: Molecular structure, physicochemical properties, and uses in food products–a Review. *Food Research International, 41*, 850-868.

Jane, J. (2009). Structural features of starch granules II. In J. BeMiller & R. Whistler (Eds.). *Starch: Chemistry and Technology* (pp. 193-236). New York, USA.: Academic Press of Elsevier Inc.

Jenkins P. J., Cameron R. E., Donald A. M., Bras W., Derbyshire G. E., Mant G. R., & Ryan A. J. (1994). In-Situ Simultaneous Small and Wide-Angle X-Ray-Scattering - a New Technique to Study Starch Gelatinization. *Journal of Polymer Science Part B-Polymer Physics, 32*, 1579-1583.

Lee S. & BeMiller J. N. (2008). Lysophosphatidylcholine identified as channel-associated phospholipid of maize starch granules. *Cereal Chemistry, 85*, 776-779.

Li J., Vasanthan T., Hoover R., & Rossnagel B. (2003). Starch from hull-less barley: Ultrastructure and distribution of granule-bound proteins. *Cereal Chemistry, 80*, 524-532.

Liu, Q. (2005). Understanding starches and their role in foods. In S. W. Cui (Ed.). *Food Carbohydrates: Chemistry, Physical Properties, and Applications* (pp. 309-355). Boca Raton, FL., USA.: CRC Press, Taylor & Francis Group, LLC.

Manners D. J. & Matheson N. K. (1981). Alpha-(1-]4)-D-Glucans .24. the Fine-Structure of Amylopectin. *Carbohydrate Research, 90*, 99-110.

Mason, W. R. (2009). Starch use in foods. In J. BeMiller & R. Whistler (Eds.). *Starch: Chemistry and Technology* (pp. 745-795). New York, USA.: Academic Press of Elsevier Inc.

Miao M., Zhang T., Mu W., & Jiang B. (2011). Structural characterizations of waxy maize starch residue following in vitro pancreatin and amyloglucosidase synergistic hydrolysis. *Food Hydrocolloids, 25*, 214-220.

Mira I., Villwock V. K., & Persson K. (2007). On the effect of surface active agents and their structure on the temperature-induced changes of normal and waxy wheat starch in aqueous suspension. Part II: A confocal laser scanning microscopy study. *Carbohydrate Polymers, 68*, 637-646.

Murthy G. S., Johnston D. B., Rausch K. D., Tumbleson M. E., & Singh V. (2011). Starch hydrolysis modeling: application to fuel ethanol production. *Bioprocess and Biosystems Engineering, 34*, 879-890.

Naik S. N., Goud V. V., Rout P. K., & Dalai A. K. (2010). Production of first and second generation biofuels: A comprehensive review. *Renewable & Sustainable Energy Reviews, 14*, 578-597.

Natural Resources Canada (2011). Ethanol. http://oee.nrcan.gc.ca.login.ezproxy.library.ualberta.ca/transportation/alternative-fuels/fuel-facts/ethanol/4929. Accessed on Jul 19, 2012.

Oates C. G. (1997). Towards an understanding of starch granule structure and hydrolysis. *Trends in Food Science & Technology, 8*, 375-382.

Pejin D., Mojovic L. J., Vucurovic V., Pejin J., Dencic S., & Rakin M. (2009). Fermentation of wheat and triticale hydrolysates: A comparative study. *Fuel, 88*, 1625-1628.

Planchot V., Colonna P., & Buleon A. (1997). Enzymatic hydrolysis of alpha-glucan crystallites. *Carbohydrate Research, 298*, 319-326.

Power, R. F. (2003). Enzymatic conversion of starch to fermentable sugars. In K. A. Jacques, T. P. Lyons, & D. R. Kelsall (Eds.). *The Alcohol Textbook: A Reference for the Beverage, Fuel and Industrial Alcohol Industries* (pp. 23-32). Nottingham, UK.: Nottingham University Press.

Ratnayake W. S., Hoover R., & Warkentin T. (2002). Pea starch: Composition, structure and properties - A review. *Starch/Stärke, 54*, 217-234.

Reed D. K. (2012). Evaluation of Residual Starch Determination Methods for Dried Distillers' Grains with Solubles (DDGS). MSc Thesis, University of Alberta.

Robin J. P., Mercier C., Charbonn.R, & Guilbot A. (1974). Lintnerized Starches Gel-Filtration and Enzymatic Studies of Insoluble Residues from Prolonged Acid Treatment of Potato Starch. *Cereal Chemistry, 51*, 389-406.

Robyt, J. F. (2009). Enzymes and their action on starch. In J. BeMiller & R. Whistler (Eds.). *Starch: Chemistry and Technology* (pp. 237-292). New York, USA.: Academic Press of Elsevier Inc.

Rolland-Sabate A., Colonna P., Mendez-Montealvo M. G., & Planchot V. (2007). Branching features of amylopectins and glycogen determined by asymmetrical flow field flow fractionation coupled with multiangle laser light scattering. *Biomacromolecules, 8*, 2520-2532.

Rosillo-Calle F. & Walter A. (2006). Global market for bioethanol: historical trends and future prospects. *Energy for Sustainable Development, 10*, 20-32.

Sanchez O. J. & Cardona C. A. (2008). Trends in biotechnological production of fuel ethanol from different feedstocks. *Bioresource Technology, 99*, 5270-5295.

Sharma V., Rausch K. D., Tumbleson M. E., & Singh V. (2007). Comparison between granular starch hydrolyzing enzyme and conventional enzymes for ethanol production from maize starch with different amylose: Amylopectin ratios. *Starch-Starke, 59*, 549-556.

Stevnebø A., Sahlström S., & Svihus B. (2006). Starch structure and degree of starch hydrolysis of small and large starch granules from barley varieties with varying amylose content. *Animal Feed Science and Technology, 130*, 23-38.

Sujka M. & Jamroz J. (2007). Starch granule porosity and its changes by means of amylolysis. *International Agrophysics, 21*, 107-113.

Sujka M. & Jamroz J. (2009). Alpha-amylolysis of native potato and corn starches - SEM, AFM, nitrogen and iodine sorption investigations. *Lwt-Food Science and Technology, 42*, 1219-1224.

Sujka M. & Jamroz J. (2010). Characteristics of pores in native and hydrolyzed starch granules. *Starch-Starke, 62*, 229-235.

Svihus B., Uhlen A. K., & Harstad O. M. (2005). Effect of starch granule structure, associated components and processing on nutritive value of cereal starch: A review. *Animal Feed Science and Technology, 122*, 303-320.

Tester R. F., Karkalas J., & Qi X. (2004). Starch—composition, fine structure and architecture. *Journal of Cereal Science, 39*, 151-165.

Tester R. F., Qi X., & Karkalas J. (2006). Hydrolysis of native starches with amylases. *Animal Feed Science and Technology, 130*, 39-54.

Vasanthan T. & Bhatty R. S. (1996). Physicochemical properties of small- and large-granule starches of waxy, regular, and high-amylose barleys. *Cereal Chemistry, 73*, 199-207.

Vermeylen R., Goderis B., Reynaers H., & Delcour J. (2005). Gelatinisation related structural aspects of small and large wheat starch granules. *Carbohydrate Polymers, 62*, 170-181.

Vinh, N. T. T. (2003). Ethanol production from cassava. In K. A. Jacques, T. P. Lyons, & D. R. Kelsall (Eds.). *The Alcohol Textbook: A Reference for the Beverage, Fuel and Industrial Alcohol Industries* (pp. 59-64). Nottingham, UK.: Nottingham University Press.

Wang S., Thomas K., Ingledew W., Sosulski K., & Sosulski F. (1997). Rye and triticale as feedstock for fuel ethanol production. *Cereal Chemistry, 74*, 621-625.

Wu H., Harold & Sarko A. (1978). The double-helical molecular structure of crystalline a-amylose. *Carbohydrate Research, 61*, 27-40.

CHAPTER 3

Distribution of granule channels, protein and phospholipid in triticale and corn starches as revealed by confocal laser scanning microscopy (CLSM)*

3.1. INTRODUCTION

Triticale (x *Triticosecale* Wittmack) is a hybrid cereal species developed by crossing wheat (*Triticum aestivum*) with rye (*Secale cereale*). Agronomic advantages of triticale such as high grain yield, high test weight, tolerance to climatic and soil-related abiotic stresses, resistance to disease and pest-related biotic stresses, and low input requirements compared to other widely grown cereals (Pejin et al., 2009), have resulted in its adoption in more than 30 countries and a steady increase in world production. Triticale is an economically favorable source of carbohydrate for industrial and energy end-uses since it has several demonstrated industrial attributes. For instance, due to its lower temperature requirement for liquefaction and saccharification, and the presence of high levels of autoamylolytic enzymes (Pejin et al., 2009), it can be efficiently used for bioethanol production (Davis-Knight & Weightman, 2008). However, the available knowledge on the structural characteristics of triticale starch is very limited, even though some of its physicochemical properties have been characterized (Berry et al., 1971; Leon et al., 1998; Palasinski et al., 1987).

* A version of this chapter has been published in *Cereal Chemistry*, 2011, 88(1):87-94. This publication was ranked one of the top 10 articles published in *Cereal Chemistry* journal in 2011. (Adapted with permission of AACC International).

The presence of surface pores, internal channels and central cavities have been reported in corn, wheat, barley, rye, sorghum, and millet starch granules (Fannon et al., 1992; Fannon et al., 1993; Huber & BeMiller, 1997; Kim & Huber, 2008; Li et al., 2003; Sujka & Jamroz, 2007). They appear to facilitate the transfer of chemical reagents and enzymes into the granule matrix (Huber & BeMiller, 2000, 2001; Kim & Huber, 2008; Sujka & Jamroz, 2007). Starches with high pore and channel density show higher susceptibility to enzymes than those with low density (Benmoussa et al., 2006; Fannon et al., 1992).

Protein, lipid, and minerals exist in starch granules as minor components. Starch granule-associated proteins are defined as proteins, which are distinctly different from storage proteins and are bound to the granule surface and/or are integral components within the starch granule (Baldwin, 2001). Surface protein is mainly present on the granule surface as aggregates, whereas the internal protein is deposited within granules as separate monomers (Mu-Forster & Wasserman, 1998). Phosphorus is present in starches in three major forms, starch phosphate monoester, phospholipid, and inorganic phosphate. In most cereal starches, phosphorus is dominantly in the form of phospholipid (Kasemsuwan & Jane, 1996; Lim et al., 1994). Thus, the phosphorus content is an index of phospholipid concentration, and its concentration has been used as a measure of lysophospholipid content by multiplying the phosphorus content by a factor of 16.3 (Morrison, 1988, 1995). Granule-associated protein and lipid on the granule surface and interior have significant and disproportionate impacts on

the surface chemistry and physicochemical properties of starch (ex: swelling, pasting, gelatinization, retrogradation, and enzyme resistance) (Baldwin, 2001; Debet & Gidley, 2006; Lin & Czuchajowska, 1998) as well as on chemical modification reactions (ex: cross-linking) (Han & BeMiller, 2008). However, the localization of starch associated protein and phospholipid have not received much attention in the case of triticale starch.

CLSM, in conjunction with fluorescent staining, is being used as a powerful imaging technique to characterize the morphological and structural features of starch granules. Examples include visualization of granule morphology and microstructure including surface pores, internal channels and the molecular distribution pattern of native and heated starches (Blennow et al., 2003; Chen et al., 2009; Fannon et al., 2003; Glaring et al., 2006; Kim & Huber, 2008; van de Velde et al., 2002), identification of granule-associated protein and lipid and their effect on starch modification (Glaring et al., 2006; Han & BeMiller, 2008; Han et al., 2005; Han & Hamaker, 2002; Israkarn & Hongsprabhas, 2007; Lee & BeMiller, 2008), and localization of chemical reaction sites and reaction patterns (Chung & Lai, 2006; Gray & BeMiller, 2004; Kuo & Lai, 2007; Mira et al., 2007). Among the various fluorophores used, single specific-dye staining has been used to distinguish starch or protein molecules from the background in various cereal, tuber, root, and legume starches, but not in triticale starch. Multiple staining techniques allow the simultaneous visualization of several individual components in complex mixtures (van de Velde et al., 2003). However,

such techniques have not been used for starch structural examination (ex: double staining of starch and non-starch minor components). Aminofluorophore 8-aminopyrene-1,3,6-trisulfonic acid (APTS) is one of the specific dyes that reacts with the reducing-ends of starch molecules (Blennow et al., 2003; Glaring et al., 2006; O'Shea et al., 1998). Fluorescamine is a specific dye for sensitive fluorometric detection of amino acids, peptides, and proteins and has been used to stain starch surface proteins (Bantan-Polak et al., 2001; Hayashi & Seguchi, 2004; Seguchi, 1986). Pro-Q Diamond phosphoprotein stain allows sensitive detection of phosphorylation levels of protein in gels. Recently, Glaring et al. (2006) successfully used this staining technique to detect the presence of phosphate and/or phospholipids within various starch granules.

Considering the value of triticale as an economically viable, industrial cereal grain, along with the demand for new starch derivatives, it is of academic and industrial importance to study the structural and physicochemical aspects of triticale starch relevant to its biorefining applications. The present work was undertaken to: 1) characterize surface pores and internal channels by localization of starch molecules, starch-associated protein and phospholipid within granules of triticale and corn starches using SEM and CLSM in conjunction with fluorescent staining; 2) study the effect of chemical and protease treatments on the concentration of starch-associated protein and phospholipid in order to better understand the relationship among starch structure, non-starch minor components and amylolysis.

3.2. MATERIALS AND METHODS

3.2.1. Materials

The Field Crop Development Centre of Alberta Agriculture, Food, and Rural Development in Lacombe (AB, Canada) supplied samples of two varieties of triticale (x *Triticosecale* cv. Pronghorn and cv. AC Ultima). Triticale grains were ground in a Retsch mill (Model ZM 200, Haan, Germany) using a ring sieve with an aperture size of 0.5 mm. Normal corn starch (Melojel) was provided by National Starch Food Innovation in Bridgewater (NJ, USA). The granular starch hydrolyzing enzyme, Stargen 002 (a mixture of alpha-amylase and glucoamylase, 570 GAU/g), was donated by Genencor International in Rochester (NY, USA). Thermolysin from *Bacillus thermoproteolyticus rokko* (EC 3.4.24.27) was purchased from Sigma-Aldrich, Inc. in St. Louis (MO, USA). All other chemicals and reagents used in this study were of ACS grade.

3.2.2. Starch isolation and purification

Triticale starch was isolated using a dough ball washing technique developed in our laboratory. A detailed starch isolation procedure is presented in appendix. The purified starch had nitrogen and phosphorus contents comparable to those of commercial cereal starches with a starch purity of 97% (dry basis).

3.2.3. Compositional analysis

Moisture content was determined by AACC Method 44-15A (AACC International 2004). The total nitrogen content of starch was determined by the Dumas

combustion method (Rutherford et al., 2008) using a Costech ECS 4010 Elemental Combustion System (Costech Analytical Technologies Inc., Valencia, CA). Total phosphorus was measured with an automated spectrophotometer (SmartChem 200 Discrete Analyzer, Westco Scientific Instruments, Inc. in Brookfield, CT, USA) following EPA Method 365.4 (U.S. Environmental Protection Agency, 1983). Starch content was estimated according to the total starch assay of Megazyme International Ireland Ltd. (Wicklow, Ireland). Apparent amylose content was determined according to the Standard Analytical Methods of the Member Companies of the Corn Refiners Association Inc. (Washington DC., USA).

3.2.4. Scanning electron microscopy (SEM)

Starch samples were mounted on circular aluminum stubs with double-sided sticky tape, coated with gold to a thickness of 12 nm, and examined and photographed in a JEOL Model JSM 6301 FXV scanning electron microscope (JEOL Ltd. in Tokyo, Japan) at an accelerating voltage of 5 kV.

3.2.5. Staining of starch granules with fluorescamine

Starch granules were stained with fluorescamine (Molecular Probes in Eugene, OR, USA) according to the procedure of Bantan-Polak et al., (2001). Starch samples (10 – 20 mg) were stained in 0.3 mL of 0.1% (w/v) fluorescamine in acetonitrile and 0.15 mL of 0.1M borate buffer (pH 8.0) at room temperature for 1h, then centrifuged, and rinsed five times with deionized water to remove excess dye. The stained starch granules were suspended in 0.5 mL of 50% glycerol for CLSM observation.

3.2.6. Double staining of starch granules with APTS and Pro-Q Diamond

A double staining technique was used to label starch molecules and phosphorus-associated molecules within starch granules. Starch molecules were stained with APTS (Molecular Probes in Eugene, OR, USA) according to the method described by Blennow et al. (2003). Phosphorus was stained with Pro-Q Diamond stain (Molecular Probes, Eugene, OR) based on the method of Glaring et al. (2006). Starch samples (10 – 15 mg) were stained in 10 µL of freshly made APTS solution (20 mM APTS in 15% acetic acid) and 10 µL of 1M sodium cyanoborohydride at 30°C for 15h. The APTS-stained starch granules were washed five times with deionized water and then dispersed in 0.5 mL of Pro-Q Diamond solution at room temperature for 1h. After thoroughly washing with deionized water five times, the stained starch granules were finally suspended in 0.5 mL of 50% glycerol for CLSM observation.

3.2.7. Confocal Laser Scanning Microscopy (CLSM)

Stained starch granules in 50% glycerol (10 µL) were dropped into a glass bottom culture dish (MatTek Coporation in Ashland, MA, USA), mixed with 0.1 mL of deionized water, covered with a glass slip, and then visualized under a confocal laser scanning microscope (Zeiss LSM 710, Carl Zeiss MicroImaging GmbH in Jena, Germany) equipped with a x40 1.3 oil objective lens. For fluorescamine-stained samples, the excitation wavelength achieved with a Diode laser was at 405 nm operating at 4% of power capacity and the emission light was detected at an interval wavelength of 406 – 493 nm. For samples stained with APTS and

Pro-Q, the excitation was at 488 nm and 561 nm operating at 1% and 4% of power capacity, respectively, with an emission light interval of 490 – 560 nm. Images of optical sections of starch granules were recorded with ZEN 2009 software (Carl Zeiss MicroImaging GmbH, Jena, Germany).

3.2.8. Chemical and protease treatments of starches

A set of chemical and protease treatments were performed at a starch-solution ratio of 1:2.5 (w/v) with continuous shaking as follows: 1) water washing at 25°C for 0.5h, 2) treatment with 2.0% (w/v) sodium dodecyl sulfate (SDS) solution at 25°C for 2h, 3) treatment with 0.2% SO_2 (w/v) solution (prepared from sodium metabisulfite) at 25°C for 16h, 4) sequential treatment with 2.0% (w/v) SDS solution at 25°C for 2h and then 0.2% SO_2 (w/v) solution at 25°C for 16h, 5) treatment with 0.15% (w/v) thermolysin in 50 mM sodium acetate buffer (pH 7.4) at 40°C for 16h (Han et al., 2005), 6) treatment with 2.0% (w/v) SDS solution at 25°C for 2h followed by digestion with 0.15% (w/v) thermolysin in 50 mM sodium acetate buffer (pH 7.4) at 40°C for 16h, 7) treatment with n-propanol: water (3:1, v/v) at 25°C for 16h (Lee & BeMiller, 2008), 8) treatment with 2.0% (w/v) SDS solution at 25°C for 2h followed by extraction with n-propanol:water (3:1, v/v) at 25°C for 16h. Soon after chemical and/or enzyme treatments, the starch slurry was centrifuged at 1500 x*g* for 10 min and then thoroughly washed with deionized water three times. The starch residue was finally washed with 95% ethanol and dried in a forced air oven at 40°C for 15h.

3.2.9. Statistical analysis

All treatments and analyses were carried out in duplicate. Analysis of variance using the General Linear Model (GLM) procedure and correlation statistics were performed using SAS Statistical Software (V 9.1.2, SAS Institute Inc., Cary, NC, 2004). Multiple comparisons of the means were done using LSD test ($p < 0.05$).

3.3. RESULTS AND DISCUSSION

3.3.1. Granule morphology

Figure 3.1 shows the starch granule morphology as revealed by SEM. Triticale starch granules were round, oval, disk-like or somewhat irregular in shape, and exhibited a bimodal size distribution (Figure 3.1A, B, C & D). Granules of triticale starch ranged in length from 2 to 36 μm, as reported earlier (Jane et al., 1994; Leon et al., 1998). Granule surfaces appeared to be relatively smooth with modest furrows and shallow depressions on some. Under high magnification, oval-shaped pores along equatorial grooves and some aggregates of small pores with the appearance of slit-like cracks were clearly observed on the large granule surfaces of triticale starches. Surface pores were more frequently visible on Pronghorn triticale starch granules (Figure 3.1A & B) than on Ultima triticale starch granules (Figure 3.1C & D), whereas corn starch showed polyhedral shaped granules with numerous large, individual pores on the granule surfaces (Figure 3.1E & F). After starches had been treated with thermolysin, pores were more frequently observed on the granule surfaces (Figure 3.2). The rendering of

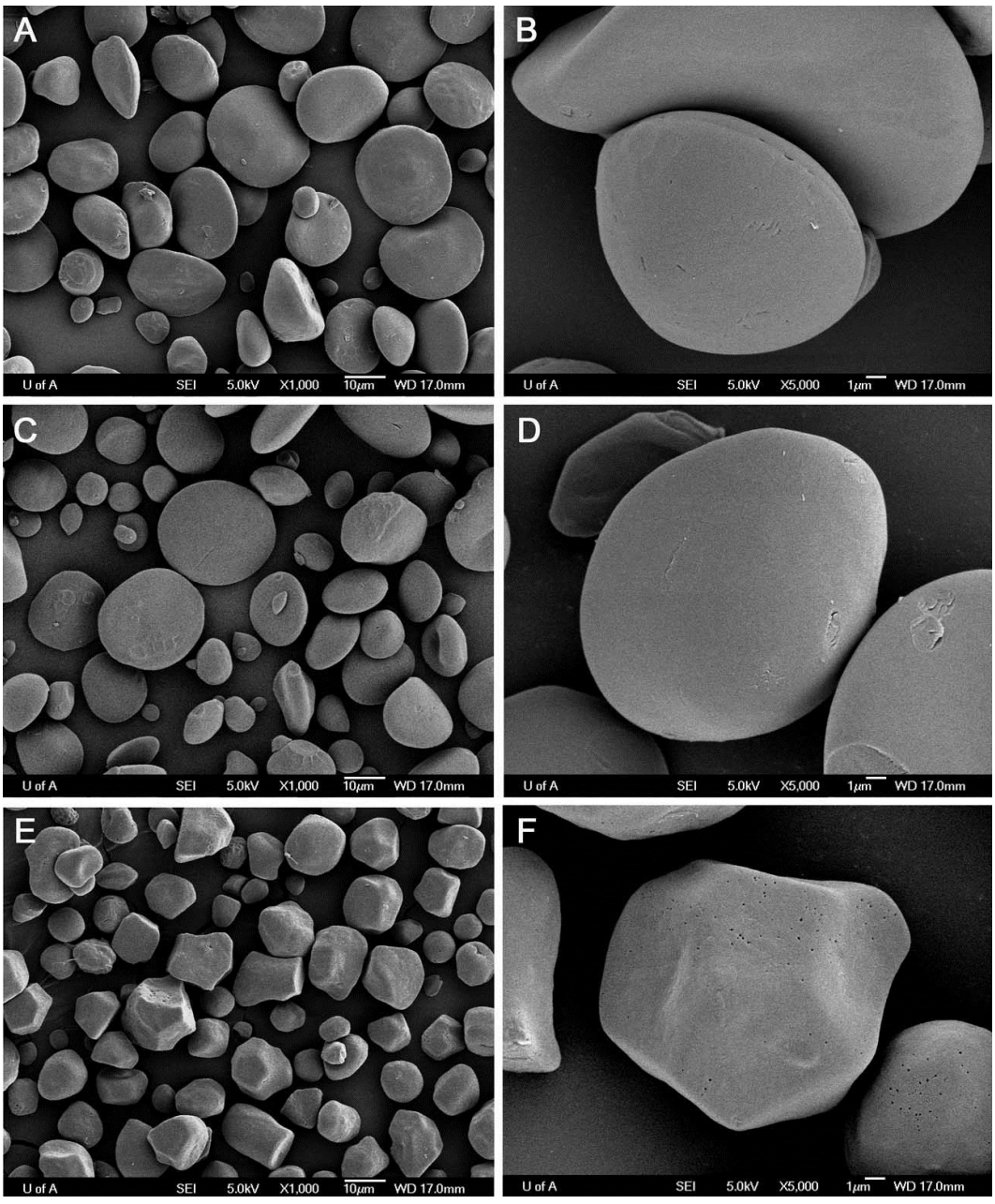

Figure 3.1: Scanning electron micrographs of triticale (A, B: Pronghorn, C, D: Ultima) and corn (E, F) starch granules.

more pores indicated that the protease treatment removed the surface impurities (principally residual endosperm-derived storage protein) that may have been covered to granule surface. This was in agreement with the observation of Kim and Huber (2008), who reported that protease treatment removed both the surface and channel proteins exposing additional surface pores on starch granules from soft wheat. Non-contact atomic force microscopy (Juszczak, 2003) showed the existence of small pores (less than 100 nm in diameter, typically 40 – 50 nm) in addition to large pores (over 100 nm in diameter) on the surfaces of triticale starch granules, which provided evidence that some small pores were not visible under SEM, even at high magnification. Pore characteristics have been correlated to starch pasting parameters (Fortuna et al., 2000) and proven to influence the chemical and enzymatic reactivity of starches (Huber & BeMiller, 2001; Kim & Huber, 2008; Sujka & Jamroz, 2007).

3.3.2. CLSM of starch granules with fluorescamine staining

After staining of starch granules with fluorescamine, the distribution of granule surface and internal protein, along with the granule internal structure, were revealed by CLSM. Though populations of both large and small granules were visualized, our attention was focused mainly on large granules, because they represented the majority of the granule population (weight/volume) of whole starch. In addition, there were some technical limitations in CLSM to focus the small granules with high resolution due to fast fluorescent leaching under high

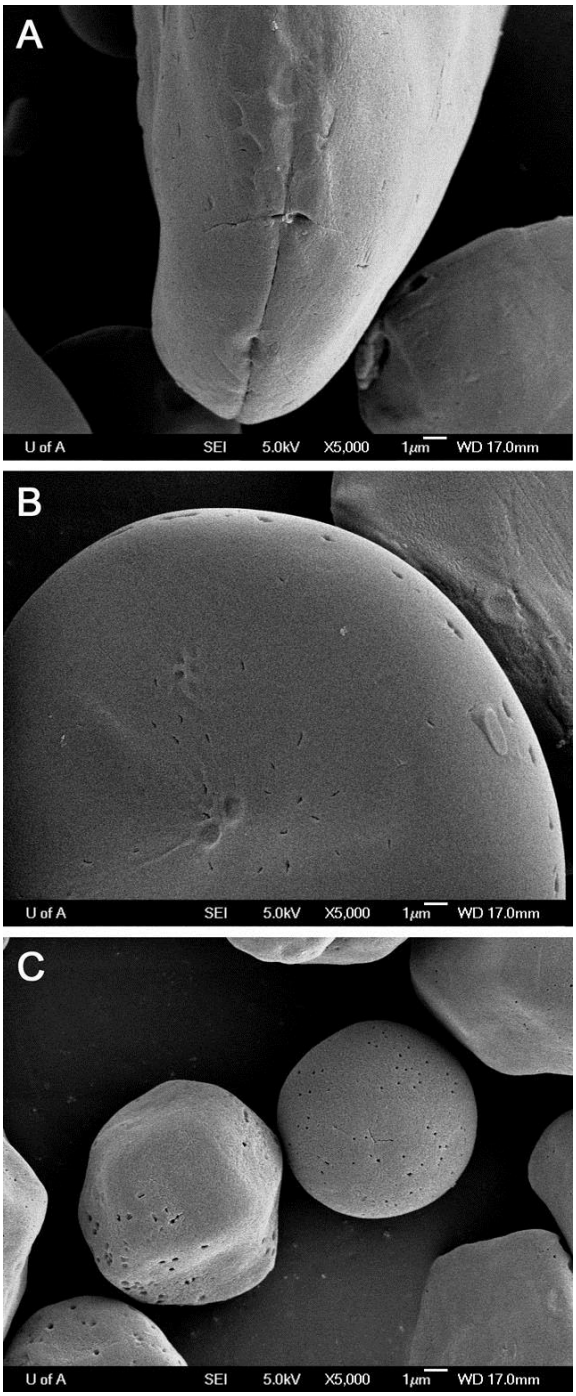

Figure 3.2: Scanning electron micrographs of triticale (A: Pronghorn, B: Ultima) and corn (C) starch granules treated with protease.

magnification and high laser power. As shown in Figure 3.3, the high fluorescent intensity in starch granules by reaction of fluorescamine with primary aliphatic amines (green in color) indicated the presence of protein on the granule surface and in the interior of the granules in triticale (Figure 3.3A, B, C & D) and corn starches (Figure 3.3E & F). In both triticale and corn starches, the surface protein was distributed uniformly in the peripheral layer of the starch granule, forming a thin coating or film with strong fluorescence intensity. Protein aggregates were intermittently observed as bright fluorescent spots on the granule surface, indicating the presence of adsorbed storage protein from the endosperm. Radially distributed channels, filled or rich in protein, extending inward from the surface of the granule were observed frequently in starch from Pronghorn triticale (Figure 3.3A & B), whereas only a few, short channels were observed in starch from Ultima triticale (Figure 3.3C & D). In corn starch, numerous irregularly shaped channels (varying in penetration depth and dimension) were present in a radial orientation, and connected to the central region of the granule (Figure 3.3E & F). A very weak fluorescent intensity in the interior of most granules, compared to that of high intensity on granule surface in triticale starches could indicate that the distribution of protein within granule matrix may not be completely revealed by CLSM under the conditions applied for staining of starches. It may be due to the limited access of the tightly packed peripheral region near to the granule surface that could act as a barrier for processes such as granule hydration, enzyme attack, and reaction with chemical reagents

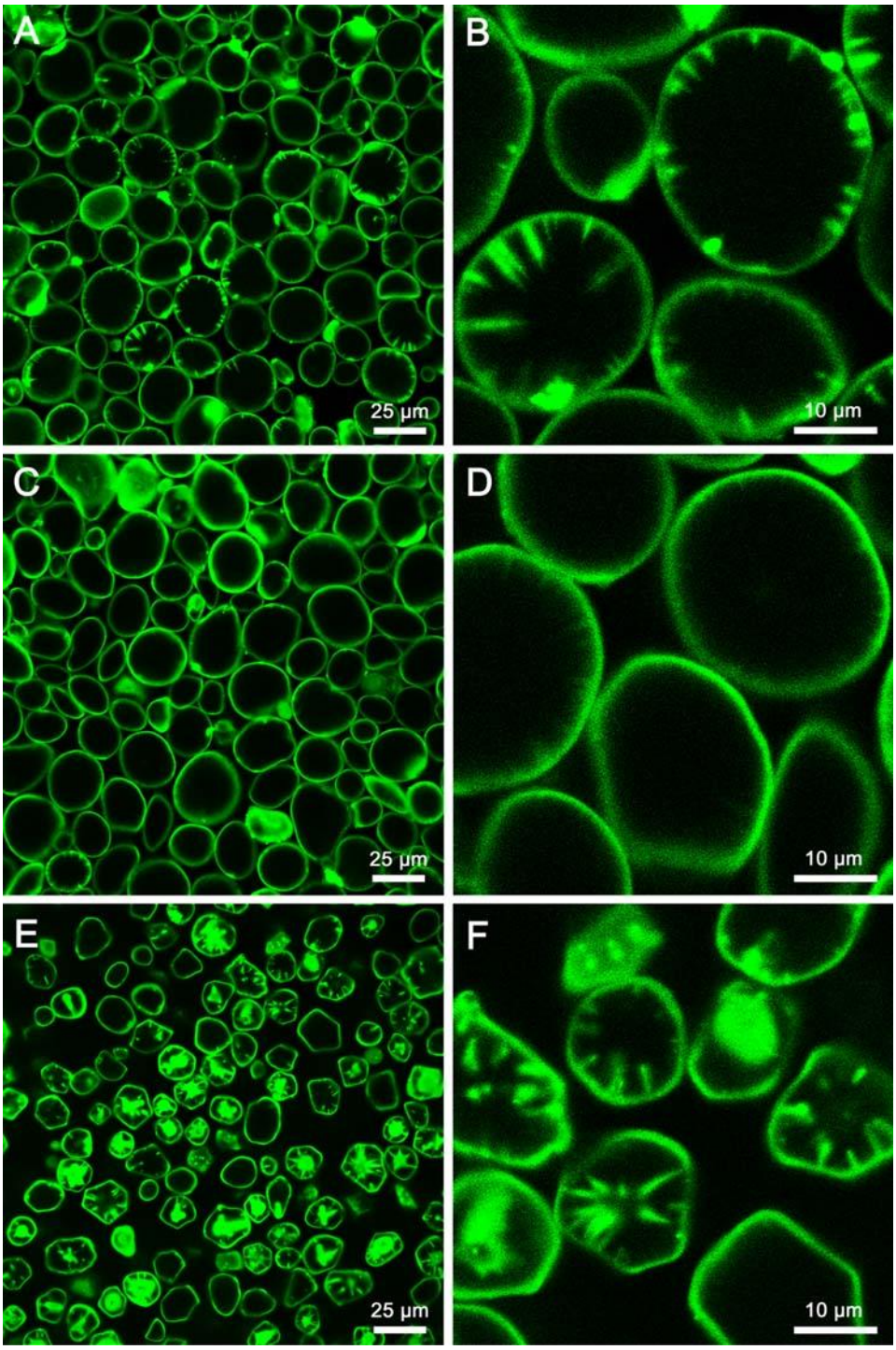

Figure 3.3: Confocal laser scanning micrographs of triticale (A, B: Pronghorn, C, D: Ultima) and corn (E, F) starch granules stained with fluorescamine.

(Baldwin, 2001). Alternatively, it may be due to blocking of the internal channels and the fluorescamine pathway. Thus, some of the chemically and protease treated starches were stained for further CLSM observation.

After the treatments with 2% SDS or 0.2% SO_2, triticale starch granules were stained more extensively to whole granule matrix, though the general fluorescence intensities were greatly reduced due to partial removal of protein (Figure 3.4A, B, C & D). Numerous channels, which extend to the central region of granules, were exposed (Figure 3.4A, B, C & D). The channel arrangement (i.e. orientation, penetration depth and dimension) in triticale starch was similar to that of wheat starch, which was stained with 3-(4-carboxybenzoyl)-quinoline-2-carboxaldehyde (CBQCA, a protein specific stain) and observed by CLSM (Han et al., 2005). As the protein in channels was hydrolyzed by protease, most channels disappeared in stained starch granules (Figure 3.4E & F). These observations indicate that the pathway for flurescamine diffusion, such as internal channels, was unblocked by partial removal of protein and thus facilitated the reaction of flurescamine with the protein in the interior of granules. The results also confirm that small channels, which were filled with or rich in protein, do exist in triticale starch granules. Kim and Huber (2008) reported that small channels originating from granule surface other than the equatorial grooves were present in waxy and normal wheat starches and some hydration/swelling or protease treatment was required for channels to be accessed by fluorescent dye.

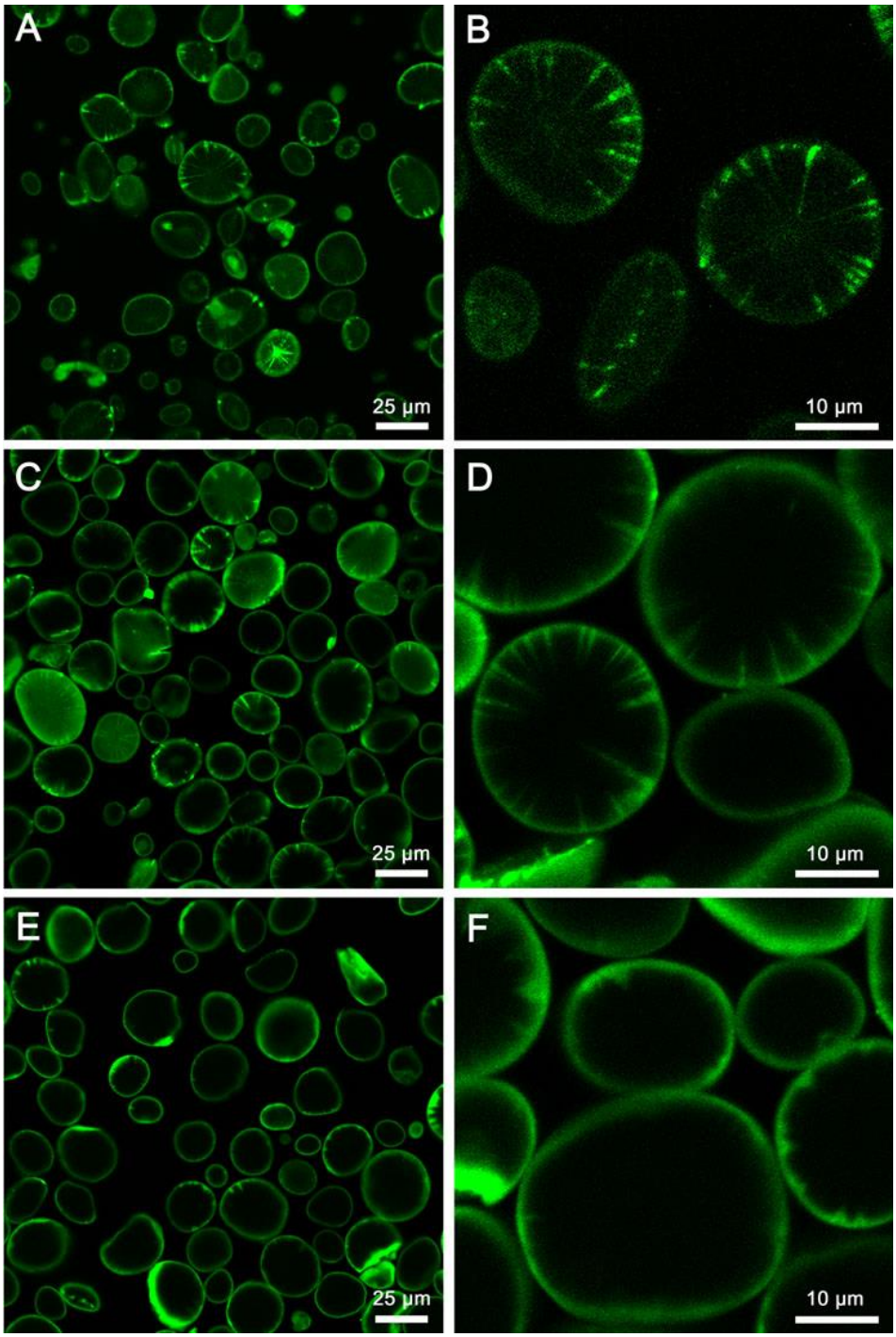

Figure 3.4: Confocal laser scanning micrographs of treated Pronghorn triticale starch granules (A, B: 2% SDS, C, D: 0.2% SO_2, E, F: 0.15% Thermolysin) stained with fluorescamine.

3.3.3. CLSM of native starches with APTS and Pro-Q Diamond staining

Double staining of starch granules with APTS and Pro-Q Diamond stain enabled the simultaneous visualization of the internal structure of starch and phosphorus molecules in one single focal plane of the starch granule by CLSM (Figure 3.5). APTS specifically reacts with the reducing ends of starch molecules, resulting in a positive correlation between the fluorescence intensity (brightness) and amylose content due to the higher molar ratio of reducing ends in amylose compared to amylopectin (Blennow et al., 2003). Pro-Q Diamond dye binds to phosphate and phospholipid with high sensitivity in various starches (Glaring et al., 2006). Thus, it was used to stain the starch-associated phosphorus as an index of phospholipid (dominant form in cereal starches). A population of granules for each starch are shown in Figure 3.5, with a representative few granules from each starch enlarged to visualize the structural features at high magnification (Figure 3.6). Alternating bright and dark rings and bright areas in the central region of the granule were frequently observed in APTS-stained triticale (Figures 3.5A & B and 3.6A & B) and corn starch granules (Figures 3.5C and 3.6C), representing typical internal structural features of growth rings, and the central amorphous region, respectively. A bright band along a flat, oval-shaped optical section (a side view of a disc-shaped granule), which represents the equatorial grooves plane, also was observed in triticale starch granules (Figures 3.5A & B and 3.6A & B). The strong fluorescence intensity in the central region and the equatorial groove plane of the granule indicated a high concentration of amylose

molecules in these areas. In triticale starch, the granule channels mostly appeared as dark, straight lines (voids, no staining), crossing growth rings and oriented towards the center of the granule (Figures 3.5A & B and 3.6A & B).

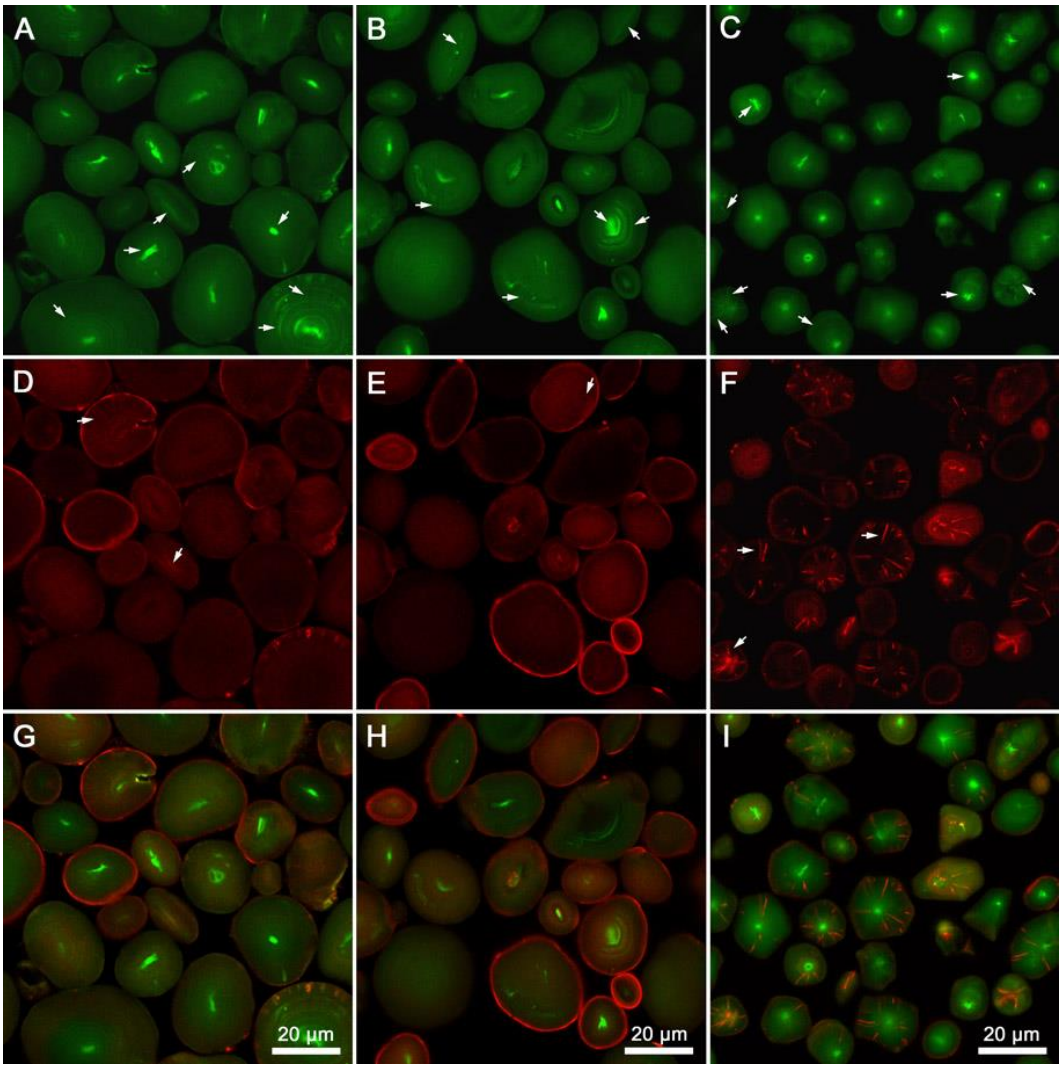

Figure 3.5: Confocal laser scanning micrographs of triticale (A, D, G: Pronghorn, B, E, H: Ultima) and corn (C, F, I) starch granules stained with APTS (A, B, C) and Pro-Q Diamond (D, E, F). G, H and I are overlays of A, B, C and D, E, F, respectively. Arrows indicate the locations of the growth rings, central region, channels, and equatorial grooves of starch granules.

In some cases, the outer regions of channels appeared bright (Figures 3.5A and 3.6A). In corn starch, bright channels and the central cavity or crack (voids, no staining) were observed in some granules (Figures 3.5C and 3.6C). The dark channels in triticale starch granules (Figure 3.5A, D & G) and bright channels in corn starch granules (Figure 3.5C, F & I) were rich in phosphorus after starches were stained with Pro-Q Diamond.

CLSM revealed the presence of starch-associated phosphorus (stained by Pro-Q Diamond) in both triticale and corn starch granules (Figure 3.5D, E & F). However, the distribution of phosphorus in these two starches was markedly different. In most triticale starch granules, a relatively high level of fluorescence was visible as a thin layer on and just beneath the granule surface and in radially orientated channels (Figure 3.5D & G). In addition, a low to intermediate level of fluorescence was uniformly distributed throughout most triticale starch granules (Figure 3.5D & E). In most corn starch granules, phosphorus was much more concentrated in channels and near the granule surface, with only weak staining observed elsewhere in the granule (Figure 3.5F & H). Overlay images (Figure 3.5G, H & I) of APTS and Pro-Q staining provided excellent contrast and clearly showed the detailed structural features and the molecular distributions described above. Phosphorus was found to be distributed throughout the large granules of wheat starch with the highest concentrations in the granule periphery (Morrison, 1981). Glaring et al. (2006) reported that wheat starch granules stained uniformly with Pro-Q Diamond with a trend toward a greater

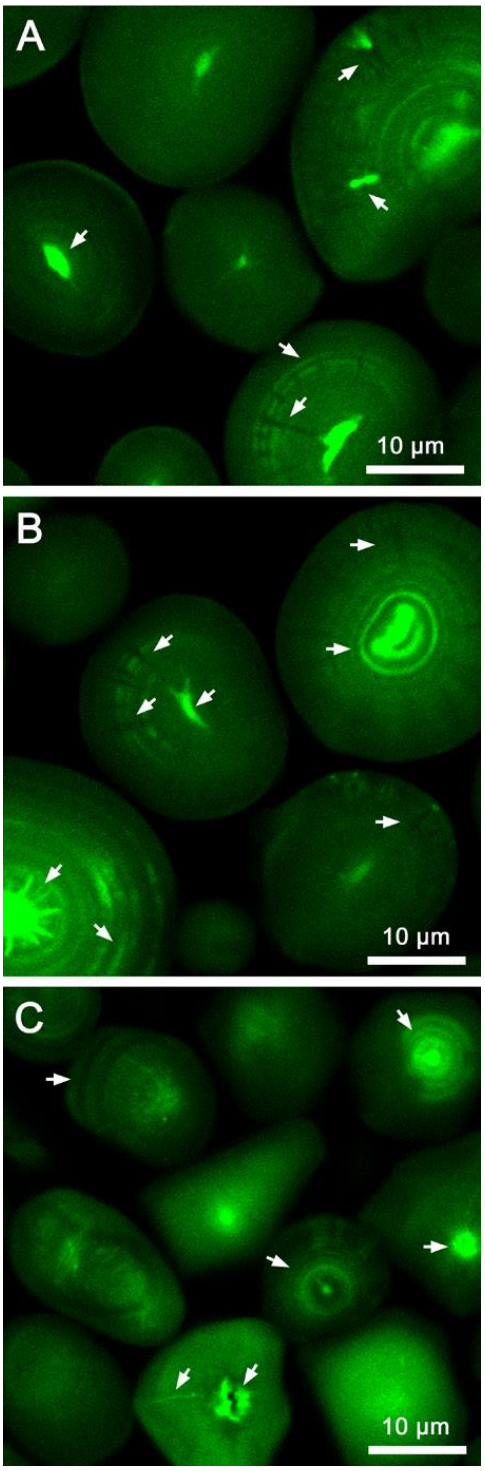

Figure 3.6: Confocal laser scanning micrographs of triticale (A: Pronghorn, B: Ultima) and corn (C) starch granules stained with APTS at higher magnification. Arrows indicate the locations of the growth rings, central region, channels, and equatorial grooves of granules.

intensity of surface staining in some granules. Using X-ray photoelectron spectroscopy, Russell et al. (1987) observed in soft wheat starch that the nitrogen and phosphorus concentrations in the granule periphery (to a depth of 5 nm) were approximately 19- and 7-fold higher, respectively, than the concentrations in the granule overall. Baldwin et al. (1997) identified phosphatidylcholine as the only major phospholipid occurring on the granule surfaces of wheat starch. Thus, the distribution of phosphorus in triticale starches is similar to that in wheat starch since phospholipid is highly associated with the surface of starch granules.

3.3.4. Effect of chemical and protease treatments on concentrations of starch-associated protein and phospholipid

A variety of chemical solutions and a protease (thermolysin) treatment were used to remove the protein and phospholipid in triticale and corn starches. The nitrogen and phosphorus contents of starches measured after treatments are shown in Table 3.1. The amount of protein and phospholipid removed by chemicals and enzyme varied with starch source and treatment conditions. Generally, the selected treatments resulted in partial removal of protein (up to 47% in starch from Pronghorn triticale, up to 17% in starch from Ultima triticale and up to 26% in corn starch) and phosphorus (up to 42% in starch from Pronghorn triticale, 39% in starch from Ultima triticale and 10% in corn starch). Though commercial corn starch may have already treated extensively with an

SO_2 solution during the wet-milling process, a certain quantity of protein from corn starch was removed by most treatments in the present study. However, less phosphorus was removed in corn starch than in triticale starches. A close association between the protein and phosphorus in triticale starches exists, since nitrogen content was positively correlated ($P < 0.05$) with the phosphorus content in treated Pronghorn ($r = 0.8994$) and Ultima ($r = 0.6033$) triticale starches, but not in treated corn starch (Figure 3.7).

Table 3.1: The contents of nitrogen and phosphorus of starches treated with selective chemicals and protease.

Treatment	Starch	Nitrogen (%)	Phosphorus (%)
Water	Pronghorn triticale	0.045	0.055
	Ultima triticale	0.030	0.054
	Corn	0.046	0.030
2% SDS	Pronghorn triticale	0.028	0.047
	Ultima triticale	0.027	0.059
	Corn	0.038	0.039
0.2% SO_2	Pronghorn triticale	0.039	0.052
	Ultima triticale	0.030	0.047
	Corn	0.041	0.032
2% SDS + 0.2% SO_2	Pronghorn triticale	0.024	0.034
	Ultima triticale	0.025	0.033
	Corn	0.035	0.027
0.15% Thermolysin	Pronghorn triticale	0.033	0.051
	Ultima triticale	0.033	0.048
	Corn	0.040	0.030
2% SDS + 0.15% Thermolysin	Pronghorn triticale	0.027	0.041
	Ultima triticale	0.028	0.041
	Corn	0.034	0.027
n-Propanol: Water (3:1)	Pronghorn triticale	0.054	0.059
	Ultima triticale	0.036	0.058
	Corn	0.043	0.029
2% SDS + n-Propanol:Water (3:1)	Pronghorn triticale	0.028	0.042
	Ultima triticale	0.025	0.038
	Corn	0.035	0.032
LSD[a]		0.003	0.004

[a] Least significant difference at $P<0.05$.

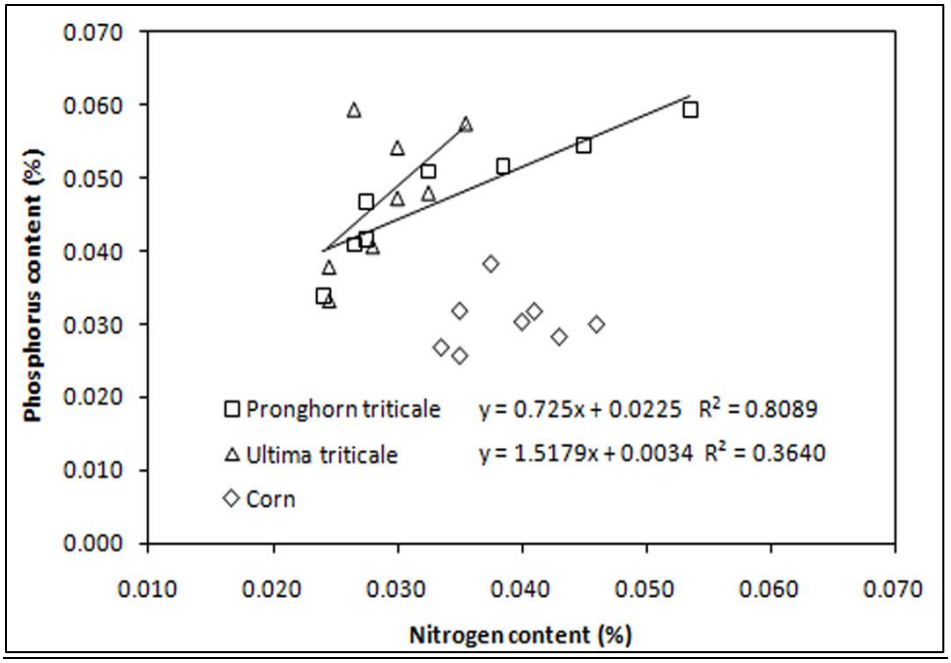

Figure 3.7: Correlations between the contents of nitrogen and phosphorus in chemically and enzymatically treated starches

A number of studies have reported an association between protein and phosphorus in starch granules (Debet & Gidley, 2006; Greenblatt et al., 1995; Tester et al., 2008). Lipid removed from the granule surface with cold SDS-ME (sodium dodecyl sulfate-mercaptoethanol) and subsequent extraction with thermolysin and propanol-water was identified as phospholipid (mainly lysophosphatidylcholine) in wheat and corn starches (Blaszczak et al., 2003; Jimeno et al., 2002; Lee & BeMiller, 2008; Seguchi, 1995). Greenblatt et al. (1995) suggested that the interaction of surface protein in starch from soft wheat with starch molecules was mediated through surface-bound glycolipids and phospholipids. Debet and Gidley (2006) suggested that phospholipid is associated with both glucan and surface protein in wheat starch, whereas it is

associated with glucan only in corn starch. This may explain why the correlation between the contents of nitrogen and phosphorus was not found in treated corn starch in present study. However, Lee and Bemiller (2008) found the phospholipid in the channels of corn starch granules where there is protein, not glucan, possibly due to the different extraction method. The different associations among glucan, surface protein and phosphorus amongst triticale and corn starches also describes the complexity and diversity of starch granule surface chemistry. This complexity is demonstrated in the composition of non-starch components, typically protein and lipid, and their associations with glucans on the granule surface, including channels in different starches. It has been reported that protein and phosphorus bound to starch molecules may stabilize the double-helical cross-linking of glucan chains, especially in the outer region of the granule (Debet & Gidley, 2007) and possibly within internal channels.

3.4. CONCLUSIONS

Starches from different origins varied with respect to the morphological features of their granules, such as granule shape, and the size, density, and dimensions of the surface pores. CLSM in conjunction with fluorescent staining using specific dyes clearly revealed the microstructure of the granule and the distribution in the internal channels, protein, and phosphorus. Small pores and internal channels existed in large granules of triticale starches. Removal of protein and phospholipid by chemical treatments made them more visible under CLSM.

Starch-associated protein was predominantly distributed on the granule surface and internal channels in both triticale and corn starches and also in the central region of corn starch granules. In triticale starches, phospholipid was mainly located on the granule surface and also in channels and throughout granules, whereas in corn starch it was mainly in the internal channels. Protein and phospholipid were found to be distributed in the channels, which blocked the pathway for the diffusion of chemicals or enzymes into starch matrix. The nitrogen and phospholipid contents were positively correlated with each other in treated triticale starches. The starch-associated protein and phospholipid in starches may play an important role in maintaining the structural stability of both the granule surface and the internal channels.

REFERENCES

AACC International. (2004). Approved methods of the AACC. AACC International, St. Paul, MN, USA.

Baldwin, P. M. (2001). Starch granule-associated proteins and polypeptides: A review. *Starch-Starke 53*:475-503.

Baldwin, P. M., Melia, C. D., & Davies, M. C. (1997). The surface chemistry of starch granules studied by time-of-flight secondary ion mass spectrometry. *J. Cereal Sci. 26*:329-346.

Bantan-Polak, T., Kassai, M., & Grant, K. B. (2001). A comparison of fluorescamine and naphthalene-2,3-dicarboxaldehyde fluorogenic reagents for microplate-based detection of amino acids. *Anal. Biochem. 297*:128-136.

Benmoussa, M., Suhendra, B., Aboubacar, A., & Hamaker, B. R. (2006). Distinctive sorghum starch granule morphologies appear to improve raw starch digestibility. *Starch-Starke 58*:92-99.

Berry, C. P., D'Appolonia, B. L., & Gilles, K. A. (1971). The Characterization of triticale starch and its comparison with starches of rye, durum, and HRS wheat. *Cereal Chem. 48*:415-426.

Blaszczak, W., Valverde, S., Fornal, J., Amarowicz, R., Lewandowicz, G., & Borkowski, K. (2003). Changes in the microstructure of wheat, corn and potato starch granules during extraction of non-starch compounds with sodium dodecyl sulfate and mercaptoethanol. *Carbohydr. Polym. 53*:63-73.

Blennow, A., Hansen, M., Schulz, A., Jorgensen, K., Donald, A. M., & Sanderson, J. (2003). The molecular deposition of transgenically modified starch in the starch granule as imaged by functional microscopy. *J. Struct. Biol. 143*:229-241.

Chen, P., Yu, L., Simon, G., Petinakis, E., Dean, K., & Chen, L. (2009). Morphologies and microstructures of corn starches with different amylose-amylopectin ratios studied by confocal laser scanning microscope. *J. Cereal Sci. 50*:241-247.

Chung, Y. L., & Lai, H. M. (2006). Molecular and granular characteristics of corn starch modified by HCl-methanol at different temperatures. *Carbohydr. Polym. 63*:527-534.

Davis-Knight, H. R., & Weightman, R. M. (2008). The potential of triticale as a low input cereal for bioethanol production, the Home-Grown Cereals Authority (HGCA) Project Rep No. 434. ADAS UK Ltd, Centre for Sustainable Crop Management: Cambridge, UK.

Debet, M. R., & Gidley, M. J. (2006). Three classes of starch granule swelling: Influence of surface proteins and lipids. *Carbohydr. Polym. 64*:452-465.

Debet, M. R., & Gidley, M. J. (2007). Why do gelatinized starch granules not dissolve completely? Roles for amylose, protein, and lipid in granule "Ghost" integrity. *J. Agric. Food Chem. 55*:4752-4760.

Fannon, J. E., Gray, J. A., Gunawan, N., Huber, K. C., & BeMiller, J. N. (2003). The channels of starch granules. *Food Sci. Biotechnol. 12*:700-704.

Fannon, J. E., Hauber, R. J., & Bemiller, J. N. (1992). Surface pores of starch granules. *Cereal Chem. 69*:284-288.

Fannon, J. E., Shull, J. M., & Bemiller, J. N. (1993). Interior channels of starch granules. *Cereal Chem*. 70:611-613.

Fortuna, T., Januszewska, R., Juszczak, L., Kielski, A., & Palasinski, M. (2000). The influence of starch pore characteristics on pasting behaviour. *Int. J. Food Sci. Technol. 35*:285-291.

Glaring, M. A., Koch, C. B., & Blennow, A. (2006). Genotype-specific spatial distribution of starch molecules in the starch granule: A combined CLSM and SEM approach. *Biomacromolecules 7*:2310-2320.

Gray, J. A., & BeMiller, J. N. (2004). Development and utilization of reflectance confocal laser scanning microscopy to locate reaction sites in modified starch granules. *Cereal Chem. 81*:278-286.

Greenblatt, G. A., Bettge, A. D., & Morris, C. F. (1995). Relationship between endosperm texture and the occurrence of friabilin and bound polar lipids on wheat-starch. *Cereal Chem. 72*:172-176.

Han, J. A., & BeMiller, J. N. (2008). Effects of protein on crosslinking of normal maize, waxy maize, and potato starches. *Carbohydr. Polym. 73*:532-540.

Han, X. Z., Benmoussa, M., Gray, J. A., BeMiller, J. N., & Hamaker, B. R. (2005). Detection of proteins in starch granule channels. *Cereal Chem. 82*:351-355.

Han, X. Z., & Hamaker, B. R. (2002). Location of starch granule-associated proteins revealed by confocal laser scanning microscopy. *J. Cereal Sci. 35*:109-116.

Hayashi, M., & Seguchi, M. (2004). Oil binding of heat-treated waxy wheat starch granules and starch granule ghosts produced with concentrated KI and I_2. *Cereal Chem. 81*:621-625.

Huber, K. C., & BeMiller, J. N. (1997). Visualization of channels and cavities of corn and sorghum starch granules. *Cereal Chem. 74*:537-541.

Huber, K. C., & BeMiller, J. N. (2000). Channels of maize and sorghum starch granules. *Carbohydr. Polym. 41*:269-276.

Huber, K. C., & BeMiller, J. N. (2001). Location of sites of reaction within starch granules. *Cereal Chem. 78*:173-180.

Israkarn, K., & Hongsprabhas, P. (2007). Influences of granule-associated proteins on physicochemical properties of mungbean and cassava starches. *Carbohydr. Polym. 68*:314-322.

Jane, J. L., Kasemsuwan, T., Leas, S., Zobel, H., & Robyt, J. F. (1994). Anthology of starch granule morphology by scanning electron-microscopy. *Starch-Starke 46*:121-129.

Jimeno, M. L., Valverde, S., Blaszczak, W., Fornal, J., & Amarowicz, R. (2002). C-13 and H-1 NMR study of lysophosphatidylcholine (LPC) isolated from the surface of wheat starch granules. *Food Sci. Technol. Int. 8*:179-183.

Juszczak, L. (2003). Surface of triticale starch granules - NC-AFM observations. Electron. *J. Pol. Agric. Univ. 6*:#08.

Kasemsuwan, T., & Jane, J. L. (1996). Quantitative method for the survey of starch phosphate derivatives and starch phospholipids by P-31 nuclear magnetic resonance spectroscopy. *Cereal Chem. 73*:702-707.

Kim, H. S., & Huber, K. C. (2008). Channels within soft wheat starch A- and B-type granules. *J. Cereal Sci. 48*:159-172.

Kuo, W. Y., & Lai, H. M. (2007). Changes of property and morphology of cationic corn starches. *Carbohydr. Polym. 69*:544-553.

Lee, S. H., & BeMiller, J. N. (2008). Lysophosphatidylcholine Identified as Channel-Associated Phospholipid of Maize Starch Granules. *Cereal Chem. 85*:776-779.

Leon, A. E., Jovanovich, G., & Anon, M. C. (1998). Gelatinization profiles of triticale starch in cookies as influenced by moisture and solutes. *Cereal Chem. 75*:617-623.

Li, J. H., Vasanthan, T., Hoover, R., & Rossnagel, B. G. (2003). Starch from hull-less barley: Ultrastructure and distribution of granule-bound proteins. *Cereal Chem. 80*:524-532.

Lim, S. T., Kasemsuwan, T., & Jane, J. L. (1994). Characterization of phosphorus in starch by P-31-nuclear magnetic-resonance spectroscopy. *Cereal Chem. 71*:488-493.

Lin, P. Y., & Czuchajowska, Z. (1998). Role of phosphorus in viscosity, gelatinization, and retrogradation of starch. *Cereal Chem. 75*:705-709.

Mira, I., Villwock, V. K., & Persson, K. (2007). On the effect of surface active agents and their structure on the temperature-induced changes of normal and waxy wheat starch in aqueous suspension. Part II: A confocal laser scanning microscopy study. *Carbohydr. Polym. 68*:637-646.

Morrison, W. R. (1981). Starch lipids: A reappraisal. *Starch-Starke 33*:408-410.

Morrison, W. R. (1988). Lipids in cereal starches: A review. *J. Cereal Sci. 8*:1-15.

Morrison, W. R. (1995). Starch lipids and how they relate to starch granule structure and functionality. *Cereal Foods World 40*:437-446.

Mu-Forster, C., & Wasserman, B. P. (1998). Surface localization of zein storage proteins in starch granules from maize endosperm - Proteolytic removal by thermolysin and in vitro cross-linking of granule-associated polypeptides. *Plant Physiol. 116*:1563-1571.

O'Shea, M. G., Samuel, M. S., Konik, C. M., & Morell, M. K. (1998). Fluorophore-assisted carbohydrate electrophoresis (FACE) of oligosaccharides: efficiency of labelling and high-resolution separation. *Carbohydr. Res. 307*:1-12.

Palasinski, M., Fortuna, T., Gambus, H., & Nowotna, A. (1987). Properties of triticale starch referred to polish triticale varieties. *Starch-Starke 39*:343-346.

Pejin, D., Mojovic, L. J., Vucurovic, V., Pejin, J., Dencic, S., & Rakin, M. (2009). Fermentation of wheat and triticale hydrolysates: A comparative study. *Fuel 88*:1625-1628.

Russell, P. L., Gough, B. M., Greenwell, P., Fowler, A., & Munro, H. S. (1987). A study by ESCA of the surface of native and chlorine-treated wheat-starch granules: The effects of various surface treatments. *J. Cereal Sci. 5*:83-100.

Rutherford, P. M., McCarthy, O. J., Arendt, E. K., & Figueiredo, C. T. (2008). Total nitrogen. Pages 239-240 in: Soil sampling and methods of analysis. M. R. Carter and E. G. Gregorich, eds. CRC Press, Boca Raton, FL, USA.

Seguchi, M. (1986). Dye binding to the surface of wheat-starch granules. *Cereal Chem. 63*:518-520.

Seguchi, M. (1995). Surface staining of wheat-starch granules with remazolbrilliant blue-r-dye and their extraction with aqueous sodium dodecyl-sulfate and mercaptoethanol. *Cereal Chem. 72*:602-608.

Sujka, M., & Jamroz, J. (2007). Starch granule porosity and its changes by means of amylolysis. *Int. Agrophys. 21*:107-113.

Tester, R. F., Yousuf, R., Karkalas, J., Kettlitz, B., & Roper, H. (2008). Properties of protease-treated maize starches. *Food Chem. 109*:257-263.

U.S. Environmental Protection Agency. (1983). Phosphorous, Total (Colorimetric, Automated, Block Digester AA II), Method 365.4 in: Methods for the chemical analysis of water and wastes, EPA/600/4-79/020. U.S. Environmental Protection Agency, Cincinnati, OH, USA.

van de Velde, F., van Riel, J., & Tromp, R. H. (2002). Visualisation of starch granule morphologies using confocal scanning laser microscopy (CSLM). *J. Sci. Food Agric. 82*:1528-1536.

van de Velde, F., Weinbreck, F., Edelman, M. W., van der Linden, E., & Tromp, R. H. (2003). Visualization of biopolymer mixtures using confocal scanning laser microscopy (CSLM) and covalent labeling techniques. *Colloid Surf. B-Biointerfaces 31*:159-168.

CHAPTER 4

Amylolysis of large and small granules of native triticale, wheat, and corn starches using a mixture of α-amylase and glucoamylase*

4.1. INTRODUCTION

In the midst of fast growing global demand for energy and progressive depletion of fossil fuel warrants innovative research efforts towards alternative energy sources (ex: bioethanol) that are renewable and environmentally friendly. Bioethanol production from energy crops (ex: sugar based and starchy materials) is referred to as the first-generation technique (Gomez, Steele-King & McQueen-Mason, 2008). Starch is a cheap, clean, nontoxic and renewable carbon source, and available in abundance, thus it is widely used as a feedstock in bioethanol production (Chen, Wu & Fukuda, 2008; Sanchez & Cardona, 2008). Corn, wheat and cassava are used to a greater extent than barley, rye and triticale in bioethanol production (das Neves, Kimura, Shimizu & Nakajima, 2007; Sanchez & Cardona, 2008). In Canada, most of the ethanol currently produced is distilled from corn and wheat (Natural Resources Canada, 2011). However due to the increasing cost of wheat and less availability of corn, triticale may be a best choice for bioethanol production in Canada (Alberta Agriculture and Rural Development, 2011; Wang et al., 1997). Triticale (x *Triticosecale* Wittmack) is a hybrid cereal species developed by crossing wheat (*Triticum turgidum* or

* A version of this chapter has been published in *Carbohydrate Polymers*, 2012, 88:864-874. (Adapted with permission of Elsevier Ltd)

Triticum aestivum) with rye (*Secale cereale*) and it has been shown to be an economically favorable source of carbohydrate for bioethanol production (Davis-Knight & Weightman, 2008; Pejin et al., 2009; Wang et al., 1997).

The current trend in bioethanol production towards continuous process involves the saccharification of dextrin (liquefied starch) into sugars in parallel to yeast fermentation in a single reactor (Balat, 2009; das Neves, Kimura, Shimizu & Nakajima, 2007). However, the initial step in current bioethanol production that converts native starch into sugars (amylolysis) is expensive since excessive heat energy is used in gelatinizing starch. Improved granular starch hydrolyzing enzymes (a mixture of α-amylase and glucoamylase) were recently developed to hydrolyze native starch granules into fermentable sugars at sub-gelatinization temperature. It could be used in simultaneous saccharification and fermentation (SSF) at low temperature, thus it reduces the cost and can effectively work on uncooked (raw) starches. However, the semicrystalline structure of native starch granules highly influences the amylolysis of starches at low temperature.

The structure, physicochemical properties and *in vitro* hydrolysis of cereal starches including triticale, wheat, barley and corn have been characterized (Ao & Jane, 2007; Bertolini, Souza, Nelson & Huber, 2003; Dhital, Shrestha & Gidley, 2010; Liu et al., 2007; Peng et al., 1999; Salman et al., 2009; Stevnebo, Sahlstrom & Svihus, 2006; Tang et al., 2001a; Utrilla-Coello et al., 2010; Vermeylen, Goderis, Reynaers & Delcour, 2005). Most recently, the characterization on

density and dimension of surface pores and the distribution of internal channels, protein, and phospholipids of triticale and corn starches using scanning electron microscopy (SEM) and confocal laser scanning microscopy (CLSM) has been studied (Naguleswaran et al., 2011). However, investigation on amylolysis of large and small granules of triticale starch using granular starch hydrolyzing enzyme has not been reported. SEM has been the main technique for investigating the morphological changes of hydrolyzed cereal starch granules. Recently, CLSM in conjunction with fluorescent staining using specific dyes has been used in studying enzyme hydrolyzed potato starch granules (Apinan et al., 2007; Varatharajan et al., 2011). However, no reports were found on enzyme hydrolyzed cereal starches. The objective of this study was to understand the relationship among morphological, architectural and physicochemical characteristics, and the degree of amylolysis of large and small starch granules from triticale, wheat, and corn starches (normal genotypes) using granular starch hydrolyzing enzymes at sub-gelatinization temperatures.

4.2. MATERIALS AND METHODS

4.2.1. Materials

Two cultivars of wheat (*Triticum aestivum* L.) grains, Canada Prairie Spring Red (CPSR) and AC Reed, were provided by Alberta Agriculture and Food in Barrhead (AB, Canada). The Field Crop Development Centre of Alberta Agriculture and Rural Development in Lacombe (AB, Canada) supplied two cultivars of triticale (x

Triticosecale) grains, Pronghorn and AC Ultima. Normal corn starch (Melojel) was donated by National Starch Food Innovation in Bridgewater (NJ, USA). Granular starch hydrolyzing enzyme, Stargen 002 (570 GAU/g), was donated by Genencor International in Rochester (NY, USA). 8-aminopyrene-1,3,6-trisulfonic acid, trisodium salt (APTS) was purchased from Invitrogen (Molecular Probes, Eugene, OR, USA). All other chemicals and reagents used in this study were of ACS grade.

4.2.2. Grain grinding and starch isolation

The triticale and wheat grains were ground into meals in a Retsch mill (Model ZM 200, Haan, Germany) using a ring sieve with an aperture size of 0.5 mm. Pure starch (purity >95%, w/w) was isolated from grain meal using the procedure described by Kandil et al. (2011). The detailed protocols are given in appendix.

4.2.3. Chemical composition of starches

Moisture and ash contents were determined by AACC Methods 44-15A and 08-01, respectively (AACC International, 2004). Starch content was measured according to the total starch assay kit of Megazyme (Megazyme International Ireland Ltd., Wicklow, Ireland). The total nitrogen (TN) content of starch was determined by the Dumas combustion method (Rutherford, McCarthy, Arendt & Figueiredo, 2008) using a Costech ECS 4010 Elemental Combustion System (Costech Analytical Technologies Inc., Valencia, CA, USA) and the protein contents were calculated by TN x 5.7. Starch lipid was determined by the procedures outlined in an earlier publication (Vasanthan & Hoover, 1992).

Apparent amylose content was determined according to the Standard Analytical Methods of the Member Companies of the Corn Refiners Association Inc. (Washington DC., USA). The amylose standard curve was prepared using pure amylose and amylopectin from potato starch (Sigma-Aldrich, Co., St. Louis, MO, USA) as described in the methodology. A detailed procedure of amylose determination is presented in appendix.

4.2.4. Fractionation of large and small starch granules

Isolated triticale and wheat starches and commercial corn starch were fractionated into large and small granules using a centrifugal sedimentation protocol adapted and modified from Peng et al. (1999). In brief, starch was slurried in water (1:10, w/v) and centrifuged (Fisher Scientific accuSpin^{TM} 400 bench top centrifuge, Germany) at 13 x*g* for 5 min. After centrifugation, the supernatant that contained small granules was collected and the residue was reslurried in water. The above centrifugal sedimentation step was repeated at least twenty times. Finally, the supernatant containing small granules and slurry of residue containing large granules were then passed independently through #41 Whatman^{TM} filter paper (GE Healthcare UK Ltd., Buckinghamshire, UK) using a vacuum filtration system. The residue on the top of filter paper was washed few times with deionized water followed by washing with anhydrous ethanol. The fractionated small and large granules were then air-dried at 40^{o}C and stored in glass vials until further analyses.

4.2.5. Granule size analysis

Granule size and size distribution of unfractionated native starches was determined following the method of Li, Guiltinan & Thompson (2007). About 50 mg of starch was slurried with 5 mL of distilled water and vortexed thoroughly before analysis. The starch solution was then loaded in the Aqueous Liquid Module system of Beckman Coulter LS 13 320 Particle Size Analyser (Beckman Coulter, Inc., Fullerton, CA, USA) with sonication for 1 min. The standard refractive indices applied for water and starch were 1.31 and 1.52, respectively. Number percentage of granules was recorded and weight percentage of starch granules was derived assuming all starch granules were spherical in shape.

4.2.6. X-ray powder diffraction analysis

X-ray diffractograms of starches were obtained with cross beam optics (CBO) technology of Rigaku Ultima IV multipurpose X-ray diffraction meter (Rigaku Americas, The Woodlands, TX, USA) according to the method described by Gao, Vasanthan & Hoover (2009). A detailed methodology is presented in appendix.

4.2.7. Amylolysis of starches using granular starch hydrolyzing enzyme

Starch samples (0.3% db, w/v) were hydrolyzed with Stargen 002 enzyme (24 U/30 mg starch) in 50 mM sodium acetate buffer (pH 4.0) at 55^{o}C for 1h followed by at 30^{o}C for 72h in a shaking water bath (Model BS-11, Jeio Tech Inc., Korea) according to the instructions given by enzyme manufacturer. The hydrolysates

were withdrawn at 1, 24, 48 and 72h for the determination of degree of hydrolysis (DH). DH was expressed as a percentage of reducing value by the 3,5-dintro salicylic acid (1%, w/v) method (Bruner, 1964). The control starch samples were concurrently run without enzyme addition.

4.2.8. Morphological and structural characterization of starch granules

The morphology and structure of unfractionated and fractionated (large and small) starch granules were characterized using SEM and CLSM according to the methods described in Chapter 3. The enzymatically hydrolyzed starch residues were recovered with addition of anhydrous ethanol followed by centrifugation (Fisher Scientific accuSpin^{TM} 400 bench top centrifuge, Germany) at 5000 x*g* for 10 min. The starch granules without addition of enzyme (control) and the enzymatically hydrolyzed starch residues after 1h and 24h were examined microscopically.

For SEM, starch samples were examined and photographed in a JEOL scanning electron microscope (Model JSM 6301 FXV, JEOL Ltd., Tokyo, Japan) at an accelerating voltage of 5 kV. In the CLSM procedure, the starch granules were stained with APTS dye and visualized under a confocal laser-scanning microscope (Zeiss LSM 710, Carl Zeiss MicroImaging GmbH, Jena, Germany) equipped with a x40 1.3 oil objective lens. Images of optical sections of starch granules were recorded and analyzed with ZEN 2009 Light Edition software (Carl Zeiss MicroImaging GmbH, Jena, Germany).

4.2.9. Statistical analyses

All treatments and analyses were carried out in triplicate. Analysis of variance using the General Linear Model (GLM) procedure and Pearson correlation statistics were performed using SAS Statistical Software, Version 9.1.2 (SAS Institute Inc., Cary, NC, 2004). Multiple comparisons of the means were carried out using Tukey's Studentized Range (HSD) Test at $\alpha = 0.05$.

4.3. RESULTS AND DISCUSSION

4.3.1. Composition of unfractionated and fractionated starches

As shown in Table 4.1, triticale and wheat starches had similar purity (≈97%) and ash content (0.2%) but lower protein content compared to those of corn starch (0.40–0.52% vs. 0.86%). The lipid contents in triticale starches (0.22%) were also lower than compared to wheat (0.77–0.87%) and corn (0.69%) starches. For fractionated starches, large starch granules generally showed lower protein and lipid contents than that those of small granules in triticale, wheat and corn starches. Other researchers (Liu et al., 2007; Raeker, Gaines, Finney & Donelson, 1998; Soulaka & Morrison, 1985) also reported similar results.

4.3.2. Granule size distribution of unfractionated starches

Triticale, wheat and corn starch granules showed a bimodal size distribution in the diameter range of 3–33 μm, 2–29 μm and 2–27 μm, respectively (Table 4.2 and Figure 4.1). The large granules (>10 μm) of triticale and wheat starches were

Table 4.1: Composition of triticale, wheat and corn starches (%, db)

Starch sources	Starch	Protein	Lipid	Ash
Triticale				
Pronghorn – Unfractionated	$97.2^{a} \pm 0.5$	$0.50^{c} \pm 0.02$	$0.22^{gh} \pm 0.001$	$0.19^{bcd} \pm 0.008$
– Large	$98.4^{a} \pm 0.3$	$0.43^{de} \pm 0.03$	$0.19^{hi} \pm 0.002$	$0.09^{f} \pm 0.002$
– Small	$98.1^{a} \pm 0.4$	$0.47^{cd} \pm 0.01$	$0.23^{g} \pm 0.009$	$0.08^{f} \pm 0.003$
Ultima – Unfractionated	$97.5^{a} \pm 0.9$	$0.40^{e} \pm 0.03$	$0.22^{gh} \pm 0.005$	$0.17^{de} \pm 0.008$
– Large	$98.0^{a} \pm 1.0$	$0.32^{f} \pm 0.01$	$0.18^{j} \pm 0.006$	$0.08^{f} \pm 0.002$
– Small	$98.4^{a} \pm 0.4$	$0.39^{e} \pm 0.01$	$0.22^{g} \pm 0.002$	$0.07^{f} \pm 0.013$
Wheat				
CPSR – Unfractionated	$96.6^{a} \pm 0.1$	$0.52^{bc} \pm 0.01$	$0.87^{b} \pm 0.005$	$0.20^{bc} \pm 0.007$
– Large	$97.9^{a} \pm 0.1$	$0.43^{de} \pm 0.01$	$0.76^{d} \pm 0.005$	$0.18^{cde} \pm 0.003$
– Small	$98.3^{a} \pm 0.2$	$0.51^{c} \pm 0.01$	$0.90^{a} \pm 0.009$	$0.16^{e} \pm 0.002$
AC Reed – Unfractionated	$96.8^{a} \pm 0.6$	$0.51^{c} \pm 0.03$	$0.77^{d} \pm 0.005$	$0.22^{a} \pm 0.001$
– Large	$97.4^{a} \pm 0.7$	$0.42^{de} \pm 0.01$	$0.75^{d} \pm 0.006$	$0.19^{bc} \pm 0.002$
– Small	$97.3^{a} \pm 0.3$	$0.50^{c} \pm 0.00$	$0.84^{c} \pm 0.009$	$0.18^{cde} \pm 0.002$
Normal Corn				
– Unfractionated	$97.1^{a} \pm 0.9$	$0.86^{a} \pm 0.01$	$0.69^{e} \pm 0.005$	$0.21^{ab} \pm 0.005$
– Large	$97.7^{a} \pm 1.0$	$0.58^{b} \pm 0.02$	$0.64^{f} \pm 0.005$	$0.09^{f} \pm 0.005$
– Small	$98.0^{a} \pm 1.0$	$0.83^{a} \pm 0.02$	$0.72^{e} \pm 0.007$	$0.08^{f} \pm 0.002$

Values are percentage of mean ± standard deviation in dry weight basis and values with the same superscript in the same column are not significantly different at $\alpha = 0.05$.

Table 4.2: Granule size distribution of unfractionated triticale, wheat and corn starches

Starch sources	Granule size range (μm)	Mean granule size			Number (%)		Weight (%)	
		O[1]	L[2]	S[3]	Large	Small	Large	Small
Triticale								
Pronghorn	3–33	15.9	20.2	7.2	$44.6^{a} \pm 0.3$	$55.4^{d} \pm 0.3$	$95.2^{a} \pm 0.0$	$4.8^{e} \pm 0.0$
Ultima	3–31	14.9	19.1	7.2	$35.9^{b} \pm 0.1$	$64.1^{c} \pm 0.1$	$93.0^{b} \pm 0.1$	$7.0^{d} \pm 0.1$
Wheat								
CPSR	2–29	9.6	18.1	4.4	$3.0^{d} \pm 0.1$	$97.0^{a} \pm 0.1$	$76.7^{e} \pm 0.4$	$23.3^{a} \pm 0.4$
AC Reed	1.5–26	8.7	17.1	4.3	$4.1^{d} \pm 0.1$	$95.9^{a} \pm 0.1$	$80.7^{d} \pm 0.1$	$19.3^{b} \pm 0.1$
Normal corn	2–27	9.4	17.1	4.8	$16.8^{c} \pm 0.6$	$83.2^{b} \pm 0.6$	$84.9^{c} \pm 0.3$	$15.1^{c} \pm 0.3$

[1] Overall mean (μm)
[2] Large granules mean (μm)
[3] Small granules mean (μm)
Values of number and weight percentages are mean ± standard deviation in number and weight basis, respectively. Values with the same superscript in the same column are not significantly different at $\alpha = 0.05$. Large starch granule was defined as granule diameter >10μm.

lenticular and the large corn starch granules were polyhedral in shape. The small granules (<10 μm) in all starches were mostly spherical in shape. As shown in Table 4.2, the average granule sizes of triticale starches were larger than those of wheat and corn starches, whereas those of wheat and corn starches were comparable. The proportions of large and small granules by number and by weight varied with starch sources (Table 4.2). In triticale starches, large granules contained the highest proportion of total granules by number (36–45%) and by weight (93–95%) compared to those of wheat and corn starches (3–17% by number and 77–85% by weight). The lower number percentage of large granules in total starch represents major mass of the starch (Li et al., 2001). The granule size and size distribution of triticale, wheat and corn starch granules are in agreement with previous studies (Ao & Jane, 2007; Salman et al., 2009).

4.3.3. Morphology and microstructure of large and small starch granules

The morphological and microstructural features of fractionated large and small granules of triticale, wheat and corn starches were revealed by SEM (Figures 4.2–4.4) and CLSM (Figures 4.5–4.7). Under SEM, the surfaces of both large and small granules of triticale and wheat starches appeared to be relatively smooth with reduced furrows and shallow depressions (Figures 4.2A & D and 4.3A & D). Surface pores were more frequently visualized on large granule surfaces of triticale and wheat starches. Oval-shaped pores along equatorial grooves and some aggregates of small pores with the appearance of slit-like cracks were

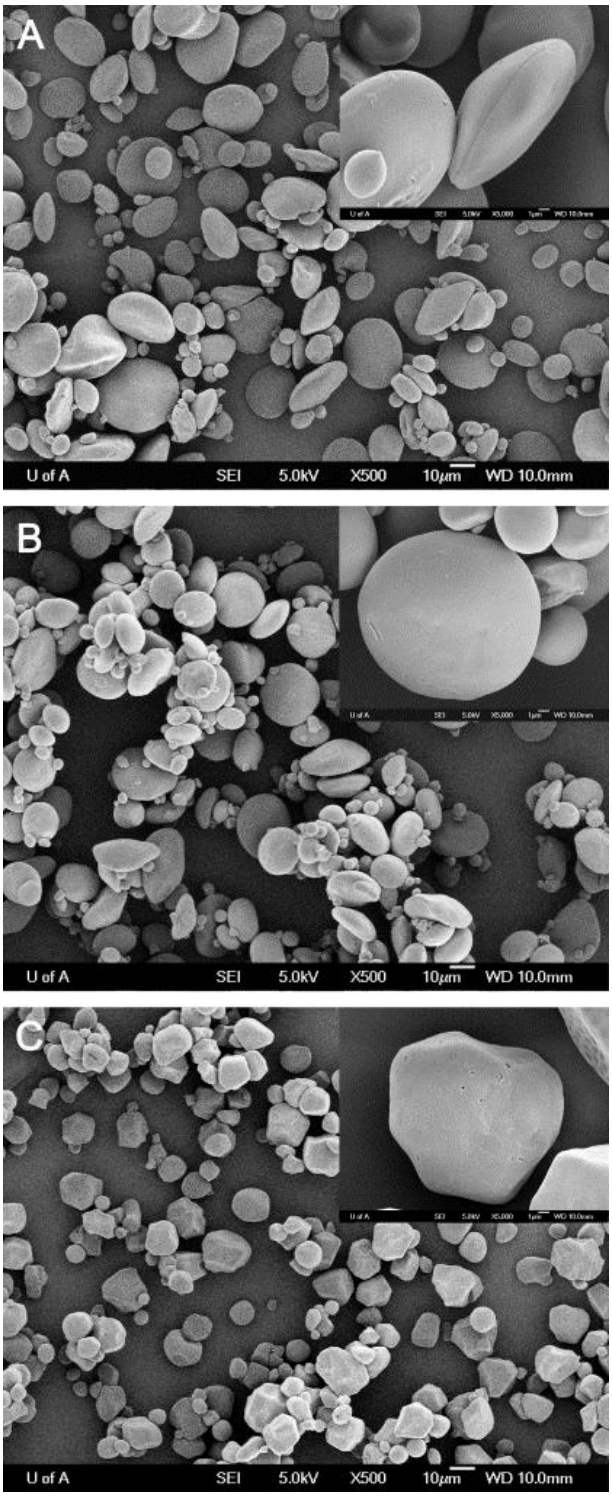

Figure 4.1: Scanning electron micrographs of unfractionated triticale (Pronghorn, A), wheat (CPSR, B) and corn (C) starch granules. Inserts are individual granules at high magnification.

present on some large granule surfaces of triticale and wheat starches (Figures 4.2A and 4.3A). Compared to those of triticale and wheat starch granules, corn starch granules showed markedly numerous pores of varying size that were unevenly distributed on the granule surface. These pores were more pronounced on the surface of large granules (Figure 4.4A).

Atomic force microscopy (AFM) has revealed that the starch granule surface is undulated as shown by protrusions and depressions even though there are rather smooth, flat or low rough regions (Juszczak, Fortuna & Krok, 2003; Tomoaia-Cotisel et al., 2010). The nitrogen absorption analyses of corn starch granules showed that the above protrusions are composed of large agglomerates (100-200 nm in size), which further consists of fine particles (20-30

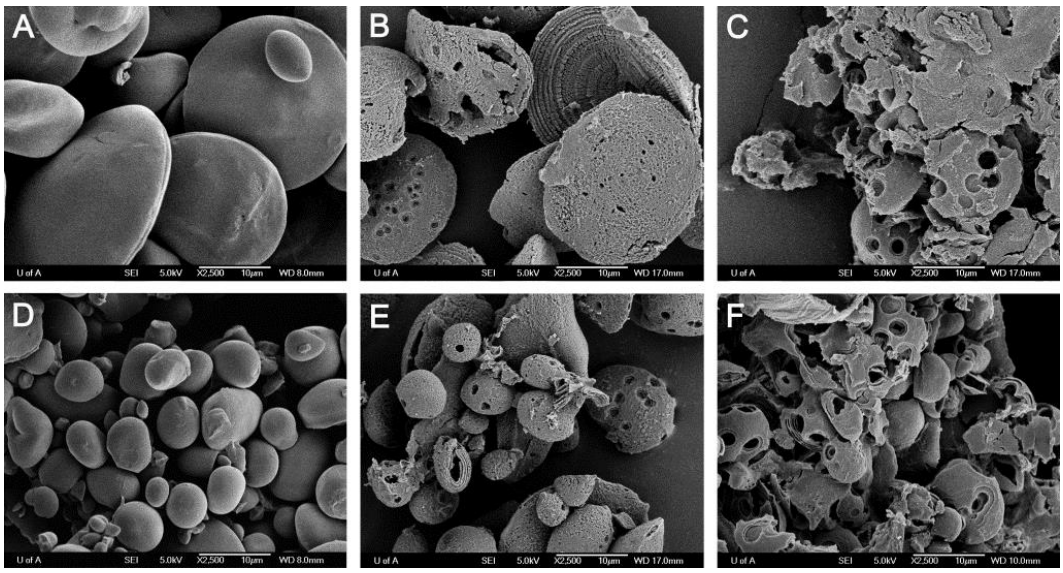

Figure 4.2: Scanning electron micrographs of large (A, B, C) and small (D, E, F) triticale (Pronghorn) starch granules hydrolyzed by granular starch hydrolyzing enzyme at 55°C for 0h (A, D), 1h (B, E) and at 30°C for 24 h (C, F).

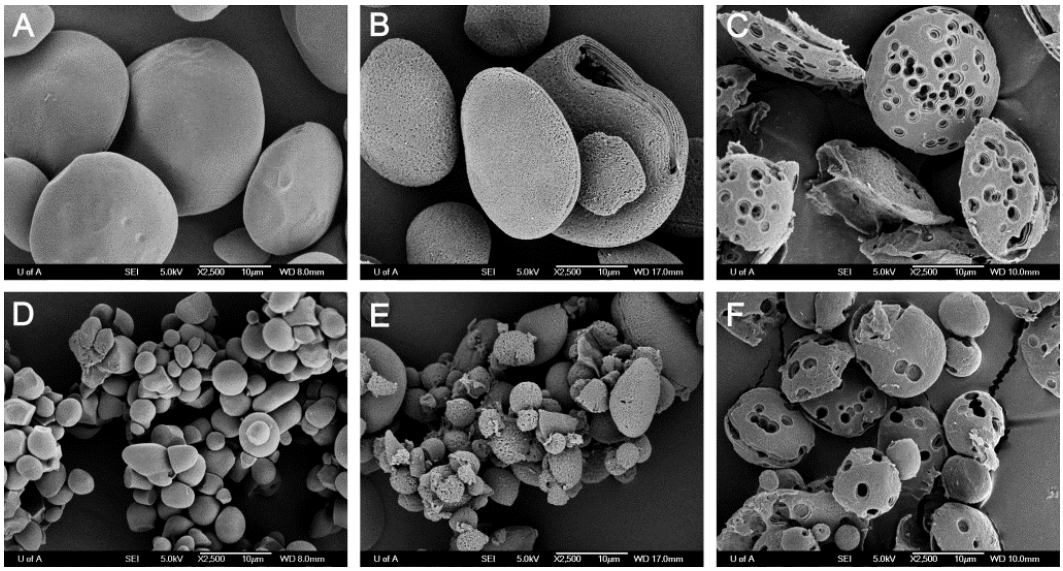

Figure 4.3: Scanning electron micrographs of large (A, B, C) and small (D, E, F) wheat (CPSR) starch granules hydrolyzed by granular starch hydrolyzing enzyme at 55°C for 0h (A, D), 1h (B, E) and at 30°C for 24h (C, F).

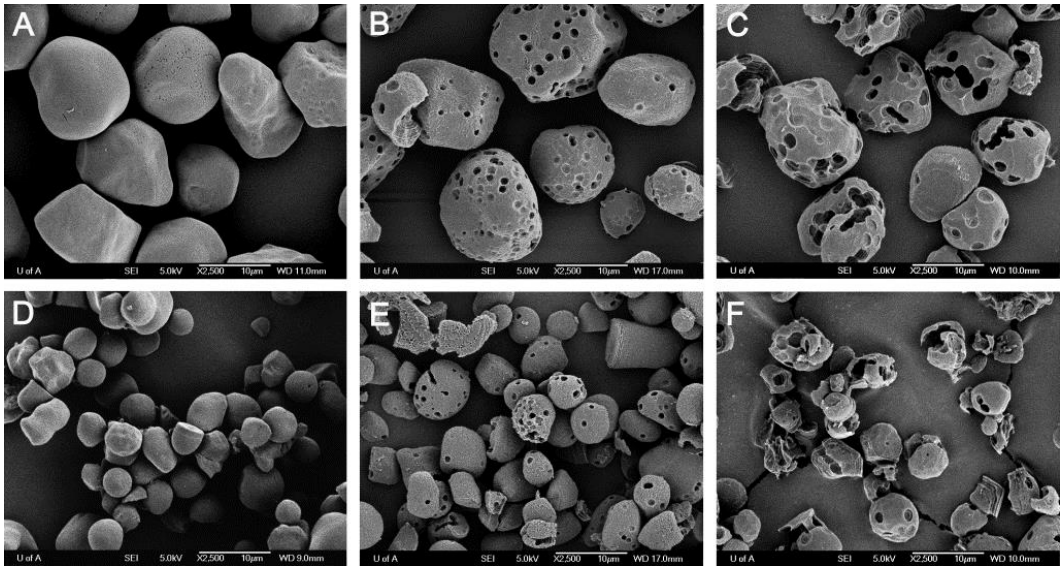

Figure 4.4: Scanning electron micrographs of large (A, B, C) and small (D, E, F) corn starch granules hydrolyzed by granular starch hydrolyzing enzyme at 55 °C for 0 h (A, D), 1 h (B, E) and at 30 °C for 24 h (C, F).

nm in diameter) surrounded by much shallow depressions (Park, Xu & Seetharaman, 2011), while dominant mesopores of 2-3 nm and macropores of 100-200 nm in diameter are also present on surfaces of corn starch granules (Sujka & Jamroz, 2009, 2010). AFM of triticale starch (Juszczak, 2003) has revealed that shallow depressions (<1 μm) with irregularly distributed pores in oval or circular or slit-like shape in a broad range of size (40-100 nm in diameter) as well as surface protrusion structure of 50-200 nm in size. In wheat starch granules, the surface protrusions consist of structures in the diameter range of 10-50 nm (Baldwin et al., 1997, 1998). The fine particle structure in the size of ≈30 nm on starch granule surfaces commonly exists in cereal and tuber starches (Ohtani et al., 2000; Sujka & Jamroz, 2009). These surface structure are believed to be the ends of starch macromolecules within the crystalline amylopectin side chain clusters (Baldwin et al., 1998; Baldwin et al., 1997; Sujka & Jamroz, 2009), corresponding to the blocklet structure proposed by Gallant, Bouchet & Baldwin (1997). Most recently, a hair-like structure in the length of 1-5 nm was found on the surface of corn and potato starch granules by AFM when granules are exposed to iodine vapor under a humid environment (Park, Xu & Seetharaman, 2011), which is believed to be extensions of either amylose or amylopectin molecules that are free to complex with iodine.

In agreement with our previous study (Chapter 3), growth rings, internal channels, equatorial grooves, and a central amorphous region were easily distinguished in all starch granules by florescence intensity under CLSM (Figures

4.5A, 4.6A and 4.7A). Recent studies on removal of channel proteins have shown the presence of tiny channels in both large and small granules of wheat, triticale and corn starches when viewed under CLSM (Kim & Huber, 2008; Naguleswaran et al., 2011). CLSM has proven that granule surface and internal channels are rich in protein and phospholipids (Chapter 3) which together with starch molecules may contribute to the complex nature of granule surface (Debet & Gidley, 2007; Naguleswaran et al., 2011; Tomoaia-Cotisel et al., 2010). The number and size distribution of pores, internal channels, and glucan polymer particles (topology) have been shown to vary with botanical origin of starch (Juszczak, Fortuna & Krok, 2003).

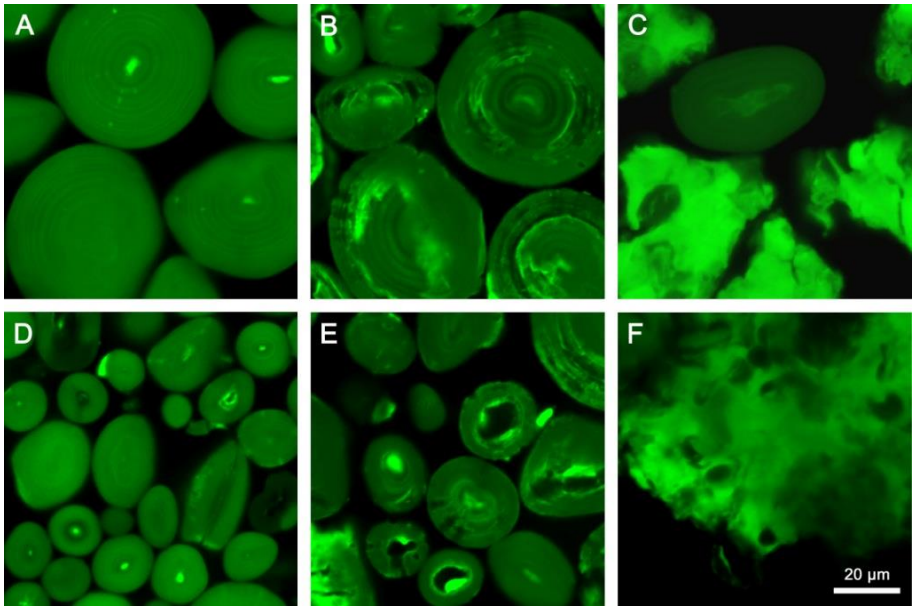

Figure 4.5: Confocal laser scanning micrographs of large (A, B, C) and small (D, E, F) triticale (Pronghorn) starch granules hydrolyzed by granular starch hydrolyzing enzyme at 55°C for 0h (A, D), 1h (B, E) and at 30°C for 24h (C, F).

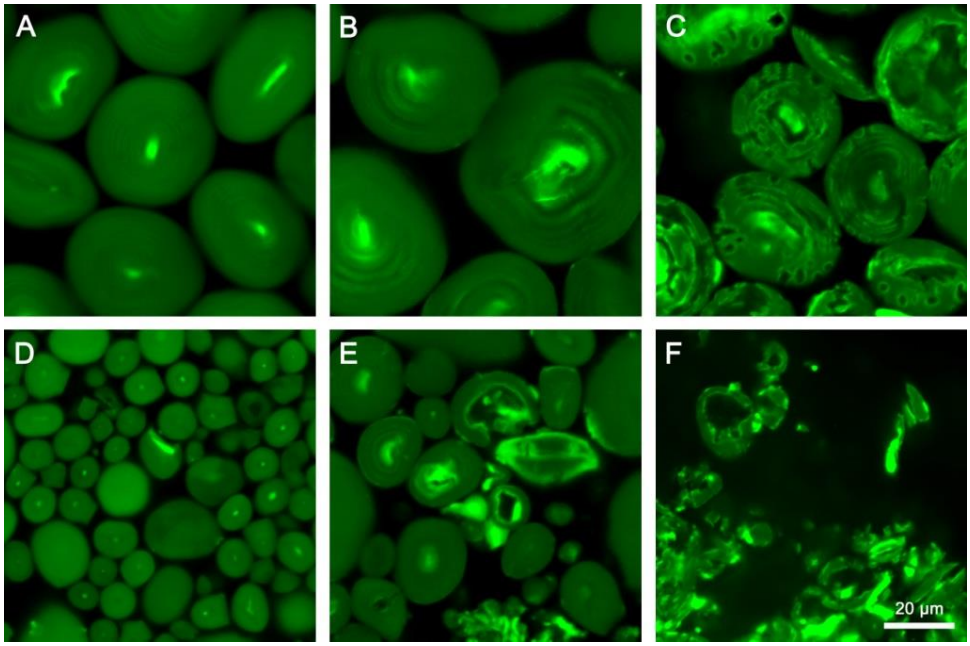

Figure 4.6: Confocal laser scanning micrographs of large (A, B, C) and small (D, E, F) wheat (CPSR) starch granules hydrolyzed by granular starch hydrolyzing enzyme at 55°C for 0h (A, D), 1h (B, E) and at 30°C for 24h (C, F).

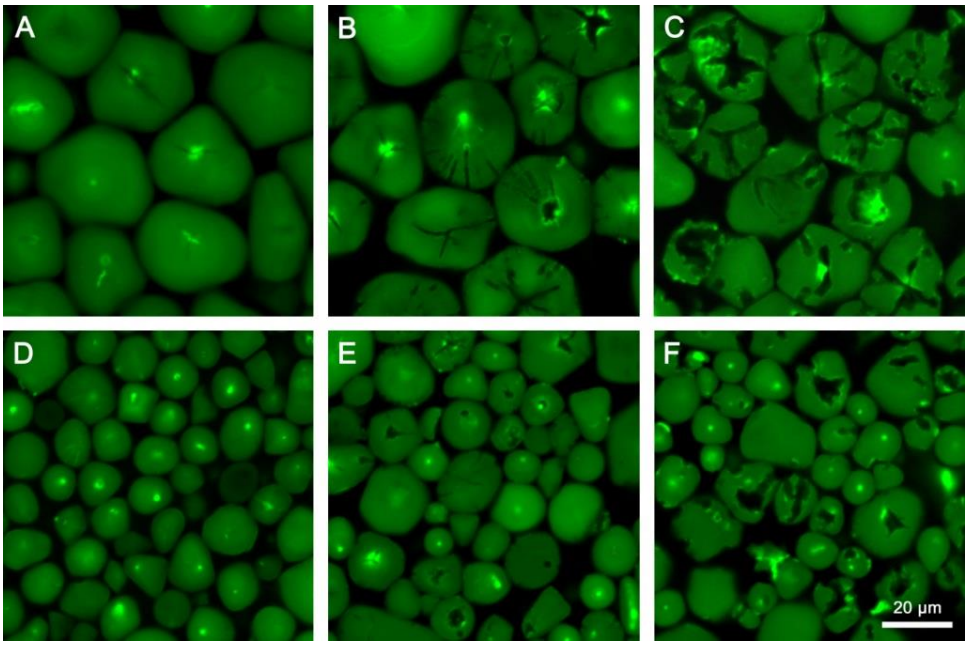

Figure 4.7: Confocal laser scanning micrographs of large (A, B, C) and small (D, E, F) corn starch granules hydrolyzed by granular starch hydrolyzing enzyme at 55°C for 0h (A, D), 1h (B, E) and at 30°C for 24h (C, F).

4.3.4. Amylose content and relative crystallinity of large and small starch granules

Apparent amylose contents of unfractionated starches from triticale, wheat and corn were in a narrow range of 22.5–26.4% (Table 4.3). However, the apparent amylose content differed significantly between large and small granules of each starch (Table 4.4). The large granules of triticale, wheat and corn starches contained significantly higher apparent amylose content (23.0–28.5%, db) than the small granules (12.4–21.0%, db). The difference in amylose contents between large and small granules in triticale, wheat and corn starches were 2.4–10.0%, 8.0–13.4%, and 5% (percentage unit difference), respectively, indicating that the apparent amylose content of starch varied with starch granule size within and between starch sources. The present results are in agreement with previous studies, where the apparent amylose content of large granules was 5–9% higher than that of small granules in wheat (Ao & Jane, 2007; Bertolini, Souza, Nelson & Huber, 2003; Liu et al., 2007), 10% in triticale (Ao & Jane, 2007), 1.3% in corn (Utrilla-Coello et al., 2010), and 3–7% in barley (Ao & Jane, 2007; Tang et al., 2001b). Amylose content has been found to be positively correlated with the proportion of small granules and the overall granule size in barley starches (Li, Vasanthan, Rossnagel & Hoover, 2001) and with the volume percentage of large granules (9.9–18.5 μm in diameter) in wheat starches (Raeker, Gaines, Finney & Donelson, 1998).

Table 4.3: Apparent amylose content and degree of hydrolysis of unfractionated triticale, wheat and corn starches

Starch sources	Apparent amylose (%, db)	Degree of hydrolysis (%)			
		1h[1]	24h[2]	48h[2]	72h[2]
Triticale					
Pronghorn	23.0^{b} ± 0.8	76.5^{a} ± 1.5	89.3^{ab} ± 0.8	92.2^{a} ± 0.7	92.4^{b} ± 1.0
Ultima	23.2^{b} ± 0.7	69.0^{b} ± 1.1	87.5^{b} ± 1.6	92.2^{a} ± 1.6	92.5^{b} ± 0.9
Wheat					
CPSR	22.5^{b} ± 1.1	53.8^{c} ± 1.1	91.3^{a} ± 0.5	92.8^{a} ± 0.5	96.9^{a} ± 0.9
AC Reed	26.4^{a} ± 0.7	22.1^{d} ± 1.3	88.6^{b} ± 0.3	89.7^{b} ± 0.9	96.2^{a} ± 0.5
Normal Corn	24.4^{ab} ± 0.9	3.5^{e} ± 0.4	59.8^{c} ± 1.0	84.9^{c} ± 0.4	90.6^{b} ± 1.4

[1] degree of hydrolysis at 55°C for 1h
[2] degree of hydrolysis at 30°C for 24, 48, and 72h, respectively
Values are mean ± standard deviation and values with the same superscript in the same column are not significantly different at $\alpha = 0.05$.

Amylopectin in large granules of barley starch showed higher molecular size, average chain length and number of chains than in small granules (Tang et al., 2001a, 2001b). Debranching of amylopectin molecules in wheat, triticale and corn starches indicated a longer average branch chain length, less short branch chains (A and B1 chains with DP 6-12 and DP 13-24) and more long branch chains (B2 and longer chains with DP>25) in large granules than in small granules (Ao & Jane, 2007; Liu et al., 2007). Salman et al. (2009) also reported a lower proportion of short chains (DP 6-12) and a higher proportion of long chains (DP 25-36) in large granules than in small granules of normal wheat starches. Thus, large starch granules differ from small granules in their composition and amylopectin structure (ex: molecular size, branch chain length and chain distribution of amylopectin, and crystallinity).

Table 4.4: Apparent amylose content, relative crystallinity and degree of hydrolysis of large and small granules of triticale, wheat and corn starches

Starch sources	Apparent amylose (%, db)	Crystallinity (%, db)	Degree of hydrolysis (%, db)			
			1h[1]	24h[2]	48h[2]	72h[2]
Triticale						
Pronghorn – Large	$23.0^{c} \pm 1.2$	$26.2^{b} \pm 0.0$	$44.5^{e} \pm 1.1$	$76.6^{d} \pm 0.9$	$80.7^{de} \pm 0.8$	$82.3^{def} \pm 0.8$
– Small	$20.6^{de} \pm 0.2$	$24.4^{d} \pm 0.2$	$62.5^{c} \pm 1.2$	$81.7^{bc} \pm 1.2$	$83.2^{bcd} \pm 0.4$	$83.9^{cd} \pm 0.9$
Ultima – Large	$28.5^{a} \pm 0.7$	$24.9^{c} \pm 0.2$	$64.5^{c} \pm 0.7$	$79.5^{c} \pm 1.0$	$81.4^{cde} \pm 1.0$	$84.5^{cd} \pm 0.4$
– Small	$18.5^{e} \pm 0.7$	$20.8^{f} \pm 0.2$	$73.8^{a} \pm 1.1$	$82.4^{ab} \pm 0.7$	$83.4^{bc} \pm 0.8$	$84.3^{cd} \pm 0.6$
Wheat						
CPSR – Large	$25.8^{b} \pm 0.4$	$25.2^{c} \pm 0.1$	$44.0^{e} \pm 1.1$	$84.4^{a} \pm 0.9$	$85.3^{b} \pm 0.8$	$90.8^{b} \pm 1.4$
– Small	$12.4^{f} \pm 1.4$	$23.7^{e} \pm 0.2$	$68.7^{b} \pm 0.8$	$84.9^{a} \pm 0.7$	$85.6^{b} \pm 1.1$	$86.2^{c} \pm 1.2$
AC Reed – Large	$27.6^{ab} \pm 0.4$	$25.9^{b} \pm 0.2$	$14.3^{g} \pm 1.0$	$83.8^{ab} \pm 0.4$	$91.3^{a} \pm 0.7$	$95.1^{a} \pm 1.4$
– Small	$19.6^{de} \pm 0.9$	$24.4^{d} \pm 0.0$	$54.6^{d} \pm 1.5$	$74.0^{d} \pm 1.1$	$77.2^{fg} \pm 1.1$	$79.6^{f} \pm 1.0$
Normal corn						
– Large	$26.0^{b} \pm 0.9$	$26.8^{a} \pm 0.1$	$3.2^{h} \pm 0.4$	$51.8^{f} \pm 0.9$	$75.3^{g} \pm 1.1$	$83.4^{cde} \pm 1.3$
– Small	$21.0^{cd} \pm 0.3$	$23.5^{e} \pm 0.3$	$20.9^{f} \pm 0.6$	$66.5^{e} \pm 1.1$	$79.2^{ef} \pm 0.8$	$80.8^{ef} \pm 0.1$

[1] degree of hydrolysis at 55°C for 1h

[2] degree of hydrolysis at 30°C for 24, 48, and 72h, respectively

Values are mean ± standard deviation and values with the same superscript in the same column are not significantly different at $\alpha = 0.05$

X-ray diffraction revealed that both large and small granules of triticale, wheat and corn starches exhibited the typical A-type polymorph pattern with characteristic peaks at 2θ angles of 15°, 17°, 18°, and 23°. As shown in Table 4.4, the relative crystallinities (RC) of large and small granules of triticale, wheat and corn starches were in the range of 24.9–26.8 % and 20.8–24.4 %, respectively. In the present study, the RC of large granules was significantly higher compared to small granules in all starches. Vermeylen et al., (2005) also reported higher RC in large starch granules of different wheat varieties. Ao and Jane (2007) proposed that the more long-branch chains (B2 chains) and lesser short-branch chains (A and B1 chains) of amylopectin in large granules form cylindrical shaped amylopectin molecules. The cylindrical shaped amylopectin molecules better align in a parallel arrangement into disk-shaped granules, which are expected to expose greater percentage of RC when compared to cone-shaped amylopectin molecules arranged radially in small spherical granules. Small-angle X-ray scattering (SAXS) and DSC study suggested that small granules of wheat starch consist of denser crystalline lamellae and longer double-helices connected to shorter single-stranded chains of the amylopectin backbone than larger granules (Vermeylen et al., 2005), which may hinder or delay enzyme absorption and diffusion in the later stage of hydrolysis. Compared to small granules, large granules of wheat starches had thicker lamellae and larger repeat distance, which may be related to the higher proportion of medium (DP 13-24) and long amylopectin chains (DP 25-36) (Salman et al., 2009).

4.3.5. Amylolysis of large and small starch granules

The unfractionated and fractionated large and small granules of triticale, wheat and corn starches were hydrolyzed to evaluate their susceptibilities towards a granular starch hydrolyzing enzyme at sub-gelatinization temperatures (55^{o}C for 1h and then at 30^{o}C for up to 72h). The degree of hydrolysis (DH) as a percentage of reducing value is summarized in Table 4.3 for unfractionated starches and in Table 4.4 for fractionated large and small starch granules. Unfractionated triticale starches showed rapid hydrolysis (DH 76.5% for Pronghorn and DH 69.0% for Ultima) followed by wheat (DH 53.8% for CPSR and DH 22.1% for AC Reed) and corn (DH 3.5%) starches when hydrolyzed at 55°C for 1h (Table 4.3). However, wheat starches were hydrolyzed to a greater extent (DH 96.2–96.9%) than triticale and corn starches (DH 90.6–92.5%) at 30°C for 72h. For each starch, small granules were hydrolyzed significantly faster than large granules at 1h hydrolysis. The DH of small granules were 9.3–18.0%, 24.7–40.3%, 17.7% (percentage unit difference) higher than those of large granules of triticale, wheat, and corn starches, respectively, at 55°C for 1h (Table 4.4). The higher DH of small granules can be attributed to their relatively larger surface area per unit mass. Surface pores and internal channels of granules are assumed to increase effective surface area for fast enzyme diffusion. However, the presence of minor components, such as proteins and lipids on granule surface and in channels largely block the binding sites of enzyme (Naguleswaran et al., 2011), thereby reducing the rate of hydrolysis, especially in larger granules that

have numerous pores and channels. Hydrolysis progressed more rapidly in the large granules possibly due to the gradual release of protein and lipid from associated glucan molecules, resulting in a narrowed difference of DH between large and small granules after 24h (Table 4.4). At a later stage, the densely packed crystalline lamellae (Vermeylen, Goderis, Reynaers & Delcour, 2005) and higher concentration of protein and lipid (Table 4.1) in small granules may greatly reduce the hydrolysis rate. The difference in DH between large and small granules became minimal in triticale after 48h and in corn after 72h (Table 4.4). In wheat, the difference in DH minimized at or less than 24h (Table 4.4). However, a significant difference in DH between small and large granules of CPSR and AC Reed wheat starches was observed at or after 48h (Table 4.4). The results for wheat starches are in agreement with Salman et al. (2009). Significant negative correlations at $p<0.05$ were found between the amylose content of small granules and the DH at 24h ($r = –0.62$), 48h ($r = –0.6$), and 72h ($r = –0.65$) and between the relative crystallinity of large granules and the DH at 1h and 24h ($r= –0.83$ and $–0.75$, respectively, $p<0.01$). Salman et al., (2009) reported that the DH of wheat starches was positively correlated with the proportion of short amylopectin branch chains (DP 6-12) and negatively correlated with the proportions of medium (DP 13-24) and long chains (DP 25-36) at initial hydrolysis but positively correlated with the proportion of medium chains at longer time of hydrolysis. This study and previous studies (Naguleswaran et al., 2011; Dhital, Shrestha & Gidley, 2010; Salman et al., 2009; Ao & Jane, 2007) suggested that

amylolysis of large and small starch granules is closely related to granule morphology, composition and structure at granular micro, and nano levels, such as shape, size, pores, channels, amylose content, associated protein and lipid, degree of crystallinity, lamellae size, and ratio of long and short amylopectin chains. It was noticed that the variation of DH between unfractionated starches (Table 4.3) and those of fractionated large and small granules (Table 4.4) differed among starches. This could be attributed to the presence of diverse proportion of large and small granules in each unfractionated starch and some cross contamination of large and small granules in fractionated starches.

4.3.6. Morphological and microstructural changes of hydrolyzed large and small starch granules

The morphological and microstructural changes of hydrolyzed starch granules (0, 1 and 24h) revealed by SEM and CLSM are shown in Figures 4.2–4.4 and Figures 4.5–4.7, respectively. One hour hydrolysis resulted in roughly pitted honeycomb-like structures on the surfaces of both large and small triticale (Figures 4.2B & E) and wheat starch granules (Figures 4.3B & E), even though individual granules were unevenly hydrolyzed. A few enlarged surface pores were observed on the surfaces of large and small triticale starch granules (Figures 4.2B & E) and even fewer on the surfaces of large and small wheat starch granules (Figures 4.3B & E). Hydrolysis occurred extensively along the equatorial groove of large triticale and wheat starch granules, resulting in

frequent appearance of half pieces of granules at 1h hydrolysis (Figures 4.2B and 4.3B). Corn starch was also roughened after 1h hydrolysis showing more perforated erosion pits and enlarged pores on the surfaces of large and small granules and much less granule fragments (Figures 4.4B & E). Generally, the visible layered structures were more pronounced on large granule surfaces (Figures 4.2B, 4.3B and 4.4B) than on small granules (Figures 4.2E, 4.3E and 4.4E). SEM suggested that enzymatic hydrolysis initiated from granule surfaces by generating pits, size enlargement of existing pores, and penetration into granule interior. The roughened surfaces in hydrolyzed corn starch granules may have been due to uneven shortening of amylopectin molecules by the action of α-amylase (Sujka & Jamroz, 2009). Hydrolysis for 24h at 30°C resulted in degradation of most large granules into fragments in triticale (Figure 4.2C) and layered residual granules with many enlarged hollows in wheat and corn (Figures 4.3C and 4.4C). However, many smaller granules were degraded into thin-layered structures with less number of hollows (Figures 4.2F, 4.3F and 4.4F).

CLSM showed that the enzyme degradation pattern of triticale and wheat starches were different from that of corn starch (Figures 4.5, 4.6 and 4.7). In triticale and wheat starches, enzyme erosion occurred along both channels (radially) and growth rings (perpendicularly), forming a large central cavity in the center of small granules (Figures 4.5E and 4.6E & F), while uneven hydrolysis took place in the outer layers of large granules, resulting in fragments with internal ring structure (Figures 4.5B and 4.6B & C). Hydrolysis was more

extensive in triticale starches (Figures 4.5C & F) than in wheat starches (Figures 4.6C & F). Nearly complete loss of structure of both large and small granules was observed in triticale starch after 24h hydrolysis (Figures 4.5C & F). Compared to triticale and wheat starches, erosion of granule interior in corn starch occurred mainly along internal channels resulting in hollowed intact granule residues (Figures 4.7B, C, E & F). With respect to corn starch, enlarged channels irregularly crossed in different size and depth in large granules, while a relatively large central cavity with less number of channels was formed in small granules after 24h hydrolysis (Figures 4.7C & F). The disappearance of internal structure of large and small granules in corn starch revealed by CLSM was consistent with the DH as shown in Table 4.4 (3.2% vs. 20.9% for 1h and 51.8% vs. 66.5% for 24h).

Hydrolysis patterns revealed by SEM and CLSM were caused by synergistic degradation of α-amylase and glucoamylase. Each enzyme erodes starch granules in a manner of exocorrosion and endocorrosion but at different hydrolysis rate and extent between starches (Kimura & Robyt, 1995; Li et al., 2004; Li et al., 2011; Quigley, Kelly, Doyle & Fogarty, 1998). As reported previously (Li et al., 2004; Li et al., 2011), α -amylase preferentially hydrolyzes the amorphous regions of the granule leaving granule residues with a sharp saw-toothed layer structure and a large cavity in the granule center, whereas glucoamylase hydrolyze amorphous and crystalline regions of the granule simultaneously by formation of shallow and circular pits with much smooth edges of internal layered structure due to confined hydrolysis along tangential

direction of the granule. Separated and fragmented layer structure revealed by CLSM in hydrolyzed starch granules indicated that α-amylase played a predominant role in hydrolyzing amorphous regions during amylolysis. This is also supported by X-ray diffraction and amylose content analysis (Blazek & Gilbert, 2010; Chen et al., 2011; Shariffa, Karim, Fazilah & Zaidul, 2009; Uthumporn, Zaidul & Karim, 2010), in which an increases of crystallinity intensity and a decrease of amylose content in hydrolyzed starches by both enzymes were found. Thus, the accessibility of α -amylase and amyloglucosidase towards large and small starch granules differ with starch origin, contributing to different hydrolysis kinetics (rate and extent) and hydrolysis patterns.

4.4. CONCLUSIONS

Large and small granules of triticale, wheat and corn starches differed in granule morphology, amylose content, presence of protein and lipid, relative crystallinity, amylolysis pattern, and hydrolysis rate and extent, indicating that the nature of starch granules (composition and macro-, micro-, nano-structures) controls starch amylolysis. Triticale starch was comparable to wheat and corn starches in terms of granular starch hydrolysis for use in ethanol production. This study suggests that the genetic manipulation of grains with different ratio of large and small starch granules could be used for precise control of liquefaction and saccharification in simultaneous hydrolysis and fermentation process.

REFERENCES

AACC International. (2004). Approved methods of the AACC. St. Paul, MN: AACC International.

Alberta Agriculture and Rural Development. (2011). Triticale grain for other uses. http://www1.agric.gov.ab.ca/$department/deptdocs.nsf/all/fcd10568. (Accessed in April 2011).

Ao, Z. H., & Jane, J. L. (2007). Characterization and modeling of the A- and B-granule starches of wheat, triticale, and barley. *Carbohydrate Polymers, 67*(1), 46-55.

Apinan, S., Yujiro, I., Hidefumi, Y., Takeshi, F., Myllarinen, P., Forssell, P., & Poutanen, K. (2007). Visual observation of hydrolyzed potato starch granules by alpha-amylase with confocal laser scanning microscopy. *Starch/Starke, 59*(11), 543-548.

Balat, M. (2009). Bioethanol as a Vehicular Fuel: A Critical Review. *Energy Sources Part A-Recovery Utilization and Environmental Effects, 31*(14), 1242-1255.

Baldwin, P. M., Adler, J., Davies, M. C., & Melia, C. D. (1998). High resolution imaging of starch granule surfaces by atomic force microscopy. *Journal of Cereal Science, 27*(3), 255-265.

Baldwin, P. M., Davies, M. C., & Melia, C. D. (1997). Starch granule surface imaging using low-voltage scanning electron microscopy and atomic force microscopy. *International Journal of Biological Macromolecules, 21*(1-2), 103-107.

Bertolini, A. C., Souza, E., Nelson, J. E., & Huber, K. C. (2003). Composition and reactivity of A- and B-type starch granules of normal, partial waxy, and waxy wheat. *Cereal Chemistry, 80*(5), 544-549.

Blazek, J., & Gilbert, E. P. (2010). Effect of enzymatic hydrolysis on native starch granule structure. *Biomacromolecules, 11*(12), 3275-3289.

Bruner, R. L. (1964). Determination of reducing value: 3, 5-dinitrosalicylic acid method. In R. L. Whistler, R. J. Smith, J. N. BeMiller & M. L. Wolform (Eds.). Methods in carbohydrate chemistry (Vol. 4, pp. 67-71). New York and London: Academic Press.

Chen, J. P., Wu, K. W., & Fukuda, H. (2008). Bioethanol production from uncooked raw starch by immobilized surface-engineered yeast cells. *Applied Biochemistry and Biotechnology, 145*(1-3), 59-67.

Chen, Y. S., Huang, S. R., Tang, Z. F., Chen, X. W., & Zhang, Z. F. (2011). Structural changes of cassava starch granules hydrolyzed by a mixture of alpha-amylase and glucoamylase. *Carbohydrate Polymers, 85*(1), 272-275.

das Neves, M. A., Kimura, T., Shimizu, C., & Nakajima, M. (2007). State of the art and future trends of bioethanol production. *Dynamic Biochemistry, Process Biotechnology and Molecular Biology, 1*(1), 1-14.

Davis-Knight, H. R., & Weightman, R. M. (2008). The potential of triticale as a low input cereal for bioethanol production, the Home-Grown Cereals Authority (HGCA) Project Cambridge, UK: ADAS UK Ltd, Centre for Sustainable Crop Management.

Debet, M. R., & Gidley, M. J. (2007). Why do gelatinized starch granules not dissolve completely? Roles for amylose, protein, and lipid in granule "Ghost" integrity. *Journal of Agricultural and Food Chemistry, 55*(12), 4752-4760.

Dhital, S., Shrestha, A. K., & Gidley, M. J. (2010). Relationship between granule size and in vitro digestibility of maize and potato starches. *Carbohydrate Polymers, 82*(2), 480-488.

Gallant, D. J., Bouchet, B., & Baldwin, P. M. (1997). Microscopy of starch: Evidence of a new level of granule organization. *Carbohydrate Polymers, 32*(3-4), 177-191.

Gao, J., Vasanthan, T., & Hoover, R. (2009). Isolation and characterization of high-purity starch isolates from regular, waxy, and high-amylose hulless barley grains. *Cereal Chemistry, 86*(2), 157-163.

Gomez, L. D., Steele-King, C. G., & McQueen-Mason, S. J. (2008). Sustainable liquid biofuels from biomass: the writing's on the walls. *New Phytologist, 178*(3), 473-485.

Juszczak, L. (2003). Surface of triticale starch granules - NC-AFM observations. *Electronic Journal of Polish Agricultural Universities, 6*(1), #08.

Juszczak, L., Fortuna, T., & Krok, F. (2003). Non-contact atomic force microscopy of starch granules surface. Part II. Selected cereal starches. *Starch/Starke, 55*(1), 8-16.

Kandil, A., Li, J., Vasanthan, T., Bressler, D. C., & Tyler, R. T. (2011). Compositional changes in whole grain flours as a result of solvent washing and their effect on starch amylolysis. *Food Research International, 44*(1), 167-173.

Kim, H. S., & Huber, K. C. (2008). Channels within soft wheat starch A- and B-type granules. *Journal of Cereal Science, 48*(1), 159-172.

Kimura, A., & Robyt, J. F. (1995). Reaction of enzymes with starch granules: kinetics and products of the reaction with glucoamylase. *Carbohydrate Research, 277*(1), 87-107.

Li, J. H., Guiltinan, M. J., & Thompson, D. B. (2007). Mutation of the maize sbela and ae genes alters morphology and physical behavior of wx-type endosperm starch granules. *Carbohydrate Research, 342*(17), 2619-2627.

Li, J. H., Vasanthan, T., Hoover, R., & Rossnagel, B. G. (2004). Starch from hull-less barley: V. In-vitro susceptibility of waxy, normal, and high-amylose starches towards hydrolysis by alpha-amylases and amyloglucosidase. *Food Chemistry, 84*(4), 621-632.

Li, J. H., Vasanthan, T., Rossnagel, B., & Hoover, R. (2001). Starch from hull-less barley: I. Granule morphology, composition and amylopectin structure. *Food Chemistry, 74*(4), 395-405.

Li, X., Gao, W. Y., Wang, Y. L., Jiang, Q. Q., & Huang, L. Q. (2011). Granule structural, crystalline, and thermal changes in native Chinese yam starch after hydrolysis with two different enzymes-alpha-amylase and gluco-amylase. *Starch-Starke, 63*(2), 75-82.

Liu, Q., Gu, Z., Donner, E., Tetlow, I., & Emes, M. (2007). Investigation of digestibility in vitro and physicochemical properties of A- and B-type starch from soft and hard wheat flour. *Cereal Chemistry, 84*(1), 15-21.

Naguleswaran, S., Li, J., Vasanthan, T., & Bressler, D. (2011). Distribution of granule channels, protein, and phospholipid in triticale and corn starches as revealed by confocal laser scanning microscopy. *Cereal Chemistry, 88*(1), 87-94.

Natural Resources Canada. (2011). Ethanol. http://www.oee.nrcan.gc.ca/transportation/alternative-fuels/fuel-facts/ethanol/about-ethanol.cfm?attr=16. (Accessed in April 2011).

Ohtani, T., Yoshino, T., Hagiwara, S., & Maekawa, T. (2000). High-resolution imaging of starch granule structure using atomic force microscopy. *Starch-Starke, 52*(5), 150-153.

Park, H., Xu, S., & Seetharaman, K. (2011). A novel in situ atomic force microscopy imaging technique to probe surface morphological features of starch granules. *Carbohydrate Research, 346*(6), 847-853.

Pejin, D., Mojovic, L. J., Vucurovic, V., Pejin, J., Dencic, S., & Rakin, M. (2009). Fermentation of wheat and triticale hydrolysates: A comparative study. *Fuel, 88*(9), 1625-1628.

Peng, M., Gao, M., Abdel-Aal, E. S. M., Hucl, P., & Chibbar, R. N. (1999). Separation and characterization of A- and B-type starch granules in wheat endosperm. *Cereal Chemistry, 76*(3), 375-379.

Quigley, T. A., Kelly, C. T., Doyle, E. M., & Fogarty, W. M. (1998). Patterns of raw starch digestion by the glucoamylase of Cladosporium gossypiicola ATCC 38026. *Process Biochemistry, 33*(6), 677-681.

Raeker, M. O., Gaines, C. S., Finney, P. L., & Donelson, T. (1998). Granule size distribution and chemical composition of starches from 12 soft wheat cultivars. *Cereal Chemistry, 75*(5), 721-728.

Rutherford, P. M., McCarthy, O. J., Arendt, E. K., & Figueiredo, C. T. (2008). Total nitrogen. In M. R. Carter & E. G. Gregorich (Eds.). Soil sampling and methods of analysis (pp. 239-240). Boca Raton, FL, USA: CRC Press.

Salman, H., Blazek, J., Lopez-Rubio, A., Gilbert, E. P., Hanley, T., & Copeland, L. (2009). Structure-function relationships in A and B granules from wheat starches of similar amylose content. *Carbohydrate Polymers, 75*(3), 420-427.

Sanchez, O. J., & Cardona, C. A. (2008). Trends in biotechnological production of fuel ethanol from different feedstocks. *Bioresource Technology, 99*(13), 5270-5295.

Shariffa, Y. N., Karim, A. A., Fazilah, A., & Zaidul, I. S. M. (2009). Enzymatic hydrolysis of granular native and mildly heat-treated tapioca and sweet potato starches at sub-gelatinization temperature. *Food Hydrocolloids, 23*(2), 434-440.

Soulaka, A. B., & Morrison, W. R. (1985). The amylose and lipid contents, dimensions, and gelatinization characteristics of some wheat starches and their A-granule and B-granule fractions. *Journal of the Science of Food and Agriculture, 36*(8), 709-718.

Stevnebo, A., Sahlstrom, S., & Svihus, B. (2006). Starch structure and degree of starch hydrolysis of small and large starch granules from barley varieties with varying amylose content. *Animal Feed Science and Technology, 130*(1-2), 23-38.

Sujka, M., & Jamroz, J. (2009). alpha-Amylolysis of native potato and corn starches - SEM, AFM, nitrogen and iodine sorption investigations. *LWT-Food Science and Technology, 42*(7), 1219-1224.

Sujka, M., & Jamroz, J. (2010). Characteristics of pores in native and hydrolyzed starch granules. *Starch/Starke, 62*(5), 229-235.

Tang, H., Ando, H., Watanabe, K., Takeda, Y., & Mitsunaga, T. (2001a). Fine structures of amylose and amylopectin from large, medium, and small waxy barley starch granules. *Cereal Chemistry, 78*(2), 111-115.

Tang, H. J., Ando, H., Watanabe, K., Takeda, Y., & Mitsunaga, T. (2001b). Physicochemical properties and structure of large, medium and small granule starches in fractions of normal barley endosperm. *Carbohydrate Research, 330*(2), 241-248.

Tomoaia-Cotisel, M., Cioica, N., Cota, C., Racz, C., Petean, I., Bobos, L. D., Mocanu, A., & Horovitz, O. (2010). Structure of starch granules revealed by atomic force microscopy. *Studia Universitatis Babes-Bolyai Chemia, 55*(2), 313-326.

Tomoaia-Cotisel, M., Cota, C., Mocanu, A., & Horovitz, O. (2010). Micro and nanostructure of starch granules from potato and maize. *Materiale Plastice, 47*(4), 426-432.

Uthumporn, U., Zaidul, I. S. M., & Karim, A. A. (2010). Hydrolysis of granular starch at sub-gelatinization temperature using a mixture of amylolytic enzymes. *Food and Bioproducts Processing, 88*(C1), 47-54.

Utrilla-Coello, R. G., Agama-Acevedo, E., de la Rosa, A. P. B., Rodriguez-Ambriz, S. L., & Bello-Perez, L. A. (2010). Physicochemical and enzyme characterization of small and large starch granules isolated from two maize cultivars. *Cereal Chemistry, 87*(1), 50-56.

Varatharajan, V., Hoover, R., Li, J., Vasanthan, T., Nantanga, K. K. M., Seetharaman, K., Liu, Q., Donner, E., Jaiswal, S., & Chibbar, R. N. (2011). Impact of structural changes due to heat-moisture treatment at different temperatures on the susceptibility of normal and waxy potato starches towards hydrolysis by porcine pancreatic alpha amylase. *Food Research International, 44*(9), 2594-2606.

Vasanthan, T., & Hoover, R. (1992). Effect of defatting on starch structure and physicochemical properties. *Food Chemistry, 45*(5), 337-347.

Vermeylen, R., Goderis, B., Reynaers, H., & Delcour, J. A. (2005). Gelatinisation related structural aspects of small and large wheat starch granules. *Carbohydrate Polymers, 62*(2), 170-181.

Wang, S., Thomas, K. C., Ingledew, W. M., Sosulski, K., & Sosulski, F. W. (1997). Rye and triticale as feedstock for fuel ethanol production. *Cereal Chemistry, 74*(5), 621-625.

CHAPTER 5

The susceptibility of large and small granules of waxy, normal and high-amylose genotypes of barley and corn starches towards amylolysis at sub-gelatinization temperatures*

5.1. INTRODUCTION

The importance of starch amylolysis in energy end-uses of grains has been discussed in the previous sections. Cereal grains are one of the raw materials used for bioethanol production; corn and wheat are used to a greater extent than barley, rye and triticale (das Neves, Kimura, Shimizu, & Nakajima, 2007; Sanchez & Cardona, 2008). In Canada, most of the ethanol currently produced is from corn and wheat grains. However due to the increasing cost of wheat and less availability of corn, there is a need to find out an alternative source for bioethanol production in Canada (Naguleswaran et al., 2012). Barley is a cheaper potential feedstock for bioethanol production compared to corn and wheat (Gibreel et al., 2009; Li, Vasanthan, Hoover, & Rossnagel, 2004). In Canada, barley has been ranked as the third cereal crop cultivated after wheat and corn [7.6 million tonnes in 2010 (Food and Agriculture Organization of the United Nations, 2012)]. Barley is a good source for bioethanol production, since it has high starch content and a diverse amylose composition (Asare et al., 2011; Gao, Vasanthan, & Hoover, 2009).

* A version of this chapter has been published in *Food Research International*, 51:771-782. (Adapted with permission of Elsevier Ltd.)

As discussed in Chapters 1 and 4, the current trend in bioethanol production using a non-cooking process (starch in grains are not gelatinized and liquefied by jet cooking) is getting popular in bioethanol industries due to the cost efficiency and a better recovery of co-products. Granular starch hydrolyzing enzymes (GSHE, a mixture of α-amylase and glucoamylase) was developed to hydrolyze the native starch granules into fermentable sugars at a sub-gelatinization temperature as GSHE has been shown to work effectively on non-cooking process. This technique is known as "raw starch hydrolysis" or "cold-cook process" in bioethanol industries, since starch is not cooked at a high temperature. In addition, raw starch hydrolysis has been shown to produce a better recovery of value-added co-products such as dried distiller's grain plus solubles (DDGS) due to the high stability of components such as proteins at low temperature (Gibreel et al., 2009).

However, the efficient conversion of native starch into sugars using GSHE primarily depends on starch composition, morphology, and molecular and granular structural features, which have been shown to influence the rate and extent of amylolysis. Native starch hydrolysis with amylases occurs in several steps, which include diffusion to the solid surface, adsorption and finally catalysis, and the rate of hydrolysis is initially fast but continues at a slower and more persistent rate (Oates, 1997). The influence of structure and physicochemical properties of starches such as granule size, granule ultrastructure, amylose:amylopectin content ratio, granule porosity, and

amylose-lipid complex on *in vitro* hydrolysis have been studied (Asare et al., 2011; Dhital, Shrestha, & Gidley, 2010; Holm et al., 1983; Liu et al., 2007; Naguleswaran et al., 2012; Salman at al., 2009; Sharma et al., 2007; Stevnebø, Sahlström, & Svihus, 2006; Sujka & Jamroz, 2007; Uthumporn et al., 2010; Zhang, Ao, & Hamaker, 2006). Recently, the effect of granule size, surface pores, internal channels, protein, and phospholipids in starch granules of normal genotypes from triticale, wheat and corn on amylolysis has been reported (Naguleswaran et al., 2011, 2012). However, there are no reports on the susceptibility of large and small granules of pure hull-less barley starches (differing in amylose content) in relation to hydrolysis by GSHE at sub-gelatinization temperatures.

The objective of this study was to ascertain whether the hydrolysis of unfractionated and fractionated (large and small) starch granules of waxy (<10% amylose), normal (20 – 30% amylose), high-amylose (>40% amylose) hull-less barley and corn starches of varying amylose content (0 – 70%) by GSHE at sub-gelatinization temperature are influenced by the morphology, architecture and physicochemical properties of the above starches. The results of this study may enable scientists to maximize the conversion of native starch into sugars at low temperatures and to optimize ethanol yield for a cost efficient bioethanol production or to optimize the sugar content in syrup production.

5.2. MATERIALS AND METHODS

5.2.1. Materials

Grains from three hull-less barley cultivars (waxy, CDC Candle; normal, CDC McGwire; and high-amylose, SH 99250) were obtained from the Crop Development Center at the University of Saskatchewan in Saskatoon (SK, Canada). Commercial corn starches of waxy (Amioca), normal (Melojel) and high-amylose (Hylon VII) were from National Starch Food Innovation in Bridgewater (NJ, USA). The Stargen 002 (570 GAU/g) was donated by Genencor International in Rochester (NY, USA). 8-aminopyrene-1,3,6-trisulfonic acid, trisodium salt (APTS) was purchased from Invitrogen (Molecular Probes, Eugene, OR, USA). All other chemicals and reagents used in this study were of ACS grade.

5.2.2. Grain grinding and starch isolation

The barley grains were ground into meals in a Retsch mill (Model ZM 200, Haan, Germany) using a ring sieve with an aperture size of 0.5 mm. Pure starch (purity >95%, w/w) was isolated from grain meal using the procedure described by Gao, Vasanthan, & Hoover (2009). A detailed procedure is presented in appendix.

5.2.3. Fractionation of large and small starch granules

Isolated barley starches and commercial corn starches were fractionated into large and small granules using a centrifugal sedimentation protocol as described in Chapter 4.2.4.

5.2.4. Chemical composition and granule size analysis of starches

Granule size and size distribution of unfractionated native starches and moisture, ash, starch, protein, lipid and apparent amylose contents of unfractionated and fractionated (large and small) starches were determined following the methods and techniques described in Chapter 4.

5.2.5. Morphological characterization of starches

The morphology of unfractionated and fractionated starch granules were characterized using SEM and CLSM techniques according to the methods described in Chapter 3. The enzymatically hydrolysed starch residues were recovered with addition of anhydrous ethanol followed by centrifugation (Fisher Scientific accuSpin^{TM} 400 bench top Centrifuge, Germany) at 5000 x*g* for 10 min. The starch granules without addition of enzyme (control) and the enzymatically hydrolysed starch residues after 24h and 72h were also examined microscopically.

5.2.5.1. Scanning Electron Microscopy (SEM)

Starch samples were mounted on circular aluminum stubs with double-sided sticky tape, coated with gold to a thickness of 12 nm followed by examined and photographed in a JEOL scanning electron microscope (Model JSM 6301 FXV, JEOL Ltd., Tokyo, Japan) at an accelerating voltage of 5 kV.

5.2.5.2. Confocal Laser Scanning Microscopy (CLSM)

The native starch granules were stained with 8-aminopyrene-1,3,6-trisulfonic acid (APTS) dye and visualized under a confocal laser scanning microscope (Zeiss LSM 710, Carl Zeiss MicroImaging GmbH, Jena, Germany), which was equipped with a 40x/1.3 oil objective lens. Images of optical sections of starch granules were recorded and examined with ZEN 2009 Light Edition software (Carl Zeiss MicroImaging GmbH, Jena, Germany).

5.2.6. Structural characterization of starches

5.2.6.1. Wide Angle X-Ray Diffraction (WAXD)

X-ray diffractograms of all starches were obtained with cross beam optics (CBO) technology of Rigaku Ultima IV multipurpose X-ray diffraction meter (Rigaku Americas, The Woodlands, TX, USA) according to the method described by Gao, Vasanthan, & Hoover (2009). A detailed procedure of X-Ray analysis is presented in appendix.

5.2.6.2. Differential Scanning Calorimetry (DSC)

Gelatinization parameters of barley and corn starches were measured using a DSC Q100 (TA Instruments, New Castle, DE, USA) equipped with a data acquisition and processing station. Water (15 μL) was added with a microsyringe to native starch (5 mg, dry basis) in a large volume stainless steel DSC pan (PerkinElmer Inc., Shelton, CT, USA) which was then sealed, and allowed to

equilibrate for 24h at room temperature. The scanning temperature range and the heating rate were 10–150°C and 10°C/min, respectively. In all measurements, the thermogram was recorded with an empty sealed-stainless pan as a reference. The thermal transitions of starch were defined in terms of temperature at T_o (onset), T_p (peak), and T_c (conclusion). ΔH refers to the enthalpy associated with the transition. This enthalpy corresponds to the area enclosed by drawing a straight line between T_o and T_c and is expressed as weight of dry starch (J/g).

5.2.7. Amylolysis of starches using granular starch hydrolyzing enzyme

Starch samples (0.3% dry basis , w/v) were hydrolyzed with Stargen 002 enzyme (24 U/30 mg starch) in 50 mM sodium acetate buffer (pH 4.0) at 55^{o}C for 1h followed by at 30^{o}C for 72h in a shaking water bath (Model BS-11, Jeio Tech Inc., Korea) according to the instructions given by enzyme manufacturer (Genencor Intl. in Rochester, NY, USA). The hydrolysates were withdrawn at 1, 24, 48 and 72h for the determination of degree of hydrolysis (DH). DH was expressed as a percentage of reducing value measured by the 3, 5-dintrosalicylic acid (1%, w/v) method (Bruner, 1964). Control starch samples were run concurrently without enzyme addition.

5.2.8. Statistical analyses

All treatments and analyses were carried out in triplicate. Analysis of variance using the General Linear Model (GLM) procedure and Pearson correlation

statistics were performed using the SAS® Statistical Software, Version 9.3 (SAS Institute Inc., Cary, NC, USA, 2011). Multiple comparisons of the means were carried out using Tukey's Studentized Range (HSD) Test at $\alpha = 0.05$.

5.3. RESULTS AND DISCUSSION

5.3.1. Composition of unfractionated and fractionated starches

The chemical composition of unfractionated and fractionated (large and small) starches from waxy (WX), normal (NM) and high-amylose (HA) genotypes of corn and barley are presented in Table 5.1. The purity of the starches was judged on the basis of low protein (<0.5%) and low ash (<0.3%) contents (Table 5.1), and microscopic observations (Figure 5.1), where the granules appeared smooth with free of other grain components. As shown in Table 5.1, isolated pure starches from barley flours and commercial corn starches had higher starch content (>95%). However, the starch content of HA corn starches ranged between 87 and 88% and this low value may have been due to greater resistance of HA starch to amylase hydrolysis (Lauro et al., 1993; Sharma et al., 2010) during the starch determination procedure. In both unfractionated and fractionated starches, starch and amylose contents were strongly correlated ($r = – 0.9$, $p<0.05$). In corn and barley starches, the lipid contents were higher in HA than in WX and NM genotypes (Table 5.1). Apparent amylose (AM) and lipid contents were strongly correlated in unfractionated ($r = 0.93$, $p<0.05$) and fractionated ($r = 0.88$ at $p<0.05$) starch granules.

Table 5.1: Composition of corn and barley starches (%, db[1])

Starches	Starch	Protein	Lipid	Ash
Corn				
Waxy				
Unfractionated	$98.9^{abc} \pm 0.2$	$0.36^{e} \pm 0.02$	$0.51^{jk} \pm 0.005$	$0.19^{e} \pm 0.004$
Large	$98.5^{a-d} \pm 0.5$	$0.25^{h} \pm 0.01$	$0.42^{n} \pm 0.004$	$0.11^{h} \pm 0.003$
Small	$98.5^{a-d} \pm 0.4$	$0.31^{f} \pm 0.01$	$0.48^{l} \pm 0.001$	$0.08^{kj} \pm 0.005$
Normal				
Unfractionated	$98.5^{a-d} \pm 0.3$	$0.46^{bc} \pm 0.01$	$0.69^{h} \pm 0.004$	$0.20^{d} \pm 0.004$
Large	$98.0^{b-e} \pm 0.4$	$0.30^{fg} \pm 0.02$	$0.64^{i} \pm 0.003$	$0.09^{ij} \pm 0.004$
Small	$97.9^{c-f} \pm 0.2$	$0.37^{e} \pm 0.02$	$0.72^{g} \pm 0.005$	$0.07^{k} \pm 0.002$
High Amylose				
Unfractionated	$87.3^{h} \pm 0.4$	$0.51^{a} \pm 0.01$	$1.04^{a} \pm 0.005$	$0.25^{c} \pm 0.004$
Large	$88.1^{h} \pm 0.5$	$0.43^{bcd} \pm 0.02$	$0.91^{d} \pm 0.002$	$0.14^{g} \pm 0.002$
Small	$87.7^{h} \pm 0.2$	$0.46^{b} \pm 0.02$	$0.98^{b} \pm 0.004$	$0.12^{h} \pm 0.003$
Barley				
Waxy				
Unfractionated	$99.0^{ab} \pm 0.2$	$0.26^{gh} \pm 0.01$	$0.52^{j} \pm 0.005$	$0.20^{d} \pm 0.004$
Large	$99.1^{a} \pm 0.1$	$0.20^{i} \pm 0.01$	$0.45^{m} \pm 0.004$	$0.13^{g} \pm 0.003$
Small	$98.9^{ab} \pm 0.3$	$0.24^{hi} \pm 0.02$	$0.50^{k} \pm 0.005$	$0.10^{i} \pm 0.004$
Normal				
Unfractionated	$97.5^{def} \pm 0.4$	$0.30^{fg} \pm 0.02$	$0.83^{e} \pm 0.005$	$0.27^{b} \pm 0.005$
Large	$97.2^{ef} \pm 0.1$	$0.25^{h} \pm 0.00$	$0.72^{g} \pm 0.004$	$0.16^{f} \pm 0.003$
Small	$96.9^{f} \pm 0.1$	$0.27^{f-h} \pm 0.01$	$0.77^{f} \pm 0.003$	$0.14^{g} \pm 0.001$
High Amylose				
Unfractionated	$95.7^{g} \pm 0.4$	$0.42^{cd} \pm 0.01$	$0.97^{b} \pm 0.005$	$0.35^{a} \pm 0.002$
Large	$95.6^{g} \pm 0.4$	$0.36^{e} \pm 0.02$	$0.90^{d} \pm 0.004$	$0.25^{c} \pm 0.005$
Small	$95.5^{g} \pm 0.3$	$0.40^{de} \pm 0.01$	$0.95^{c} \pm 0.005$	$0.20^{d} \pm 0.003$

[1] dry basis.
Values are a percentage of mean ± standard deviation in dry weight basis, and values with the same superscript in the same column are not significantly different at $\alpha = 0.05$.

Overall, in large granules, protein and lipid contents were lower than in small granules (Table 5.1). A higher protein and lipid content in small granules may be due to their greater surface to volume ratio, which could be associated with more protein and lipids than their large counterparts. The above results are in

agreement with previous reports on corn, barley, triticale and wheat starches (Liu et al., 2007; MacGregor & Ballance, 1980; Naguleswaran et al., 2012).

5.3.2. Granule size distribution of unfractionated starches

Corn and barley starch granules showed a bimodal size distribution with a diameter range of 2–26 μm and 1–24 μm respectively (Figures 5.1 & 5.2, and Table 5.2). The mean granule size of large and small granules were >14 μm and <5 μm, respectively, in both corn and barley starches. The proportions of large and small granules by number and by weight significantly varied among genotypes of corn and barley starches (Table 5.2). In both corn and barley starches, large granules contained a lower proportion of total granules by number (6–20%) and had a higher proportion of total granules by weight (53 – 89%) than small granules (80–94% by number and 11–47% by weight). A higher number of small granules in total starch increase the surface area per unit mass for fast chemical reaction and/or enzyme diffusion. Compared to WX and NM starches, the HA corn and HA barley starches had greater proportion of small granules by number (90– 94%) and by weight (32–47%) than their large granules. Correlations were seen between AM content, and number percent ($r = 0.6$, $p<0.05$) or weight percent ($r = 0.7$, $p<0.05$) in small granules of both corn and barley starches. The results on granule size and size distribution of barley and corn starch granules are in agreement with previous studies (Ao & Jane, 2007; Li, Vasanthan, Rossnagel, & Hoover, 2001).

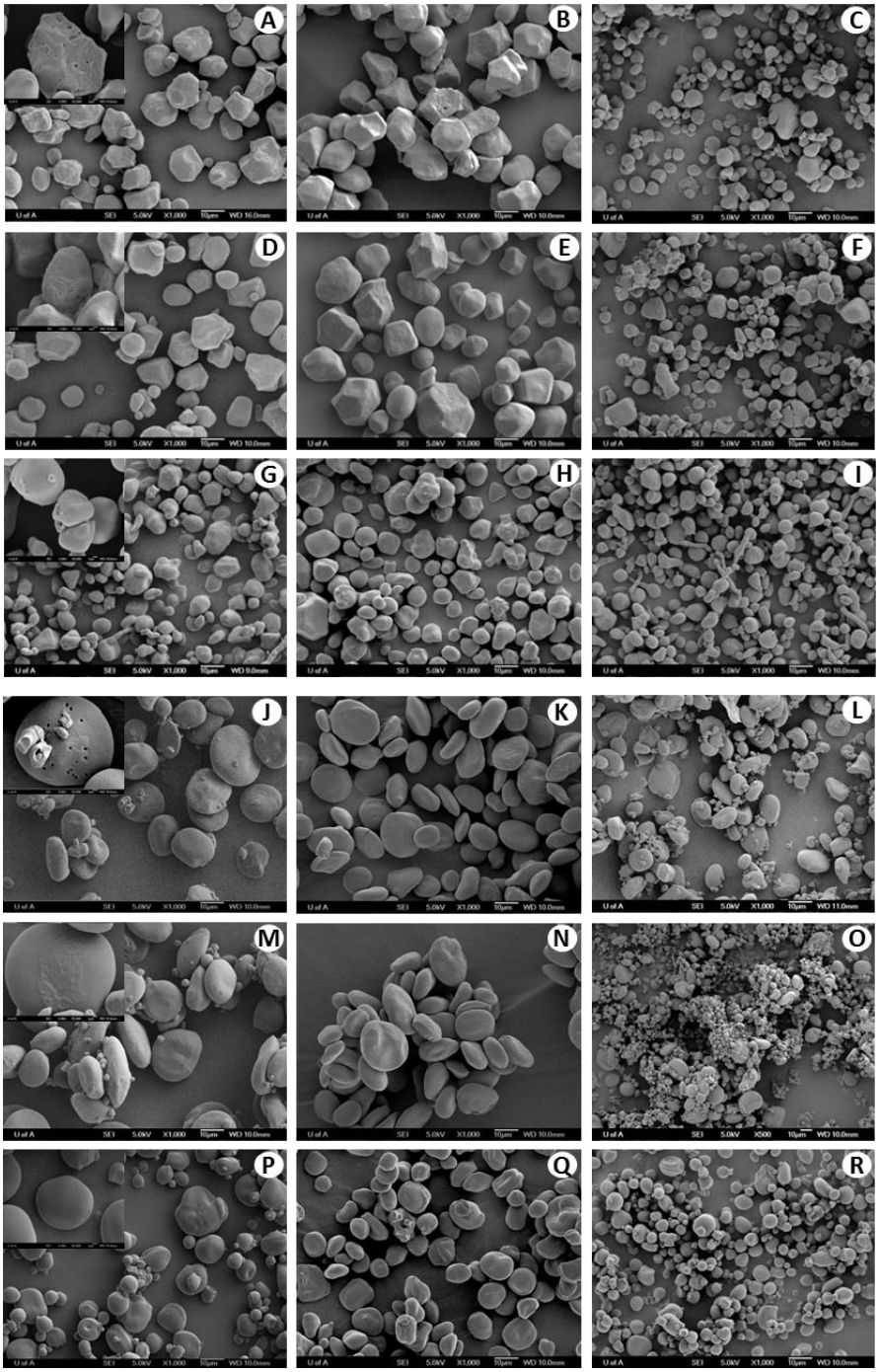

Figure 5.1: Scanning electron microscopy (SEM) images of waxy corn (A-unfractionated; B-large granules; C-small granules), normal corn (D-unfractionated; E-large granules; F-small granules), high-amylose corn (G-unfractionated; H-large granules; I-small granules), waxy barley (J-unfractionated; K-large granules; L-small granules), normal barley (M-unfractionated; N-large granules; O-small granules) and high-amylose barley (P-unfractionated; Q-large granules; R-small granules) starches (x1000, scale bar=10µm). Insets in A, D, G, J, M & P were at x5000, scale bar=1µm

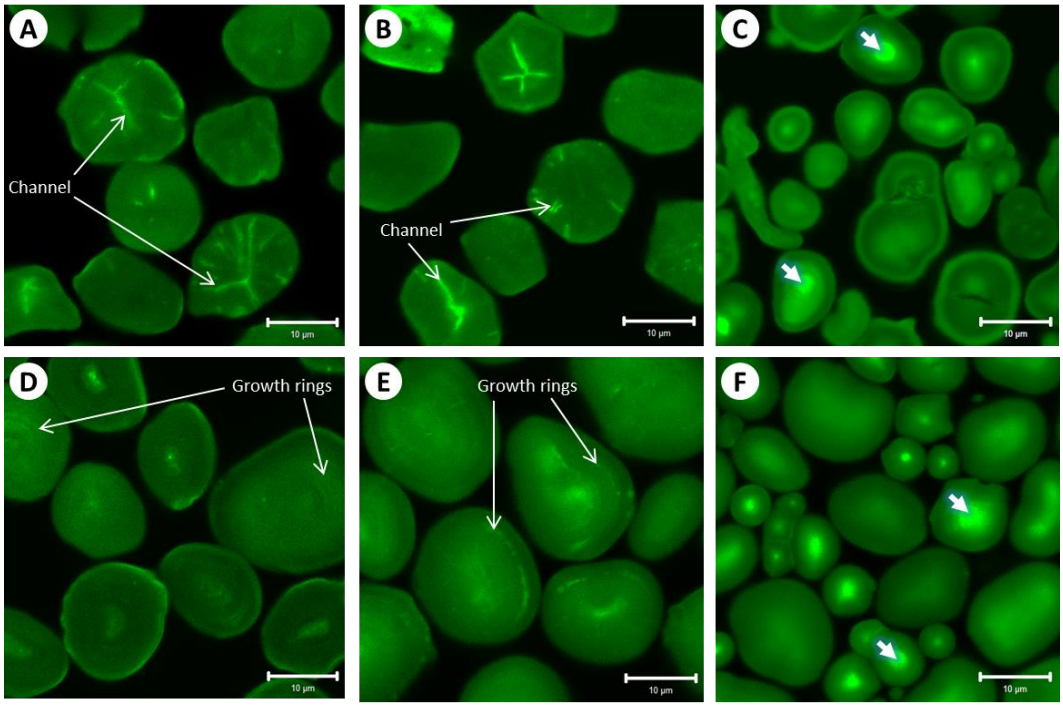

Figure 5.2: Confocal laser scanning microscopy (CLSM) images of unfractionated corn (A-waxy; B-normal; C-high-amylose) and barley (D-waxy; E-normal; F-high-amylose) starches. Small thick arrows indicate the central amorphous regions of granules (scale bar = 10 µm).

Table 5.2: Granule size distribution of corn and barley starches

Starches	Granule size (µm)	Mean			Number (%)		Weight (%)	
		O[1]	L[2]	S[3]	Large	Small	Large	Small
Corn								
Waxy	2 - 20	7.8	14.6	4.8	$19.8^{a} \pm 1.1$	$80.2^{d} \pm 1.1$	$86.5^{b} \pm 0.6$	$13.5^{d} \pm 0.6$
Normal	2 - 26	9.4	17.1	4.8	$16.8^{b} \pm 1.8$	$83.2^{c} \pm 1.8$	$84.9^{c} \pm 0.3$	$15.1^{c} \pm 0.3$
High amylose	2 - 22	8.5	15.4	4.9	$10.2^{c} \pm 0.5$	$89.8^{b} \pm 0.5$	$67.6^{d} \pm 1.5$	$32.4^{b} \pm 1.5$
Barley								
Waxy	1.5 - 22	8.5	15.4	4.9	$20.0^{a} \pm 1.5$	$80.0^{d} \pm 1.5$	$88.8^{a} \pm 0.1$	$11.2^{e} \pm 0.1$
Normal	1 - 24	8.6	16.2	4.6	$7.0^{d} \pm 0.1$	$93.0^{a} \pm 0.1$	$86.9^{b} \pm 0.1$	$13.1^{d} \pm 0.1$
High amylose	1 - 20	8	14.6	4.9	$6.2^{d} \pm 0.1$	$93.8^{a} \pm 0.1$	$53.5^{e} \pm 0.1$	$46.5^{a} \pm 0.1$

[1] Overall mean (µm)
[2] Mean of large granules (µm)
[3] Mean of small granules (µm)
Values of number and weight percentages are mean ± standard deviation in number and weight basis, respectively. Values with the same superscript in the same column are not significantly different at α = 0.05. Large starch granule was defined as granule diameter >10µm.

5.3.3. Morphology and microstructure of starch granules

SEM (Figure 5.1) and CLSM (Figure 5.2) revealed the morphological and microstructural features of corn and barley starches. As discussed in the previous section, both corn and barley starches consisted of a mixture of large and small granules (Figures 5.1 and 5.2). The large granules of corn starches were polyhedral in shape (Figures 5.1B, E & H), whereas the large granules of barley starches were spherical/disk/lenticular in shape (Figures 5.1K, N & Q). The shape of the small granules was irregular/spherical in both corn (Figures 5.1C, F & I) and barley (Figures 5.1L, O & R) starches, and most of the small granules in barley starches were present as clusters (Figures 5.1L, O & R). Compared to those of large granules of NM and HA genotypes, large granules of WX genotype exhibited numerous large pores that were unevenly distributed on the granule surface (Figures 5.1A & J-insets). These pores naturally exist on the granule surface and may reflect the ends of tube like channels within starch granules.

CLSM is a versatile tool for examining the cross-sections and internal structure of starch granules without disturbing the microstructural features of starch. An aminofluorophore, 8-aminopyrene-1,3,6-trisulfonic acid (APTS) is one of the specific dyes that reacts with the reducing ends of amylose and amylopectin in a starch granule (Blennow et al., 2003). In the current study, growth rings, internal channels, and a central amorphous region of corn and barley starch granules were visible by fluorescence intensity under CLSM (Figure 5.2). Compared to WX and NM genotypes, the HA genotypes of both corn and

barley showed higher fluorescence intensity in the center (hilum) of the granules (Figures 5.2C & F). This could reflect a higher concentration of amylose molecules in the hilum region. The internal channels were more visible in WX and NM genotypes of corn starches (Figures 5.2A & B) compared to other genotypes, and these observations are in agreement with previous reports on corn starches. According to recent studies on wheat, triticale and corn starches by CLSM, the internal channels and the surface of starch granules were found to be rich in protein and phospholipids (Lee & BeMiller, 2008; Naguleswaran et al., 2011). These starch associated minor components together with starch molecules (amylose and amylopectin) may contribute to the complex morphological structure of the starch granules (Naguleswaran et al., 2011; Tomoaia-Cotisel et al., 2010). It is interesting to highlight that the HA genotype of corn starch contained some elongated starch granules that were prevalent in the small granules (Figures 5.1I and 5.2C). Jiang et al. (2010) reported that two or more starch granules could fuse together during granule development resulting in the formation of elongated starch granules which are highly resistant to amylase digestion.

5.3.4. Amylose content and relative crystallinity of starches

Apparent amylose (AM) content and relative crystallinity (RC) of corn and barley starches are summarized in Table 5.4. The AM content significantly varied among genotypes of both corn (1 – 70%) and barley (4 – 40%) starches. These results are in agreement with previous reports on corn and barley starches (Asare et al.,

2011; Gao, Vasanthan, & Hoover, 2009; Li et al., 2001; Stevnebø, Sahlström, & Svihus, 2006). Regardless of genotypes, large granules of corn and barley starches had a higher AM content (1.1 – 69.8% and 6.0 – 39.5%, respectively) than their small granule counterparts did (1.0 – 65.7 % and 4.0 – 34.8 %, respectively), indicating that the AM content varies with granule size within and between starch sources. This was in agreement with previous studies, where the difference in AM content between large and small granules was 1.3% in corn (Utrilla-Coello, Agama-Acevedo, de la Rosa, Rodriguez-Ambriz, & Bello-Perez, 2010) and 3–7% in barley (Ao & Jane, 2007; Tang, Ando, Watanabe, Takeda, & Mitsunaga, 2001) starches. Correlations were also found between AM content and proportion of small granules (by number basis, $r = 0.6$ and by weight basis, $r = 0.7$, $p<0.05$), this was in agreement with previous findings reported for barley starches (Asare et al., 2011; Li et al., 2001).

The crystalline structure of starch is often analysed by wide angle X-ray diffraction (WAXD) technique. In the present study, WAXD revealed that both unfractionated and fractionated starches from the genotypes WX and NM corn, and WX, NM and HA barley starches exhibited the typical 'A'-type polymorph pattern with characteristic peaks at Bragg angles (2ϑ) of 15°, 17°, 18°, and 23° (Figure 5.3). However, the HA genotype of corn of both unfractionated and fractionated (large and small) starches showed a mixture of 'A'- and 'V'-type polymorph patterns (Tawil et al., 2012) with strong peaks at Bragg angles 2ϑ = 17° and 20°, and weak peaks at 2ϑ = 15° and 23° (Figure 5.3). The peak at 2ϑ =

20° represents the amylose-lipid complex (V-type) in starch granules (Tawil et al., 2012; Waduge et al., 2006) which was more pronounced in the HA genotype of corn starches followed by HA genotype of barley starches (Figure 5.3). The intensity of the 20° 2ϑ peak increased with increase in both amylose (Table 5.4) and lipid (Table 5.1) contents indicating a higher proportion of V-type lipid-amylose complexes in HA genotypes. The WX starches had minimal AM content, however the presence of a weak peak at 2ϑ = 20° in WX starches may be due to V-complex formation between lipids and the outer branches of amylopectin (Waduge et al., 2006). The difference in WAXD peaks between large and small granules of corn and barley starches was marginal (Figure 5.3). A small peak at $2\vartheta = 5.5^{o}$, which represents the presence of 'B'-type crystals was visible (indicated by arrows in Figure 5.3) in both unfractionated (Figure 5.3A) and fractionated (Figures 5.3B & C) HA corn starches. A similar peak has been reported in barley starches (Waduge et al., 2006). However, in this study, the peak at $2\vartheta = 5.6^{o}$ did not appear in the X-ray diffractograms of barley starches. This may have been due to variations in starch isolation protocol and starch cultivars.

RC significantly varied among genotypes of corn and barley starches and was in the range of 20.3 – 35.9% and 20.2 – 34.3%, respectively (Table 5.4). The RC values decreased with increasing amylose content of starches and a strong correlation was found between RC and AM content in both unfractionated ($r = -0.95$, $p<0.05$) and fractionated ($r = -0.88$, $p<0.05$) granules.

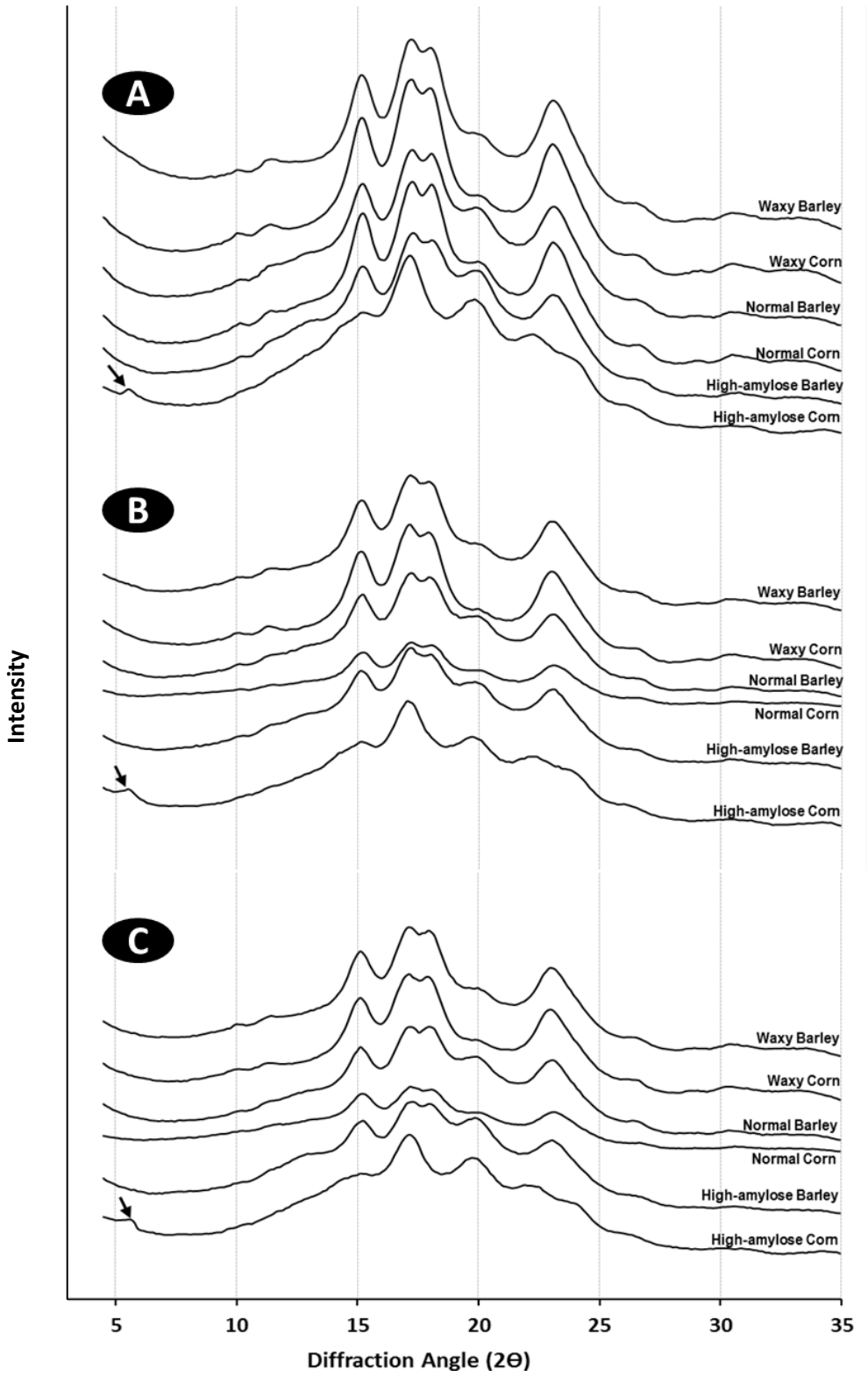

Figure 5.3: X-ray diffractograms of corn and barley starches (A-Unfractionated, B-Large granules and C-Small granules). Small arrows point out the peak at $2\theta \approx 5.5^{o}$.

These findings are in agreement with earlier work on unfractionated granules (Gao, Vasanthan, & Hoover, 2009); however in the present study the RC values were lower than those of reported values for corn (20.8 – 41.1%) and barley (29.1 – 39.1%) starches. The progressive decrease in RC (WX>NM>HA) with increase in amylose content (WX<NM<HA) in unfractionated and fractionated corn and barley starches, reflects the interplay between the amount of amorphous regions (HA>NM>WX) and the extent to which amylose chains are co-crystallized (HA>NM>WX) with the amylopectin side chains and/or with the α-(1-6) branch points that are present in the amorphous lamella of amylopectin. Both types of co-crystallization could disrupt the alignment of double helices, thereby changing the orientation of ordered crystallites to the X-ray beam. Since amylose in starch granules is amorphous (Ao & Jane, 2007; Luo, Fu, Gao, & Yu, 2011), the higher RC of WX genotypes may have been due to their lower AM content (Table 5.4). The large granules of WX, NM and HA genotypes had higher RC than their small granule counterparts in both corn (2 – 4% higher) and barley (2 – 3% higher) starches (Table 5.4). DSC studies showed that large granules of WX, NM and HA genotypes of both corn and barley starches had a lower gelatinization temperature range than their small granule counterparts (Table 5.3). This suggests that crystallites of large granules are more perfectly aligned within the crystalline lamella. This would then explain the higher degree of crystallinity seen with the large granules (Table 5.4).

5.3.5. Thermal characteristics of starches

The gelatinization transition temperatures and enthalpy of gelatinization of corn and barley starches are presented in Table 5.3. The onset (T_o), peak (T_p), conclusion (T_c), gelatinization temperature range (T_c–T_o) and gelatinization enthalpy (ΔH) significantly varied between corn and barley starches. In unfractionated corn starches, T_o, T_c, T_c-T_o and ΔH followed the order: HA>NM>WX, HA>NM≈WX, HA>WX>NM and WX>NM>HA, respectively. The corresponding order for unfractionated barley starches was WX>NM=HA, HA>WX>NM, HA>NM≈WX, and WX>NM>HA, respectively. Differences in T_o between large and small granules of WX, NM and HA genotypes of barley and corn starches was only marginal. In corn starches, small granules of the NM genotype exhibited a wider T_c-T_o than the large granules. However, there was no significant difference in T_c-T_o between large and small granules of WX and HA genotypes. Also, there was no significant difference in T_p between large and small granules in all three genotypes of barley starch. However, in corn starches, T_p of small granules of HA genotype was much higher than that of the large granules. Whereas, there was no significant difference found in T_p between small and large granules of WX and NM genotypes of corn starches. Difference in T_c between small and large granules in all three genotypes of corn starch was not significant. However, in barley starches, T_c was significantly higher in small granules of all three genotypes. The T_o represents the melting of the weakest crystallites. The results showed that crystallites of barley starches are much

Table 5.3: Thermal characteristics of corn and barley starches

Starches	T_o [1]	T_p [1]	T_c [1]	T_c-T_o [2]	ΔH [3]
Corn					
Waxy					
Unfractionated	63.4^{d} ± 0.1	71.8^{de} ± 0.1	81.2^{b} ± 0.0	17.9^{e} ± 0.1	20.9^{b} ± 0.9
Large	62.2^{e} ± 0.6	70.6^{ef} ± 0.3	80.6^{b} ± 0.3	18.3^{de} ± 0.9	20.4^{bc} ± 1.5
Small	61.5^{e} ± 0.5	71.4^{d-f} ± 1.3	79.9^{bc} ± 0.6	18.4^{de} ± 0.1	14.5^{gh} ± 0.1
Normal					
Unfractionated	66.8^{b} ± 0.3	72.3^{d} ± 0.3	80.7^{b} ± 0.5	13.8^{g} ± 0.8	18.5^{cd} ± 0.2
Large	65.3^{c} ± 0.2	70.6^{ef} ± 0.5	77.5^{de} ± 0.2	12.2^{h} ± 0.4	15.5^{fgh} ± 1.0
Small	63.4^{d} ± 0.0	70.1^{f} ± 0.2	78.9^{cd} ± 0.0	15.5^{f} ± 0.0	13.7^{h} ± 0.2
High Amylose					
Unfractionated	69.4^{a} ± 0.2	83.7^{b} ± 1.6	109.9^{a} ± 0.2	40.5^{b} ± 0.5	16.0^{efg} ± 0.9
Large	67.7^{b} ± 0.2	80.3^{c} ± 0.5	109.6^{a} ± 1.1	41.9^{a} ± 0.9	23.9^{a} ± 1.6
Small	67.4^{b} ± 0.2	86.0^{a} ± 1.4	110.2^{a} ± 1.4	42.8^{ab} ± 1.1	21.2^{b} ± 0.4
Barley					
Waxy					
Unfractionated	57.5^{f} ± 0.0	62.9^{ij} ± 0.4	70.2^{h} ± 0.4	12.7^{gh} ± 0.4	17.9^{de} ± 1.2
Large	57.5^{f} ± 0.3	62.7^{j} ± 0.3	70.1^{h} ± 0.7	12.6^{gh} ± 0.4	16.1^{efg} ± 1.5
Small	55.6^{g} ± 0.0	63.1^{ij} ± 0.4	71.7^{g} ± 0.8	16.1^{f} ± 0.8	15.3^{fgh} ± 0.9
Normal					
Unfractionated	54.6^{hi} ± 0.2	59.6^{k} ± 0.4	67.4^{i} ± 1.0	12.8^{gh} ± 1.2	16.3^{efg} ± 0.6
Large	55.3^{gh} ± 0.1	59.4^{k} ± 0.0	66.5^{i} ± 0.3	11.1^{h} ± 0.2	17.0^{def} ± 0.3
Small	53.1^{j} ± 0.4	59.5^{k} ± 0.2	68.9^{h} ± 0.2	15.8^{f} ± 0.2	16.1^{efg} ± 0.0
High Amylose					
Unfractionated	54.6^{hi} ± 0.3	66.1^{g} ± 0.6	76.6^{e} ± 0.2	22.0^{c} ± 0.1	13.6^{h} ± 1.2
Large	53.9^{ij} ± 1.3	64.2^{hi} ± 0.4	73.7^{f} ± 0.7	19.8^{d} ± 1.9	13.4^{h} ± 0.9
Small	54.0^{i} ± 0.3	65.2^{gh} ± 0.0	77.5^{de} ± 0.8	23.5^{c} ± 0.5	9.7^{i} ± 1.2

[1] T_o, T_p and T_c indicate the gelatinization temperatures of onset, peak and conclusion, respectively (^{o}C).
[2] $T_c - T_o$ indicate the gelatinization temperature range (^{o}C).
[3] Enthalpy of gelatinization (J/g)
Values are mean ± standard deviation, and values with the same superscript in the same column are not significantly different at $\alpha = 0.05$.

weaker (reflected in lower T_o values) than those of corn starches. Among genotypes of corn and barley starches, there was no significant variation in crystallite strength between large and small granules. The difference in

crystallite strength was also reflected by higher values of T_p, T_c and ΔH for corn starches. The difference in ΔH between corn and barley starches, suggest that double helices that are aligned within the crystalline lamella are more strongly associated in the former. In both corn and barley starches, variation in strength of double helical association between large and small granules was significant in all three genotypes. This difference was more pronounced in WX and HA genotypes of corn and barley starches, respectively. T_c-T_o represents the crystalline heterogeneity. In corn starches, with the exception of the NM genotype, the degree of heterogeneity between small and large granules was not significant in WX and HA genotypes. The heterogeneity, however, was higher in the small granules (WX ≈ NM < HA) of barley starches. Differences in heterogeneity between small and large granules could reflect the interplay among differences in: 1) crystallite size, 2) type of crystallite association (crystallites formed between AM-AM and or AM-AP chains), and 3) crystallite perfection.

5.3.6. Amylolysis of corn and barley starches

The unfractionated and fractionated granules of WX, NM and HA genotypes of corn and barley starches were hydrolysed to evaluate their susceptibilities towards the granular starch hydrolysing enzymes at sub-gelatinization temperatures (55^{o}C for 1h followed by at 30^{o}C for periods ranging from 24 to 72h). The degree of hydrolysis (DH) measured as a percentage of reducing value is shown in Figure 5.4 (55^{o}C for 1h) and Table 5.4 (30^{o}C for 24-72h). During

hydrolysis at 55°C, the DH of unfractionated corn starches followed the order: WX > NM > HA. The corresponding order for unfractionated barley starches was: NM > WX > HA. The difference in DH between NM and HA unfractionated corn starches, reflect the higher lipid content (Table 5.1) and higher amylose content (Table 5.4) in the latter. The very low DH seen with unfractionated HA corn starch (Figure 5.4), suggests that due to its very high amylose content (Table 5.4), the amylose chains may have been compactly packed (reduces amylose chain flexibility) within the bulk amorphous regions of the granule, thereby rendering the conformational transformation of the D-glucopyranosyl units (chair to half chair) during hydrolysis difficult. This would decrease the accessibility of the glycosidic linkages to hydrolysis by the starch enzymes. The higher DH seen with unfractionated WX corn starch is a reflection of its low content of amylose and

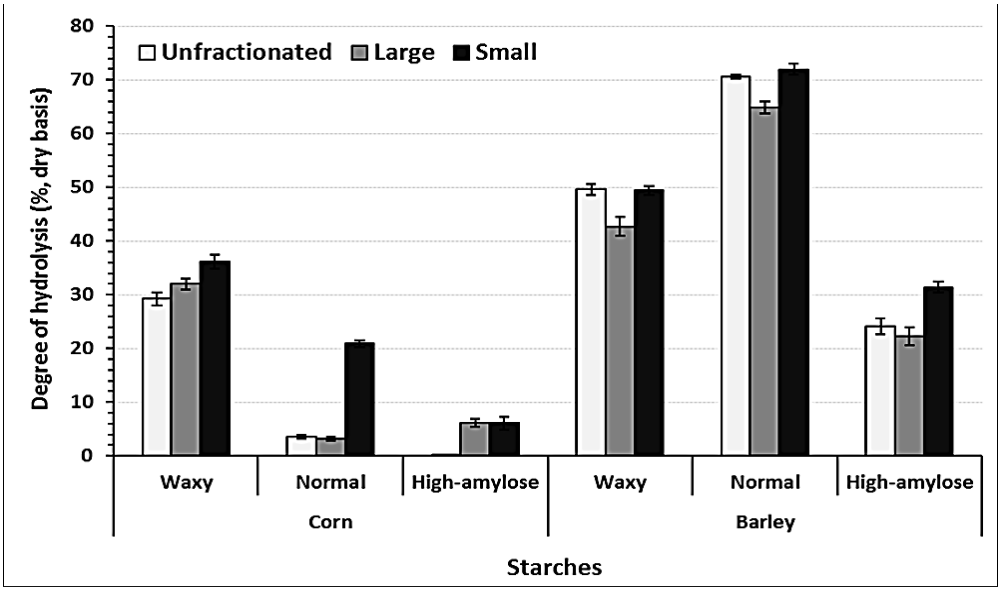

Figure 5.4: Degree of hydrolysis (%) of unfractionated, large and small granules of corn and barley starches, hydrolyzed at 55°C for 1h.

bound lipids. CLSM images (Figure 5.2) showed that the intensity of APTS staining was more pronounced at the granule periphery of NM barley starch. Since hydrolysis has been shown to begin near the granule periphery, amylose chains in NM barley starch would be more rapidly hydrolyzed than those of NM corn starch during the first hour of hydrolysis. This would then explain the difference in hydrolysis between NM and WX starches of corn (WX > NM) and barley (NM > WX) after 1h hydrolysis at 55^{o}C (Figure 5.4). SEM images showed the presence of pores on the granule surface of both unfractionated corn and barley (corn > barley) starches (Figure 5.1), and CLSM images showed the presence of channels extending from the granule periphery to the interior in corn starch (Figures 5.2A & B). Surface pores and internal channels of granules are assumed to increase effective surface area for fast enzyme diffusion. Therefore, on this basis, unfractionated corn starches should have been theoretically hydrolyzed to a greater extent than barley starches. Thus, the observed DH (barley > corn, Figure 5.4) suggests that the presence of weaker crystallites in barley starch [reflected by lower T_o values (Table 5.3)] may have rendered barley starches more susceptible to hydrolysis. A significant correlation ($r = -0.80$, $p<0.05$) also found between T_o and DH of unfractionated starches, hydrolyzed at 55^{o}C for 1h. Furthermore, the presence of minor components, such as protein and lipid on granule surface and in channels could have been largely blocked the binding sites of enzyme (Naguleswaran et al., 2011), thereby reducing the rate of hydrolysis of corn starches.

Table 5.4: Apparent amylose content, relative crystallinity and degree of hydrolysis of corn and barley starches

Starches	Amylose (%, db[1])	RC[2] (%)	Degree of hydrolysis (%, db[1])		
			24h[3]	48h[3]	72h[3]
Corn					
Waxy					
Unfractionated	$1.1^{k} \pm 0.0$	$34.2^{b} \pm 0.2$	$77.3^{e} \pm 0.7$	$87.3^{abc} \pm 1.0$	$88.1^{a-d} \pm 0.7$
Large	$1.1^{k} \pm 0.1$	$35.9^{a} \pm 0.2$	$85.5^{ab} \pm 0.4$	$87.1^{abc} \pm 1.2$	$88.6^{a-d} \pm 1.4$
Small	$1.0^{k} \pm 0.0$	$32.2^{c} \pm 0.2$	$79.1^{de} \pm 1.0$	$80.0^{f} \pm 0.4$	$81.9^{f} \pm 0.0$
Normal					
Unfractionated	$24.4^{ef} \pm 0.9$	$28.1^{e} \pm 0.2$	$59.8^{g} \pm 1.0$	$84.9^{cde} \pm 0.4$	$90.6^{a} \pm 1.4$
Large	$26.0^{e} \pm 0.9$	$27.6^{e} \pm 0.3$	$51.8^{h} \pm 0.9$	$75.3^{g} \pm 1.1$	$83.4^{ef} \pm 1.3$
Small	$21.0^{g} \pm 0.3$	$24.0^{gh} \pm 0.5$	$66.5^{f} \pm 1.1$	$79.2^{f} \pm 0.8$	$80.8^{f} \pm 0.1$
High Amylose					
Unfractionated	$69.7^{a} \pm 0.1$	$21.6^{jk} \pm 0.1$	$2.6^{j} \pm 0.4$	$2.8^{j} \pm 0.4$	$9.4^{h} \pm 0.7$
Large	$69.8^{a} \pm 1.3$	$22.5^{ij} \pm 0.3$	$6.5^{i} \pm 1.0$	$6.7^{i} \pm 0.7$	$7.1^{h} \pm 0.7$
Small	$65.7^{b} \pm 0.1$	$20.3^{k} \pm 0.1$	$8.1^{i} \pm 0.7$	$8.9^{i} \pm 0.8$	$9.2^{h} \pm 0.4$
Barley					
Waxy					
Unfractionated	$5.3^{ij} \pm 0.5$	$34.3^{b} \pm 0.4$	$83.8^{bc} \pm 1.0$	$88.1^{ab} \pm 1.3$	$89.4^{abc} \pm 0.7$
Large	$6.0^{i} \pm 0.3$	$32.0^{c} \pm 0.9$	$88.7^{a} \pm 1.3$	$89.6^{a} \pm 1.0$	$90.4^{ab} \pm 1.2$
Small	$4.0^{j} \pm 0.2$	$30.3^{d} \pm 0.2$	$82.6^{bc} \pm 1.0$	$86.3^{b-d} \pm 0.6$	$88.2^{a-d} \pm 1.0$
Normal					
Unfractionated	$23.6^{f} \pm 1.1$	$25.2^{fg} \pm 0.4$	$81.3^{cd} \pm 1.1$	$84.0^{de} \pm 0.9$	$89.8^{ab} \pm 0.5$
Large	$23.2^{fg} \pm 0.3$	$25.8^{f} \pm 0.3$	$85.6^{ab} \pm 1.6$	$86.1^{bcd} \pm 0.8$	$87.6^{bcd} \pm 1.5$
Small	$16.8^{h} \pm 1.2$	$23.2^{hi} \pm 0.4$	$83.0^{bc} \pm 1.9$	$85.0^{cde} \pm 0.6$	$86.6^{cd} \pm 0.6$
High Amylose					
Unfractionated	$38.4^{c} \pm 0.9$	$20.8^{k} \pm 0.1$	$78.8^{de} \pm 1.0$	$83.1^{e} \pm 0.4$	$86.2^{de} \pm 1.4$
Large	$39.5^{c} \pm 0.9$	$22.6^{hij} \pm 0.5$	$65.6^{f} \pm 1.0$	$75.0^{g} \pm 0.8$	$86.3^{de} \pm 1.3$
Small	$34.8^{d} \pm 0.8$	$20.2^{k} \pm 0.3$	$63.6^{f} \pm 1.2$	$71.9^{h} \pm 1.1$	$75.8^{g} \pm 0.5$

[1] dry basis
[2] relative crystallinity
[3] degree of hydrolysis at 30°C for 24h, 48h, and 72h, respectively
Values are mean ± standard deviation, and values with the same superscript in the same column are not significantly different at $\alpha = 0.05$.

In the fractionated starches after 1h hydrolysis, the small granules were hydrolyzed to a greater extent than large granules (Figure 5.4). This finding is in agreement with previously reported results for corn (Dhital, Shrestha, & Gidley, 2010), barley (Stevnebø, Sahlström, & Svihus, 2006), triticale and wheat (Naguleswaran et al., 2012) starches. The difference in DH between large and small granules hydrolysed at 55^{o}C for 1h greatly varied among the genotypes and followed the order: NM corn (18%) > HA barley (9%) > NB Barley (7%) ≈ WX barley (6.7%) > WX corn (4%) > HA corn (0%). The higher DH of small granules can be attributed to their relatively larger surface area per unit mass (proportional to higher number of small granules, Table 5.2), weak association of double helices within the crystalline lamellae reflected by lesser Δ*H* (Table 5.3) and lower crystallinity (Table 5.4) than those of large granules (Kim et al., 2008; Stevnebø, Sahlström, & Svihus, 2006). However, in the fractionated starches at all time periods of hydrolysis (at 30^{o}C), there was no definite trend in the DH between small and large granules (Table 5.4). The variation in DH between unfractionated starches and their fractionated large and small granules (Table 5.4) could be attributed to the presence of diverse proportion of large and small granules in each unfractionated starch and some cross contamination of large and small granules in fractionated starches.

5.3.7. Morphology of hydrolyzed starch residues

The enzyme mixture used in this study was composed of both α-amylase (endo-attack on α-(1,4)-glycosidic linkages) and glucoamylase (exo-attack on

both α-(1,4)- and α-(1,6)-linkages). SEM revealed that the hydrolysis patterns of starch granules were caused by synergistic degradation of α-amylase and glucoamylase. Each enzyme digests starch granules by exocorrosion (erosion of entire granule surface or sections of it) and/or endocorrosion (erosion from the surface towards the centre of granule) but at different rates and extent between starches (Li et al., 2004; Li et al., 2011; Naguleswaran et al., 2012; Quigley et al., 1998; Sujka & Jamroz, 2007). The α-amylase has been shown to cause large pores while glucoamylase forms small pores on the granule surface (Sujka & Jamroz, 2007). The digestion pattern in the interior of starch granule also varies with enzymes source. SEM of hydrolyzed (72h, at 30^{o}C) unfractionated starches (Figure 5.5) showed that WX, NM and HA barley starches (Figures 5.5J, K & L) were more extensively eroded than WX, NM and HA corn starches (Figures 5.5D, E &F). No evidence of granule structure was seen in WX and NM barley starches (Figures 5.5J & K), whereas the granules of WX and NM corn starches were fragmented (Figures 5.5D & E). HA barley starch was more extensively eroded than HA corn starch (Figures 5.5F & L).

The morphological changes of hydrolyzed large and small starch granules of corn and barley revealed by SEM are shown in Figure 5.6. Hydrolysis for 24h at 30^{o}C resulted in roughly pitted honeycomb-like structures on the surfaces of both large and small WX corn (Figures 5.6A & D) and NM corn (Figures 5.6B & E) starch granules, even though some individual granules were intact (particularly in small granules). It explains that enzymatic hydrolysis by α-amylase and

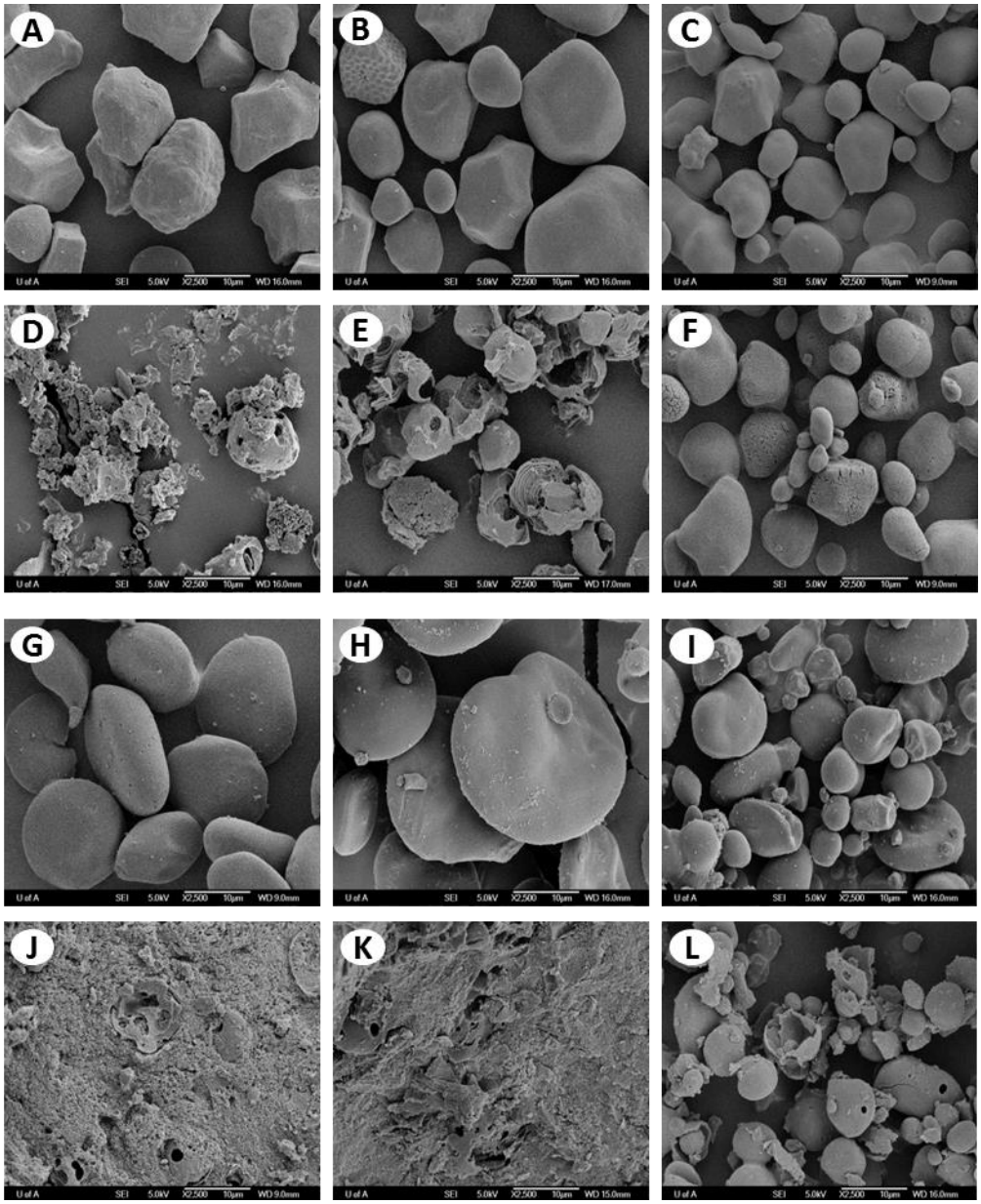

Figure 5.5: Scanning electron microscopy (SEM) images of starch residues of unfractionated corn (A, B & C were the control of waxy, normal and high-amylose, respectively; D, E & F were the enzyme treated waxy, normal and high-amylose, respectively) and barley (G, H & I were the control of waxy, normal and high-amylose, respectively; J, K & L were the enzyme treated waxy, normal and high-amylose, respectively) starches after 72h hydrolysis (x2500, scale bar = 10 µm)

glucoamylase initiated from granule surfaces by generating pits, size enlargement of existing pores, and penetration into granule interior. The pitted holes on the granules surface suggested that amylases hydrolyzed both crystalline and amorphous lamellae of starch granules through endocorrosion attack and this pattern was highly pronounced in NM corn than WX corn (Figure 5.6). However, some granules in both large (Figure 5.6A) and small (Figure 5.6D) WX corn starch had roughened surface and fragmented pieces so that their interior parts were exposed. The roughened surfaces in hydrolyzed WX corn starch granules may have been due to uneven shortening of amylopectin molecules by the action of α-amylase (Sujka & Jamroz, 2009). Interior structure of fragmented granule residues suggests that α-amylase favourably hydrolyzed the amorphous regions of the starch granule leaving the crystalline regions which were more resistant to amylase attack even after 24h hydrolysis (Figures 5.6A & D). This is indicative of the higher AP content (≈99%) of WX corn starch. In hydrolyzed HA corn, drilled pore like structures were found both in large and small granules; however the size and frequency of pores were higher in small (Figure 5.6F) than in large (Figure 5.6C) granules. This suggests that the glucoamylase predominantly attacks the granule surface of HA corn starch. SEM also revealed that the hydrolysis pattern of large and small granules of barley starches were different to that of corn starch granules. Extensive hydrolysis (most likely by glucoamylase) along the equatorial groove of large granules of WX and NM barley starches (after 24h) resulted in the formation of fragmented

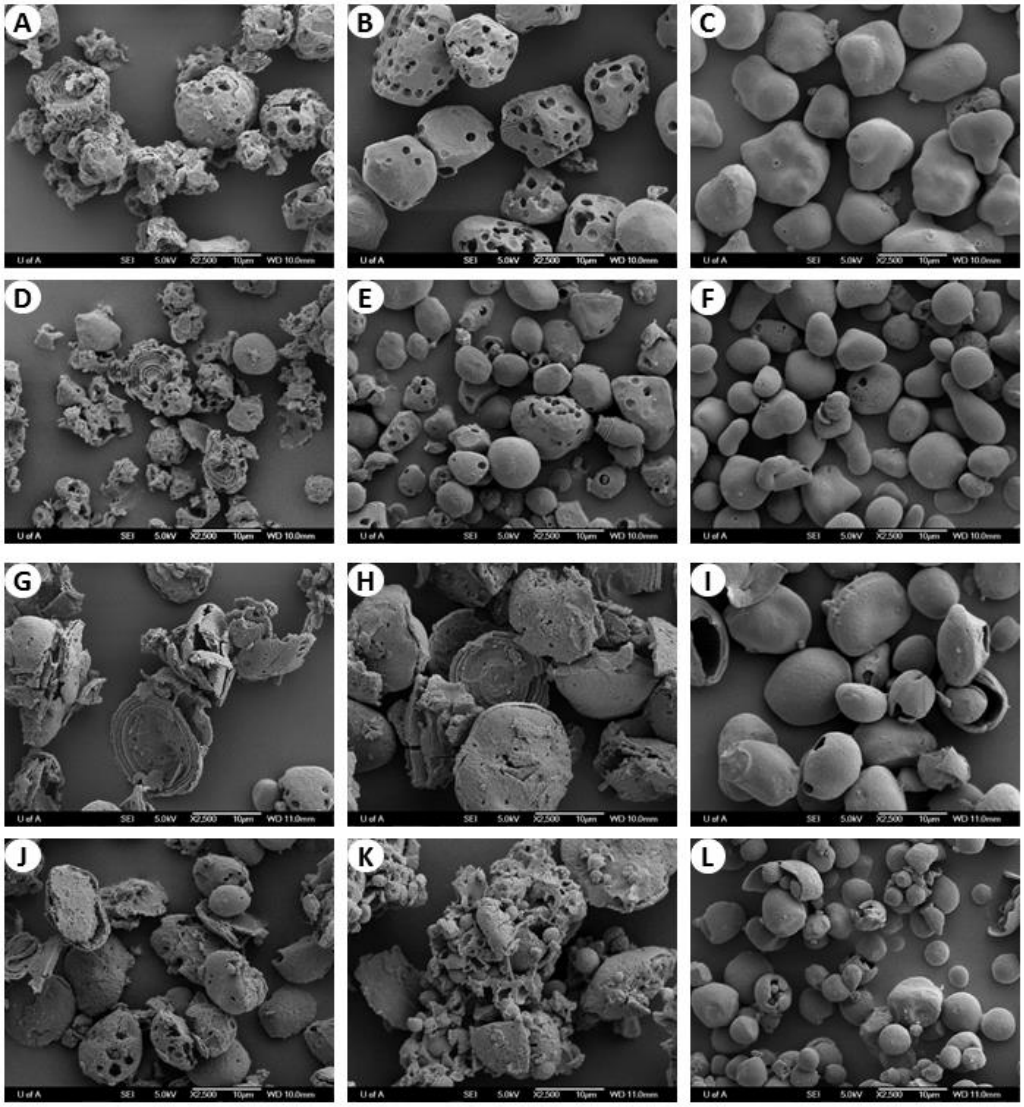

Figure 5.6: Scanning electron microscopy (SEM) images of starch residues of fractionated corn (A, B & C were the large granules of waxy, normal and high-amylose, respectively; D, E & F were the small granules of waxy, normal and high-amylose, respectively) and barley (G, H & I were the large granules of waxy, normal and high-amylose, respectively; J, K & L were the small granules of waxy, normal and high-amylose, respectively) starches after 24h hydrolysis (x2500, scale bar=10µm).

granules (Figures 5.6G & H). The interior structure of fragmented granules (Figures 5.6G & H) suggests that the amorphous regions were extensively hydrolyzed by α-amylase leaving behind the crystalline layers of starch granules. However, the sharpness of crystalline regions in the barley starch residues (Figures 5.6G & H) were lower than in corn starch residues (Figures 5.6A & D). In small granules of WX barley (Figure 5.6J) and NM barley (Figure 5.6K) starches, more perforated erosion pits and enlarged pores on the surfaces and much less fragmented granules were observed. Generally, the visible layered structures were more pronounced on large granule surfaces (Figures 5.6G & H) than on small granules (Figures 5.6J & K). Hydrolysis of large (Figure 5.6I) and small (Figure 5.6L) granules of HA barley starches resulted in eroded surfaces and enlarged hollows. This would then explain why the central region (cavity) rather than the periphery region of HA barley starch granules is more susceptible to amylase hydrolysis. Thus, the accessibility of α-amylase and glucoamylase towards large and small starch granules differ with starch origin and genotypes. This leads to different hydrolysis kinetics (rate and extent) and hydrolysis patterns.

The present study has demonstrated that at initial stages of amylolysis, small starch granules were hydrolysed to a higher extent than large granules. This difference was more pronounced in NM corn. Since NM corn is widely used for the bioethanol industry, its initial rate of hydrolysis may be too low for optimum yeast function at the initial stages of fermentation (underperformance

of yeast due to lack of available fermentable sugars). In contrast, the NM barley starches showed high initial rate of hydrolysis that may be too high for optimum yeast function (i.e. underperformance of yeast due to high amounts of fermentable sugar and osmotic pressure). Barley starches which rather new to the bioethanol industries are equally comparable (except in the initial rate of amylolysis) to corn starches (the benchmark raw materials used in North American bioethanol industries). In addition, although small variations exist between the NM corn and NM barley starches with respect to their proximate composition and amylose content, the observed large variations in the extent of amylolysis at the initial stages of hydrolysis is indicative that the molecular architecture and granule porosity (i.e. the number of granule surface pores and whether or not they are blocked with protein and lipids) influence amylolysis.

5.4. CONCLUSIONS

The North American bioethanol industry is expanding rapidly and the business is becoming more competitive. Quantitative conversion of starch (at a desired rate of amylolysis) and release of fermentable sugar is very important for optimum yeast function and maximum ethanol yield. The novelty of this study relies on the findings related to starch amylolysis (barley vs. corn starches), and how its rate and extent are influenced by varying combinations of granule size and amylose content. The study suggested that blending of NM corn and NM barley starches (i.e. flours) may benefit the bioethanol production.

REFERENCES

Ao, Z., & Jane, J. (2007). Characterization and modeling of the A- and B-granule starches of wheat, triticale, and barley. *Carbohydrate Polymers, 67*(1), 46-55.

Asare, E. K., Jaiswal, S., Maley, J., Baga, M., Sammynaiken, R., Rossnagel, B. G., & Chibbar, R. N. (2011). Barley grain constituents, starch composition, and structure affect starch *in vitro* enzymatic hydrolysis. *Journal of Agricultural and Food Chemistry, 59*(9), 4743-4754.

Bruner, R. L. (1964). Determination of reducing value: 3, 5-dinitrosalicylic acid method. In R. L. Whistler, R. J. Smith, J. N. BeMiller, & M. L. Wolform, *Methods in carbohydrate chemistry (Vol 4)*(pp. 67-71). New York and London: Academic Press.

Blennow, A., Hansen, M., Schulz, A., Jorgensen, K., Donald, A. M. and Sanderson, J. (2003). The molecular deposition of transgenically modified starch in the starch granule as imaged by functional microscopy. *Journal of Structural Biology, 143*, 229-241.

das Neves, M. A., Kimura, T., Shimizu, C., & Nakajima, M. (2007). State of the art and future trends of bioethanol production. *Dynamic Biochemistry, Process Biotechnology and Molecular Biology*, *1*(1), 1-14.

Dhital, S., Shrestha, A. K., & Gidley, M. J. (2010). Relationship between granule size and *in vitro* digestibility of maize and potato starches. *Carbohydrate Polymers, 82*(2), 480-488.

Food and Agriculture Organization of the United Nations (2012). FAOSTAT 2010. http://faostat.fao.org/site/339/default.aspx . (Accesesed in Oct 2012).

Gao, J., Vasanthan, T., & Hoover, R. (2009). Isolation and characterization of high-purity starch isolates from regular, waxy, and high-amylose hulless barley grains. *Cereal Chemistry, 86*(2), 157-163.

Gibreel, A., Sandercock, J. R., Lan, J., Goonewardene, L. A., Zijlstra, R. T., Curtis, J. M., & Bressler, D. C. (2009). Fermentation of barley by using *Saccharomyces cerevisiae*: Examination of barley as a feedstock for bioethanol production and value-added products. *Applied and Environmental Microbiology, 75*(5), 1363-1372.

Holm, J., Bjorck, I., Ostrowska, S., Eliasson, A. C., Asp, N. G., Larsson, K., & Lundquist, I. (1983). Digestibility of amylose-lipid complexes *In vitro* and *In vivo*. *Starch/Starke, 35*(9), 294-297.

Jiang, H., Horner, H. T., Pepper, T. M., Blanco, M., Campbell, M., & Jane, J. (2010). Formation of elongated starch granules in high-amylose maize. *Carbohydrate Polymers, 80*(2), 533-538.

Kim, J. C., Kong, B. W., Kim, M. J., & Lee, S. H. (2008). Amylolytic hydrolysis of native starch granules affected by granule surface area. *Journal of Food Science, 73*(9), C621-C624.

Lauro, M., Suortti, T., Autio, K., Linko, P., & Poutanen, K. (1993). Accessibility of Barley Starch Granules to Alpha-Amylase during Different Phases of Gelatinization. *Journal of Cereal Science, 17*(2), 125-136.

Lee, S., & BeMiller, J. N. (2008). Lysophosphatidylcholine Identified as Channel-Associated Phospholipid of Maize Starch Granules. *Cereal Chemistry, 85*(6), 776-779.

Li, J., Vasanthan, T., Hoover, R., & Rossnagel, B. (2004). Starch from hull-less barley: V. In-vitro susceptibility of waxy, normal, and high-amylose starches towards hydrolysis by alpha-amylases and amyloglucosidase. *Food Chemistry, 84*(4), 621-632.

Li, J., Vasanthan, T., Rossnagel, B., & Hoover, R. (2001). Starch from hull-less barley: I. Granule morphology, composition and amylopectin structure. *Food Chemistry, 74*(4), 395-405.

Li, X., Gao, W., Wang, Y., Jiang, Q., & Huang, L. (2011). Granule structural, crystalline, and thermal changes in native Chinese yam starch after hydrolysis with two different enzymes, alpha-amylase and gluco-amylase. *Starch-Starke, 63*(2), 75-82.

Liu, Q., Gu, Z., Donner, E., Tetlow, I., & Emes, M. (2007). Investigation of digestibility *in vitro* and physicochemical properties of A- and B-type starch from soft and hard wheat flour. *Cereal Chemistry, 84*(1), 15-21.

Luo, Z., Fu, X., Gao, Q., & Yu, S. (2011). Effect of acid hydrolysis in the presence of anhydrous alcohols on the structure, thermal and pasting properties of normal, waxy and high-amylose maize starches. *International Journal of Food Science and Technology, 46*(2), 429-435.

MacGregor, A. W., & Ballance, D. L. (1980). Hydrolysis of large and small starch granules from normal and waxy barley cultivars by alpha-amylases from barley malt. *Cereal Chemistry, 57*(6), 397-402.

Naguleswaran, S., Li, J., Vasanthan, T., & Bressler, D. (2011). Distribution of granule channels, protein, and phospholipid in triticale and corn starches as revealed by confocal laser scanning microscopy. *Cereal Chemistry, 88*(1), 87-94.

Naguleswaran, S., Li, J., Vasanthan, T., Bressler, D., & Hoover, R. (2012). Amylolysis of large and small granules of native triticale, wheat and corn starches using a mixture of α-amylase and glucoamylase. *Carbohydrate Polymers, 88*(3), 864-874.

Oates, C. G. (1997). Towards an understanding of starch granule structure and hydrolysis. *Trends in Food Science & Technology, 8*, 375-382.

Quigley, T., Kelly, C., Doyle, E., & Fogarty, W. (1998). Patterns of raw starch digestion by the glucoamylase of Cladosporium gossypiicola ATCC 38026. *Process Biochemistry, 33*(6), 677-681.

Salman, H., Blazek, J., Lopez-Rubio, A., Gilbert, E. P., Hanley, T., & Copeland, L. (2009). Structure-function relationships in A and B granules from wheat starches of similar amylose content. *Carbohydrate Polymers, 75*(3), 420-427.

Sanchez, O. J., & Cardona, C. A. (2008). Trends in biotechnological production of fuel ethanol from different feedstocks. *Bioresource Technology, 99*(13), 5270-5295.

Sharma, V., Rausch, K. D., Graeber, J. V., Schmidt, S. J., Buriak, P., Tumbleson, M. E., & Singh, V. (2010). Effect of resistant starch on hydrolysis and fermentation of corn starch for ethanol. *Applied Biochemistry and Biotechnology, 160*(3), 800-811.

Sharma, V., Rausch, K. D., Tumbleson, M. E., & Singh, V. (2007). Comparison between granular starch hydrolyzing enzyme and conventional enzymes for ethanol production from maize starch with different amylose: amylopectin ratios. *Starch/Starke, 59*(11), 549-556.

Stevnebø, A., Sahlström, S., & Svihus, B. (2006). Starch structure and degree of starch hydrolysis of small and large starch granules from barley varieties with varying amylose content. *Animal Feed Science and Technology, 130*(1–2), 23-38.

Sujka, M., & Jamroz, J. (2009). α-Amylolysis of native potato and corn starches - SEM, AFM, nitrogen and iodine sorption investigations. *LWT-Food Science and Technology*, *42*(7), 1219-1224.

Sujka, M., & Jamroz, J. (2007). Starch granule porosity and its changes by means of amylolysis. *International Agrophysics, 21*(1), 107-113.

Tang, H., Ando, H., Watanabe, K., Takeda, Y., & Mitsunaga, T. (2001). Fine structures of amylose and amylopectin from large, medium, and small waxy barley starch granules. *Cereal Chemistry, 78*(2), 111-115.

Tawil, G., Vikso-Nielsen, A., Rolland-Sabate, A., Colonna, P., & Buleon, A. (2012). Hydrolysis of concentrated raw starch: A new very efficient alpha-amylase from *Anoxybacillus flavothermus*. *Carbohydrate Polymers, 87*(1), 46-52.

Tomoaia-Cotisel, M., Cota, C., Mocanu, A., & Horovitz, O. (2010). Micro and nanostructure of starch granules from potato and maize. *Materiale Plastice, 47*(4), 426-432.

Uthumporn, U., Zaidul, I. S. M., & Karim, A. A. (2010). Hydrolysis of granular starch at sub-gelatinization temperature using a mixture of amylolytic enzymes. *Food and Bioproducts Processing, 88*(C1), 47-54.

Utrilla-Coello, R. G., Agama-Acevedo, E., de la Rosa, A. P. B., Rodriguez-Ambriz, S. L., & Bello-Perez, L. A. (2010). Physicochemical and Enzyme Characterization of Small and Large Starch Granules Isolated from Two Maize Cultivars. *Cereal Chemistry, 87*(1), 50-56.

Waduge, R., Hoover, R., Vasanthan, T., Gao, J., & Li, J. (2006). Effect of annealing on the structure and physicochemical properties of barley starches of varying araylose content. *Food Research International, 39*(1), 59-77.

Zhang, G., Ao, Z., & Hamaker, B. R. (2006). Slow digestion property of native cereal starches. *Biomacromolecules, 7*(11), 3252-3258.

CHAPTER 6

Molecular characteristics of amylopectin and amylose isolated from triticale, wheat, corn, and barley starches*

6.1. INTRODUCTION

Starch is an important source of energy for many plants and animals, including humans. The uses of starch are not limited for food consumption; it can be a raw material for various industrial applications. For instance, starch is popularly known for the manufacturing of paper and boards, textiles, cosmetics, pharmaceuticals, agrochemicals, detergents, bioplastics, and for bioethanol production (Liu, 2005; Murthy, et al., 2011). However, understanding the starch structure-property relationship is important for efficient utilization of starch for food and industrial applications. Starch is deposited as granules in the amyloplast of various storage organs such as grains or seeds, tubers, roots, fruits, leaves and stems. Two polymers such as amylose (AM) and amylopectin (AP) build up the architecture of a starch granule. The AM and AP molecules are highly organized by inter- and intra-molecular hydrogen-bonding to form the architecture of a starch granule. The architecture differs in starch granules since the proportion of AM and AP varies with different starch sources and among cultivars within a source. A detail description of the molecular structures of AM and AP, and the architecture of a starch granule is presented in Chapter 2.1.2.

* A version of this chapter has been submitted for publication.

Molecular properties of AM and AP such as molar mass (molecular weight, M_w), molecular size or dimension (radius of gyration, R_g), molecular density (ρ), specific volume for gyration (SV_g), polydispersity index (*PDI*), branch chain length distribution or degree of polymerization (*DP*), degree of branching (*DB*), branching ratio or shrinking factor (*gM*), number of branch points (*B*) and average-chain length (*CL*) influence the physicochemical and functional properties of starches (Arturo Bello-Perez, et al., 2009; Chen & Bergman, 2007; Gilbert, et al., 2010; Goesaert, et al., 2010; Miao, et al., 2011; Radosta, et al., 2001; Rojas, et al., 2008; Rolland-Sabate, et al., 2007; Yoo & Jane, 2002). Starch properties are mainly influenced by the molecular characteristics of AP (Goesaert, et al., 2010; Miao, et al., 2011; Murthy, et al., 2011). For example, two AP molecules with the same size can have different molar mass if their degree of branching is different, thus influencing their hydrolysis (Gilbert, et al., 2010; Goesaert, et al., 2010; Rolland-Sabate, et al., 2007).

To study the molecular properties of AM and AP, the starch granules must be completely solubilized and dispersed as separate molecules without degradation. High-Performance Size Exclusion Chromatography (HPSEC) coupled with Multi-Angle Laser Light Scattering (MALLS) and Refractive Index (RI) detectors are widely used to study the molecular properties of starch polymers. Starch dissolving solvents [dimethylsulfoxide (DMSO), NaOH, and KOH] and physical separation techniques (aqueous leaching, microwave heating, autoclaving, homogenization, and sonication) have been used in the study of

starch molecular characteristics using HPSEC-MALLS-RI system (Arturo Bello-Perez, et al., 2009; Charoenkul, et al., 2006; Chen & Bergman, 2007; Evans & Thompson, 2008; Gilbert, et al., 2010; Mua & Jackson, 1997; Yokoyama, et al., 1998; Yoo & Jane, 2002; You & Lim, 2000). In addition, Asymmetric Flow Field-Flow Fractionation (AFFFF) coupled with MALLS and RI detectors has also been used for characterization of molecular structure of various starches (Kim, et al., 2007; Rojas, et al., 2008; Rolland-Sabate, et al., 2007; You, et al., 2002).

The objective of this study was twofold: a) to determine the molecular characteristics of AM and AP of normal, waxy and high amylose starches from cereals such as triticale, wheat, corn and barley in their unfractionated and fractionated (i.e. large and small granules) forms, and b) to compare the molecular characteristics between sources as well as between large and small granules within each source.

6.2. MATERIALS AND METHODS

6.2.1. Materials

Two cultivars of wheat (*Triticum aestivum* L.) grains, Canada prairie spring red (CPS Red) and AC Reed, were provided by Alberta Agriculture and Food in Barrhead (AB, Canada). The Field Crop Development Centre at the Alberta Agriculture and Rural Development in Lacombe (AB, Canada) supplied two cultivars of triticale (x *Triticosecale*) grains, Pronghorn and AC Ultima. Grains from three hull-less barley cultivars (waxy, CDC Candle; normal, CDC McGwire;

and high-amylose, SH 99250) were obtained from the Crop Development Center at University of Saskatchewan in Saskatoon (SK, Canada). Commercial corn starches of waxy (Amioca), normal (Melojel) and high-amylose (Hylon VII) were obtained from National Starch Food Innovation in Bridgewater (NJ, USA). All other chemicals and reagents used in this study were of ACS grade.

6.2.2. Grain grinding and starch isolation

Triticale, wheat and barley grains were ground into meals in a Retsch mill (Model ZM 200, Haan, Germany) using a ring sieve with an aperture size of 0.5 mm. Pure starch (purity >95%, w/w) was isolated from a grain meal of triticale and wheat, and barley using the procedures described by Kandil et al. (2011) and Gao et al. (2009), respectively. The detailed starch isolation protocols are presented in appendix.

6.2.3. Fractionation of large and small starch granules

Isolated triticale, wheat and barley starches, and commercial corn starches were fractionated into large and small granules using a centrifugal sedimentation protocol as described in Chapter 4.2.4.

6.2.4. Preparation of starches for HPSEC-MALLS-RI system

Starch sample (20 mg, dry basis) of unfractionated, large, and small granules was solubilized with the addition of 2 mL of 95% DMSO followed by heating (85–90^{o}C) in a water bath for 30 min with vortexing every 5 min. The solubilized

starch solution was cooled to room temperature followed by the addition of absolute ethanol (6 mL). The solution was then kept at 4^{o}C for 2 h, centrifuged (6000 x*g* for 10 min) and the residue washed with cold ethanol (5 mL). The residue was then resolubilized by the addition of 2M KOH (2 mL) followed by mechanical mixing for 1h in an ice-bath (tubes containing the samples were covered with ice in a Styrofoam box) and then for 15 h at room temperature (22^{o}C). The alkaline solution containing starch molecules was diluted with 0.2M $NaNO_3$ (15 mL) solution, neutralized by 2M HCL and then made up to volume (20 mL) with 0.2M $NaNO_3$ (starch polymer concentration was 1 mg/mL) followed by filtration through a nylon membrane filter (1 µm) device (Puradisc 25 NYL, Whatman Inc., NJ, USA). An aliquot (50 µL) of the filtrate was injected into an HPSEC-MALLS-RI system. In order to avoid aggregation of dispersed starch molecules, the solubilized starch in KOH solution was neutralized instantly before each injection.

6.2.5. HPSEC-MALLS-RI system

The HPSEC-MALLS-RI consisted of an Agilent 1200 HPLC system (Agilent Technologies in Santa Clara, CA, USA) coupled with a multi-angle laser light scattering detector which had a laser wavelength of 658 nm (MALLS, DAWN-HELEOS II, Wyatt Technology in Santa Barbara, CA, USA), and a refractive index detector (RID, Agilent Technologies in Santa Clara, CA, USA). A guard column (Ultrahydrogel^{TM}, 6x40 mm, Waters Corporation in Milford, MA, USA) and an SEC

column (Ultrahydrogel^{TM} Linear, 7.8x300 mm, Waters Corporation in Milford, MA, USA) were connected to the HPLC system. The mobile phase used in HPSEC system was aqueous $NaNO_3$ (0.2M) solution with a flow rate of 0.5 mL/min, which was degassed in a sonication-assisted water bath for 20 min and filtered through 0.22 μm cellulose acetate filter system (Corning Inc. in Corning, NY, USA). The column and RI detector temperatures were maintained at 40^{o}C and 35^{o}C, respectively. Before injection of starch samples, two types of dextran with different molecular weight (M_w) were analyzed to test the chromatography system. The M_w of tested dextrans were ($2.45x10^5$ and $1.01x10^7$ g/mol) in agreement with reported values by the manufacturer (Sigma-Aldrich Canada Ltd. in Oakville, ON, Canada).

6.2.6. Molecular data analyses

The ASTRA software (Version 5.3.4.20, Wyatt Technology in Santa Barbara, CA, USA) was used to collect and analyze data from the HPSEC-MALLS-RI system. An dn/dc value of 0.146 mL/g for starch was applied in calculations using the Berry extrapolation model [$\sqrt{K^* c}/R_\Theta$ vs. $\sin^2(\Theta/2)$] with a first-degree polynomial fit, where c is the mass concentration of the solute, R_Θ is the excess intensity of scattered light at angle Θ, and K^* is the optical constant equal to $4\pi^2 n_0^2 (dn/dc)^2/(\lambda_0^4 N_A)$, where n_0 is the refractive index (RI) of the solvent, λ_0 is the wavelength of the scattered light in vacuum, dn/dc is the change in RI with solute concentration at λ_0, and N_A is Avogadro's number. The ASTRA software

quantitatively measures M_i (molar mass) and R_{gi} (radius of gyration) of i^{th} slice of a peak obtained from the MALLS and RI detections according to Berry's equation (1) as shown below (Chen & Bergman, 2007; Rolland-Sabate, et al., 2007; Yoo & Jane, 2002).

$$\sqrt{\left(\frac{K^*c}{R_\theta}\right)_i} = \sqrt{\frac{1}{M_i}\left(1 + \frac{16\pi^2}{3\lambda^2}R_{gi}^2 \ sin^2\left(\frac{\theta}{2}\right)\right)} \quad \text{..... (1)}$$

The M_n (number-average molecular weight, g/mol), M_w (weight-average molecular weight, g/mol), R_z (z-average radius of gyration, nm), and R_w (weight-average radius of gyration, nm) of AM and AP were automatically calculated by ASTRA according to the summation of all the slices over a selected peak using the following equations, respectively.

$$M_n = \frac{\sum c_i}{\sum(c_i/M_i)} \quad \text{.....(2)}$$

$$M_w = \frac{\sum(c_i M_i)}{\sum c_i} \quad \text{..... (3)}$$

$$R_z = \sqrt{\frac{\sum c_i M_i R_{gi}^2}{\sum(c_i M_i)}} \quad \text{..... (4)}$$

$$R_w = \sqrt{\frac{\sum\left(c_i R_{gi}^2\right)}{\sum c_i}} \quad \text{..... (5)}$$

The following molecular characteristics, including branching parameters of starch polymers were derived based on the abovementioned key features (molar mass and molecular size). The polydispersity index was measured by M_w/M_n. The number-average degree of polymerization (DP_n) and weight-average degree of

polymerization (DP_w) of AM and AP were calculated as per the equations M_n/162 and M_w/162, respectively, where molar mass of an anhydrous glucose molecule was 162 g/mol (Chen & Bergman, 2007). The branching parameters such as average dispersed-molecular density (ρ) equals to M_w/R_z^3 (g/mol/nm^3), average number of branch points (B), average unit chain length ($CL = DP_w/B$), and average degree of branching [$DB = (B/DP_w)$x100%] of starch polymers were also computed (Rolland-Sabate, et al., 2007; Yoo & Jane, 2002). The average specific volume for gyration (SV_g in cm^3/g) and average branching ratio or shrinking factor (gM) were calculated using the equations (6) and (7), respectively (Rolland-Sabate, et al., 2007; You & Lim, 2000).

$$SV_g = 2.522\left(\frac{{R_z}^3}{M_w}\right) \quad \text{..... (6)}$$

$$g_M = \frac{{R_{w(br)}}^2}{{R_{w(lin)}}^2} = 4\left[\frac{\sqrt{(1+2B)}}{\left(1+\sqrt{(1+2B)}\right)^2}\right] \quad \text{..... (7)}$$

The shrinking factor is the ratio between the weight-average mean-square radius of gyration of branched [$R_{w(br)}^2$] and linear [$R_{w(lin)}^2$] polymers with the same molar mass, where $R_{w(br)}$ was obtained from ASTRA result and $R_{w(lin)}$ is calculated by using the equation, $(5.96/1000)M_w^{0.63}$ (Rolland-Sabate, et al., 2007).

6.3. RESULTS AND DISCUSSION

6.3.1. Granular starch solubilization and chromatograms

A complete solubilization of starch granules was achieved with a dual starch dissolution protocol using DMSO and KOH, which enabled us to study the molecular characteristics of AP and AM in detail. The light scattering (LS) chromatograms of unfractionated (Figure 6.1), large (Figure 6.2), and small (Figure 6.3) granules of triticale, wheat, corn, and barley starches showed complete separation of AP and AM. All normal (NM) and high-amylose (HA) starches showed two sharp peaks to represent the distribution of AP and AM molecules (Figures 6.1 – 6.3). However, the waxy (WX) starches of corn and barley showed (Figures 6.1 – 6.3) only a single AP peak (since the AM content of the WX starches were ≈1 and ≈6%, respectively). DMSO (95%, v/v) and alkali (2M KOH) disrupt inter- and intra-molecular H-bonds between AP and AM molecules, thereby increasing starch solubility. At a higher pH (12.5), the majority of –OH groups in the anhydrous glucose units of AP and AM are ionized (Han & Lim, 2004). This prevents agglomeration of dispersed starch molecules. Filtration of starch solution before injecting into HPSEC system was much easier with HA starches due to their higher amylose content that made HA starches more amorphous, thus increasing their solubility in DMSO and alkali solution (Han & Lim, 2004).

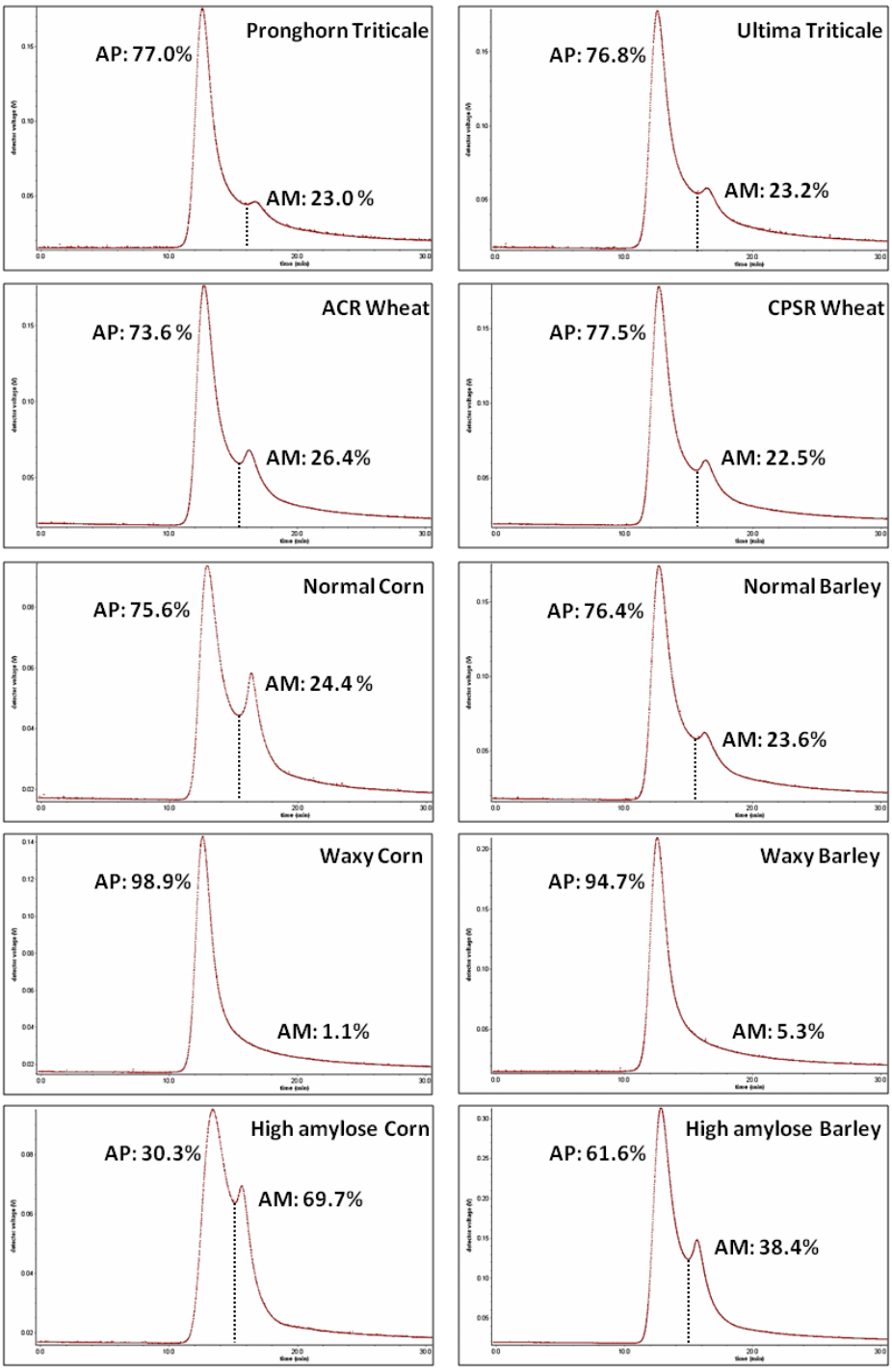

Figure 6.1: Light scattering signal (V) profile is shown throughout the elution time (min) for amylopectin (AP) and amylose (AM) of unfractionated starches, determined by the HPSEC-MALLS-RI system. Composition of AM and AP measured by a colorimetric method is presented for comparison.

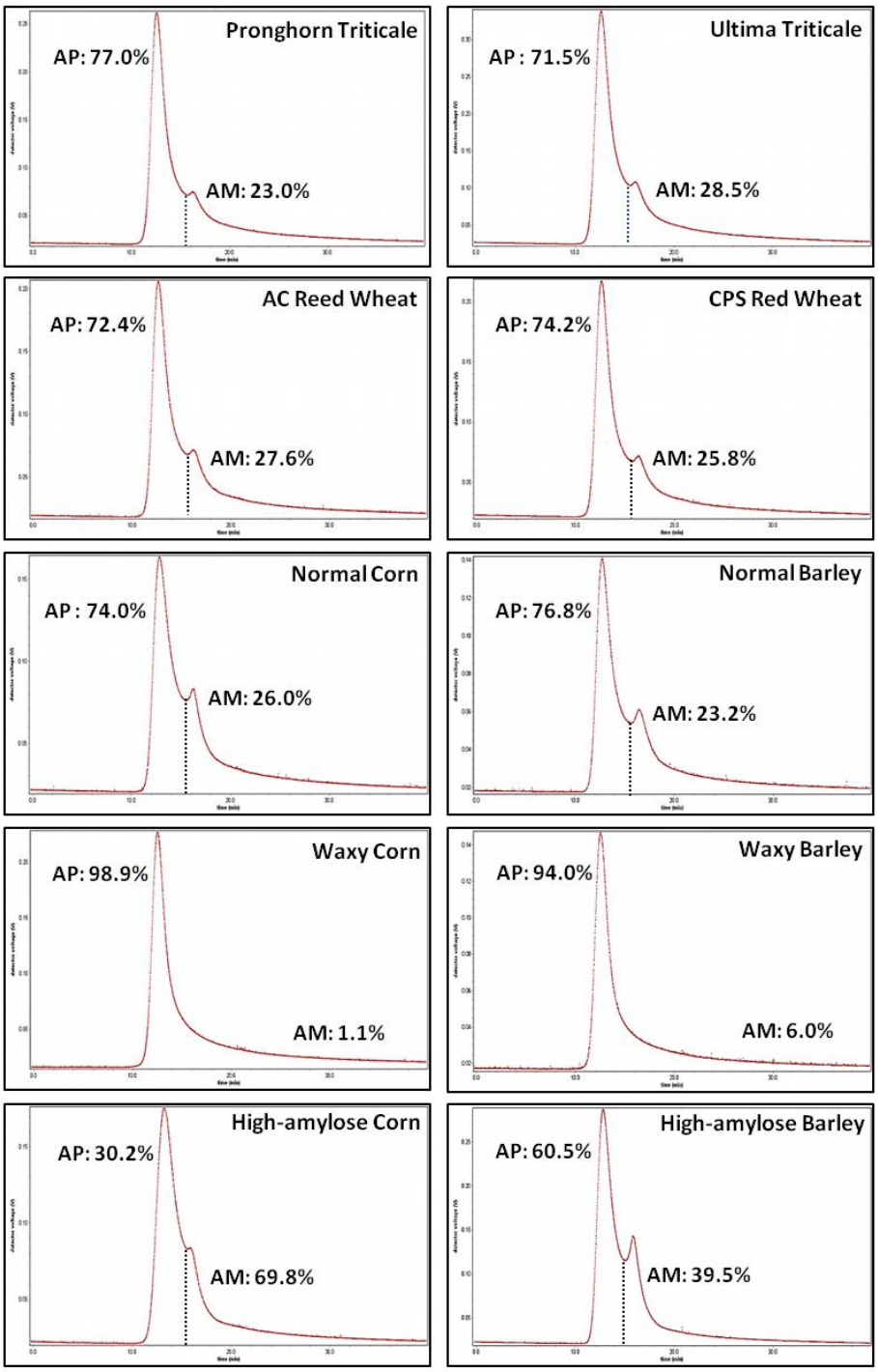

Figure 6.2: Light scattering signal (V) profile is shown throughout the elution time (min) for amylopectin (AP) and amylose (AM) of large starch granules, determined by the HPSEC-MALLS-RI system. Composition of AM and AP measured by a colorimetric method is presented for comparison.

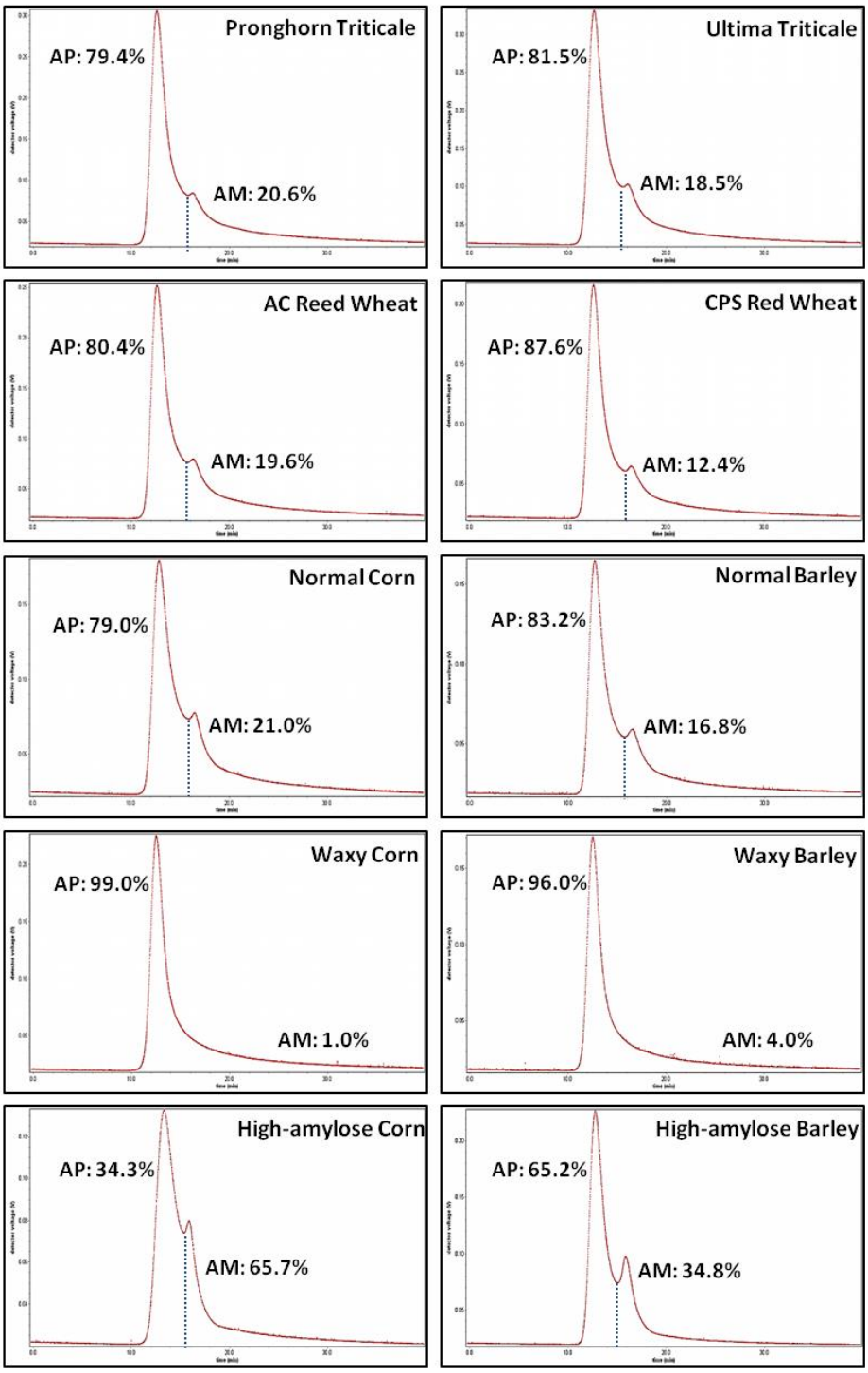

Figure 6.3: Light scattering signal (V) profile is shown throughout the elution time (min) for amylopectin (AP) and amylose (AM) of small starch granules, determined by the HPSEC-MALLS-RI system. Composition of AM and AP measured by a colorimetric method is presented for comparison.

6.3.2. Relationships among molar masses, molecular sizes, and polydispersity indices

Molecular characteristics of AP and AM [molar masses (number-average, M_n and weight-average, M_w), degree of polymerization (number-average, DP_n and weight-average, DP_w), radii of gyration (*z*-average, R_z and weight-average, R_w) and polydispersity indices (*PDI*, a ratio between weight-average molar mass and number-average molar mass)] are presented in Table 6.1 and Table 6.2, respectively. Overall, the M_n of AP and AM were lower than that of M_w, thus $DP_n < DP_w$ in both AM and AP of all starches.

6.3.2.1. Amylopectin

As shown in Table 6.1, the M_w of AP in unfractionated NM starches ranged between $6.5x10^6$ g/mol (corn) and $2.5x10^7$ g/mol (Pronghorn triticale). There was no definite trend observed in the M_w of AP between large and small granules of NM starches. The molecular size (R_z) of AP in unfractionated NM starches was between 63.9 nm (corn) and 72.4 nm (barley). A trend was seen in R_z of AP between unfractionated and fractionated NM starches, where R_z of large and small granules was higher than their unfractionated counterparts (Table 6.1). In WX starches, the M_w and R_z of AP in corn was higher than that in barley, and the ranges were $6.2x10^6$–$1.7x10^7$ g/mol and 67.0–69.6 nm, respectively. As in NM starches, the R_z of AP in large and small granules of WX corn and barley was also higher than the R_z of AP in their corresponding unfractionated starches.

Table 6.1: Molecular characteristics of amylopectin of triticale, wheat, corn and barley starches

Starches		M_n [1]	M_w [2]	DP_n [3]	DP_w [4]	R_z [5]	R_w [6]	PDI [7]
Normal								
Pronghorn Triticale	Unfractionated	2.40E+07	2.46E+07	1.48E+05	1.52E+05	71.9	72.4	1.025
	Large	2.13E+07	2.22E+07	1.32E+05	1.37E+05	76.0	75.3	1.040
	Small	1.94E+07	1.98E+07	1.19E+05	1.22E+05	81.1	80.8	1.021
Ultima Triticale	Unfractionated	1.43E+07	1.49E+07	8.85E+04	9.19E+04	69.5	69.3	1.039
	Large	1.94E+07	1.95E+07	1.19E+05	1.20E+05	82.8	83.2	1.006
	Small	2.45E+07	2.46E+07	1.51E+05	1.52E+05	76.7	77.0	1.003
AC Reed Wheat	Unfractionated	7.73E+06	9.35E+06	4.77E+04	5.77E+04	71.4	70.4	1.209
	Large	9.00E+06	9.14E+06	5.55E+04	5.64E+04	75.9	75.4	1.016
	Small	1.19E+07	1.23E+07	7.36E+04	7.56E+04	75.4	75.5	1.028
CPS Red Wheat	Unfractionated	1.40E+07	1.97E+07	8.61E+04	1.21E+05	66.7	68.6	1.410
	Large	1.08E+07	1.61E+07	6.69E+04	9.94E+04	77.6	78.0	1.260
	Small	1.04E+07	1.19E+07	6.43E+04	7.33E+04	75.3	75.9	1.140
Corn	Unfractionated	5.73E+06	6.48E+06	3.54E+04	4.00E+04	63.9	64.8	1.130
	Large	1.95E+07	2.07E+07	1.20E+05	1.28E+05	69.3	69.2	1.063
	Small	1.54E+07	1.54E+07	9.48E+04	9.49E+04	72.2	72.1	1.001
Barley	Unfractionated	2.19E+07	2.24E+07	1.35E+05	1.39E+05	72.4	72.1	1.025
	Large	1.28E+07	1.28E+07	7.89E+04	7.91E+04	71.6	71.8	1.003
	Small	1.46E+07	1.51E+07	8.98E+04	9.30E+04	70.5	71.2	1.036
Waxy								
Corn	Unfractionated	1.67E+07	1.69E+07	1.03E+05	1.04E+05	69.6	69.5	1.011
	Large	3.30E+07	3.45E+07	2.04E+05	2.13E+05	78.1	78.0	1.045
	Small	2.79E+07	2.85E+07	1.72E+05	1.76E+05	73.9	73.9	1.019
Barley	Unfractionated	6.14E+06	6.15E+06	3.79E+04	3.80E+04	67.0	66.9	1.002
	Large	1.97E+07	2.05E+07	1.22E+05	1.26E+05	73.7	72.8	1.038
	Small	1.64E+07	1.67E+07	1.01E+05	1.03E+05	68.6	68.4	1.021
High-Amylose								
Corn	Unfractionated	6.71E+06	7.02E+06	4.14E+04	4.33E+04	53.1	54.1	1.046
	Large	1.04E+07	1.08E+07	6.39E+04	6.67E+04	63.3	62.7	1.044
	Small	8.82E+06	1.07E+07	5.45E+04	6.57E+04	58.9	57.5	1.207
Barley	Unfractionated	1.90E+07	2.05E+07	1.17E+05	1.27E+05	59.9	60.1	1.081
	Large	1.58E+07	1.64E+07	9.74E+04	1.01E+05	57.0	57.1	1.039
	Small	1.49E+07	1.63E+07	9.21E+04	1.01E+05	53.3	53.3	1.092

[1] number-average molecular weight (g/mol)
[2] weight-average molecular weight (g/mol)
[3] number-average degree of polymerization
[4] weight-average degree of polymerization
[5] z-average radius of gyration (nm)
[6] weight-average radius of gyration (nm)
[7] polydispersity index (M_w/M_n)

Regardless of starch granule size, in corn and barley starches, AP molecules of HA genotypes were much smaller than those of NM and WX genotypes. This could be attributed the lower R_z value for HA starches (53.1–63.3 nm). However, the M_w of AP in HA starches of corn and barley was comparable to their NM and WX genotypes. Our data on M_w and R_z of AP from unfractionated starches were much lower than that reported in the literature (Rolland-Sabate, et al., 2007; Yoo & Jane, 2002; You & Izydorczyk, 2002). In these reports, the ranges of M_w and R_z were 1.3 to 4.9x10^8 g/mol and 201 to 312 nm, respectively, for NM starches of corn, wheat, and barley and 1.9 to 8.3x10^8 and 183 to 372 nm, respectively, for WX starches of corn and barley. The corresponding values for HA corn and barley were 1.4 to 1.7x10^8 and 164 to 389 nm, respectively. The discrepancies in M_w and R_z of AP might have been due to different starch cultivars, starch solubilization methods, and analytical approaches (HPSEC or Flow Field-Flow Fractionation) used in studies.

6.3.2.2. Amylose

The molecular characteristics of AM (Table 6.2) were different to those of AP (Table 6.1). In comparison to AP, the M_w of AM was lower and R_z was higher. R_z is related to the volume occupied by a molecule in a solution. Thus, the lower M_w and higher R_z suggest a higher proportion of loosely packed, long, unbranched AM chains. Whereas, the higher M_w and lower R_z of AP suggest a highly compact, highly branched structure. In NM starches, the M_w of AM in unfractionated

Table 6.2: Molecular characteristics of amylose of triticale, wheat, corn and barley starches

Starches		M_n[1]	M_w[2]	DP_n[3]	DP_w[4]	R_z[5]	R_w[6]	PDI[7]
Normal								
Pronghorn Triticale	Unfractionated	1.10E+06	1.13E+06	6.81E+03	6.96E+03	82.4	82.9	1.022
	Large	6.49E+06	7.48E+06	4.01E+04	4.61E+04	99.6	97.4	1.151
	Small	9.62E+06	1.07E+07	5.94E+04	6.62E+04	98.8	97.1	1.116
Ultima Triticale	Unfractionated	2.25E+06	2.25E+06	1.39E+04	1.39E+04	80.5	80.3	1.000
	Large	7.40E+06	7.67E+06	4.57E+04	4.73E+04	102.7	101.2	1.036
	Small	1.76E+07	1.79E+07	1.09E+05	1.11E+05	90.7	90.5	1.017
AC Reed Wheat	Unfractionated	1.73E+06	2.06E+06	1.07E+04	1.27E+04	87.7	89.7	1.190
	Large	4.50E+06	4.52E+06	2.78E+04	2.79E+04	91.5	91.4	1.004
	Small	3.63E+06	3.67E+06	2.24E+04	2.26E+04	91.1	90.9	1.010
CPS Red Wheat	Unfractionated	4.42E+06	4.55E+06	2.73E+04	2.81E+04	80.7	80.2	1.029
	Large	3.03E+06	3.05E+06	1.87E+04	1.88E+04	94.6	93.3	1.006
	Small	2.20E+06	2.51E+06	1.36E+04	1.55E+04	92.2	93.2	1.138
Corn	Unfractionated	2.28E+06	2.38E+06	1.41E+04	1.47E+04	77.9	78.4	1.042
	Large	3.06E+06	3.10E+06	1.89E+04	1.92E+04	97.6	98.3	1.013
	Small	4.16E+06	5.08E+06	2.57E+04	3.13E+04	91.3	93.5	1.220
Barley	Unfractionated	5.04E+06	5.11E+06	3.11E+04	3.15E+04	88.3	88.9	1.014
	Large	5.00E+06	5.04E+06	3.08E+04	3.11E+04	81.8	81.5	1.009
	Small	4.69E+06	4.73E+06	2.89E+04	2.92E+04	86.8	87.1	1.009
High-Amylose								
Corn	Unfractionated	8.74E+05	8.88E+05	5.39E+03	5.48E+03	69.2	70.3	1.016
	Large	1.57E+06	1.68E+06	9.72E+03	1.04E+04	88.7	86.6	1.066
	Small	9.49E+05	9.50E+05	5.86E+03	5.86E+03	80.0	80.3	1.001
Barley	Unfractionated	4.69E+06	4.71E+06	2.89E+04	2.91E+04	71.5	71.1	1.005
	Large	3.55E+06	3.61E+06	2.19E+04	2.23E+04	70.4	71.0	1.019
	Small	2.80E+06	2.80E+06	1.73E+04	1.73E+04	64.8	64.9	1.002

[1] number-average molecular weight (g/mol)
[2] weight-average molecular weight (g/mol)
[3] number-average degree of polymerization
[4] weight-average degree of polymerization
[5] *z*-average radius of gyration (nm)
[6] weight-average radius of gyration (nm)
[7] polydispersity index (M_w/M_n)

starches ranged from 1.1x10^6 g/mol (Pronghorn triticale) to 5.1x10^6 g/mol (barley). However, a broad range in M_w distribution was not seen between small and large granules of these starches (Table 6.2). The R_z of AM in NM unfractionated starches was between 77.9 nm (corn) and 88.3 nm (barley), which were lower than in their fractionated starches (Table 6.2). In fractionated NM starches, the R_z of AM in large granules (91.5–102.7 nm) was higher than in their small granules (90.7–98.8 nm). However, such a trend was not seen with NM barley starch. The molecular characteristics of AM in unfractionated HA starches also varied between corn and barley. Corn AM had a lower M_w (8.9x10^5 g/mol) and a smaller size (69.2 nm). Whereas, the corresponding values for barley AM were 4.7x10^6 g/mol and 71.5 nm, respectively. The R_z of AM in large and small granules of HA starches followed the order: corn (80–88.7 nm) > barley (64.8–70.4 nm). The M_w and R_z of AM from unfractionated barley were within the reported values (2.7–5.7x10^6 and 64–107 nm, respectively) for NM and HA genotypes (You & Izydorczyk, 2002).

As shown in Tables 6.1 and 6.2, the polydispersity index (*PDI*) of AP and AM were in the range 1.0–1.41 and 1.0–1.19, respectively. This is indicative of a broad range of polymer populations (regardless of starch sources and genotypes) in both AP and AM. When compared to other starches, wheat starches had the highest variation in the population of their polymer molecules (Tables 6.1 & 6.2). The results obtained from this study showed that the molar mass and molecular size or dimensions of AM and AP vary between and within starch sources.

6.3.3. Branching parameters

The branching parameters such as average molecular density (ρ), average specific volume for gyration (*SV*g), average degree of branching (*DB*), average chain length (*CL*) and the branching ratio or shrinking factor (*gM*) of AP and AM of triticale, wheat, corn and barley starches are presented in Table 6.3 and Table 6.4, respectively.

6.3.3.1. Amylopectin

The ρ of AP has been shown to influence starch properties (Yoo & Jane, 2002). In this study, AP density of unfractionated NM starches ranged from 24.8 (corn) to 66.3 (CPS Red wheat) g/mol/nm^3. This suggests that AP of CPS Red wheat is more compactly packed and more extensively branched than AP of corn. AP density of large granules of NM starches ranged from 20.9 (AC Reed wheat) to 62.1 (corn) g/mol/nm^3, whereas the AP density of small granules of NM starches ranged from 27.8 (CPS Red wheat) to 54.5 (Ultima triticale) g/mol/nm^3. In WX starches, the density of AP followed the order: fractionated corn >unfractionated corn >fractionated barley > unfractionated barley (Table 6.3). However, a reverse order was seen in HA starches, where the density of AP in fractionated barley was higher than in fractionated corn (Table 6.3). Regardless of starch sources and genotypes, the AP of small granules in most starches had a higher molecular density than those of large counterparts. This could be attributed to presence of a higher ratio of short-chains/long-chains in small granules (Ao & Jane, 2007).

Table 6.3: Branching parameters of amylopectin of triticale, wheat, corn and barley starches

Starches		Density[1]	*SV*g[2]	*gM*[3]	*CL*[4]	*DB*[5]
Normal						
Pronghorn Triticale	Unfractionated	66.1	0.038	0.07	12.7	7.9
	Large	50.5	0.050	0.09	17.7	5.7
	Small	37.0	0.068	0.12	28.9	3.5
Ultima Triticale	Unfractionated	44.4	0.057	0.12	24.1	4.1
	Large	34.3	0.074	0.13	33.5	3.0
	Small	54.5	0.046	0.08	16.4	6.1
AC Reed Wheat	Unfractionated	25.7	0.098	0.23	59.2	1.7
	Large	20.9	0.121	0.27	85.1	1.2
	Small	28.6	0.088	0.19	49.3	2.0
CPS Red Wheat	Unfractionated	66.3	0.038	0.09	14.6	6.9
	Large	34.5	0.073	0.14	35.1	2.8
	Small	27.8	0.091	0.20	53.4	1.9
Corn	Unfractionated	24.8	0.102	0.31	82.3	1.2
	Large	62.1	0.041	0.08	13.9	7.2
	Small	40.8	0.062	0.13	27.1	3.7
Barley	Unfractionated	59.1	0.043	0.08	14.5	6.9
	Large	34.9	0.072	0.16	36.4	2.7
	Small	43.0	0.059	0.13	26.6	3.8
Waxy						
Corn	Unfractionated	50.1	0.050	0.11	19.8	5.1
	Large	72.4	0.035	0.05	10.0	10.0
	Small	70.5	0.036	0.06	10.9	9.2
Barley	Unfractionated	20.5	0.123	0.35	107.3	0.9
	Large	51.2	0.049	0.09	17.5	5.7
	Small	51.8	0.049	0.10	18.8	5.3
High-Amylose						
Corn	Unfractionated	46.9	0.054	0.19	30.5	3.3
	Large	42.6	0.059	0.15	27.2	3.7
	Small	52.1	0.048	0.13	19.2	5.2
Barley	Unfractionated	95.5	0.026	0.06	7.8	12.8
	Large	88.6	0.028	0.07	9.1	11.0
	Small	107.6	0.023	0.07	6.9	14.5

[1] molecular density (g/mol/nm^3)
[2] specific volume for gyration (cm^3/g)
[3] branching ratio or shrinking factor = $R_{w\,(branched)}^2 / R_{w\,(linear)}^2$
[4] average chain length
[5] degree of branching (%)

The specific volume for gyration (*SV*g) of a molecule provides the theoretical gyration volume (in cm^3) per unit of molar mass (g), which can be further used to understand the mass-based information on the density and degree of branching of a molecule (You & Lim, 2000). The current study showed that the *SV*g of AP molecules (Table 6.3) were lower than those of AM molecules (Table 6.4), because the R_z of AP (Table 6.1) was lower than that of AM (Table 6.2). In unfractionated NM starches, the *SV*g of AP ranged from 0.038 cm^3/g (Pronghorn triticale and CPS Red wheat) to 0.102 cm^3/g (corn). This again confirms that the compactness of Pronghorn triticale or CPS Red wheat AP was much higher than that of corn AP. There was no noticeable relationship seen in *SV*g of AP from NM starches of unfractionated and fractionated forms (Table 6.3). In unfractionated WX starches, the *SV*g of AP was higher in barley (0.123 cm^3/g) than in corn (0.05 cm^3/g). However, there was no difference in *SV*g between large (0.035 cm^3/g) and small (0.049 cm^3/g) granules of corn and barley. *SV*g of AP in unfractionated HA starches was higher in corn (0.054 cm^3/g) than in barley (0.026 cm^3/g), and the AP in large granules of HA corn and HA barley starches had a higher *SV*g (0.028 – 0.059 cm^3/g) than their small granule counterparts (0.023 – 0.048 cm^3/g). Regardless of starch sources and genotypes, correlations were found between M_w, density, and SVg of AP in unfractionated starches. M_w was positively correlated to density ($r = 0.8$, $p<0.01$) and negatively correlated to *SV*g ($r = –0.8$, $p<0.01$). A strong negative correlation was also found between the molecular density and *SV*g of AP ($r = –0.9$, $p<0.001$).

The branching ratio or shrinking factor (*gM*) was used to calculate the number of branch points in starch molecules as shown in the equation (7), which was based on a simple ABC model proposed for hyper-branched macromolecules (Rolland-Sabate, et al., 2007). This model describes how polymerization or polycondensation occurs between the functional groups of its monomer molecules, thus is also a three-functional ploycondensation model (Rolland-Sabate, et al., 2007). For instance, in the ABC model of an AP, each glucose monomer has a reducing end (i.e. functional group 'A') which can connect to two hydroxyl (functional) groups, one in the C_4 position (i.e. group 'B') and another in the C_6 (i.e. group 'C') position. Polymerization reaction between groups 'A' and 'B' to form a linear chain is 25 times more recurrent than a reaction between groups 'A' and 'C' to form a branch chain, and ultimately an AP molecule. Accordingly, the average degree of polymerization (*DP*) of a molecule depends on the reactivity between 'A' and 'C' functional groups. In the present study, average chain length ($CL = DP_w/B$) and degree of branching ($DB = [B/DP_w]x100\%$) were measured by considering a "modified number" of branch points (B) in an AP molecule, which was calculated (Rolland-Sabate, et al., 2007) according to Hizukuri (Hizukuri, 1986) structural model of AP. In the Hizukuri model of AP, the longest B3-chain carries fourteen A-chains and one B1-chain, and two B2-chains each linked to four A-chains and one B1-chain. As a result, every long B-chain (one B3 + two B2) in an AP is connected to 8.33 (i.e. twenty five short chains divided by three long chains) chains on average (Rolland-Sabate, et al., 2007).

Thus, to get the "modified number" of branch points in an AP molecule, the number of branch points from equation (7) was multiplied by the factor of 8.33.

The average-*CL* of the AP molecules varied greatly between and within starch sources (differing in both amylose content and granule size). In this study, the average-*CL* of AP in unfractionated NM starches ranged from 12.7 (Pronghorn triticale) to 82.3 (corn). According to the Hizukuri (1986) model, the AP of unfractionated starches from Pronghorn triticale, Ultima triticale, CPS Red wheat, and NM barley may have been built up mainly of short-branch chains such as A- and B1-chains (*CL* = 12.7–24.1), whereas AC Reed wheat and NM corn may have been built up primarily of B2-chains (*CL* = 59.2), and B3-chains (*CL* = 82.3), respectively. The average-*CL* of AP of large and small granules from NM starches ranged from 13.9 to 85.1 and 16.4 to 53.4, respectively. With respect to unfractionated WX starches, the average-*CL* of corn AP (19.8) was lower than that of barley (107.3). The results on average-*CL* of WX barley suggest that AP of unfractionated starch is built up mainly of B4-chains, whereas its large and small granules are built up of B1-chains (*CL* = 17.5–18.8). This suggests that granule size influences the average-*CL* of AP. Similarly, AP of unfractionated WX corn was composed mainly of B1-chains, but its fractionated portions were composed mainly of A-chains. There was only a marginal difference (within a source) between large and small granules of the above starches (Table 6.3). In HA genotypes (irrespective to granule size distribution), the AP of corn and barley are mainly composed of B1-chains (*CL* = 19.2–30.5), and A-chains (*CL* = 6.9–9.1),

respectively. Our results differed from those of Evans and Thompson (2008), who showed that AP of HA corn starch had a lower *DB*, and was composed mainly of longer external and internal chains when compared to the AP of starch from NM corn. Regardless of starch sources, the AP of large and small granules from WX and HA genotypes had a higher proportion of short-branch chains than that of NM starches (Table 6.3). The average-*CL* was inversely correlated to both molecular density ($r = –0.84$, $p<0.01$) and *DB* ($r = –0.79$, $p<0.01$), regardless of starch sources and genotypes. The distribution of AP short A-chains (*DP* 6-11) has been shown to influence the gelatinization temperatures, thereby affecting the hydrolysis and other functional properties of native starch granules (Ao & Jane, 2007; Miao, et al., 2011).

The *DB* of AP is another branching parameter that is often considered in evaluating the suitability of starches for various applications. In unfractionated NM starches, the *DB* was found to be in the range from 1.2% (corn) to 7.9% (Pronghorn triticale). The average *DB* for most common starches is 3–6% (Rolland-Sabate, et al., 2007). In the present study, the *DB* of AP from Ultima triticale (4.1%), CPS Red wheat (6.9%), and barley (6.9%) were within or close to the reported range (3–6%) for *DB*. In contrast, the Pronghorn triticale (7.9%) had a higher *DB*, whereas AC Reed wheat (1.7%) and corn (1.2%) contained a lower *DB* than that of the reported range (3–6%) for *DB*. Although the *DB* of AP (1.2–7.2%) in fractionated starches was within the range for unfractionated starches, no trend was seen in *DB* between large and small granules of NM starches (Table

6.3). In WX starches, barley AP appeared to be less branched (*DB* = 0.9%) than corn AP (*DB* = 5.1%). The lower *DB* of WX barley suggests that the AP fraction may have been contaminated with AM. The *DB* of AP of large and small granules of WX barley starch ranged from 5.3 to 5.7%, whereas the corresponding range for WX corn was 9.2–10.0% (Table 6.3). The *DB* of AP molecules in HA corn starches ranged from 3.3–5.2% with 5.2% being highest in their small granules (Table 6.3). In contrast, AP molecules of HA barley starches appeared to be highly branched compared to HA corn, since the *DB* was higher (11.0–14.5%) in the former. The *DB* (directly proportional to number of branch points) greatly influences AP density; a highly branched AP molecule would be denser than a less branched molecule. A strong correlation was found between *DB* and density of AP in unfractionated starches ($r = 0.99$, $p<0.001$).

Molecular characteristics of AP of cereal and tuber starches have been shown to influence amylolysis (Gilbert, et al., 2010; Goesaert, et al., 2010; Rolland-Sabate, et al., 2007). However, none of these studies have reported in detail how molecular properties influence starch hydrolysis. The present study showed that the structure and properties of AP varied significantly among starches as illustrated using the Hizukuri (1986) model of AP below.

AP of unfractionated WX corn vs. AP of unfractionated Ultima triticale (Figure 6.4)

The AP from unfractionated starches of WX corn and Ultima triticale had a comparable molecular size (Figure 6.4). However, their *DB* varied by 1% (Table

6.3). WX corn AP showed a higher molecular-density (50.1 g/mol/nm^3) than that of Ultima triticale AP (44.4 g/mol/nm^3). The M_w of AP also varied by 2.0x10^6 g/mol (Table 6.1) between the above starches, being highest in WX corn AP (1.7x10^7 g/mol). A comparable average-*CL* (20–24) of AP implies that the difference in length of short unit chains (A and B1) between AP molecules of the above starches is not significant. This suggests then when branched chains of AP are densely packed (Figure 6.4A), they hinder amylolysis. Whereas, branch chains loosely packed within the same volume of AP (Figure 6.4B) are readily hydrolyzed. Furthermore, in a densely packed AP, intra-molecular H-bonding would result in a large number of crystallites, as formed within and between AP molecules, which may confer high thermal stability.

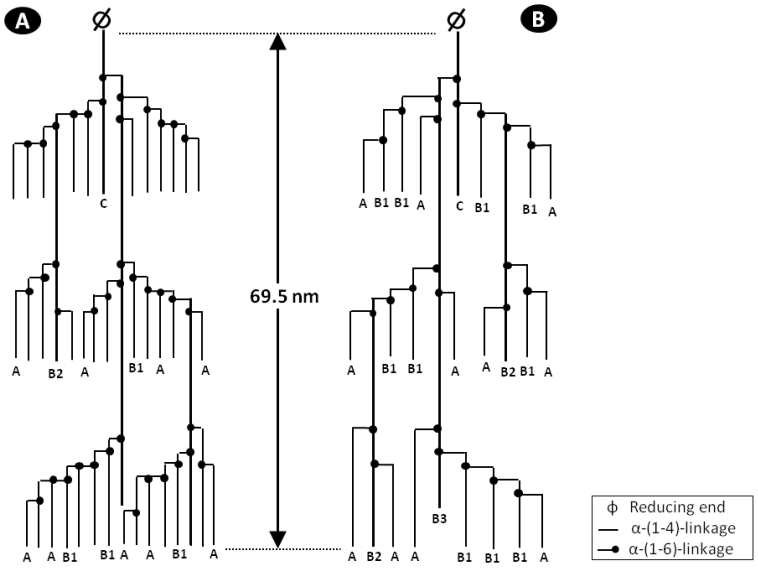

Figure 6.4: Structure models of amylopectins with comparable molecular size; isolated from unfractionated starches of waxy corn (**A**) and Ultima triticale (**B**). A, B1, B2, B3 and C in the models are the unit chains of amylopectin.

AP of unfractionated NM barley vs. AP of unfractionated CPS Red wheat (Figure 6.5)

Although the AP molecules from the above starches had equal *DB* (6.9%), their molecular sizes were different; R_z of NM barley was higher than that of CPS Red wheat (Figure 6.5). The difference in R_z indicates that the AP of NM barley starch is probably composed mainly of longer B2- and B3-chains or in other words, amorphous lamellae of NM barley AP is bigger than CPSR wheat AP (Figure 6.5). This would result in the size of AP of NM barley starch being larger than AP of CPS Red wheat starch (Figure 6.5). In addition, the higher M_w of NM barley AP ($2.2x10^7$ g/mol) suggests that its structure is different to that of CPS Red wheat AP. Accordingly, NM barley AP has more space between clusters which would confer high susceptibility to enzymatic and chemical reactions (Figure 6.5A).

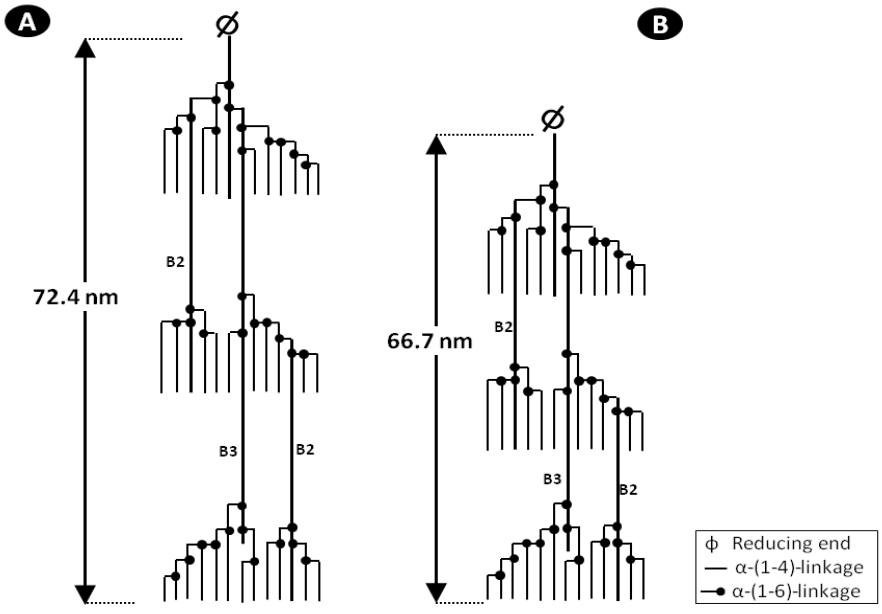

Figure 6.5: Structure models of amylopectins with equal degree of branching; isolated from unfractionated starches of normal barley (**A**) and CPS Red wheat (**B**).

In contrast, the clusters of CPS Red wheat AP are compactly organized, and therefore more resistant to hydrolysis (Figure 6.5B). In addition, the AP molecules of CPS Red wheat starch would be more resistant to thermal degradation than AP of NM barley starch.

AP of large granules of Pronghorn triticale vs. AP of large granules of AC Reed wheat (Figure 6.6)

Although the molecular size of AP from the above starches are comparable (76 nm), their variation in density, average-*CL*, and *DB* (Table 6.3) indicates that the unit chains in each AP have different length. High values for density (50.5 g/mol/nm^3) and *DB* (5.7%), and a lower value of average-*CL* (17.7) are seen in the AP of large granules from Pronghorn triticale. The corresponding values for the AP of large granules from AC Reed wheat are 20.9 g/mol/nm^3, 1.2% and 85.1. This implies that AC Reed AP is composed mainly of longer unit chains, which will have a fewer number of branch points (Figure 6.6B). Furthermore, the AP of large granules from Pronghorn triticale had a higher M_w when compared to the AP of large granules of AC Reed wheat (Table 6.1). This suggests that Pronghorn triticale AP had a higher molecular density due to a higher ratio of short-unit chains to long-unit chains (Figure 6.6A). Since an AP that is composed mainly of short-chains is highly stabilized by H-bonding in a starch granule, AP of Pronghorn triticale starch may resist enzyme hydrolysis. In addition, AP of Pronghorn triticale is better able to withstand applied thermal stresses than that of AC Reed wheat AP (Huber & Praznik, 2004).

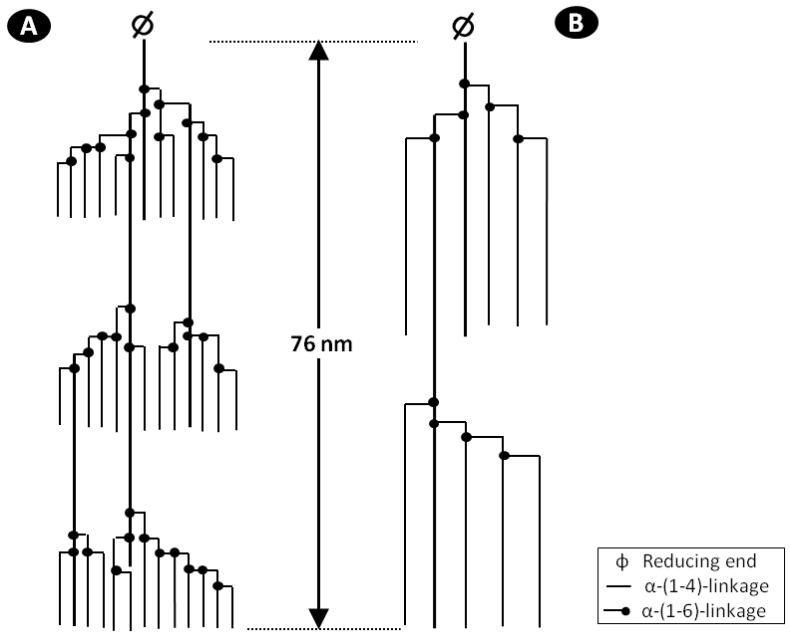

Figure 6.6: Structure models of amylopectins with comparable molecular size but differing in unit chain length; isolated from large granules of Pronghorn triticale (**A**) and AC Reed wheat (**B**) starches.

6.3.3.2. Amylose

Branching is uncommon in AM molecules; they are predominantly linear chains of glucopyronosyl units. However, the AM molecules of some starches appeared to be branched. A small degree of branching was seen in unfractionated starches of CPS Red wheat, NM barley and HA barley, and their average-*CL* per branching point were 801.9, 1182.6 and 291, respectively (Table 6.4). In contrast, the AM from large and small granules of NM and HA barley starches showed only a marginal *DB* (0.1–0.3%). A contamination of AP molecules with AM could explain the inconsistency in the results with respect to AM branching in other starches

Table 6.4: Branching parameters of amylose of triticale, wheat, corn and barley starches

Starches		Density[1]	*SVg*[2]	*gM*[3]	*CL*[4]	*DB*[5]
Normal						
Pronghorn Triticale	Unfractionated	2.0	1.251	4.58	0.0	0.0
	Large	7.6	0.333	0.58	537.8	0.2
	Small	11.1	0.227	0.37	209.8	0.5
Ultima Triticale	Unfractionated	4.3	0.585	1.80	0.0	0.0
	Large	7.1	0.356	0.61	645.8	0.2
	Small	24.0	0.105	0.17	55.8	1.8
AC Reed Wheat	Unfractionated	3.0	0.828	2.52	0.0	0.0
	Large	6.0	0.422	0.96	5580.0	0.0
	Small	4.8	0.527	1.26	0.0	0.0
CPS Red Wheat	Unfractionated	8.6	0.292	0.74	801.9	0.1
	Large	3.6	0.701	1.66	0.0	0.0
	Small	3.2	0.789	2.12	0.0	0.0
Corn	Unfractionated	5.0	0.502	1.60	0.0	0.0
	Large	3.3	0.755	1.80	0.0	0.0
	Small	6.7	0.378	0.88	2212.6	0.0
Barley	Unfractionated	7.4	0.340	0.79	1182.6	0.1
	Large	9.2	0.274	0.67	592.8	0.2
	Small	7.2	0.349	0.83	1459.2	0.1
High-Amylose						
Corn	Unfractionated	2.7	0.941	4.45	0.0	0.0
	Large	2.4	1.049	3.03	0.0	0.0
	Small	1.9	1.359	5.33	0.0	0.0
Barley	Unfractionated	12.9	0.196	0.56	291.0	0.3
	Large	10.4	0.243	0.77	787.7	0.1
	Small	10.3	0.245	0.89	1383.8	0.1

[1] molecular density (g/mol/nm^3)
[2] specific volume for gyration (cm^3/g)
[3] branching ratio or shrinking factor = $R_w{}^2{}_{(branched)}/R_w{}^2{}_{(linear)}$
[4] average chain length
[5] degree of branching (%)

(unfractionated or fractionated granules). AM molecules of WX, NM and HA barley starches have been reported to exhibit some branching (Yoshimoto, et al., 2002; You & Izydorczyk, 2002). In the present study, AM from the WX starches of both corn and barley was not separated well in the HPSEC-MALLS-RI system, likely due to their low AM contents (Figures 6.1–6.3).

Compared to AP molecules, the AM of unfractionated NM and HA starches showed a lower molecular density (2.0 to 12.9 g/mol/nm^3). In large and small granules, the AM of NM starches showed a higher density range (3.2–24.0 g/mol/nm^3), whereas the HA starches exhibited a lower density (1.9–10.4 g/mol/nm^3) than their corresponding unfractionated starches. A higher density of AM molecules in barley genotypes, such as NM and HA, was likely due to their branched chains. AM molecules exhibited a higher *SV*g than AP molecules (Table 6.4), indicating that AM chains are longer than AP molecules.

Significant correlations were seen between the molecular characteristics and branching parameters such as M_w, density and *SV*g of AP and AM of unfractionated starches regardless of their genotypes. The M_w was highly correlated to molecular density of both AP and AM ($r = 0.8$, $p<0.01$ and $r = 0.9$, $p<0.01$, respectively), whereas it was negatively correlated to *SV*g ($r = –0.8$, $p<0.01$ and $r = –0.9$, $p<0.01$, respectively). Furthermore, a strong inverse correlation between molecular density and *SV*g of AP and AM also found ($r = –0.9$, $p < 0.001$ and $r = –0.9$, $p < 0.01$, respectively).

6.4. CONCLUSIONS

Structural characteristics of AP and AM from wheat, triticale, barley and corn were determined by HPSEC-MALLS-RI. The molecular characteristics and branching parameters of AP and AM of these starches varied significantly among these starches, as a function of botanical origin, genotypes, and granule size. In comparison to the other starches, AP and AM of HA barley starches were smaller, denser and more branched. In addition, AP of HA barley starches were composed mainly of shorter chains. Whereas, AP of wheat starches were less branched, less compact and composed mainly of longer chains. The AP molecular size of Ultima triticale and WX corn starches were comparable, however, they differed with respect to molar mass and degree of branching. The AP of the two NM starches (CPS Red wheat and barley) was composed mainly of similar type of unit chains (with equal degree of branching). However, they differed with respect to their molar mass and molecular size, suggesting that variations in molecular characteristics of AP will significantly influence starch properties such as susceptibility towards enzyme hydrolysis, gelatinization, extent of crystallization during retrogradation, and granular swelling.

REFERENCES

Ao Z. & Jane J. (2007). Characterization and modeling of the A- and B-granule starches of wheat, triticale, and barley. *Carbohydrate Polymers 67*, 46-55.

Arturo Bello-Perez L., Rodriguez-Ambriz S. L., Agama-Acevedo E., & Sanchez-Rivera M. M. (2009). Solubilization Effects on Molecular Weights of Amylose and Amylopectins of Normal Maize and Barley Starches. *Cereal Chemistry 86*, 701-705.

Charoenkul N., Uttapap D., Pathipanawat W., & Takeda Y. (2006). Simultaneous determination of amylose content & unit chain distribution of amylopectins of cassava starches by fluorescent labeling/HPSEC. *Carbohydrate Polymers 65*, 102-108.

Chen M. & Bergman C. J. (2007). Method for determining the amylose content, molecular weights, and weight- and molar-based distributions of degree of polymerization of amylose and fine-structure of amylopectin. *Carbohydrate Polymers 69*, 562-578.

Evans A. & Thompson D. B. (2008). Enzyme susceptibility of high-amylose starch precipitated from sodium hydroxide dispersions. *Cereal Chemistry 85*, 480-487.

Gao J., Vasanthan T., & Hoover R. (2009). Isolation and Characterization of High-Purity Starch Isolates from Regular, Waxy, and High-Amylose Hulless Barley Grains. *Cereal Chemistry 86*, 157-163.

Gilbert R. G., Gidley M. J., Hill S., Kilz P., Rolland-Sabate A., Stevenson D. G., & Cave R. A. (2010). Characterizing the Size and Molecular Weight Distribution of Stach: Why it Is Important and Why it Is Hard. *Cereal Foods World 55*, 139-143.

Goesaert H., Bijttebier A., & Delcour J. A. (2010). Hydrolysis of amylopectin by amylolytic enzymes: level of inner chain attack as an important analytical differentiation criterion. *Carbohydrate Research 345*, 397-401.

Han J. & Lim S. (2004). Structural changes in corn starches during alkaline dissolution by vortexing. *Carbohydrate Polymers 55*, 193-199.

Hizukuri S. (1986). Polymodal Distribution of the Chain Lengths of Amylopectins, and its Significance. *Carbohydrate Research 147*, 342-347.

Huber, A. & Praznik, W. (2004). Analysis of Molecular characteristics of starch polysaccharides. In P. Thomasik (Ed.). *Chemical and Functional Properties of Food Saccharides* (pp. 333-353). Boca Raton, Florida, USA.: CRC Press LLC.

Kandil A., Li J., Vasanthan T., Bressler D. C., & Tyler R. T. (2011). Compositional changes in whole grain flours as a result of solvent washing and their effect on starch amylolysis. *Food Research International 44*, 167-173.

Kim W., Eum C. H., Lim S., Han J., You S., & Lee S. (2007). Separation of amylose and amylopectin in corn starch using dual-programmed flow field-flow Fractionation. *Bulletin of the Korean Chemical Society 28*, 2489-2492.

Liu, Q. (2005). Understanding starches and their role in foods. In S. W. Cui (Ed.). *Food Carbohydrates: Chemistry, Physical Properties, and Applications* (pp. 309-355). Boca Raton, FL., USA.: CRC Press, Taylor & Francis Group, LLC.

Miao M., Zhang T., Mu W., & Jiang B. (2011). Structural characterizations of waxy maize starch residue following in vitro pancreatin and amyloglucosidase synergistic hydrolysis. *Food Hydrocolloids 25*, 214-220.

Mua J. & Jackson D. (1997). Relationships between functional attributes and molecular structures of amylose and amylopectin fractions from corn starch. *Journal of Agricultural and Food Chemistry 45*, 3848-3854.

Murthy G. S., Johnston D. B., Rausch K. D., Tumbleson M. E., & Singh V. (2011). Starch hydrolysis modeling: application to fuel ethanol production. *Bioprocess and Biosystems Engineering 34*, 879-890.

Naguleswaran S., Li J., Vasanthan T., Bressler D., & Hoover R. (2012). Amylolysis of large and small granules of native triticale, wheat and corn starches using a mixture of α-amylase and glucoamylase. *Carbohydrate Polymers 88*, 864-874.

Radosta S., Haberer M., & Vorwerg W. (2001). Molecular characteristics of amylose and starch in dimethyl sulfoxide. *Biomacromolecules 2*, 970-978.

Rojas C. C., Wahlund K., Bergenstahl B., & Nilsson L. (2008). Macromolecular Geometries Determined with Field-Flow Fractionation and their Impact on the Overlap Concentration. *Biomacromolecules 9*, 1684-1690.

Rolland-Sabate A., Colonna P., Mendez-Montealvo M. G., & Planchot V. (2007). Branching features of amylopectins and glycogen determined by asymmetrical flow field flow fractionation coupled with multiangle laser light scattering. *Biomacromolecules 8*, 2520-2532.

Yokoyama W., Renner-Nantz J., & Shoemaker C. (1998). Starch molecular mass and size by size-exclusion chromatography in DMSO-LiBr coupled with multiple angle laser light scattering. *Cereal Chemistry 75*, 530-535.

Yoo S. & Jane J. (2002). Molecular weights and gyration radii of amylopectins determined by high-performance size-exclusion chromatography equipped with multi-angle laser-light scattering and refractive index detectors. *Carbohydrate Polymers 49*, 307-314.

Yoshimoto Y., Takenouchi T., & Takeda Y. (2002). Molecular structure and some physicochemical properties of waxy and low-amylose barley starches. *Carbohydrate Polymers 47*, 159-167.

You S., Stevenson S., Izydorczyk M., & Preston K. (2002). Separation and characterization of barley starch polymers by a flow field-flow fractionation technique in combination with multiangle light scattering and differential refractive index detection. *Cereal Chemistry 79*, 624-630.

You S. G. & Izydorczyk M. S. (2002). Molecular characteristics of barley starches with variable amylose content. *Carbohydrate Polymers 49*, 33-42.

You S. & Lim S. (2000). Molecular characterization of corn starch using an aqueous HPSEC-MALLS-RI system under various dissolution and analytical conditions. *Cereal Chemistry 77*, 303-308.

CHAPTER 7

Amylolysis of amylopectin and amylose isolated from wheat, triticale, corn, and barley starches*

7.1. INTRODUCTION

Starch is the second abundant natural polysaccharide present in higher plants, next to cellulose and it is an inevitable source of energy for animals, including humans. The starch granules naturally exist in semicrystalline architecture, which makes the starch as a unique component with numerous functionalities (Vermeylen et al., 2005; Mua & Jackson, 1997). The architecture of a starch granule is built up by two polymers, amylose (AM) and amylopectin (AP), which are highly organized through intra- and inter-molecular hydrogen bonds resulting in a complex biopolymer. In general, enzymatic hydrolysis is used as a tool to study the architecture of starch granules (Miao, et al., 2011). Hydrolysis of starch granules with amylases (i.e. amylolysis) occurs in several steps, which include diffusion to the solid surface, adsorption, and finally catalysis. The rate of hydrolysis is initially fast but then continues at a slower and more persistent rate (Oates, 1997). Among the amylases, α-amylase and glucoamylase are most commonly used to study the hydrolysis pattern of starch granules. The α-amylases (EC 3.2.1.1) are endo-acting enzymes that internally hydrolyse α-D-(1,4)-glycosidic linkages of both AP and AM yielding soluble products such as

* A version of this chapter has been submitted for publication.

oligosaccharides, and branched and low molecular weight α-limit dextrins. However, glucoamylase (EC 3.2.1.3) is an exo-acting enzyme, which depolymerizes both α-(1,4)- and α-(1,6)-linkages of starch polymers from their non-reducing ends resulting in the complete conversion of starch into glucose (Sujka & Jamroz, 2007). Thus, a study of the action pattern of amylases is important to understand how starch structure influences physicochemical properties and functionality. In addition, cereal starches are more frequently used in various food and industrial applications than starches from other sources. Thereby, understanding the molecular structure-amylolysis relationship is important for efficient utilization of cereal starches in different applications.

The influence of structural properties of native starches such as granule size, granule architecture, and granule porosity on *in vitro* hydrolysis have been studied (Asare, et al., 2011; Dhital, et al., 2010; Liu, et al., 2007; Naguleswaran, et al., 2012; Salman, et al., 2009; Stevnebø, et al., 2006; Sujka & Jamroz, 2007; Uthumporn, et al., 2010). However, there is a dearth of information on the extent to which isolated AM and AP are hydrolyzed by α-amylase and glucoamylase at low temperatures. A comparison of the reactivity of amylases towards the intact native granule and isolated AP and AM would help us to understand the role played by molecular characteristics of AP and AM in starch amylolysis. The hypothesis of this study was AP and AM, when separated from starch granule would be hydrolyzed to a higher extent than they are present together within the granule interior.

7.2. MATERIALS AND METHODS

7.2.1. Materials

Two cultivars of wheat grains, Canada prairie spring red (CPS Red) and AC Reed, were provided by Alberta Agriculture and Food in Barrhead (AB, Canada). Triticale grains (Pronghorn and AC Ultima) were obtained from the Field Crop Development Centre of Alberta Agriculture and Rural Development in Lacombe (AB, Canada). Grains from three hull-less barley cultivars (waxy, CDC Candle; normal, CDC McGwire; and high-amylose, SH 99250) were obtained from the Crop Development Center at University of Saskatchewan in Saskatoon (SK, Canada). Commercial corn starches of waxy (Amioca), normal (Melojel) and high-amylose (Hylon VII) were obtained from the National Starch Food Innovation in Bridgewater (NJ, USA). Granular starch hydrolyzing enzyme, Stargen 002 (570 GAU/g) was a gift from Genencor International in Rochester (NY, USA). All other chemicals and reagents used in this study were of ACS grade.

7.2.2. Grain grinding and starch isolation

Triticale, wheat and barley grains were ground into meals in a Retsch mill (Model ZM 200, Haan, Germany) using a ring sieve with an aperture size of 0.5 mm. Pure starch (purity >95%, w/w) was isolated from the grain meal of triticale, wheat and barley using the procedures reported by Kandil, et al. (2011) and Gao, et al. (2009). The detailed description of the starch isolation procedures are presented in appendix.

7.2.3. Amylopectin (AP) and amylose (AM) isolation

AP and AM of triticale, wheat, corn, and barley starches were separated according to the protocols described by Charoenkul et al. (2006) and Takeda et al. (1986) with certain modifications. Starch (100 mg, dry basis) was dissolved in 10 mL of 95% dimethyl sulfoxide (DMSO) by heating (85 – 90^{o}C) in a water bath for 1h with stirring in a Vortex mixer every 10 min. Dissolved starch was cooled to room temperature (22^{o}C) followed by addition of 30 mL of anhydrous ethanol and then kept at 4^{o}C for 2h to settle the starch molecules. The pellet of AP and AM was collected and washed with 10 mL of cool anhydrous ethanol followed by centrifugation (3500 x*g* for 10 min). The starch molecules were then dispersed in 17 mL water at 70 – 80^{o}C followed by the addition of 1 mL of n-butanol and 1 mL of isopentanol (3-methyl-1-butanol). The mixture in a tightly closed tube was heated (80 – 85^{o}C) in a water bath for 1h under a fume hood with stirring (Vortex mixing every 10 min), then cooled and stored in a Styrofoam box for 15h at room temperature followed by for 24h at 4^{o}C. The supernatant liquid (≈20 mL) containing AP and the pellet of AM were separated by centrifugation (6000 x*g* for 10 min). To recover AP from the supernatant liquid, 60 mL of cold methanol (absolute) was added. The tubes were then kept at 4^{o}C for 2h and centrifuged (6000 x*g* for 10 min). After washing with cold methanol (10 mL), the AP pellet was air-dried at room temperature for 24h. AM pellet in the form of butanol-amylose complex was dispersed in 20 mL of cold ethanol (anhydrous). The tubes were then kept at 4^{o}C for 2h and centrifuged (6000 x*g* for 10 min). The pellet of

AM was washed with cold ethanol (10 mL) followed by cold acetone (10 mL), and air-dried at room temperature for 24h. The isolated AP and AM were stored at room temperature in airtight containers until further analyses. The residual contents of butanol and isopentanol in AM fractions were analyzed by Gas Chromatography coupled with a Flame-Ionization-Detector (GC-FID) according to the procedure described by Gibreel et al. (2009). An internal standard (0.4% pentanol) and two sample standards (0.4% n-butanol and 0.5% isopentanol) were included in this procedure. The n-butanol and isopentanol contents in separated amylose samples were in the range 0.1 – 2% and 0.4 – 1.5%, respectively.

7.2.4. Amylolysis of isolated AP and AM

AP and AM (30 mg, dry basis) were dissolved separately in 2 mL of 1M KOH and mechanically stirred in an orbit shaker (Lab-line Instruments, Inc., IL, USA) for 1h (tubes containing the samples were covered with ice in a Styrofoam box). The dispersed AP or AM molecules in KOH solution was then diluted with 2 mL of 50 mM sodium acetate buffer and the pH of the solution was adjusted to 4.0 with 1M HCl. Total volume of the solution was corrected to 10 mL with acetate buffer-enzyme mixture (Stargen 002 enzyme was used at 24 U/30 mg starch) to achieve the sample concentration of 0.3% (w/v). The amylolysis experiment was carried out at 55^{o}C for 1h and then at 30^{o}C for 72h in shaking water bath (Model BS-11, Jeio Tech Inc., Korea). The aliquots of hydrolyzed samples were withdrawn at 1, 24, 48, and 72h for determination of the degree of hydrolysis

(DH). DH was expressed as a percentage of reducing value (Bruner, 1964). Control samples for AP and AM were run concurrently without enzyme addition.

7.2.5. Statistical Analysis

All amylolysis treatments were carried out in triplicate. Analysis of variance using the General Linear Model (GLM) procedure and Pearson correlation statistics was performed using the SAS® Statistical Software, Version 9.3 (SAS Institute Inc., Cary, NC, USA, 2011). Multiple comparisons of the means were completed by using the Tukey's Studentized Range (HSD) Test at $\alpha = 0.05$.

7.3. RESULTS AND DISCUSSION

7.3.1. Molecular characteristics of AP and AM

The molecular characteristics of AP and AM such as weight-average molecular weight (M_w), z-average molecular dimension (R_z), dispersed-molecular density (ρ), degree of branching (*DB*), and average-chain length (*CL*) were adapted from Chapter 6 and presented in Table 7.1.

7.3.2. Amylolysis of native starch granules

Amylolysis data of native starch granules from wheat, triticale, corn, and barley were adapted from Chapters 4 and 5. The starches used in this study are categorized into three genotype groups; normal, waxy, and high-amylose depending on the AM content in their native form and the DH of their native granules are presented in Tables 7.2, 7.3 and 7.4, respectively.

Table 7.1: Molecular characteristics of amylopectin and amylose of normal, waxy, and high-amylose starches from triticale, wheat, corn, and barley

	Amylopectin					Amylose		
	M_w[1]	R_z[2]	P[3]	DB[4]	CL[5]	M_w	R_z	ρ
Normal								
Pronghorn Triticale	2.46E+07	71.9	66.1	7.9	12.7	1.13E+06	82.4	2.0
Ultima Triticale	1.49E+07	69.5	44.4	4.1	24.1	2.25E+06	80.5	4.3
AC Reed Wheat	9.35E+06	71.4	25.7	1.7	59.2	2.06E+06	87.7	3.0
CPS Red Wheat	1.97E+07	66.7	66.3	6.9	14.6	4.55E+06	80.7	8.6
Corn	6.48E+06	63.9	24.8	1.2	82.3	2.38E+06	77.9	5.0
Barley	2.24E+07	72.4	59.1	6.9	14.5	5.11E+06	88.3	7.4
Waxy								
Corn	1.69E+07	69.6	50.1	5.1	19.8	n/a	n/a	n/a
Barley	6.15E+06	67.0	20.5	0.9	107.3	n/a	n/a	n/a
High-Amylose								
Corn	7.02E+06	53.1	46.9	3.3	30.5	8.88E+05	69.2	2.7
Barley	2.05E+07	59.9	95.5	12.8	7.8	4.71E+06	71.5	12.9

[1] weight-average molecular weight (g/mol)
[2] z-average radius of gyration (nm)
[3] dispersed-molecular density (g/mol/nm^3)
[4] degree of branching (%)
[5] average chain length

7.3.3. Amylolysis of native granules, AP and AM of normal starches

The DH of native granules and their AP and AM fractions of normal starches are presented in Table 7.2. The results showed that the DH of native granules from normal starches with similar AM content (22.5 – 26.4%) increased rapidly during first 24h hydrolysis (CPS Red wheat ~ Pronghorn triticale > AC Reed wheat ~ Ultima triticale > barley > corn). The lower DH of native corn starch could be attributed to the morphological characteristics of the granule surface. Hydrolysis

of native starch granules has been shown to begin at the granule periphery (due to the presence of surface pores and channels). Pores and channels have been shown to increase the effective surface area for fast enzyme diffusion (Oates, 1997; Tester et al., 2006). Naguleswaran et al. (2011) have shown that in corn starch, surface pores and channels are blocked by protein and phospholipids and this may have been responsible for the lower DH of corn starch. After 24h, hydrolysis was gradual in all starches. At the end of 72h, DH followed the order: CPS Red wheat ~ AC Reed wheat > Ultima triticale ~ Pronghorn triticale > corn > barley (Table 7.2). The isolated AP (DH = 72.7 – 82.7%) and AM (DH = 68.7 – 81.4%) from all starches were hydrolyzed to a greater extent than native granules (DH = 3.5 – 76.5%) during the initial stage (1h) of hydrolysis. The difference in DH between native granules and their isolated fractions (AP and AM) is mainly due to the architecture of the native granules. As discussed earlier, the first point of enzyme attack is on the granule surface. The granule periphery is highly organized by short-chains of AP clusters that hinder the entry of amylases into the granule interior. This may explain the reduced DH of native granules during the early stage of hydrolysis (Figure 7.1A).

The DH after 72h was higher in native granules (89.8 – 96.9%) than in isolated AP (81.1 – 87.9%) and AM (73.6 – 87.0%). This could be attributed to increased mobility of isolated AP and AM, which facilitates interaction among AP-AP, AP-AM and AM-AM molecules resulting in the formation of junction zones that become inaccessible to amylases. Between 1 and 72h of hydrolysis,

the difference in DH between isolated AP and AM (AP > AM) could be attributed to the molecular structure of AP. The enzyme cocktail used in this study was composed of both α-amylase (random endo-attack on α-(1,4)-glycosidic linkages) and glucoamylase (exo-attack on both α-(1,4)- and α-(1,6)-linkages).

Table 7.2: Degree of hydrolysis of native granules, amylopectin and amylose of normal starches from triticale, wheat, corn, and barley

	Degree of hydrolysis (%, dry basis)			
	1h[1]	**24h[2]**	**48h[2]**	**72h[2]**
Native granules				
Pronghorn Triticale	$76.5^{c} \pm 1.5$	$89.3^{ab} \pm 0.8$	$92.2^{a} \pm 0.7$	$92.4^{b} \pm 1.0$
Ultima Triticale	$69.0^{g} \pm 1.1$	$87.5^{b} \pm 1.5$	$92.2^{a} \pm 1.6$	$92.5^{b} \pm 0.9$
AC Reed Wheat	$22.1^{i} \pm 1.3$	$88.6^{b} \pm 0.3$	$89.7^{b} \pm 0.9$	$96.2^{a} \pm 0.5$
CPS Red Wheat	$53.8^{h} \pm 1.1$	$91.3^{a} \pm 0.5$	$92.8^{a} \pm 0.5$	$96.9^{a} \pm 0.9$
Corn	$3.5^{j} \pm 0.4$	$59.8^{k} \pm 1.0$	$84.9^{cd} \pm 0.4$	$90.6^{bc} \pm 1.4$
Barley	$70.6^{fg} \pm 0.3$	$81.3^{de} \pm 1.1$	$84.0^{d} \pm 0.9$	$89.8^{bc} \pm 0.5$
Amylopectin				
Pronghorn Triticale	$79.2^{b} \pm 1.0$	$81.6^{de} \pm 1.2$	$83.7^{d} \pm 0.8$	$85.3^{def} \pm 0.6$
Ultima Triticale	$82.7^{a} \pm 0.8$	$84.8^{c} \pm 1.3$	$86.5^{c} \pm 0.8$	$87.8^{cd} \pm 1.5$
AC Reed Wheat	$72.7^{ef} \pm 1.1$	$76.0^{hi} \pm 0.8$	$77.9^{g} \pm 0.3$	$81.1^{g} \pm 1.2$
CPS Red Wheat	$76.0^{c} \pm 0.2$	$78.6^{fg} \pm 0.4$	$80.3^{f} \pm 0.8$	$81.6^{g} \pm 0.8$
Corn	$73.4^{de} \pm 0.4$	$79.4^{efg} \pm 0.7$	$83.1^{de} \pm 0.7$	$86.6^{de} \pm 0.7$
Barley	$75.4^{cd} \pm 0.5$	$81.5^{de} \pm 0.8$	$83.8^{d} \pm 1.0$	$87.9^{cd} \pm 0.7$
Amylose				
Pronghorn Triticale	$75.6^{cd} \pm 0.8$	$78.5^{fgh} \pm 0.5$	$81.0^{ef} \pm 0.7$	$83.4^{fg} \pm 1.2$
Ultima Triticale	$81.4^{ab} \pm 1.0$	$83.4^{cd} \pm 0.7$	$84.7^{cd} \pm 0.4$	$86.3^{de} \pm 0.6$
AC Reed Wheat	$68.8^{g} \pm 0.8$	$71.6^{j} \pm 0.5$	$72.7^{h} \pm 0.5$	$73.6^{h} \pm 0.3$
CPS Red Wheat	$75.1^{cde} \pm 0.4$	$77.5^{ghi} \pm 0.5$	$79.8^{fg} \pm 0.6$	$80.9^{g} \pm 0.5$
Corn	$68.7^{g} \pm 0.6$	$75.1^{i} \pm 0.3$	$79.5^{fg} \pm 0.3$	$84.5^{ef} \pm 1.3$
Barley	$74.3^{cde} \pm 0.7$	$80.7^{ef} \pm 0.5$	$83.4^{d} \pm 0.8$	$87.0^{de} \pm 1.0$

[1] hydrolysis carried out at 55°C for 1h

[2] hydrolysis carried out at 30°C for 24, 48, and 72h

values are mean ± standard deviation, and values with the same superscript in italic letters in the same column are not significantly different at α = 0.05.

Since AP molecules possess several non-reducing ends, the outer clusters of AP are rapidly hydrolyzed by exo-type glucoamylase (Figure 7.1B). The low DH of isolated AM could be attributed to the presence of only one non-reducing end for glucoamylase action (Figure 7.1C). Long-chains of AP that connect each cluster are initially hydrolyzed by endo-acting α-amylases to release individual clusters (Figure 7.1B). Thereafter, clusters composed of short-chains are extensively hydrolyzed by exo-acting glucoamylases to produce sugars. As discussed earlier, a higher number of short-chains in a cluster increases the number of access points for glucoamylase reactions (Figure 7.1B). The high DH of native granules of triticale (Pronghorn and Ultima), wheat (CPS Red wheat), barley starches, and their respective AP molecules (Table 7.2) is mainly due to the presence of high proportion of AP short-chains (average-CL 12.7–24.1). The low DH shown by native granules of AC Reed wheat and corn, and their APs at the end of 1h hydrolysis (Table 7.2) could be attributed to their AP long average-*CL* (Table 7.1).

We postulate that, the rate of hydrolysis for a longer glycosidic AM chain would be lower than that of a shorter AP chain due to the following reasons: 1) AM has only one non-reducing end per molecule compared to AP which has >1. Consequently, glucoamylase hydrolysis will progress faster with AP and 2) longer chains produced from random attack of α-amylase on AM chains would interact (Figure 7.1C) to a greater extent (reduces accessibility for amylases) than shorter AP chains during the time course of hydrolysis, resulting in a lower DH for AM.

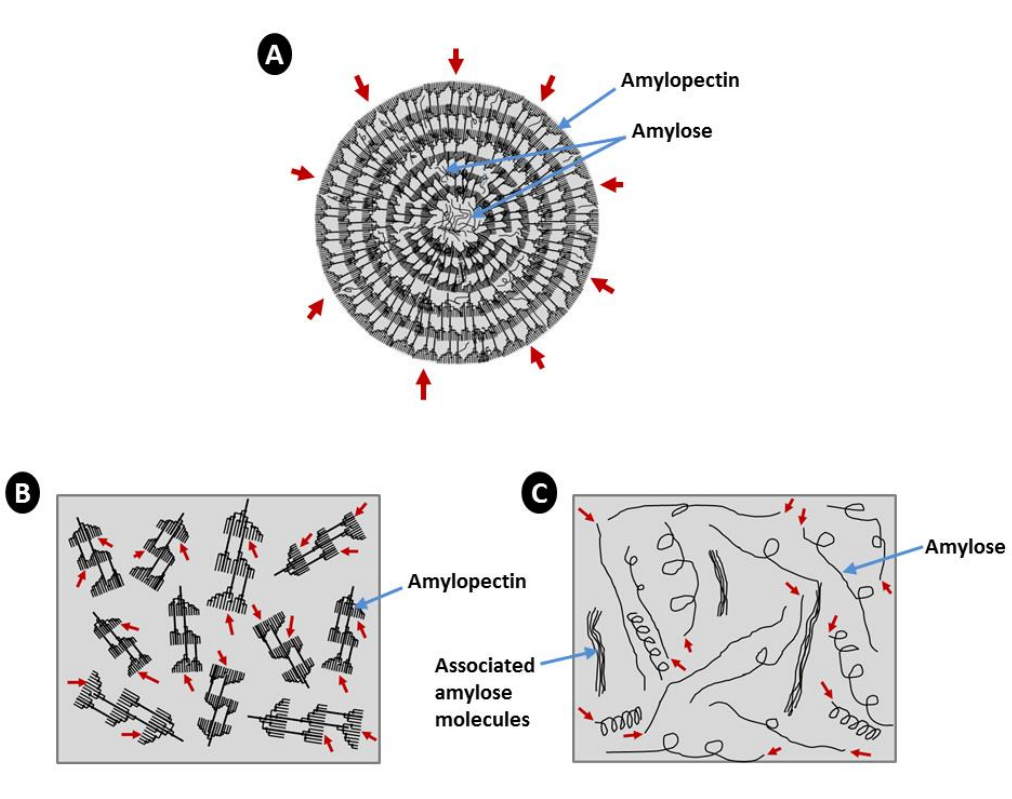

Figure 7.1: Representations to show the reaction pattern of amylases: (A) native granule showing the semicrystalline structure, (B) dispersed amylopectin molecules, and (C) dispersed amylose molecules. Small-block arrows indicate the access points of amylases towards the native granules (A), and isolated amylopectin (B) and amylose (C) of starches. Amylopectin models shown in this representation are based on the model proposed by Hizukuri (1986).

7.3.4. Amylolysis of native granules, AP and AM of waxy starches

Hydrolysis data of waxy corn and waxy barley are presented in Table 7.3. As both starches were low in AM content (1.1 – 5.3%), only the AP fraction was isolated for this study. Initially (at 1h), native granules of barley starch were hydrolyzed by amylases to a higher extent (49.6%) than corn (29.2%). However, their AP fractions showed an opposite trend in the extent of hydrolysis (Table 7.3). It is likely that the presence of weaker crystallites and a lower content of bound lipid in barley starch may have rendered waxy barley starches more susceptible to

hydrolysis (Chapter 5). In addition, a lower DH in native granules of corn than barley could be attributed to the higher molecular density (50.1 g/mol/nm^3) of its AP. The difference in DH between isolated AP of corn and barley starches during the initial stages of hydrolysis (1–48h) reflects the higher content of short-chains (*CL* = 19.8) in the former (Table 7.3). After 24h hydrolysis, the difference in DH (Table 7.3) between native granules and AP fraction of barley starches was not significant. This suggests that the structure of AP in barley starch did not influence the DH at the later stage of hydrolysis.

Table 7.3: Degree of hydrolysis of native granules and amylopectin of waxy starches from corn and barley

	Degree of hydrolysis (%, dry basis)			
	1h[1]	**24h[2]**	**48h[2]**	**72h[2]**
Native granules				
Corn	29.2^{d} ± 1.2	77.3^{c} ± 0.7	87.3^{b} ± 1.0	88.1^{b} ± 0.7
Barley	49.6^{c} ± 1.0	83.8^{b} ± 1.0	88.1^{b} ± 1.3	89.4^{ab} ± 0.7
Amylopectin				
Corn	86.1^{a} ± 0.8	88.3^{a} ± 0.5	90.8^{a} ± 0.5	91.4^{a} ± 0.4
Barley	78.0^{b} ± 1.0	84.0^{b} ± 1.3	86.6^{b} ± 0.4	91.3^{a} ± 1.2

[1] hydrolysis carried out at 55^{o}C for 1h

[2] hydrolysis carried out at 30^{o}C for 24, 48, and 72h

values are mean ± standard deviation, and values with the same superscript in italic letters in the same column are not significantly different at α = 0.05.

7.3.5. Amylolysis of native granules, AP and AM of high-amylose starches

The DH results of starches from high-amylose genotypes of corn and barley are presented in Table 7.4. As seen in both normal (Table 7.2) and waxy (Table 7.3) genotypes of corn and barley starches, the native granules of high-amylose corn

and barley starches also showed a lower DH during 1h hydrolysis than did their AP and AM fractions. Native granules of corn showed only a DH of 9.4% even after 72h. This suggests that in corn starch AM content (69.7%) had greater influence than AP structure on DH. The granule size range of high-amylose corn (2 – 22 μm) and barley (1 – 20 μm) starches was comparable; however, their AM content varied greatly (corn > barley, Chapter 5). In addition, the molecular size (R_z) of AM between high-amylose corn and barley starches is comparable and compared to normal starches, AM in the above starches are smaller (Table 7.1). This would explain then the architecture of AM is greatly varied between high-amylose corn and barley starch granules. AM (high proportion) being compactly

Table 7.4: Degree of hydrolysis of native granules, amylopectin and amylose of high-amylose starches from corn and barley

	Degree of hydrolysis (%, dry basis)			
	1h[1]	**24h[2]**	**48h[2]**	**72h[2]**
Native granules				
Corn	$0.3^{e} \pm 0.0$	$2.6^{c} \pm 0.4$	$2.8^{c} \pm 0.4$	$9.4^{d} \pm 0.7$
Barley	$24.1^{d} \pm 1.4$	$78.8^{a} \pm 1.0$	$83.1^{a} \pm 0.4$	$86.2^{a} \pm 1.4$
Amylopectin				
Corn	$71.4^{b} \pm 0.9$	$78.9^{a} \pm 1.0$	$83.0^{a} \pm 0.6$	$84.7^{ab} \pm 0.8$
Barley	$74.5^{a} \pm 1.3$	$77.3^{ab} \pm 1.1$	$82.2^{a} \pm 0.8$	$84.8^{ab} \pm 0.7$
Amylose				
Corn	$66.4^{c} \pm 0.8$	$74.9^{b} \pm 0.9$	$78.5^{b} \pm 1.0$	$82.9^{bc} \pm 1.0$
Barley	$68.3^{c} \pm 1.0$	$75.7^{b} \pm 1.3$	$78.4^{b} \pm 0.5$	$82.0^{c} \pm 1.0$

[1] hydrolysis carried out at 55°C for 1h

[2] hydrolysis carried out at 30°C for 24, 48, and 72h

values are mean ± standard deviation, and values with the same superscript in the same column are not significantly different at α = 0.05.

packed (reduces amylose chain flexibility) in high-amylose corn starch within the bulk amorphous would hinder the conformational transformation (chair to half chair) required for hydrolysis of D-glucopyranosyl units. Consequently, this would decrease the accessibility of the glycosidic linkages to hydrolysis by amylases. It is highly unlikely that AM-lipid complexes could be a factor contributing to difference in DH, since isolated AM from high-amylose corn and barley starches are hydrolyzed nearly to the same extent (Table 7.4). The higher proportion of short-chains (indicated by high degree of branching and high molecular density) in barley AP (Table 7.1) could be attributed to DH of native barley (24.1%) being higher than that of corn (0.3%) during the early stage (1h) of hydrolysis. Similarly, isolated barley AP (74.5%) was hydrolyzed to greater extent than corn AP (71.4%) due to the presence of a higher proportion of short-chains (average-*CL* 7.8) in the former. However, the difference in DH between corn AP and barley AP was insignificant after 24h (Table 7.4). Miao et al. (2011), Evans & Thompson (2008) and Sevenou et al. (2002) reported that native granules of high-amylose corn are resistant to amylase hydrolysis due the presence of a high level of double helical order of AP short-chains in the external region of granules that were highly resistant to amylase hydrolysis. The DH of isolated corn and barley AM was lower than that of AP counterparts (Table 7.4). This could be attributed to association between AM and AM chains, which hinder amylase hydrolysis (Figure 7.1C). Although the molecular characteristics of AM between barley and corn were different (Table 7.1), the difference in DH

of AM during the progress of hydrolysis (1 to 72h, Table 7.4) was not significant. This suggests that the DH of AM was not influenced by the molecular characteristics of AM isolated from high-amylose barley and corn. Since both AP and AM of high-amylose corn and barley were hydrolyzed to the same extent, the difference in DH between native corn and barley probably reflects the denser packing of AM within the granule interior of corn starch. Densely packed AM chains would decrease the accessibility of α-amylase towards the glycosidic linkages.

7.3.6. Relations between molecular characteristics and degree of hydrolysis

The statistical correlations between molecular characteristics of AP and AM, and DH of starches are presented in Figures 7.2 and 7.3. The correlation results suggest that the initial rate of hydrolysis of AP and AM are greatly influenced by amylases, when they are within native granules rather than in dispersed solutions. As shown in Figures 7.2A and 7.2C, the molar mass (M_w) and molecular size (R_z) of AP significantly correlated to the DH of native granules (r = 0.66 and 0.71, $p<0.05$, respectively). A similar trend was seen with AM; however, correlations between molecular characteristics and DH of AM were not significant (Figures 7.2B and 7.2D). The branching parameters of AP also predominantly influence the reaction of amylases on native starch granules. The results showed that the average-*CL*, *DB*, and *ρ* of AP highly influenced the DH of native granules at the initial stages of hydrolysis (Figure 7.3). As explained

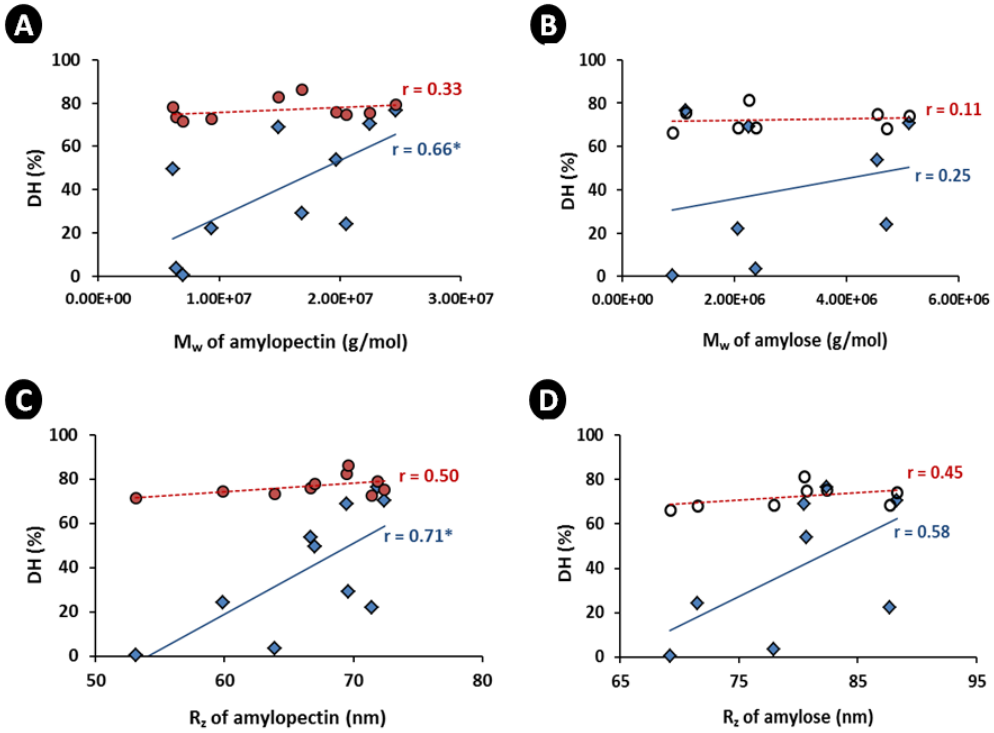

Figure 7.2: Statistical correlations between the molecular characteristics of starch molecules and degree of hydrolysis (DH) of native granules (◆), amylopectin (●) and amylose (○) at 1h hydrolysis: molecular weight vs. degree of hydrolysis, (A) amylopectin and (B) amylose; radius of gyration vs. degree of hydrolysis, (C) amylopectin and (D) amylose. Correlation coefficient (r) and level of significance (*) presented in the figures are measured at $\alpha = 0.05$.

earlier, AP molecules that are composed mainly of short-chains (indicated by low average-*CL*), showed a higher DH in native granules (Figure 7.3A). Correlations of *DB* (Figure 7.3B) and ρ (Figure 7.3C) of AP with DH of native granules were further indicative of the effect of short-chains on hydrolysis. The high *DB* in AP molecules was found in Pronghorn triticale, CPS Red wheat and barley (normal and high-amylose) starches perhaps due to heavily branched and densely packed short-chains (Table 7.1). The positive relationships between M_w or R_z and DH

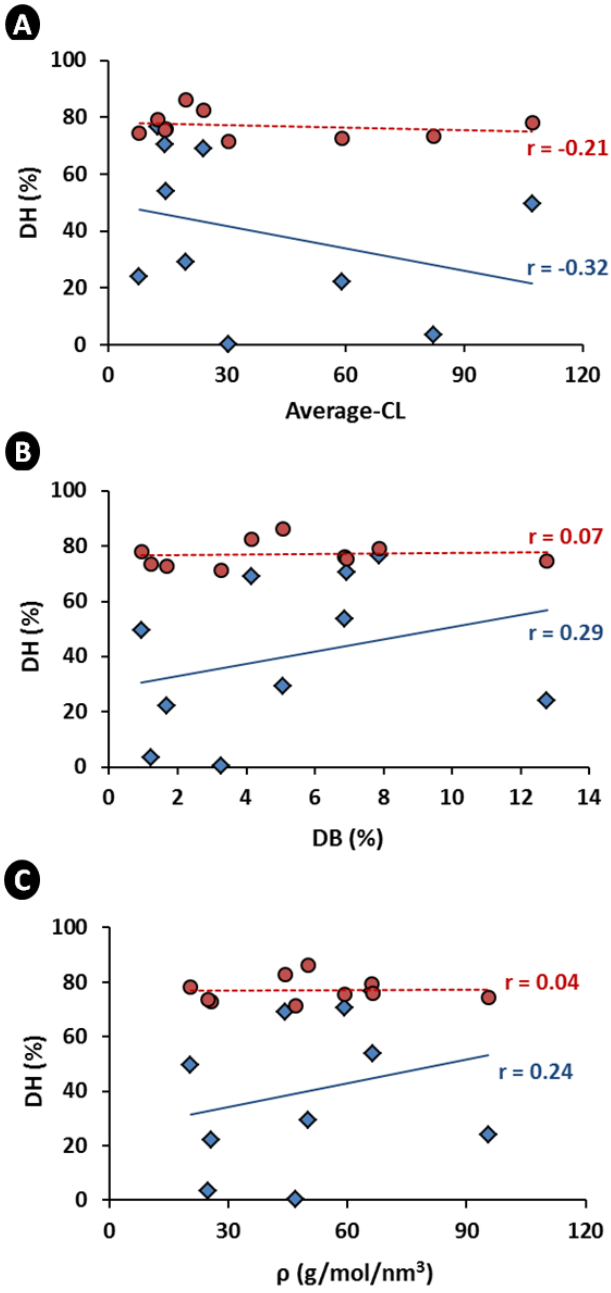

Figure 7.3: Statistical correlations between branching parameters of amylopectin and degree of hydrolysis (DH) of native granules (◆) and amylopectin (●) at 1h hydrolysis: (A) average chain-length (*CL*) vs. degree of hydrolysis, degree of branching (*DB*) vs. degree of hydrolysis, and (C) molecular density (ρ) vs. degree of hydrolysis. Correlation coefficient (r) presented in the figures are measured at $\alpha = 0.05$.

(Figures 7.2A and 7.2C) and an inverse relationship between average-*CL* and DH (Figure 7.3A) were indicative that large molecules of AP increase the DH of native granules initially due to their higher proportion of short-chains.

Correlations between molecular characteristics and the DH of isolated AP (Figures 7.2A, 7.2C, 7.3A, 7.3B and 7.3C), and between the molecular characteristics and DH of isolated AM (Figures 7.2B and 7.2C) were not significant. This suggests that the molecular characteristics AP and AM are similar between starches and that they had no direct influence on amylase hydrolysis when they were present in a dispersed solution.

7.4. CONCLUSIONS

The study was conducted to understand the relationship between molecular architecture and DH of starches (normal, waxy, and high-amylose genotypes) from two common cereals such as wheat and corn, which are extensively used in food and industrial applications, with two less utilized starches such as triticale and barley. In all starches, isolated AP and AM were hydrolyzed to a higher extent during the initial stages of hydrolysis than the native granules. In isolated AP and AM from normal and high-amylose starches, the AP molecules were hydrolyzed to a greater extent than their AM counterparts. The difference in DH during the initial stages of starch amylolysis by α-amylase and glucoamylase is likely due the variations in the average-*CL* of AP molecules. The AP composed of a high proportion of short branch chains showed a high DH.

REFERENCES

Asare, E. K., Jaiswal, S., Maley, J., Baga, M., Sammynaiken, R., Rossnagel, B. G., & Chibbar, R. N. (2011). Barley Grain Constituents, Starch Composition, and Structure Affect Starch in Vitro Enzymatic Hydrolysis. *Journal of Agricultural and Food Chemistry,* 59(9), 4743-4754.

Bruner, R. L. (1964). Determination of reducing value: 3, 5-dinitrosalicylic acid method.In R. L. Whistler, R. J. Smith, J. N. BeMiller, & M. L. Wolform (Eds.), *Methods in carbohydrate chemistry* (67-71). New York & London: Academic Press.

Charoenkul, N., Uttapap, D., Pathipanawat, W., & Takeda, Y. (2006). Simultaneous determination of amylose content & unit chain distribution of amylopectins of cassava starches by fluorescent labeling/HPSEC. *Carbohydrate Polymers,* 65(1), 102-108.

Chen, J., Wu, K., & Fukuda, H. (2008). Bioethanol production from uncooked raw starch by immobilized surface-engineered yeast cells. *Applied Biochemistry and Biotechnology,* 145(1-3), 59-67.

Dhital, S., Shrestha, A. K., & Gidley, M. J. (2010). Relationship between granule size and in vitro digestibility of maize and potato starches. *Carbohydrate Polymers,* 82(2), 480-488.

Englyst, H. N., Kingman, S. M., & Cummings, J. H. (1992). Classification and measurement of nutritionally important starch fractions. *Eur. J. Clin. Nutr.,* 46(2), 33-50.

Evans, A. & Thompson, D. B. (2008). Enzyme susceptibility of high-amylose starch precipitated from sodium hydroxide dispersions. *Cereal Chemistry,* 85(4), 480-487.

FAO Statistics Division. (2012). FAOSTAT 2012. http://faostat.fao.org. Accessed Oct/9, 2012.

Gaborieau, M. & Castignolles, P. (2011). Size-exclusion chromatography (SEC) of branched polymers and polysaccharides. *Analytical and Bioanalytical Chemistry,* 399(4), 1413-1423.

Gao, J., Vasanthan, T., & Hoover, R. (2009). Isolation and Characterization of High-Purity Starch Isolates from Regular, Waxy, and High-Amylose Hulless Barley Grains. *Cereal Chemistry,* 86(2), 157-163.

Gibreel, A., Sandercock, J. R., Lan, J., Goonewardene, L. A., Zijlstra, R. T., Curtis, J. M., & Bressler, D. C. (2009). Fermentation of Barley by Using Saccharomyces cerevisiae: Examination of Barley as a Feedstock for Bioethanol Production and Value-Added Products. *Applied and Environmental Microbiology,* 75(5), 1363-1372.

Goesaert, H., Bijttebier, A., & Delcour, J. A. (2010). Hydrolysis of amylopectin by amylolytic enzymes: level of inner chain attack as an important analytical differentiation criterion. *Carbohydrate Research,* 345(3), 397-401.

Gomez, L. D., Steele-King, C. G., & McQueen-Mason, S. J. (2008). Sustainable liquid biofuels from biomass: the writing's on the walls. *New Phytologist,* 178(3), 473-485.

Hizukuri, S. (1986). Polymodal Distribution of the Chain Lengths of Amylopectins, and its Significance. *Carbohydrate Research,* 147(2), 342-347.

Kandil, A., Li, J., Vasanthan, T., Bressler, D. C., & Tyler, R. T. (2011). Compositional changes in whole grain flours as a result of solvent washing and their effect on starch amylolysis. *Food Research International,* 44(1), 167-173.

Liu, Q., Gu, Z., Donner, E., Tetlow, I., & Emes, M. (2007). Investigation of digestibility in vitro and physicochemical properties of A- and B-type starch from soft and hard wheat flour. *Cereal Chemistry,* 84(1), 15-21.

Liu, Q. (2005). Understanding starches and their role in foods.In S. W. Cui (Ed.), *Food Carbohydrates: chemistry, physical properties, and applications* (309-355). Boca Raton, FL., USA.: CRC Press, Taylor & Francis Group, LLC.

Mason, W. R. (2009). Starch use in foods.In J. BeMiller & R. Whistler (Eds.), *Starch: Chemistry and Technology* (745-795). New York, USA.: Academic Press of Elsevier Inc.

Miao, M., Zhang, T., Mu, W., & Jiang, B. (2011). Structural characterizations of waxy maize starch residue following in vitro pancreatin and amyloglucosidase synergistic hydrolysis. *Food Hydrocolloids,* 25(2), 214-220.

Mua, J. & Jackson, D. (1997). Relationships between functional attributes and molecular structures of amylose and amylopectin fractions from corn starch. *Journal of Agricultural and Food Chemistry, 45*, 3848-3854.

Naguleswaran, S., Li, J., Vasanthan, T., & Bressler, D. (2011). Distribution of Granule Channels, Protein, and Phospholipid in Triticale and Corn Starches as Revealed by Confocal Laser Scanning Microscopy. *Cereal Chemistry,* 88(1), 87-94.

Naguleswaran, S., Li, J., Vasanthan, T., Bressler, D., & Hoover, R. (2012). Amylolysis of large and small granules of native triticale, wheat and corn starches using a mixture of α-amylase and glucoamylase. *Carbohydrate Polymers,* 88(3), 864-874.

Oates, C. G. (1997). Towards an understanding of starch granule structure and hydrolysis. *Trends in Food Science & Technology,* 8(11), 375-382.

Salman, H., Blazek, J., Lopez-Rubio, A., Gilbert, E. P., Hanley, T., & Copeland, L. (2009). Structure-function relationships in A and B granules from wheat starches of similar amylose content. *Carbohydrate Polymers,* 75(3), 420-427.

Sevenou, O., Hill, S., Farhat, I., & Mitchell, J. (2002). Organisation of the external region of the starch granule as determined by infrared spectroscopy. *International Journal of Biological Macromolecules,* 31(1-3), 79-85.

Sharma, V., Rausch, K. D., Tumbleson, M. E., & Singh, V. (2007). Comparison between granular starch hydrolyzing enzyme and conventional enzymes for ethanol production from maize starch with different amylose: Amylopectin ratios. *Starch-Starke,* 59(11), 549-556.

Stevnebø, A., Sahlström, S., & Svihus, B. (2006). Starch structure and degree of starch hydrolysis of small and large starch granules from barley varieties with varying amylose content. *Animal Feed Science and Technology,* 130(1–2), 23-38.

Sujka, M. & Jamroz, J. (2007). Starch granule porosity and its changes by means of amylolysis. *International Agrophysics,* 21(1), 107-113.

Takeda, Y., Hizukuri, S., & Juliano, B. O. (1986). Purification and Structure of Amylose from Rice Starch. *Carbohydrate Research,* 148(2), 299-308.

Tester, R. F., Qi, X., & Karkalas, J. (2006). Hydrolysis of native starches with amylases. *Animal Feed Science and Technology, 130*(1-2), 39-54.

Uthumporn, U., Zaidul, I. S. M., & Karim, A. A. (2010). Hydrolysis of granular starch at sub-gelatinization temperature using a mixture of amylolytic enzymes. *Food and Bioproducts Processing,* 88(C1), 47-54.

Vermeylen, R., Goderis, B., Reynaers, H., & Delcour, J. (2005). Gelatinization related structural aspects of small and large wheat starch granules. *Carbohydrate Polymers, 62*, 170-181.

CHAPTER 8

GENERAL DISCUSSION AND CONCLUSIONS

8.1. Significance of the research

Starch is a polysaccharide that solely present in higher plants. Its native granular form as a semicrystalline structure offers unique functionalities for various applications. Highly processed foods utilize various functionalities of starch-derived products such as sugars, dextrins and modified starches, which confer many specific physicochemical properties. Furthermore, rapidly growing trends in processed food have shifted towards more natural and healthy products. One of the current trends is the consumption of starchy products that are resistant to digestion, so called as resistant starches (RS). The benefits of RS-rich food products, in particular RS1 and RS2, mainly depend on the starch granular architecture. Slow release of sugar during starch digestion is important to control the dietary calorie value and blood glucose level in humans (Liu, 2005; Mason, 2009; Englyst et al., 1992). Thus, understanding the impact of starch structure on enzymatic hydrolysis is important in developing novel food products from various starch sources.

On the other hand, the use of renewable sources of energy such as bioethanol is receiving much attention due to the fast growing global demand for energy, a rapid depletion of fossil fuel, and a concern for increased greenhouse gas emission. The current conventional bioethanol production from

cereal grains is a batch process and it requires starch from grains to be enzymatically hydrolyzed completely to sugars (glucose, maltose and maltotriose), which are subsequently fermented to ethanol by yeast (Chen et al., 2008; Sharma et al., 2007). However, the initial step in this ethanol production that converts the native starch into sugars (starch hydrolysis/amylolysis) is still unnecessarily expensive (excessive heat energy is used to gelatinize the starch). This is primarily due to our lack of understanding on how starch molecular and granular structural features influence the kinetics of amylolysis. Improved granular starch-hydrolyzing enzymes (a mixture of α-amylase and glucoamylase) have been recently introduced in bioethanol production these can be used to hydrolyze the native starch granules at low temperatures, thus cooking of starch at high temperature is unnecessary for this process. However, it is important to answer the question of how do the compositional, morphological, ultrastructural and molecular properties of native starches influence amylolysis. Thereby, this thesis was designed towards understanding how variations in the granular and molecular structural properties of starch from various botanical origins would influence starch susceptibility towards hydrolysis by amylases at low temperatures. Two benchmark cereals that are most commonly utilized in both food and ethanol production in North America such as corn and wheat were considered in this research for comparison with triticale and barley that are currently receiving attention as alternative crops for food and industrial applications.

8.2. Summary and Conclusions

In North America, corn and wheat grains are extensively used for bioethanol production. However, these two grains are also widely used for various food applications. Due to the increasing cost of wheat and less availability of corn and wheat for food production, there is a need to find alternative sources for bioethanol production, particularly in Canada. Triticale and barley are less utilized cereals in Canada; however, they are a potentially favorable source of starch for bioethanol production (Davis-Knight & Weightman, 2008; Gibreel et al., 2009; Wang et al., 1997). Nevertheless, the available knowledge on the structural features of triticale starch towards its application is very limited. In Chapter 3, the morphology and microstructure of starch granules from two varieties of triticale (Pronghorn and Ultima) and from normal corn were characterized using scanning electron microscopy (SEM) and confocal laser scanning microscopy (CLSM). Compared to numerous pores distributed randomly on the surface of corn starch granules, markedly fewer pores were observed on the surface of Pronghorn triticale starch granules, and even fewer on the surface of Ultima triticale starch granules. The presence of pores, channels and cavities in starch granules facilitate improved chemical and enzyme penetration (Sujka & Jamroz, 2007). In the present study, CLSM in conjunction with fluorescent staining clearly revealed that surface pores and internal channels in both triticale and corn starch granules were associated with protein

and phospholipids, which blocked the pathway for the diffusion of chemicals or enzymes into the starch matrix.

In order to enhance the use of triticale starch in various applications, the influence of granule size and ultrastructure of starch granules on amylolysis were studied in comparison to wheat and corn starches of normal genotypes (Chapter 4). In this study, large and small granules were fractionated from native triticale, wheat and corn starches using a centrifugal sedimentation protocol and were hydrolyzed by granular starch hydrolyzing enzymes (GSHE) at sub-gelatinization temperatures. In all starches, the proportion of small granules was higher than that of large granules. Surface pores and internal channels (viewed by SEM and CLSM) were more visible in large granules than in small granules of triticale, wheat, and corn starches, but corn starch generally displayed more pores and channels than triticale and wheat starches. Large granules contained significantly higher apparent amylose content and higher relative crystallinity than did small granules in all starches. Initially (at 55 °C for 1h), small granules of triticale, wheat, and corn starches were hydrolyzed significantly faster than large granules, however the DH of small granules slowed down in later stage of hydrolysis. The initial difference in degree of hydrolysis between small and large granules was attributed to the fact that the small granules had a larger surface area per unit mass for enzyme reaction than large granules. SEM and CLSM further revealed that the hydrolysis pattern differed between large and small starch granules, and among starch sources, indicating that variation existed in

the molecular architecture of starch granules. The results suggested that the triticale starch was comparable to wheat and corn starches in terms of granular starch hydrolysis for use in bioethanol production as well as any potential food application.

In Canada, barley grains are most frequently used to make beverages like beer and whisky, and are used as feed for hogs, cattle and poultry (Canadian Grain Commission, 2011). It has been reported that barley is a cheaper potential feedstock for bioethanol production compared to corn and wheat (Gibreel et al., 2009; Li, Vasanthan, Hoover, & Rossnagel, 2004). However, the structure of native starch granules with varied amylose content of barley would affect the amylolysis in the formation of fermentable sugars for ethanol production. A study (Chapter 5) was conducted to ascertain whether the hydrolysis of unfractionated and fractionated (large and small) starch granules of waxy (<10% amylose), normal (20 – 30% amylose), high-amylose (>40% amylose) hull-less barley and corn starches of varying amylose content (0 – 70%) by GSHE at sub-gelatinization temperature are influenced by the morphology, structure and physicochemical properties of the above starches. SEM and CLSM images revealed that the distribution of surface pores and internal channels varied between genotypes of corn and barley starches; waxy and normal genotypes of corn starch granules have shown to be distributed with more surface pores and internal channels than the other starches. Compared to corn starches, barley starches were hydrolyzed to a greater extent initially due to the presence of

weaker crystallites in the latter. As seen in triticale and wheat starches (Chapter 4), at initial stages of amylolysis, small granules of corn and barley starches were hydrolyzed to a higher extent than large granules. This difference was more pronounced in normal corn. Since normal corn is widely used in bioethanol production, its initial rate of hydrolysis may be too low for optimum yeast function at the initial stages of fermentation (i.e. underperformance of yeast due to lack of available fermentable sugars). In contrast, normal barley starches showed high initial rate of hydrolysis that may be too high for optimum yeast function (i.e. underperformance of yeast due to high amounts of fermentable sugar and osmotic pressure). Although small variations existed between normal genotypes of corn and barley starches with respect to their proximate composition and amylose content, the observed large variations in the extent of amylolysis at the initial stages of hydrolysis is indicative that the molecular architecture and granule porosity (i.e. the number of granule surface pores and channels) influence amylolysis. Therefore, we suggest blending of normal corn and normal barley starches (i.e. flours) may benefit the bioethanol production.

All of the above studies (Chapters 3, 4 and 5) have suggested that the starch factors such as amylose:amylopectin content ratio, morphology, granule size and ultrastructure of native starches highly influenced the degree of hydrolysis by amylases. The architecture of a starch granule is built up by two polymers, amylose and amylopectin, which are highly organized through intra- and inter-molecular hydrogen bonds resulting in a complex biopolymer.

Molecular characteristics of amylopectin and amylose have been shown to influence the amylolysis of starches when they are within the granules (Goesaert, Bijttebier, & Delcour, 2010; Miao et al., 2011; Murthy et al., 2011). However, there is a dearth of information on the extent to which isolated amylose and amylopectin are hydrolyzed by amylases at low temperatures. Therefore, a study was initially carried out to compare the molecular characteristics of amylose and amylopectin of normal, waxy, and high-amylose genotypes from wheat, triticale, barley, and corn starches using high-performance size exclusion chromatography coupled with multi-angle laser light scattering and refractive index detectors (Chapter 6). In the last study (Chapter 7), a comparison of the reactivity of amylases towards the intact native granules and their isolated amylopectin and amylose of the above starches was carried out to understand the role played by molecular characteristics of amylopectin and amylose in starch amylolysis. Molecular characterization of starch polymers revealed that, the molecular weight (M_w) of amylopectin was higher than amylose; however, the molecular size (R_z) of amylopectin was lower than that of amylose in all starches, reflecting the heavily branched and compacted structure of amylopectin. In comparison to other starches, amylopectin of high-amylose barley starches were smaller, denser, more branched and composed mainly of shorter unit-chains. Whereas, amylopectin of wheat starches were less branched, less compact and composed mainly of longer unit-chains. Amylose of normal and high-amylose barley starches were smaller and appeared to be

branched than amylose of other starches. Variations in molecular characteristics of amylopectin isolated from triticale, wheat, corn and barley starches have been explained in this study using three structure models of amylopectin (Chapter 6). The models suggested that the structure of amylopectin would significantly influence starch properties such as susceptibility towards enzyme hydrolysis, gelatinization, extent of crystallization during retrogradation, and granular swelling.

Amylolysis of isolated amylopectin and amylose by using a mixture of α-amylase and glucoamylase at sub-gelatinization temperatures (< 55^{o}C) over a period from 1 to 72h, indicated that molecular characteristics of amylopectin greatly influenced the hydrolysis of native starches (Chapter 7). Furthermore, in most of the starches, the DH of AP was significantly higher than the corresponding AM regardless of the stages of hydrolysis. Whereas, DH among isolated AP or AM from different starch sources was generally insignificant irrelevant to the stages of hydrolysis. In addition, it was observed that the DH (at 1h) of native unfractionated starches was negatively correlated to average chain length, but positively correlated to M_w, R_z, density and degree of branching of amylopectin. The relationship between molecular characteristics of amylopectin and amylolysis of native granules suggested that the less utilized starches such as triticale and barley were comparable to the most frequently utilized starches such as corn and wheat for various food and industrial applications. For example, the triticale and barley starches (their amylopectins have been shown to be

composed mainly of short chains) can be utilized to produce sugar derivatives and bioethanol. Overall, the study indicated that starch amylolysis is influenced by: 1) composition (AM content), 1) morphological characteristics (granule size, channels/pores, and associated proteins and phospholipids) and 3) difference in granular architecture (resulting from variation in the average chain length of amylopectin).

8.3. Originality of the research investigations presented in this thesis

Cereal grains are a major source of starch that is currently utilized in various food and industrial (bioethanol production) applications in North America. In food applications, slower rate of amylolysis and gradual release of sugar (i.e. low-glycemic attribute of starch), as well as incomplete amylolysis/digestion (i.e. presence of indigestible resistant starch) of starches are preferred. In contrast, for bioethanol production, a quantitative conversion of starch to sugars by amylase enzymes at a "slow to medium" rate of hydrolysis is preferred. Several factors, including starch granular and molecular structural properties could influence amylolysis. Hence, a clear understanding of starch structure-amylolysis relationship is essential for better selection of grains and starches for different applications.

The influence of grain composition and physicochemical properties of native/raw starches such as granule size, granular architecture and porosity, and molecular structure on *in vitro* starch hydrolysis have been reported. However,

the following investigations presented in this thesis fill the research gap that exists in the literature with respect to starch structure-amylolysis relations.

- The distribution of starch associated protein and phospholipid and their influence on triticale starch hydrolysis. In this study, selective fluorescent staining techniques followed by CLSM were used to study the distribution of starch associated protein and phospholipid of triticale in comparison to that of barley, wheat and corn (Chapter 3).
- A double staining (fluorescent) technique followed by CLSM was used for structural examination of starch granules in order to study the distribution of starch molecules (amylose and amylopectin), and non-starch minor components (ex: phospholipids) simultaneously (Chapter 3).
- Benefits of triticale and barley starches with respect to their amylolytic characteristics in "raw starch hydrolysis and fermentation technology" of bioethanol production was evaluated and compared to starches from corn and wheat (bench mark grains) (Chapters 4 and 5).
- Amylolysis of the intact native starch granules (influence of granule architecture exists) and separated starch molecules (from the same starch granules) such as amylopectin or amylose (influence of granule architecture no longer exists, but molecular structural influence present) was carried out to understand the influence of granule architecture and molecular characteristics of amylopectin and amylose on starch amylolysis (Chapters 6 and 7).

8.4. Recommendations for future work

Bioethanol industries face ongoing challenges in the quantitative conversion of "starch to ethanol", also report inconsistencies in the conversion efficiency. Furthermore, determination of the residual starch content in the dried distillers' grains plus solubles (DDGS), collected from commercial facilities as well as from lab experiments (Drs. Bressler and Vasanthan labs), have clearly indicated the presence of significant starch (resistant starch) in the samples. Therefore, it is important to understand the mechanism by which starch escapes the process of ethanol production. Further studies warranted towards understanding on how conversion efficiency of "starch to ethanol" influenced by starch characteristics that are investigated in this thesis. Such a study may lead to minimize the loss of starch in the DDGS and could improve the profitability of ethanol industries. Furthermore, similar studies can be extended into applications looking for special functionalities of starch in food, and their relations to starch characteristics. Another line of research would be to carry out similar studies in grain flours instead of purified starches. This is because the grain flour contains a number of non-starch components such as fiber (soluble and insoluble), protein, phenolics, phytic acid, etc. that can potentially interfere the hydrolysis of starch by amylases. Furthermore, in this thesis we have considered only few genotypes under each grain source. Extending this study to precisely understand the effect of other genotypes along with the growing locations on the rate and extend of starch hydrolysis, and ethanol conversion efficiency would benefit the industry.

REFERENCES

Asare, E. K., Jaiswal, S., Maley, J., Baga, M., Sammynaiken, R., Rossnagel, B. G., & Chibbar, R. N. (2011). Barley grain constituents, starch composition, and structure affect starch *in vitro* enzymatic hydrolysis. *Journal of Agricultural and Food Chemistry, 59*(9), 4743-4754.

Canadian Grain Commission (2011). Canadian Barley, accessed from http://www.grainscanada.gc.ca/barley-orge/bom-mbo-eng.htm on Jan 14, 2013.

Chen, J., Wu, K., & Fukuda, H. (2008). Bioethanol production from uncooked raw starch by immobilized surface-engineered yeast cells. *Applied Biochemistry and Biotechnology, 145*, 59-67.

Davis-Knight, H. R., & Weightman, R. M. (2008). The potential of triticale as a low input cereal for bioethanol production. The Home-Grown Cereals Authority (HGCA) Project Rep No. 434. ADAS UK Ltd, Centre for Sustainable Crop Management: Cambridge, UK.

Englyst, H. N., Kingman, S. M., & Cummings, J. H. (1992). Classification and measurement of nutritionally important starch fractions. *European Journal of Clinical Nutrition, 46*, 33-50.

Gao, J., Vasanthan, T., & Hoover, R. (2009). Isolation and Characterization of High-Purity Starch Isolates from Regular, Waxy, and High-Amylose Hulless Barley Grains. *Cereal Chemistry, 86*(2), 157-163.

Gibreel, A., Sandercock, J. R., Lan, J., Goonewardene, L. A., Zijlstra, R. T., Curtis, J. M., & Bressler, D. C. (2009). Fermentation of barley by using *Saccharomyces cerevisiae*: examination of barley as a feedstock for bioethanol production and value-added products. *Applied and Environmental Microbiology, 75*, 1363-1372.

Goesaert, H., Bijttebier, A., & Delcour, J. A. (2010). Hydrolysis of amylopectin by amylolytic enzymes: Level of inner chain attack as an important analytical differentiation criterion. *Carbohydrate Research, 345*(3), 397-401.

Li, J., Vasanthan, T., Hoover, R., & Rossnagel, B. (2004). Starch from hull-less barley: V. In-vitro susceptibility of waxy, normal, and high-amylose starches towards hydrolysis by alpha-amylases and amyloglucosidase. *Food Chemistry, 84*(4), 621-632.

Liu, Q. (2005). Understanding starches and their role in foods. In S. W. Cui (Ed.), *Food Carbohydrates: chemistry, physical properties, and applications* (309-355). Boca Raton, FL., USA: CRC Press, Taylor & Francis Group, LLC.

Mason, W. R. (2009). Starch use in foods. In J. BeMiller & R. Whistler (Eds.), *Starch: Chemistry and Technology* (745-795). New York, USA: Academic Press of Elsevier Inc.

Miao, M., Zhang, T., Mu, W., & Jiang, B. (2011). Structural characterizations of waxy maize starch residue following in vitro pancreatin and amyloglucosidase synergistic hydrolysis. *Food Hydrocolloids, 25*(2), 214-220.

Murthy, G. S., Johnston, D. B., Rausch, K. D., Tumbleson, M. E., & Singh, V. (2011). Starch hydrolysis modeling: Application to fuel ethanol production. *Bioprocess and Biosystems Engineering, 34*(7), 879-890.

Sharma, V., Rausch, K. D., Tumbleson, M. E., & Singh, V. (2007). Comparison between granular starch hydrolyzing enzyme and conventional enzymes for ethanol production from maize starch with different amylose:amylopectin ratios. *Starch-Starke, 59*, 549-556.

Sujka, M., & Jamroz, J. (2007). Starch granule porosity and its changes by means of amylolysis. *International Agrophysics, 21*, 107-113.

Wang, S., Thomas, K. C., Ingledew, W. M., Sosulski, K., & Sosulski, F. W. (1997). Rye and triticale as feedstock for fuel ethanol production. *Cereal Chemistry, 74*(5), 621-625.

APPENDIX

Detailed descriptions of some methodologies used in this thesis

1. Starch isolation from wheat grains

Wheat grains were ground in a Retsch mill (Model ZM 200, Haan, Germany) using a ring sieve with an aperture size of 0.5 mm. A dough ball washing technique was used to isolate the starch from wheat flour. Stiff dough was prepared by mixing 100 g of flour with 60 mL of water (1:0.6, w/v) in a dough mixer (KitchenAid® Professional 600, Canada). The dough ball was covered with a plastic cup and tempered at room temperature for 1 h followed by mixed with water (700 mL). The slurry was then filtered on a sieve with an aperture size of 75 µm (W.S. Tyler, ON, Canada) and the fiber residue from top of the sieve was re-slurried with water (1:7, w/v) and filtered again. The filtrates were pooled, centrifuged (1500 x*g* for 10 min), and the upper brown layer of the residue was removed carefully with spatula. The bottom white starch layer was re-slurried with water (200 mL) and its pH was adjusted to 10.0 by using 0.05% (w/v) NaOH followed by mixed for 30 min and centrifuged (1500 x*g* for 10 min). The starch residue was re-slurried with water (100 mL) and the pH was neutralized using 0.1N HCl followed by centrifuged (1500 x*g* for 10 min). The supernatant and the upper brownish layer of the residue containing mainly protein were discarded. The lower whitish starch-rich residue was washed three more times with distilled water (100 mL) using centrifugation (1500 x*g* for 10 min). Pure starch isolate was

dried at 40 °C for 15 h followed by ground and screened on a sieve with an aperture size of 250 mm (W.S. Tyler, ON, Canada).

2. Starch isolation from triticale grains

Triticale grains were ground in a Retsch mill (Model ZM 200, Haan, Germany) using a ring sieve with an aperture size of 0.5 mm. As explained in wheat starch isolation, a dough ball washing technique was used to isolate the starch from triticale flour too. However, there were few modifications applied in this improved dough ball washing technique. After tempering the stiff dough at room temperature for 1 h, 200 mL water was added to the dough ball followed by the mixture was blended at high speed in a Waring blender (Dynamics Corp. of America, New Hartford, CT, USA). The slurry was then filtered on a sieve with an aperture size of 75 µm (W.S. Tyler, ON, Canada) and the fiber residue from top of the sieve was re-slurried with water (1:2.5, w/v) followed by blended and filtered as mentioned above. The filtrates were pooled and the remainder stapes in the starch isolation protocol were followed exactly similar as explained for wheat starch isolation.

3. Starch isolation from barley grains

Barley grains were ground in a Retsch mill (Model ZM 200, Haan, Germany) using a ring sieve with an aperture size of 0.5 mm. Starch was isolated from barley flour using a combination of aqueous-alcohol and aqueous extraction protocol. Ground barley flour was mixed with 50% ethanol (1:4.5, w/v) in a beaker and

gently stirred for 30 min. The slurry was filtered through a 63-µm sieve. The fiber residue on the screen was reslurried with 50% ethanol (1:2.5, w/v) and sonicated (Sonic 300 dismembrator with 90% amplitude, Systems Corporation, Farmingdale, NY) for 30 min under continuous stirring. The slurry was filtered (63-µm sieve) again. After filtering, fiber residue was reslurried with 50% ethanol (1:2, w/v) and wet-milled using a polytron homogenizer (PT 2000, Kinematica AG LITTAU, Switzerland) for 10 min (30,000 rpm) followed by the slurry was filtered (63-µm sieve) once again. All filtrates from the above three filtrations were pooled and centrifuged (1500 ×*g* for 10 min). The crude starch residue was reslurried with water (1:2, w/v, according to the original flour weight) and Sodium Dodecyl Sulfate (0.25%, w/w according to the original flour) was added followed by the mixture was sonicated (while stirring) for 30 min. The slurry was centrifuged (7500 ×*g* for 10 min) followed by the supernatant and upper gray layer of residue containing mainly protein were carefully removed. The lower starch-rich white layer was washed three more times with distilled water and finally washed with 95% ethanol. Pure starch isolate was dried at 40°C for 15 h, then ground, and screened through 250-mm sieve (W.S. Tyler, ON, Canada).

4. X-Ray analysis

X-ray diffractograms were obtained with cross beam optics (CBO) technology of Rigaku Ultima IV multipurpose X-ray diffractometer (Rigaku America in

Woodlands, TX, USA) connected to a data acquisition and processing station. Before X-ray analyses, the moisture content of all starch samples were equilibrated to ≈20% by being kept in a desiccator over saturated K_2SO_4 solution (a_w = 0.98 at 25^{o}C) for seven days. The starch powder was then scanned through the 2θ range of 5–50°. Traces were obtained using a Co-Kα X-ray tube with a D/teX Ultra counter operating under the following conditions: target voltage—40 kV, target current—40 mA, scan speed—1.0°/min, divergence slit width—1.0cm, scatter slit width—1.3cm, and receiving slit width—1.3cm. Quartz was used as the 100% reference crystal. Jade 7.1 (Materials Data, Livermore, CA, USA) was used for data interpretation. For good comparison, all data were converted from cobalt (1.78899Å) to copper (1.54059Å) by changing the radiation wavelength. Relative crystallinity (RC) was measured by the method described by Nara and Komiya (Nara, S., and Komiya, T. 1983. *Starch/Stärke 35*:407-410).

5. Amylose determination

The starch samples (100.0 ± 0.1 mg) were dispersed in 1 mL of absolute ethyl alcohol followed by the addition of 10 mL of 1N sodium hydroxide solution. After an hour of complete gelatinization and solubilization of starch, the contents were diluted to 100 mL. An aliquot of 2.5 mL was quantitatively transferred and diluted to 50 mL with distilled water. The contents were neutralized with 0.1N hydrochloric acid solution followed by the addition of 2 mL of 0.2% iodine solution. Following the dilution to 100 mL, the contents were

allowed to 30 min for amylose-iodine binding reaction. The absorbance of the blue color was read at 620 nm (at room temperature) against a blank using a spectrophotometer (Model: 6300, Jenway Ltd., Essex, UK). A reference solution (blank) was prepared by diluting 2 mL of 0.2% iodine solution with distilled water to 100 mL and the absorbance was calibrated to zero prior to read the absorbance of sample solutions. The amylose standard curve was prepared using pure amylose and amylopectin from potato starch (Sigma-Aldrich, Co., St. Louis, MO, USA) as described in the methodology.